BIOCHEMICAL CHARACTERISATION OF PIMELATE BIOSYNTHETIC GENES OF Mycobacterium tuberculosis

GUGU, MUSA,FILIBUS

BIOCHEMICAL CHARACTERISATION OF PIMELATE BIOSYNTHETIC GENES OF *Mycobacterium tuberculosis*

by

Musa Filibus Gugu

Supervisor: Dr Alistair K Brown

Durham University

May 2019

BIOCHEMICAL CHARACTERISATION OF PIMELATE BIOSYNTHETIC GENES OF *Mycobacterium tuberculosis*

A project report submitted in partial fulfilment of the requirements for a Doctor of Philosophy (PhD).

by

Musa Filibus Gugu

Durham University

May 2019

Declaration: I, *Musa Filibus Gugu* confirm that I have read and understood the University regulations concerning plagiarism and that the work contained within this project report is my own work within the meaning of the regulations.

Signed ……..……

Abstract

Emergence of drug resistant tuberculosis (TB) and comorbidity with HIV, especially in the sub-Saharan Africa and Asia, has exacerbated the problem of TB, with an estimated 1.6 million people dying of the disease worldwide in 2017 alone. This programme of work approached the problem of TB by utilising a two-pronged approach to novel drug identification.

The first approach investigated enzymes involved in pimelate biosynthesis in *Mycobacterium tuberculosis* (*Mtb*). Pimelate, the precursor of biotin synthesis in bacteria, is an essential micronutrient needed for the survival of the organism. This biochemical study identified four enzymes, Rv0089, Rv1882c, Rv3177 and Rv2715 as possible proteins involved in this pathway. Due to ongoing issues with toxicity in various expression hosts, only Rv0089 was purified and biochemical studies performed. These studies confirmed the enzyme to be a methyl transferase capable of converting S-adenosyl-methionine (SAM) into S-adenosyl-L-homocysteine (SAH) with a preference for malonyl-CoA.

The second approach analysed isoxyl and SQ109 hybrid anti-tubercular agents. A series of hybrids were synthesized to develop a potential new lead compound with multiple modes of action and decreased propensity to develop resistance. A lead compound with an MIC of 0.120 µg/mL against *Mtb* was successfully synthesised showing markedly higher activities than the parental drugs (SQ109 MIC = 0.48 µg/mL and isoxyl MIC = 0.24 µg/mL). Additionally, this compound was equally potent against rifampicin and isoniazid singularly resistant *Mtb*.

This work has therefore provided a basis by which new anti-tubercular drugs can be developed.

Acknowledgments

To God almighty the author and finisher of our faith, I say thank you Lord.

My excellent principal supervisor, Dr. Alistair K. Brown has been amazing throughout this journey, making all the sacrifices and ensuring that I pull through. This will never be possible without you. Words are not enough to say thank you. I appreciate all the efforts. You are one in a million. My co-supervisors Dr. Jonathan Harburn and Dr. Jon Sellars, thank you for the efforts too.

To my amazing parents, Pastor and Mrs F. Gugu for giving me a good training and supporting me all through, I say thank you. My siblings, Zinas, Ezekiel, Christiana, you are all amazing, thank you.

Other friends around that helped in keeping me sane during my depressed laboratory moments; Gift Jesse, Ben Kakwi, Dr. Mohammed Buhari, Dr. Abubakar Lawal, Dr. Tobechi Okoroafor, Dr. Solomon Obida, Dr. E. E. Nnadi, Josephine Daniel Kakwi, Ibrahim Samuel, Tiseh Samuel, Ishaya Zechariah, and Samson Yakubu Obasanjo, thank you all.

To all the colleagues I started this journey with from Northumbria University to Newcastle University and to the ones at Durham University, I say a special thank you to you all.

Table of contents

Thesis figures

Thesis tables

Abbreviations

5’-AMP	5’-Adenosine monophosphate
7H11 Agar	Middlebrook 7H11 agar
7H9 Broth	Middlebrook 7H9 broth
ACC	Acetyl-CoA carboxylase
ACP	Acyl carrier protein
AcpS	Acyl carrier protein synthase
ADP	Adenosine diphosphate
AG	Arabinogalactan
AGP	Arabinogalactan peptidoglycan
Amp^R	Ampicillin resistance marker
APS	Ammonium persulfate
ATP	Adenosine triphosphate
BC	Biotin carboxylase
BCCP	Biotin carboxyl carrier protein
BCG	Bacillus Calmette-Guérin
BPL	Biotin protein ligase
BirA	Bi-functional repressor A
BLAST	Basic local alignment search tools
BTZ	1,3-benzothiazin-4-ones
CFP-10	Culture filtrate antigen
cMBT	Carboxymycobactin
CoA	Coenzyme A
CT	Carboxyl transferase
DAPA	7,8-diaminopelargonic acid
D-Ara*f*	D-arabinofuranosyl
DAT	Di-acyl trehalose
D-Gal*f*	D-galactofuranosyl
DIM	Dimycocerosate

DMSO	Dimethyl sulphoxide
DNA	Deoxyribonucleic acid
dNTP	Deoxyribonucleotide triphosphate
DOA	Deoxyadenosyl
DOTS	Directly observed treatment short course
DPA	Decaprenylphosphoryl-D-arabinose
DPR	Decaprenylphosphoryl-D-ribose
DTB	Dethiobiotin
DTT	DL-Dithiothreitol
EDTA	Ethylenediaminetetraacetic acid
EMB	Ethambutol
ESAT-6	Early secretory antigenic target
EtBr	Ethidium bromide
FAS	Fatty acid synthase
FAS-I	Fatty acid synthase I
FAS-II	Fatty acid synthase II
FasA	Fatty acid synthase A
FasB	Fatty acid synthase B
FNR	Fumarate and nitrate reductase
GCC	Geranyl-CoA carboxylase
gDNA	Genomic DNA
GTE	Glucose Tris-EDTA
HBCs	High burden countries
HCl	Hydrochloric acid
HIV	Human immunodeficiency virus
Hyg^R	Hygromycin resistance marker
IAA	Iodoacetamide
ICDH	Isocitrate dehydrogenase
IMAC	Immobilised metal affinity chromatography
INH	Isoniazid

IPTG	Isopropyl β-D-1-thiogalactopyranoside
ISO	Isoxyl
Kan^R	Kanamycin resistance marker
KAPA	7-keto-8-amino-pelargonic acid
LAM	Lipoarabinomannan
LB Agar	Luria Bertani agar
LB Broth	Luria Bertani broth
LM	Lipomannan
MA	Mycolic acid
mAGP	Mycolyl-arabinogalactan-peptidoglycan
MBP	Maltose binding protein
MBT	Mycobactin
MCC	Methyl-crotonyl-CoA Carboxylase
MCS	Multiple cloning site
MDR-TB	Multi-drug resistant TB
$MgSO_4$	Magnesium sulphate
MIC	Minimum inhibitory concentration
Milli-Q	18.2 MΩ ddH_2O
MIM	Mycobacterial inner membrane
MOM	Mycobacterial outer membrane
MOPS	(3-(*N*-morpholino)propanesulfonic acid)
Mtb	*Mycobacterium tuberculosis*
MTB Complex	*Mycobacterium tuberculosis* complex
MurNGly	N-Glycolylmuramic acid
NADP	Nicotinamide adenine dinucleotide phosphate
NCBI	National Centre for Biotechnology Information
NMR	Nuclear magnetic resonance
NRPS	Non-ribosomal peptide synthetase
OADC	Oleic albumin dextrose catalase
OD_{600}	Optical density at 600 nm

ODHC	2-oxoglutarate dehydrogenase complex
OMP	Outer membrane protein
Omp	Outer membrane porins
Ori	Origin of replication
PAGE	Polyacrylamide gel electrophoresis
PAT	Penta-acyl trehalose
PC	Pyruvate carboxylase
PCC	Propionyl-CoA carboxylase
PCR	Polymerase chain reaction
PDH	Pyruvate dehydrogenase
PDIM	Phthiocerol dimycocerosate
pDNA	Plasmid DNA
PE	Phosphatidylethanolamine
PG	Peptidoglycan
PGL	Phenolic glycolipid
pI	Isoelectric point
PI	Phosphatidylinositol
PIM	Phosphatidylinositol mannosides
PKS	Polyketide synthases
PMSF	Phenylmethylsulfonyl fluoride
PZA	Pyrazinamide
REV	Reverse
RIF	Rifampicin
RNA	Ribonucleic acid
RNaseI	Ribonuclease I
RR-TB	Rifampicin resistant TB
SAH	S-Adenosyl-L-homocysteine
SAM	S-Adenosyl methionine
SAR	Structural activity relationship
SDR	Short-chain dehydrogenase reductase

SDS	Sodium dodecyl sulphate
SecA	Secretory pathway A
SecB	Secretory pathway B
SGL	Sulphoglycolipid
SL	Sulpholipids
S-layer	Surface layer
SQ109	N-Geranyl-N’-(2-adamantyl)-ethane-1,2-diamine
TAE	Tris-acetate EDTA buffer
TAT	Triacyltrehalose
TB	Tuberculosis
TDM	Trehalose dimycolate
TDRTB	Totally drug resistant TB
TEMED	N,N,N',N'-tetramethylethane-1,2-diamine
TetR	Tet repressor protein
TFB1	Transformation buffer 1
TFB2	Transformation buffer 2
T_m	Melting temperature
TMM	Trehalose monomycolate
TP	Thymidine phosphorylase
Tris	Trizma base
UC	Urea carboxylase
UN	United Nations
WHO	World Health Organisation
XDR TB	Extensively drug resistant TB
$\sum H_2O$	Sterile DNase and RNase free ultrapure ddH_2O

Chapter 1
Introduction

1 Introduction

1.1 The mycolata group

Mycobacteria are Gram-positive, filamentous, mycelia forming bacteria which belong to the taxon mycolata under the class actinobacteria. Actinobacteria represents bacteria that form spores, which are found freely in the environment and produce aerial hyphae. The order Actinomycetales, are found in soil, fresh water and marine habitats which are mostly harmless to both plants and animals (Bentley *et al*., 2002). A large number of Actinomycetes are sources of antibiotics, especially the genus *Streptomyces* that are believed to produce about 100,000 antimicrobial compounds (Watve *et al*., 2001).

Within actinobacteria, there are several important pathogenic genera including *Rhodococcus*, *Corynebacterium*, *Norcadia* and *Mycobacterium*. These organisms have characteristic complexes of mycolic acids in their outer cell envelope that confer protection to environmental stress, host immune mechanisms and drugs (Barry *et al*., 1998, Kasik, 1965).

The class is described based on its branching position in 16S rRNA gene trees, but this method of classification created ambiguity because the rRNA sequence failed to clearly differentiate between closely related species or genera. An updated classification of actinobacteria based on 16S rRNA trees was recently reported, where sub-classes and sub-orders were upgraded to classes and orders, respectively (Gao and Gupta, 2012).

1.2 Classification of actinobacteria

Within the bacteria domain, actinobacteria is one of the largest taxonomic units recognised. Organisms within this group have different morphologies, physiologies and

metabolic capabilities that are used in classifying them. Knowledge of their taxonomy has increased over time with recent advances in microbial morphology and genetics. Three major characteristics are used to describe the taxonomy of actinobacteria into genus and species levels. These are the microscopic morphology of the organism, chemotaxonomy and the molecular data of the organism (Adegboye and Babalola, 2012).

1.2.1 Classification based on microscopic morphology

Classification based on its microscopic morphology is as a result of the presence of mycelia, spore chain morphology, spore chain length and the presence of melanoid pigments. These combined features form the basis of morphological classification of the actinomycetes. Organisms such as *Sporichthya sp*., *Micropolyspora*, *Micromonospora* and *Actinobacteria* are all classified according to their morphology (Adegboye and Babalola, 2012).

1.2.2 Classification based on chemotaxonomy

Chemotaxonomy classification utilises the different chemical components within organisms to group them based on their cellular chemistries (Goodfellow and Minnikin, 1985). Notable among these cellular components are amino acids, lipids, proteins, sugars, menaquinones, muramic acid and base composition of DNA (Williams *et al*., 1983). These classifications can also be based on the information obtained from the whole-organism chemical fingerprinting techniques. *Streptomyces sp*., *Nocardioides sp*., *Frankia sp*. and *Agromyces sp.* all have different cell compositions that classify them into different groups (Goodfellow and Minnikin, 1985).

1.2.3 Classification based on molecular data

The molecular classification method looks at recent advances in genome sequencing that provides molecular taxonomic data good enough to challenge the morphological and chemical classification of actinomycetes. Molecular analysis has been used to re-classify some organisms that were inappropriately placed in certain groups (Zhi *et al*., 2009). New species can be classified if their genetic analysis data, based on sequencing the 16S rRNA gene and DNA-DNA hybridization data, is known (Euzéby, 1997).

1.2.3.1 The genus *Tropheryma*

The genus *Tropheryma*, represented by *T. whipplei* is a good example of a member of actinobacteria placed in this genus as a result of its genetic analysis data. This organism is the causative agent of Whipple's disease, an intestinal malabsorption disease in humans, leading to cachexia (loss of weight, fatigue, weakness and loss of appetite) and death (Raoult *et al*., 2001). *T. whipplei* resides inside intestinal macrophages and circulating monocytes (Raoult *et al*., 2001). Evidence suggests that *T. whipplei* has a host-restricted life cycle due to its small genome and its inability for metabolism (Bentley *et al*., 2003). The organism is reported to survive the effect of phagocytes and can replicate within macrophages by interfering with innate immune activation (Desnues *et al*., 2010).

1.2.3.2 The genus Propionibacterium

Propionibacterium sp. is also classified as an actinobacteria due to the available molecular analysis data. It includes various species of human cutaneous propionibacteria such as *P. acnes, P. avidum, P. granulosum* and *P. innocuum. P. acnes* is present on human skin within sebaceous follicles and survives as a harmless commensal. However,

the organism can be an opportunistic pathogen (Ingham, 1999) as it has been isolated from sites of infection and inflammation in patients suffering from acne, corneal ulcers, synovitis, endocarditis and pulmonary angitis (Csukás *et al*., 2004).

1.2.3.3 The genus Micromonospora

Micromonospora serve as a source of secondary metabolites for medicine (Hirsch and Valdés, 2010). The genus is second only to *Streptomyces* in terms of antibiotic production (Berdy, 2005) and can synthesise approximately 500 different molecules with different properties (Whitman *et al*., 2012). They can also synthesise hydrolytic enzymes which help them degrade organic matter in their habitat.

1.2.3.4 The genus Bifidobacterium

Bifidobacterium are typically health-promoting and have probiotic properties (Lievin *et al*., 2000). Some of the probiotic features include induction of immunoglobulin production, improvement of a food's nutritional value, anti-carcinogenic activity and folic acid synthesis (Bevilacqua *et al*., 2003). *Bifidobacterium* species are also involved in bile salt hydrolase activity, immune modulation and ability to adhere to intestinal epithelium (Lievin *et al*., 2000).

1.2.3.5 The genus *Gardnerella*

Gardnerella vaginalis is associated with bacterial vaginosis, a vaginal discharge that can also occur frequently in the vaginal microbiota of healthy individuals (Kim *et al*., 2009). This disease condition poses a serious risk factor as a sexually transmitted disease. Studies reveal that there is a correlation between *G. vaginalis* and preterm delivery (Menard *et al*., 2010).

1.2.3.6 The genus *Rhodococcus*

Rhodococcus sp. are closely related to the genus *Nocardia*. Some of them are symbionts, while others are pathogens to animals. *R. equi* is the pulmonary pathogen found in young horses and has been observed in HIV-infected humans (Prescott, 1991). A key important feature of this group is the presence of tuberculostearic acid, long chain mycolic acid and menaquinone (Bell *et al*., 1998). They produce very important metabolites such as carotenoids, bio-surfactants and bio-flocculation agents all of which have industrial potential.

1.2.3.7 The genus Streptomyces

Streptomyces species is one of the complex mycelial genera within actinobacteria. They are important in cycling carbon from insoluble organic debris of plants and fungi through the production of hydrolytic exo-enzymes. The genus also has a wide phylogenetic spread, producing divers' bioactive secondary metabolites with great interest in medicine and industry (Hopwood, 2007).

1.2.3.8 The genus Corynebacterium

Several chemotaxonomic studies and 16S rRNA sequence analysis data identified approximately 70 *Corynebacterium species* and are grouped under actinobacteria. One of the intensively studied species, *C. glutamicum*, is widely utilised industrially to produce amino acids, such as L-glutamic acid and L-lysine, for human and animal nutrition (Coco *et al*., 2001). Other sequence analysis data from *C. ulcerans*, *C. kutscheri* and *C. kroppenstedtii* provides a good insight into the genomic architecture of the genus (Rückert *et al*., 2015). *C. diphtheria* is one of the pathogenic members of this genus causing acute

communicable diphtheria disease in humans, characterised by local growth of the organism in the pharynx and the formation of inflammatory pseudomembrane (Hadfield *et al*., 2000). *C. ulcerans* is also identified to mimic *C. diphtheria* by harbouring a diphtheria toxin gene that causes symptoms of diphtheria in humans (Mattos-Guaraldi *et al*., 2008).

1.2.3.9 The genus *Nocardia*

Nocardia bacteria are known to be the causative agent of opportunistic infection and in immunocompromised hosts. Infection by these organisms can be through inhalation or percutaneous inoculation from environmental sources (Abreu *et al*., 2015). It causes disseminated nocardiosis by spreading to the brain, kidneys, joints, bones, soft tissues and eyes of humans and animals. They have also been shown to cause infection during organ and bone marrow transplant, or with long term steroid use, alcoholism, cirrhosis, ulcerative colitis and renal failure (Brown-Elliott *et al*., 2006).

1.2.3.10 The genus Mycobacterium

Mycobacterium, together with *Corynebacterium* and *Nocardia*, form a monophyletic taxon with actinobacteria and are collectively called the CMN group (Embley and Stackebrandt, 1994) or Mycolata (Table 1.1). This group is characterised by an unusual waxy cell envelope containing mycolic acids which makes them both acid fast and alcohol fast. The mycobacterial cell wall however is also made up of various polysaccharide polymers such as arabinogalactan, Lipomannan, lipoarabinomannan and phosphatidyl mannosides (Chatterjee *et al*., 1992).

Table 1.1 Table indicating the origin, pathogenic status and prevalence of the mycolata Group

Organism	Origin	Pathogenic status	Prevalence
Mycobacterium	Believe to have originated about 40, 000 years ago from East Africa. The disease was disseminated and spread between human to human and between humans to animals (Wirth *et al*., 2008).	TB affects the lungs and other parts such as lymph nodes, bones, kidney, brain and even skin. It result to coughing up blood due to perforated lungs (Ernst *et al*., 2012).	Caused 1.3 million deaths among HIV negative people and 300,000 deaths among HIV positive people in 2017. An estimated 10 million people developed TB in 2017. Amongst them are 5.8 million men, 3.2 million women and 1.0 million children (WHO, 2018).
Corynebacterium	Humans are the repository for this organism, but the organism can be isolated in soil, water, blood and human skin. The bacterium is ubiquitous in nature and can be found in mucous membranes and skin of humans. It is predominantly found in temperate regions of the world (Zink *et al.*, 2001).	It causes disease by multiplying and secreting diphtheria toxin in either nasopharyngeal or skin lesions. It can also inhibit protein synthesis in eukaryotic cells. The throat, which is usually the site of infection, become sore and swollen (Holt *et al*., 1994).	There is an estimated 5,000 cases of this disease per year from 2005-2015 (Bernard, 2012).
Nocardia	The organism was first isolated in 1888. The organism can live as a saprophyte in fresh water, salt water, dust and soil, and in decaying faecal matter from animals (Ribeiro *et al*., 2008).	The disease can cause cutaneous infection and severe diseased condition through the central nervous system and pulmonary nervous system (Holt *et al*., 1994).	There has not been any worldwide reported figure on the prevalence of this organism. It is estimated that 1 out of 125,000 people in the United States have the disease, but prevalence of this in Europe is unknown (Lerner, 1996).

In silico analysis of the *Mycobacterium tuberculosis* (*Mtb*) H37Rv genome identified larger gene duplication events (Tekaia *et al*., 1999). These events lead to the ability of the organism to secrete the T-cell antigens, 6-kDa early secretory antigenic target (ESAT-6) and culture filtrate antigen (CFP-10, lhp) through multiple copies of the genes and several other associated genes (Van Pinxteren *et al*., 2000, Sørensen *et al*., 1995). Five gene clusters described as ESAT-6 loci are present in the genome of *Mtb* H37Rv. The clusters

contain CFP-10, ESAT-6 gene families that encode the secreted T-cell antigens lacking detectable secretion signal peptides, genes encoding secreted cell-wall-associated subtilisin-like serine proteases, putative ATP binding cassettes transporters (ABC transporters) ATP-binding proteins and other membrane-associated proteins. These proteins are associated with the membrane and provide the high levels of energy required for the secretion of ESAT-6 and CFP-10 protein families. The proteases may be involved in processing the secreted peptide (van Pittius *et al*., 2001). Twelve gene families have been identified in these five regions. When protein sequences from six of the most conserved gene families present were assessed using phylogenetic analyses, the result indicated that region 4, Rv3884c-3895c, is the ancestral region. This region also has less proteins [only 6 compared to the 12 of region 1 (Rv3866-3883c) and region 2 (Rv3884c-3895c)], and indicated that the absence of proline-glutamic acid (PE) and proline-proline glutamic acid (PPE) genes was suggestive to have been inserted into the other regions after the first duplication. Additional phylogenetic analyses using different methods and protein family data also suggests that subsequent duplications took place in the following order: region 1 (Rv3866-3883c) → 3 (Rv0282-0292) → 2 (Rv3884c-3895c) → 5 (Rv1782-1798). Similar taxonomic ordering of other mycobacteria demonstrated *M. smegmatis* is taxonomically the farthest removed from *Mtb*. The presence of a copy of region 4 and its flanking genes in *C. diphtheriae* strengthens the taxonomic data that implies that the corynebacteria and mycobacteria have a common ancestor. It appears that *C. diphtheriae* diverged from the mycobacteria before the multiple duplications of the ESAT-6 gene cluster, as only one copy of this cluster could be identified in the genome of this organism (van Pittius *et al*., 2001).

Some of the members in this group are obligate pathogens in humans, while some are opportunistic pathogens. *Mtb* is the classical obligate pathogen in humans, while

Mycobacterium africanum is classed as opportunistic pathogen. *M. africanum* is mostly found in Africa which starts with a latent infection, and then progresses to an active disease state especially when the immune system of the host is compromised (Brennan and Nikaido, 1995, Brosch *et al*., 2002, de Jong *et al*., 2005, de Jong *et al*., 2010, Gehre *et al*., 2013, Meyer *et al*., 2008).

Bovine tuberculosis and Johne's disease are tuberculosis-connected diseases in livestock caused by *Mycobacterium bovis* and *Mycobacterium avium subsp. Paratuberculosis*, respectively (Beard *et al*., 2001, Hines *et al*., 1995, Salem *et al*., 2013). Recent research shows that *M. avium subsp*. *paratuberculosis* is associated with Crohn's disease in humans and can also cause inflammatory bowel conditions (Hermon-Taylor, 2009). The problem of treatment associated with mycolata worldwide is not only restricted to *Mtb*. Leprosy caused by *Mycobacterium leprae* was the first bacterial pathogen of man, living within its host as an obligate parasite (Bloom and Godal, 1983, Reibel *et al*., 2015). The World Health Organisation (WHO) states that there were 219,000 new cases of leprosy in Africa and Asia in 2011 (Espinal *et al*., 2001). The WHO planned to eliminate leprosy by 2000. The original plan, set up in 1991, succeeded in reducing leprosy cases to less than 1 case per 10,000 people. This was achieved because of the wide spread use of multi-drug therapy that saw a drastic reduction in the prevalence of leprosy (Lockwood, 2002, Noordeen *et al*., 1992). From 1985 to 2011, leprosy cases were drastically reduced from 5.2 million to 219,000 and there were no outbreaks of drug-resistant strains, as compared to cases of tuberculosis with several reports of drug resistant strains. The drug resistant strains of TB therefore, are the primary cause for the inability to eradicate the disease and require urgent steps to tackle the problem (WHO, 2013).

1.3 Epidemiology of tuberculosis

Tuberculosis (TB) is one of the most prevalent and interesting diseases in the world today. The prevalence of this disease rises to about 10 million cases in 2017 worldwide, where 5.8 million men, 3.2 million women and 1 million children were said to have TB (WHO, 2018). As a result of these high global statistics it is estimated that 1.3 million deaths were recorded among HIV-negative people and an additional 300,000 deaths among HIV-positive individuals in 2017 (WHO, 2018). TB is the leading cause of death from a single curable infectious disease (WHO, 2018). One third of the world's population is latently infected with tuberculosis. Globally, 90% of TB cases were recorded among adults aged 15 years and above, while 9% were people living with HIV among which 72% of them are from Africa. Two third of the 90% of TB infected individuals are from India (27%), China (9%), Indonesia (8%), the Philippines (6%), Pakistan (5%), Nigeria (4%), Bangladesh (4%) and South Africa (3%). These countries and 22 others form WHO's list of 30 high TB burden countries and accounted for 87% of global cases of TB. The WHO European Region accounted for 3% and WHO Region of the Americas accounted for another 3% (WHO, 2018). Different countries experienced different epidemics of TB in 2017. Most high-income countries experienced as low as 10 new cases of TB per 100,000 people in 2017. Whereas, the majority of the high TB burden countries recorded between 150-400 new cases, while an estimated 500 new TB cases being recorded in Mozambique, the Philippines and South Africa (WHO, 2018).

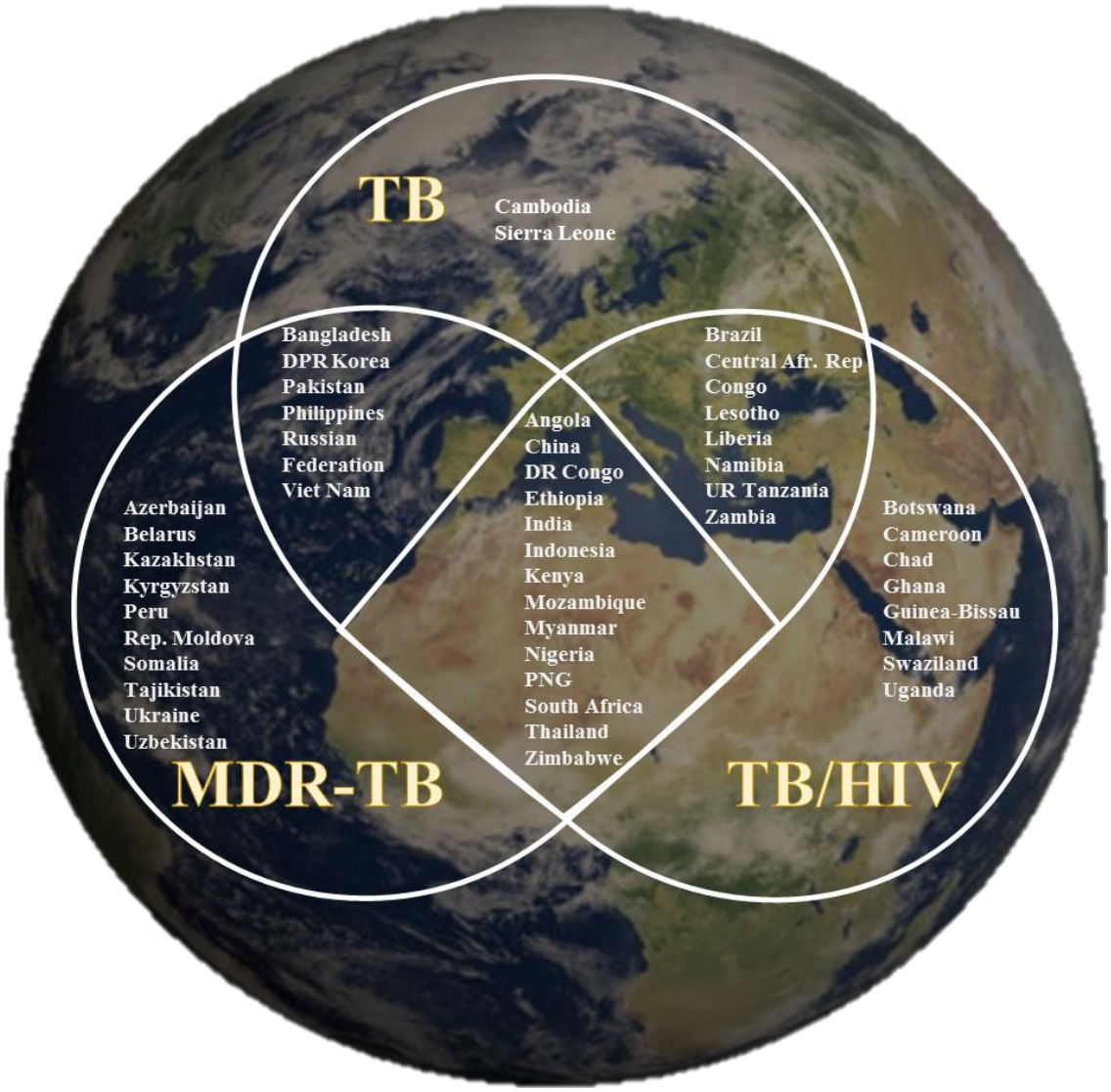

Figure 1.1 **Global cases of TB comprising of 3 lists of TB, MDR-TB and TB/HIV.** 48 countries account for 85-89% of the global burden of TB. A total of 30 countries make up the 'high burden countries' (HBCs) of TB. 14 countries represented by the central diamond in the figure are those found in all 3 lists. Poor economic conditions and sub-standard healthcare facilities is the major cause of TB cases in Eastern Europe countries listed (adapted from WHO Global tuberculosis report 2016).

A compromised immune system by diseases such as HIV, ageing, malnutrition, chemotherapeutic treatments, and diabetic infection are some of the factors contributing to the risk of developing active tuberculosis (WHO, 2013, Nam *et al*., 2013). The wide spread development of tuberculosis disease in Africa is attributed to the HIV epidemic

that has been ravaging the continent since the 1980s (Figure 1.1) (Corbett *et al*., 2003, Dye, 2006).

In Eastern Europe, TB is largely attributed to economic deterioration and sub-standard healthcare facilities, leading to an increase in TB globally since the 1990s (Dye, 2006). Globally, cases of TB are associated with HIV, with one third of active HIV infected patients being co-infected with TB. Also, 13% of new TB cases in 2012 were reported to be HIV positive (WHO, 2013). Most countries with high performance surveillance systems usually have a good proxy TB indicator well enough for TB notification cases. High quality and good access to health care facilities means most TB cases are diagnosed. In many countries that have not met the above criteria an inventory study is used to estimate TB incidences. The inventory studies are sometimes combined with capture-recapture methods to estimate TB incidences only after meeting certain conditions (Ravi and Sunita, 2013). The goal for this surveillance was to be able to determine TB incidences from all countries based on TB notifications. Unfortunately, this is not a simple task to achieve since it involves combined strengthened surveillance, better quantification of under-reporting and universal health coverage. A total of 61 countries completed a TB surveillance checklist in order to provide a direct measure of TB incidence in 2017 (WHO, 2016). The co-morbidity of TB with HIV was highest in the Sub-Saharan African region and exceeded 50% in parts of Southern Africa. The risk of developing TB in the 37 million people living with HIV was 21 times higher than the risk in the rest of the world's population (WHO, 2017).

1.4 Reduction in TB spread through DOTS and End TB Strategy

However, it's not all doom and gloom, there has been a slow but significant decline in the number of TB incidences globally since 2000. The average global decline in TB rate was

1.4% per year from 2000-2016 and 1.9% between 2015 and 2016. To achieve a milestone reduction of TB cases and deaths, WHO through its global TB programme, came up with a strategy to end the global TB epidemic. This strategy, 'End TB strategy' aim to reduce the number of TB deaths to 95% and reduce TB incidence to 90% in 2035. This would ensure no families are facing catastrophic costs due to TB by 2035 (WHO, 2018). This strategy is anchored on four basic principles that involves ensuring government stewardship and accountability with monitoring and evaluation, strong coalition with civil society organisations and communities, protection and promotion of human rights, ethics and equity and the adaptation of the strategy and targets at country level, with global collaboration. Pillars to this strategy include integrated patient-cantered care and prevention and the capability for an early diagnosis of TB, universal drug susceptibility testing and systemic screening of contacts and high-risk groups. It also involves the treatment of all people infected with TB, including drug resistant TB and the need for patient support. Additionally, collaborations of TB/HIV activities and management of co-morbidities are key to end TB. This will go with treatment of individuals with high risk of TB and vaccination against TB. Bold policies and systems put in place by governments and making political commitments by providing resources for TB care and prevention are some of the strategies adopted. Communities, civil society organisations and public and private care providers are actively engaged in the fight against TB. Other determinants of TB such as poverty and bridging the gap on social protection are actively being tackled by various governments. New research and innovations in the area of TB control and optimised implementation and impact are on-going. These combined pillars ensured a decline in TB cases globally. The end TB strategy works hand in hand with the directly observed treatment, short-course (DOTS) strategy of the WHO (WHO, 2018). The DOTS ensure technical, logistical, operational and political angles of the end TB strategy are

observed. This covers areas from detection and diagnosis of TB, provision of adequate healthcare, ensuring government commitment and policy formulations (WHO, 2018).

The European region has the fastest rate of decline, which was at about 4.6% from 2015-2016. There has been a remarkable estimated decline in incidence rate since 2010 in most of the high TB burden countries such as Kenya (6.9%), Lesotho (7%), Zimbabwe (11%), Namibia (6.0%), Ethiopia (6.9%), Tanzania (6.7%), Zambia (4.8%) and the Russian Federation (4.5%) (WHO, 2018).

1.5 Antibiotic resistance in mycobacteria

Mtb ability to persist in host cell by evading the host immune system is an effective means of infection coupled with the organism capacity to become dormant within the host and can reactivate when the host is immuno-compromised makes the organism difficult to treat. An important feature of *Mtb* is the characteristic 3-3 crosslinking of the peptidoglycan (PG) in the mycobacterial cell wall. This forms a highly impermeable wall that surrounds the cell and confers innate resistance to many antibiotics such as the β-lactams (Pisabarro, 1986). Additionally, mycobacteria secrete β-lactamase enzymes that aid in the degradation of β-lactam antibiotics (Kasik, 1965; Kasik and Peacham, 1968; Lavollay *et al.*, 2008). The mechanism of resistance in mycobacteria is not solely dependent on the production of β-lactamase enzymes, even though it is an effective system (Jarlier *et al.*, 1991). The complex structure of the mycobacterial cell wall impermeable barrier accounts for the organism's resistance to antibiotics and other stress factors caused by the host immune system. Comparatively, the mycobacterial cell envelope is 100 times less permeable than other organisms, so it can activate specific physiological states and genes (Nguyen and Thompson, 2006). A transcriptional

regulatory protein, such as whiB1-7, plays a major role in this process. The production of this protein increases in response to antibiotics and other stresses caused by the host immune system. The response mechanisms includes antibiotic inactivation and the production of drug export channels (Burian *et al.*, 2012). *Mtb* resistance to macrolides, such as clarithromycin, that inhibits protein synthesis, is as a result of the production of the 16S RNA dimethyl transferase (ksgA), even though the entire mechanism is not yet clear (Phunpruch *et al.*, 2013).

Many bacteria escape the effect of drugs or antibiotics by activating their drug export mechanism that serves as efflux pumps (Briken *et al*., 2004). Most mycobacterial genomes including *Mtb* have all the classes of major drug efflux pumps. These include the facilitator superfamily and adenosine triphosphate (ATP) binding cassette family (Briken *et al.*, 2004, Saier *et al.*, 1998). These efflux pumps have homologues in *M. smegmatis* and *M. bovis* that gives them resistance to multiple drugs like chloramphenicol, acriflavine, rifampicin and isoniazid (De Rossi *et al.*, 1998; Briken *et al.*, 2004, Paulsen *et al.*, 1996, Sander *et al.*, 2000). Multi-drug and toxic compound extrusion family efflux pumps have been discovered in mycobacteria and account for their resistance against chemicals that damage DNA and some antibiotics (Mishra and Daniels, 2013). Mycobacteria induces several of these efflux pumps as a first step towards resistance prior to chromosomal mutation (Schmalstieg *et al.*, 2012).

1.6 Pathway of TB infection and pathogenesis

Tuberculosis disease is caused by the inhalation of tubercle particles (Figure 1.2).

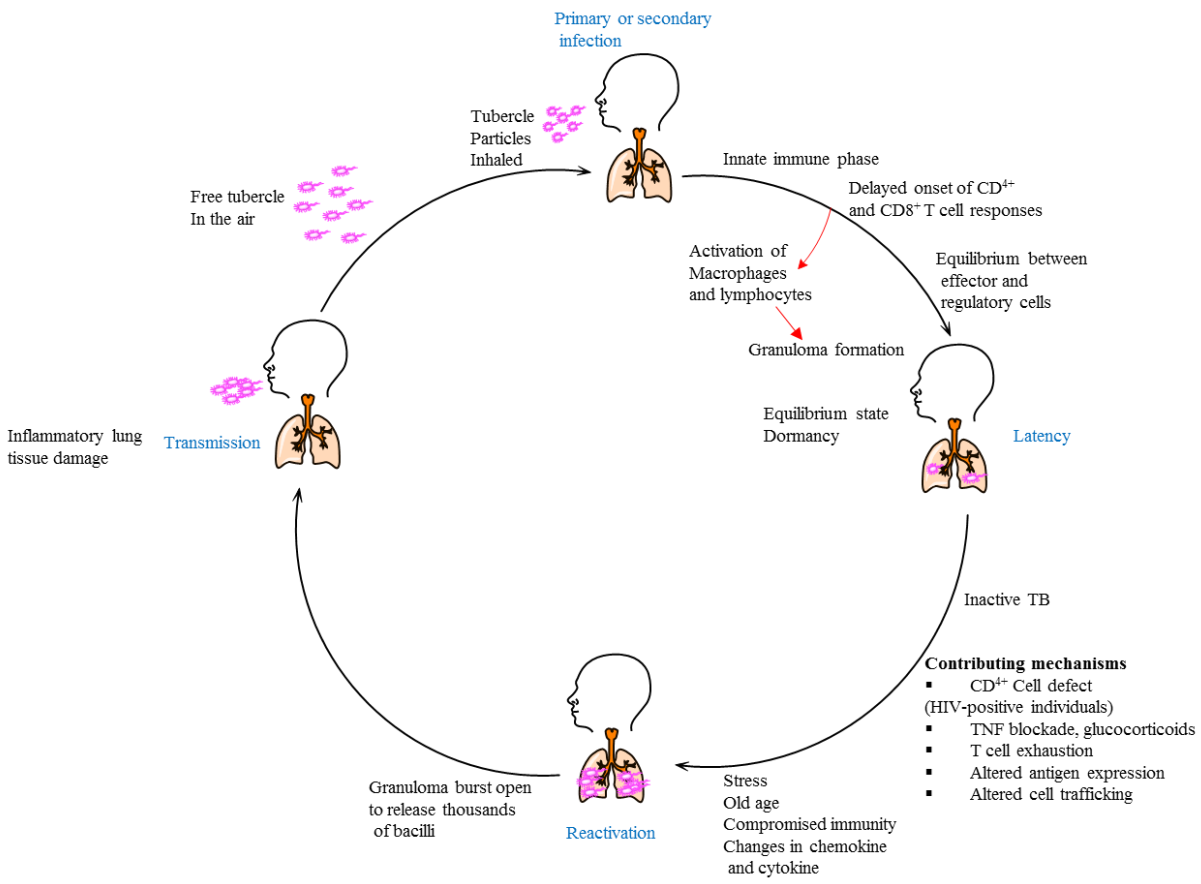

Figure 1.2 **Life cycle of TB infection.** TB disease begin when free tubercle particles are inhaled by a healthy individual. *Mtb* infects the lungs where granuloma are formed to prevent the spread of the particles. Activation of TB results in break-away of active TB cells which then spread into the lungs. An infected individual coughs out blood containing TB particles (Adapted from Ernst, 2012).

The infection occurs in three major stages. The first stage involves the inhalation of aerosol droplets containing the *Mtb* from an infected individual with TB of the lungs (pulmonary TB). The infected individual coughs, sneezes or spits and spreads the tubercle particles into the air. The expelled droplets can remain into the atmosphere for several hours because of their small nature. A single bacterium is enough to cause infection (Russel *et al*., 2010). The *Mtb* in the air are inhaled by a healthy individual and enters the lungs and come in contact with alveolar macrophages (AMs) and dendritic cells (DCs) (Cooper, 2009). It is expected that the AM ingests and kill the bacteria, but the

bactericidal activity of AM against the tubercle is still not clear (Sasindran and Torrelles, 2011). Restricting the spread of the disease at the establishment of disease depends on the genetics of the host individual and the strain of *Mtb* inhaled (Russel *et al*., 2010). The bacterium then invade the surrounding epithelial layers and multiply, leading to mild inflammations (Russel *et al*., 2010). In response to this, mononuclear cells from neighbouring blood vessels are recruited, providing fresh host cells needed by the bacterial population to expand. *Mtb* evolve mechanisms to evade host immune responses within the lungs, despite the presence of AM believed to be barriers against pathogens. They do this by initiating anti-inflammatory response, stopping the production of reactive oxygen intermediates (ROIs) and reactive nitrogen intermediates (RNIs) and acidification reduction of *Mtb* containing phagosome (Fenton *et al*., 2005, Flynn and Chan, 2001).

The second stage of *Mtb* infection involve cell-mediated immunity and granuloma formation. The fresh host cells developed as a result of inflammations, serves as building blocks for granuloma formation. The surviving *Mtb* bacilli multiply and destroy the AM, thereby attracting blood monocytes and inflammatory cells. Matured monocytes become antigens-presenting AMs and DCs and try to ingest and kill the bacteria, but this action will not be effective and eventually lead to *Mtb* growth under limited tissue damage. Antigens presenting DCs move to the lymph nodes after just 6-8 weeks of infection. T lymphocytes are then activated and migrate to the site of infection where they proliferate and form an early stage granuloma. At this stage, macrophages are activated and function as effective killers of intracellular *Mtb* (Ulrichs and Kaufmann, 2006). Continuous activation of T cells results in granuloma formation that will lead to a persistent infection stage (latency) with limited growth and spread of the bacteria into other tissues. Approximately, 90% of infected individuals at this stage remain asymptomatic, but may have surviving *Mtb* within their AMs (Russel *et al*., 2010).

In the third and final stage, latent and controlled *Mtb* infection become reactivated. Reactivation can be caused by physical or emotional stress or by weakening the patient's immune system, either through malnutrition or HIV infection. It is also as a result of the failure of the body to develop and maintain immune signals. These scenarios cause the disruption of the granuloma structure, leading to development of cavities within the lungs. This spills thousands of infectious bacilli into the airways. (Kaplan *et al*., 2003, Dheda *et al.*, 2005, Ulrichs and Kaufmann, 2006, Russell, 2007).

People infected with *Mtb* stays infected for years, and sometimes for life. Approximately 90% of those infected with *Mtb* do not develop the disease, and about 10% of those infected develop the disease.

Individuals become susceptible to TB as a result of genetic causes such as mutations in specific host C-type lectins, cytokines, chemokines and their specific receptors that plays a vital role in disrupting important signalling pathways leading to immune response against *Mtb*. Compromised immunity due to co-infection with diseases such as HIV is a major environmental or exogenous cause of TB susceptibility (Geldmacher *et al*., 2010). Reactivation of *Mtb* can also be as a result of stress or old age, largely due to changes in cytokine/chemokine networks (Turner, 2011). Reactivation can also be as a result of exogenous reinfection with another strain of *Mtb* (Sonnenberg *et al*., 2001, Behr, 2004).

1.6.1 Granuloma formation in TB infected individuals

Formation of granuloma within the lungs is key to *Mtb* infection. Granuloma infection can be advantageous to both the host and the bacterium. To the host, it serves as a barrier that restricts the spread of the organism, while to the bacterium, it provides a safe microenvironment so it can establish latency. Granuloma is formed when there is a

temporary influx of neutrophils to the site of infection, after which macrophages and lymphocytes are activated. A well-developed granuloma is made up of infected AMs and epithelioid cells, forming a necrotic central core, surrounded by $CD4^+$ and $CD8^+$ T-cell layers and some activated macrophages. This collection forms a dense cellular wall that prevents the spread of the *Mtb* and, at the same time, provides a safe microenvironment for the organism (Saunders and Cooper, 2000). Immunocompetent individuals develop small and compact granulomas with many interferon gamma (IFN-γ) CD4 T-cells, while immune-deficient individuals develop large granulomas rich in activated macrophages and few surrounding lymphocytes (Ultrichs *et al*., 2005).

The interaction of AMs and DCs with *Mtb* leads to the release of inflammatory cytokines such as tumour necrosis factor-α (TNF-α), interleukin (IL)-12 and IL-23. These are released alongside other chemokines such as C-C motif ligand 2 (CCL2), CCL5 and C-X-C motif ligand 8 (CXCL8). IL-12 and IL-23 production causes type 1 T helper (Th1) cell response which is important in granuloma formation. The inflammatory event is regulated by IFN-γ and IL-2 activated T-cell production. Cytokines that aid inflammation tend to regulate the activities of other cytokines and chemokines and this help in organising and maintaining a functional granuloma. Production of TNF, IFN-γ, IL-12, RNIs and ROIs are induced when *Mtb* infects macrophages and they are all considered as important regulatory factors in granuloma structure formation and maintenance.

1.7 Tuberculosis infection in HIV infected individuals

The development of TB primary disease is linked to a host who has recently been infected, the reactivation of latent infection, or an exogenous reinfection. Infection can occur as a result of the host organism inhaling tubercle bacilli particles of <5 µm (Edwards and

Kirkpatrick, 1986). Inhalation of the bacilli particle initiates pulmonary alveoli infection where it is phagocytosed by alveolar macrophages, which serves as the first line of defence against *Mtb*. Some of the invading particles are destroyed by the macrophages, whilst others multiply and spread to other parts of the body hematogenously. In HIV infected individuals, defective macrophages function in response to TB infection, which in part increase susceptibility to TB (Patel *et al*., 2009). However, there is no clear evidence to suggest that HIV-positive individuals have a higher likelihood of acquiring TB infection than HIV-negative individuals, even when exposed at the same degree (Whalen *et al*., 2011, Meltzer *et al*., 1990).

Once infection does occur, however, the risk of rapid progression is much greater among persons with HIV infection, because HIV impairs the host's ability to contain new TB infection. Immunocompetent individuals infected with *Mtb* have approximately a 10% lifetime risk of developing TB (Horsburgh Jr *et al*., 2000) with half of the risk occurring in the first 1-2 years after infection. In contrast, HIV-infected individuals with latent TB are approximately 20-30 times more likely to develop TB disease than those who are HIV uninfected, at a rate of 8-10% per year (Figure 1.3) (WHO, 2018).

HIV coinfection also increases the risk of progression of recently acquired infection to active disease (Whalen *et al*., 2011, Meltzer *et al*., 1990). In several outbreak settings, 35-40% of HIV-infected patients exposed to TB in health care or residential settings developed active TB disease within 60-100 days of exposure (Daley *et al*., 1992, Zachariah *et al*., 2011, Lin *et al*., 2010). Infection with *Mtb* in an immunocompetent person is thought to confer significant protective immunity against exogenous reinfection (Horsburgh *et al*., 2000).

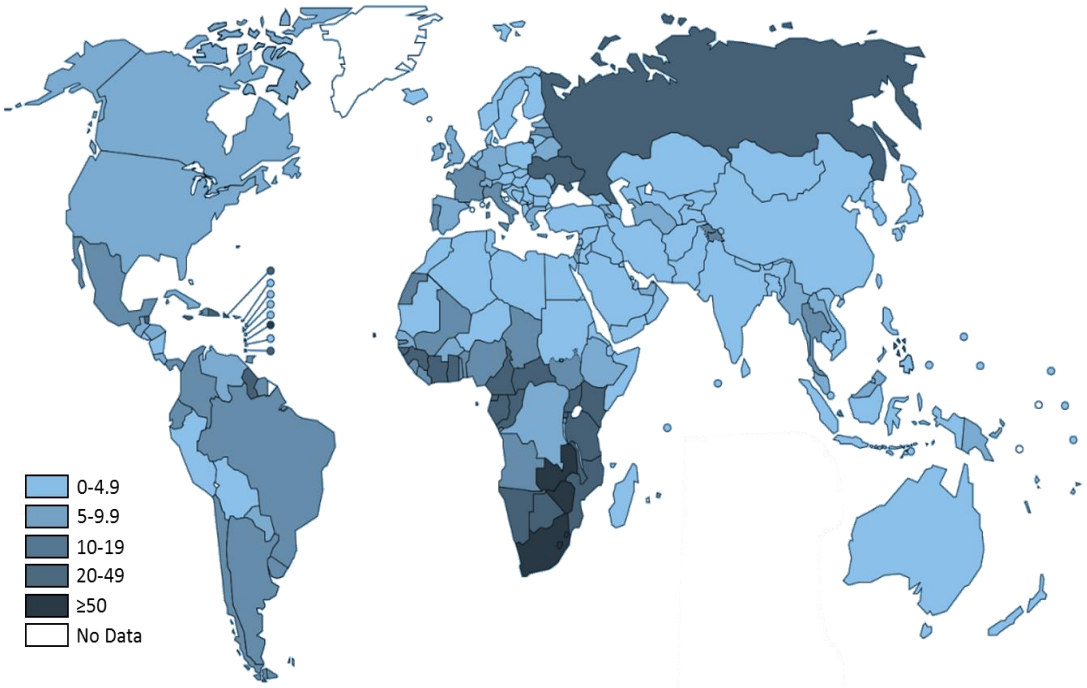

Figure 1.3 **Global burden of TB with HIV comorbidity**. HIV prevalence in new and relapse TB cases (%) Both TB and HIV suppresses the immune system and each synergistically makes the other worse. There has been a double increase in new cases of TB in countries with high HIV prevalence in the past 15 years (adapted from WHO Global tuberculosis report 2018)

However, reinfection has been reported in both HIV-seronegative (Shafer *et al*., 1995, Nardell *et al*., 1986) and HIV-seropositive individuals (Osset *et al*., 1995, Horn *et al*., 1994, Hawken *et al*., 1993, Small *et al*., 1993, Godfrey-Faussett and Stoker, 1992) although its incidence is not known. DNA fingerprinting on paired isolates of *Mtb* from 17 patients who repeatedly had positive cultures at a single hospital in New York City found 4 patients to have acquired a new, drug-resistant strain of *Mtb* through exogenous reinfection, probably as a result of nosocomial transmission (Small *et al*., 1993).

1.8 Drug Resistant TB

A major global threat to the eradication of TB has been the emergence of drug resistant strains of the organism. There are three different categories of these strains which are also used for global surveillance and treatment. First, is multi-drug resistant TB (MDR-TB), which is resistant to both rifampicin (RIF) and isoniazid (INH), which are the two most effective anti-TB drugs. There is also the RIF resistant TB (RR-TB) which is resistant to RIF but susceptible to INH. The extensively drug resistant TB (XDR-TB) is MDR-TB, plus resistance to at least one of the most important drugs in the MDR-TB regimen (WHO, 2017). New cases of MDR/RR previously treated cases of TB in 2016 alone was estimated to be at 4.1% globally. In the same year, there was an estimated 600,000 incident cases of MDR/RR-TB and MDR-TB accounted for 82% of the drug resistant cases. China, India and the Russian Federation had the largest number of MDR/RR-TB cases (47%). An estimated 240,000 deaths were recorded in 2016 from MDR/RR-TB alone (WHO, 2017).

1.9 Tuberculosis treatment

Successful treatment for drug-sensitive TB generally requires 6 months of therapy. The first 2 months of treatment is often referred to as the intensive phase, and typically entails the use of 4 drugs; RIF, INH, pyrazinamide, and ethambutol, followed by 4 months (called the continuation phase) with RIF and INH alone. Treatment duration is extended to 9 months for patients with cavitary disease at baseline, those with a positive culture after 2 months of treatment, and those who did not receive pyrazinamide during the first 2 months (Blumberg *et al*., 2003). Patients with evidence of drug resistance require a modified regimen and, often, a more-lengthy course of treatment.

Treatment for MDR-TB should be done for at least two years using second-line drugs that have severe side effects, such as fever, hepatotoxicity, dermatitis, nausea and nephrotoxicity (Nathanson *et al.*, 2004). Tuberculosis strains resistant to INH, RIF, Fluoroquinolones and any of the second line drugs such as capreomycin, amikacin or kanamycin, makes TB treatment more difficult and is termed extensive drug resistant TB (XDR-TB) (Flor de Lima and Tavares, 2014, Gandhi *et al*., 2006). The totally drug resistant strains of TB (TDR-TB) has a total resistance to drugs and all other forms of current treatment (Cegielski, 2010; Klopper *et al.*, 2013, Shah *et al.*, 2007, Velayati *et al.*, 2009).

The 2010 meta-analysis examined the efficacy of daily versus thrice-weekly dosing of TB medications and found that, in a pooled analysis, daily dosing during the continuation phase of TB treatment was associated with improved TB outcomes (Khan *et al*., 2010). The WHO currently recommends daily administration of TB treatment at least for the intensive phase of therapy in persons with HIV co-infection (WHO, 2009).

An effective method of the use of the Direct Observation Therapy, short course (DOTS) was designed in 1998 to include the treatment of TB drug-resistant strains using the DOTS-plus strategy. Eradication of tuberculosis globally is unrealistic within this century, since more drug resistant strains keep emerging, with an increase in the cost of treatment that requires about US 2.3 billion dollars yearly for research and treatment (WHO, 2013).

The United Nations Millennium Development Goals (UNMDGs) set a target in 2000 with the aim of stopping the spread and reversing the incidence of diseases, such as malaria and TB by 2015 (Dye, 2000). The World Health Organisation (WHO) founded the Stop TB partnership in 2001, setting a target of reducing the global incidence of TB disease to

half by 2015, of the 1990 levels. The organisation also targets the elimination of the disease as a threat to global public health, with an incidence of less than 1 per million by 2050 (Figueroa-Munoz and Ramon-Pardo, 2008). The spread of TB has been gradually decreasing since the 1990's, with a 37% decrease observed between 1990-2012 and with a 45% decrease in mortality rate in the same period. Reduction in TB prevalence is as a result of DOTS strategy, and the commitment of the various governments towards TB control (WHO, 2009).

Today, TB treatment can be very expensive due to the drug resistant nature of emerging strains. It costs 200-fold higher to treat MDR-TB, for example, than treating drug susceptible strains, and about 10-fold higher for the cost of associated care (WHO, 2009).

Currently, the most effective vaccine against TB is the attenuated *M. bovis* Bacillus Calmette Guerin (BCG) vaccine. The vaccine is effective against *Mtb* infection in children, which results in TB meningitis and has about 50% efficiency. Despite its effectiveness against TB in children, it is not effective in adults, especially in the case of adult pulmonary TB, which is the common TB infection and has about 10% efficacy overall (Barreto *et al.*, 2006; Rodrigues *et al.*, 1993). Although, the low efficacy of this vaccine against adult pulmonary TB infection can cause a significant protection against MDR-TB strains, there is an urgent need for novel TB vaccines to replace or supplement the current BCG vaccine that has been in existence since the 1920s (Kritski *et al.*, 1996). The use of the current BCG vaccine could be cost effective, if there were a re-vaccination with the BCG vaccine, since it can be effective for about 10 years and can avert about 17% of cases of pulmonary TB (Dye, 2013; Rodrigues *et al.*, 2011).

Recent research into vaccine production against TB focuses on trying to identify new potential vaccine antigens from active TB, antigens against latent TB, inducible CD8+T

cells antigens and substances that stimulate vaccines causing immunity against TB (Cayabyab *et al.*, 2012). A number of newly developed vaccines are currently under clinical trials with the aim to supplement or replace the current BCG vaccine including *rBCG30, Ad5Ag85A* and *AERAS-402* (Cayabyab *et al.*, 2012). These vaccines help to increase the level of secretion of Antigen 85, a protein complex that is highly immunogenic, by *Mtb* and *M. bovis* BCG which confer resistance in animals (Hoft *et al.*, 2008, Horwitz *et al.*, 1995, Horwitz *et al.*, 2000, McShane *et al.*, 2004, Wang *et al.*, 2004). TB specific CD8+T cells increased for about 50-fold after a re-vaccination with AERAS-402. This is the highest response shown to any previously used human TB vaccine on trial (Hoft *et al*., 2012).

1.10 Cell wall structure of mycolata

The class actinobacteria contain the mycolata, which are Gram-positive bacteria, yet they do not retain the crystal violet stain during Gram-staining. Empirically therefore, they do not fit into this category of grouping. However, they are classified as Gram-positive because they lack a classical outer membrane similar to that found in Gram-negative bacteria (Fu and Fu-Liu, 2002). A waxy outer layer rich in mycolic acids found in all mycolata repels the crystal violet and resists decolourisation with acid alcohol during Ziel-Neelsen staining (Yamada *et al.*, 2012). Using the differential stain carbol fuchsin in Ziel-Neelsen staining, the acid-fast cells stain red due to its affinity to mycolic acids. This is contrary to the blue non acid-fast cells counter stained with methylene blue. Therefore the mycolata can be classed as atypical diderm bacteria (Sutcliffe, 2010).

1.10.1 Mycolyl-Arabinogalactan-Peptidoglycan (mAGP) Complex

Bacteria of the mycolata have an outer pseudo-membrane responsible for the acid-fast nature, phagosome-lysosome fusion prevention and exhibition of cytokine-mediated host response (Meena, 2010, Deb *et al.*, 2009, Glickman and Jacobs, 2001). The inner layer of this outer membrane is made up of a peptidoglycan (PG), arabinogalactan (AG) and mycolic acids collectively known as the mycolyl-arabinogalactan-peptidoglycan (mAGP) core (Figure 1.4). The PG layer is similar to other Gram-positive bacteria with alternating residues of N-acetylglucosamine with muramic acid residues. A fundamental difference between the PG of mycobacteria and their close relatives is that the muramic acid residues are modified by glycolation and acetylation (Mahapatra *et al*., 2005, Raymond *et al.*, 2005, Petit *et al*., 1969).

Another key difference is the characteristic 3-3 cross-linkages in the pentapeptide aminoacyl crosslinks, which differentiates it from the 3-4 cross-linkages of other bacteria (Kana and Mizrahi, 2010, Vandal *et al*., 2009, Lavollay *et al*., 2008).

AG is a polysaccharide that is made up of D-arabinofuranosyl (D-Ara*f*) and D-galactofuranosyl (D-Gal*f*) residues. AG is linked to a PG layer through the α-L-Rhap (1→3)-D-GlcNAc-(1→p) disaccharide bridge between the galactan domain and the C-6 position of the N-glycolylmuramic acid (MurNGly) residue of the PG (Dover *et al*., 2004, Puech *et al*., 2001, Daffe *et al*., 1990). There are approximately 30 β-D-Gal*f* residues arranged in a linear structure with alternating β1-5 and β1-6 linkages in the galactan domain. The three arabinan chains are connected to the galactan chains at the reducing end and are made up of α-D-Ara*f* residues with branching introduced by α(1→3)-Ara*f* residues (Alderwick *et al*., 2011, Birch *et al*., 2008). The inner layer of the mycobacterial cell envelope is complete by the esterification of the AG molecule via the hexa-arabino

furanoside motif (McNeil *et al*., 1994, Wolucka *et al*., 1994). The intercalating layers of the lipids such as the di-acyl trehalose (DAT), penta-acyl trehalose (PAT) and the glycosylated mycolic acids trehalose monomycolate (TMM) and TDM all complete the outer layer of the cell envelope (Yamada et al., 2012).

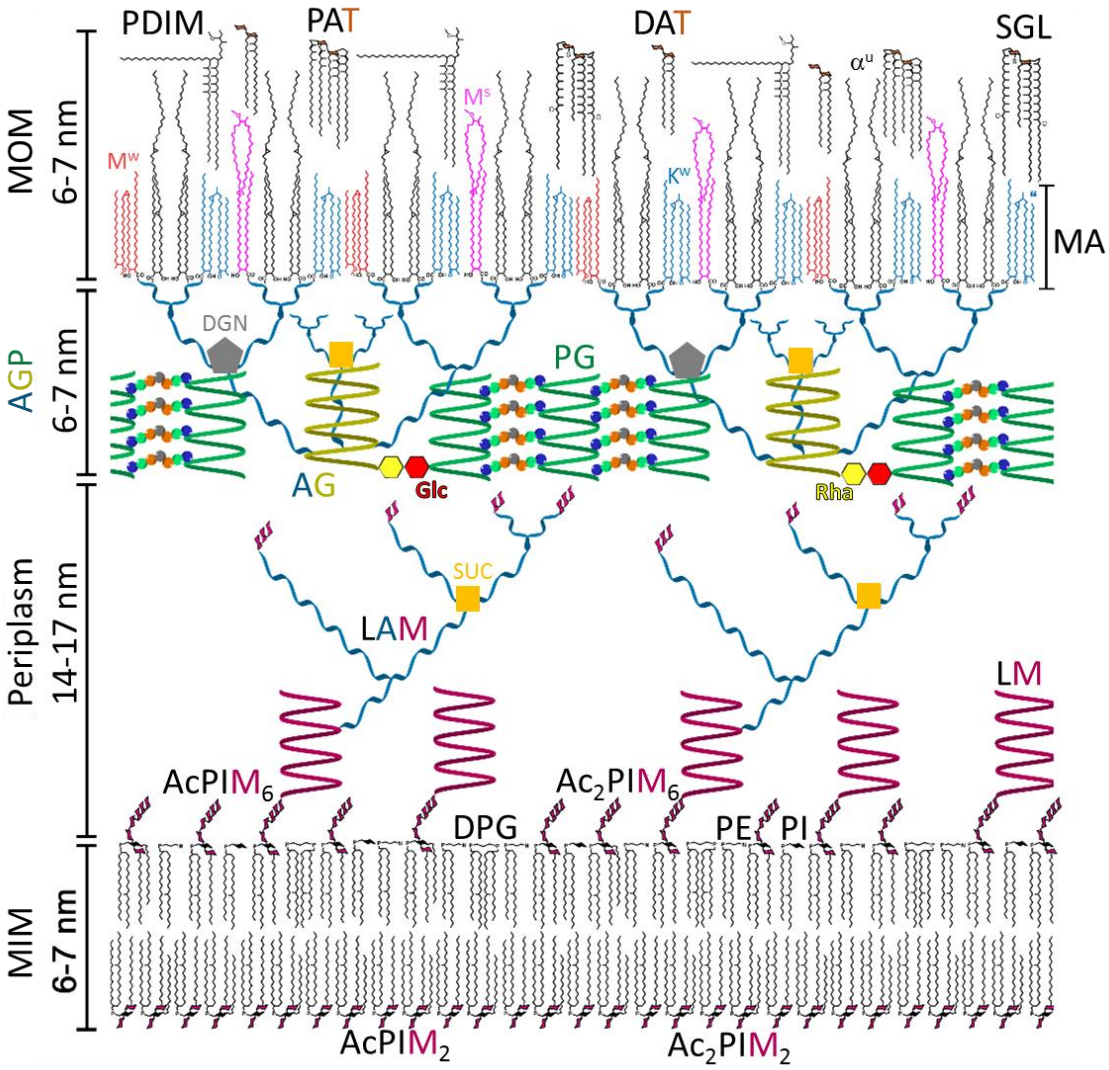

Figure 1.4 **Diagrammatic representation of the cell envelope of *M. tuberculosis*.** Mycobacterial outer membrane, MOM; Mycobacterial inner membrane, MIM; Arabinogalactan-peptidoglycan, AGP. Dimensions of all components are drawn to fit within the spatial constraints sanctioned by cryo-electron microscopy (Hoffmann *et al*., 2008; Zuber *et al*., 2008). Mycolic acid, MA, folds in the MOM are labelled "α^u" for α-mycolate for fully extended "eU" shape, Ketomycolate, K^w methoxymycolate, M^w folded in the "W" configuration. Methoxymycolate, M^s for semi-folded "sZ" configuration. Lipomannan, LM; Lipoarabinomannan, LAM; Arabinan and galactan of arabinogalactan, AG; Peptidoglycan, PG; Penta-acyl trehalose, PAT; Diacyl trehalose, DAT; Sulfated trehalose glycolipids, SGL; Phthiocerol dimycocerosate, PDIM; D-Galactoseamine, DGN; Succinyl, SUC; diphosphatidylglycerol, DPG; phosphatidylethanolamine, PE; phosphatidyl-inositol, PI; mono-acyl phosphatidylinositol dimannoside, $AcPIM_2$; diacyl phosphatidylinositol dimannoside, Ac_2PIM_2; mono-acyl phosphatidyl-inositol hexamannoside, $AcPIM_6$; diacyl phosphatidylinositol hexamannoside, Ac_2PIM_6. Contains a phosphodiester bonds to C-1 of GlcNAc-1-P (Glc), which, in turn, is (1→3) linked to L-rhamnose (Rha) residue providing the "linker unit" between the galactan of AG and PG (Adapted from Minnikin *et al*., 2015)

1.10.2 Mycolic acids as components of mycolata cell membranes

The mycolata all have mycolic acids in their outer membrane which are long chain α-alkyl β-hydroxy branched fatty acids that make up about 40% of the total dry mass of the cell (Figure 1.5) (Kowalski *et al*., 2012, Davidson *et al*., 1982). These structures form a complete monolayer that surrounds the cell (Minnikin *et al*., 2002). In mycobacteria the mycolic acids are about 60-90 carbons in length, which is much longer than the mycolic acids length in other members of the mycolata, such as *Corybacterium sp* and *Rhodococcus sp,* with a carbon length of 22-38 and 28-54 carbons, respectively (Sutcliffe, 2010). Some members of the group also have simple mycolic acids with lower functions as compared to the mycolic acids isolated from mycobacteria with a higher degree of functionality (Yang *et al*., 2012). In terms of proportions, mycobacteria has a much higher content of mycolic acids compared to other cell wall components, while in other members of the mycolata, the mycolic acid content is not in abundance and do not form a complete layer surrounding the cell (Puech *et al.*, 2001). The mycolic acids are instead found bound to certain points to the mAGP core (Dover *et al*., 2004, Barry *et al*., 1998).

The general formula for mycolic acids in mycobacteria is made up of an α-alkyl chain of 20-26 carbons and a functionalised mero-mycolate chain of up to 70 carbon atoms depending on the species in question (Figure 1.5) (Verschoor *et al*., 2012, Rezwan *et al*., 2007, Faller *et al*., 2004). There are about three major classes of mycolic acids described in *Mtb* with several others identified among the mycolata (Marrakchi *et al*., 2014). In *Mtb* the mycolic acid is modified at two sites within the mero-mycolate chain at the proximal and distal positions (Marrakchi *et al*., 2014, Barry *et al*., 1998). Many sub-classes are found within the α-, keto- and methoxy- mycolic acids. For instance, there are the α1 and α2 sub-classes within the α-mycolic acids which are functionalised by two *cis*-

cyclopropane rings or one *cis*-cyclopropane ring and one *cis*-double bond. The methoxy-mycolic acid and keto-mycolic acid have also been identified to have six sub-classes and five sub-classes of mycolic acids, respectively (Marrakchi *et al*., 2014)

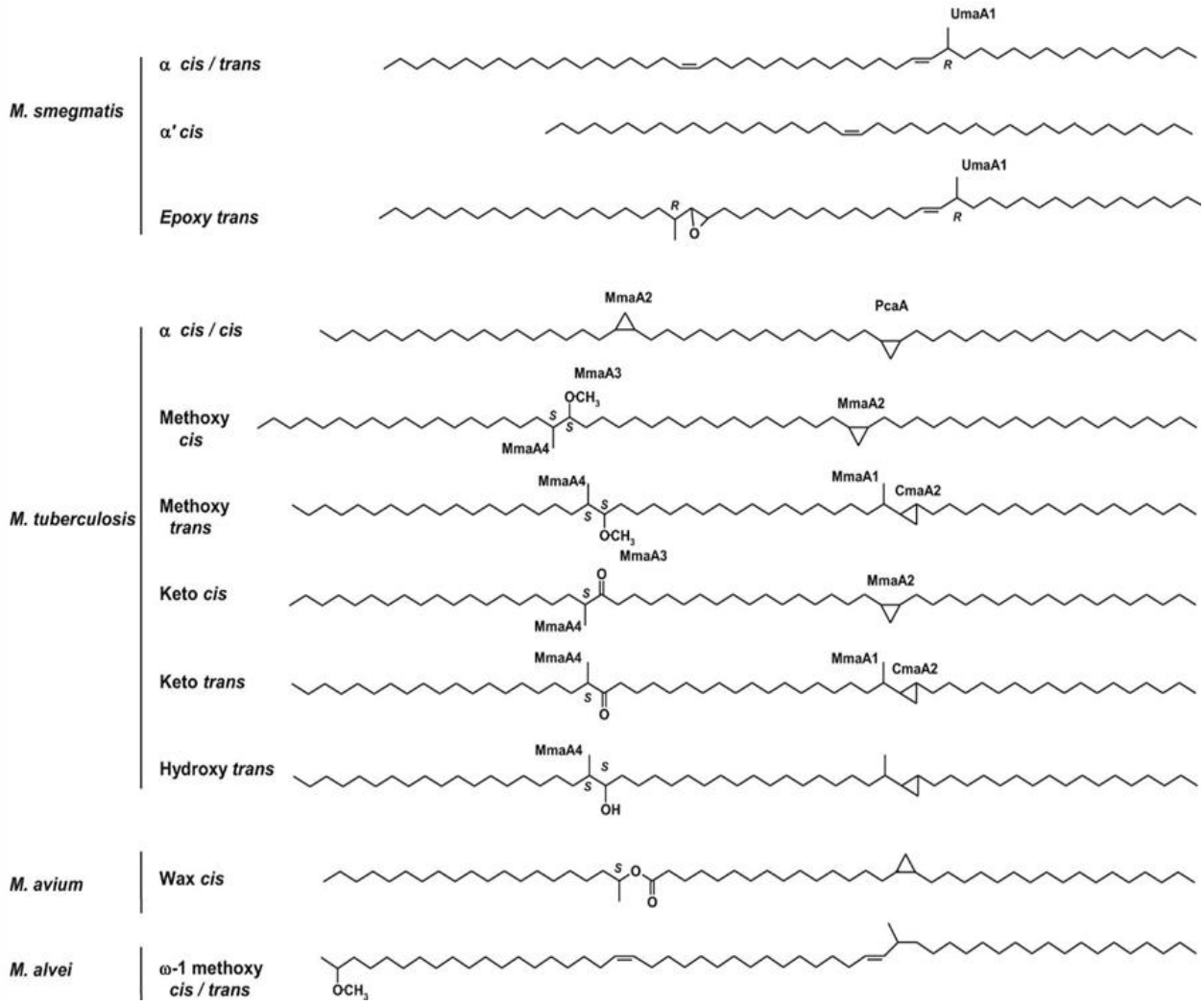

Figure 1.5 **Mycolic acid structures in *Mycobacterium* species mero-chains.** The proximal configuration of double bonds and cyclopropanes is either *cis* or *trans* (with an adjacent methyl branch). The stereochemistry of the asymmetric carbon atoms in the mero-chain is noted (S or R), i.e., carbon bearing methyl, methoxyl, or hydroxyl groups (adapted from Marrakchi et al., 2014)

The α-mycolic acid is present in nearly all mycobacterial species, representing 70% of all mycolic acids in the cell wall, making them the most structurally widespread. The

presence of α-mycolic acid allows pathogenic strains to persist in their hosts by tolerating oxidative conditions better. This special attribute is due to the α-mycolic acid functionalised by *cis*-cyclopropane rings (Yuan *et al*., 1998, Yuan *et al*., 1995). The remaining mycolic acids in mycobacterial species makes up the keto- and methoxy-mycolic acids which is about 10-15%. The mero-mycolate chains are functionalised by cyclopropanation of their proximal position. This occurs either through *cis*- or *trans*-configurations resulting in persistence and virulence of pathogenic mycobacteria. Survival and virulence in mycobacteria is largely dependent on the mycolic acid content (Barkan *et al*., 2012, Dubnau *et al*., 2000, Glickman *et al*., 2000). The presence of mycolic acid in other bacteria in the group mycolata has been shown to be primarily for growth (Gebhardt *et al*., 2007). Therefore, the mycolic acid portion of the cell envelope is of great interest to scientists and has become a target for research.

1.10.3 Additional cell wall components

The cell wall of mycolata have additional components that further complicate the structure and makes permeability difficult. These structures are part of the cell envelope and exposed on the bacterial surface. Some of these components are potential virulent factors shown to inhibit macrophage antimicrobial activity (Vergne and Daffé, 1998). This is posible because pathogenic mycobcteria infect and lives within their hosts, making them facultative intracellular parasites. The components, that differ in sruture to mammalian cell membrane components interact with the host membranes to derive their biologic function. The additional cell wall components of mycobacteria are made up of lipoarabinomannan, lipomannan, Phosphatidylinositol mannosides, and these have been shown to affect the physical and functional properties of the host membranes (Vergne and Daffé, 1998).

1.10.3.1 Lipoarabinomannan, Lipomannan, Phosphatidylinositol mannosides

Other additional virulence associated cell wall components of pathogenic mycolata include lipoarabinomannan (LAM), lipomannan (LM), phosphatidylinositol mannosides (PIM) (Stoop *et al*., 2013, Kothari *et al*., 2012, Briken *et al*., 2004, Vergne and Daffé, 1998). Within the *Mtb* cell envelope, there are the PIMs between two and six mannose residues. PIM_4 mannan chains are extended in the production of LM and LAM (Figure 1.6) (Patterson *et al*., 2003, Kordulakova *et al*., 2002, Gilleron *et al*., 2000, Jackson *et al*., 2000, Chatterjee and Khoo, 1998). LAM has been shown to prevent macrophage activation during infection and has the ability to inhibit T-cells sequestering many mycolata enabling host immune system evasion (Ray *et al*., 2013, Schroeder *et al*., 2002, Gilleron *et al*., 2000). LAM is attached to the plasma membrane through the PI portion, but it is not clear whether it is attached outside the cellular membrane or within (Verbelen *et al*., 2009, Chatterjee, 1997). A combination of PIM, LM and mAGP core causes thrombolytic complications during infection leading to intravascular and deep vein thrombosis through tissue factor production in macrophages (Kothari *et al*., 2012). Therefore these molecules play a key role in supressing the host immune system and for active growth of pathogenic mycobacterial species (Fukuda *et al*., 2013, Jackson et al., 2000).

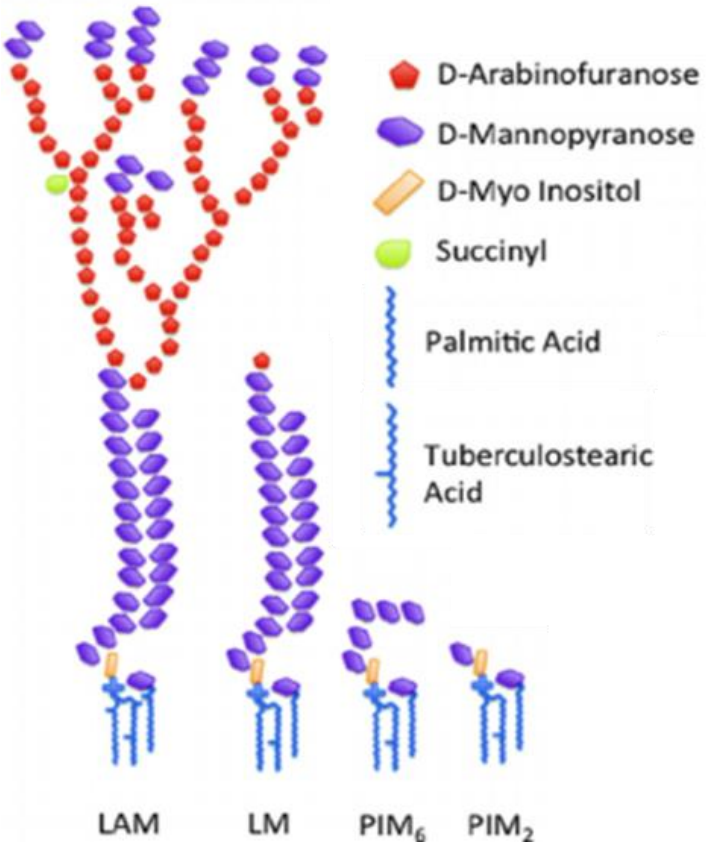

Figure 1.6 Schematic of proposed structures of LAM, LM and PIMs of *M. tuberculosis* (Adapted from Jackson, 2014).

1.10.3.2 Glycosylated mycolic acid

Trehalose monomycolate (TMM) and trehalose dimycolate (TDM) are found as a free mycolate glycolipids and together form a part of the mycolic acid layer that surrounds the bacterium by intercalating with the mycolic acids tethered to the mAGP core. They make up 6% of the total lipid content in *Mtb* (Figure 1.7) (Rath *et al*., 2013, Barry *et al*., 1998). The presence of cord-like structures in the cell surface of virulence strains of mycobacteria characterises the presence of TDM (Middlebrook *et al*., 1947). The TDM is often referred to as cord factor, although the structure is not clearly seen. It is made up of a 6,6-dimycolate of α, α-D-trehalose and small amounts can cause acute toxicity in mice. Its toxic effect is as a result of a disruption caused by the mitochondrial respiratory

chain and oxidative phosphorylation pathways when the NADase activity is stimulated (Saitoh *et al*., 2012, Brennan, 2003, Behling *et al*., 1993).

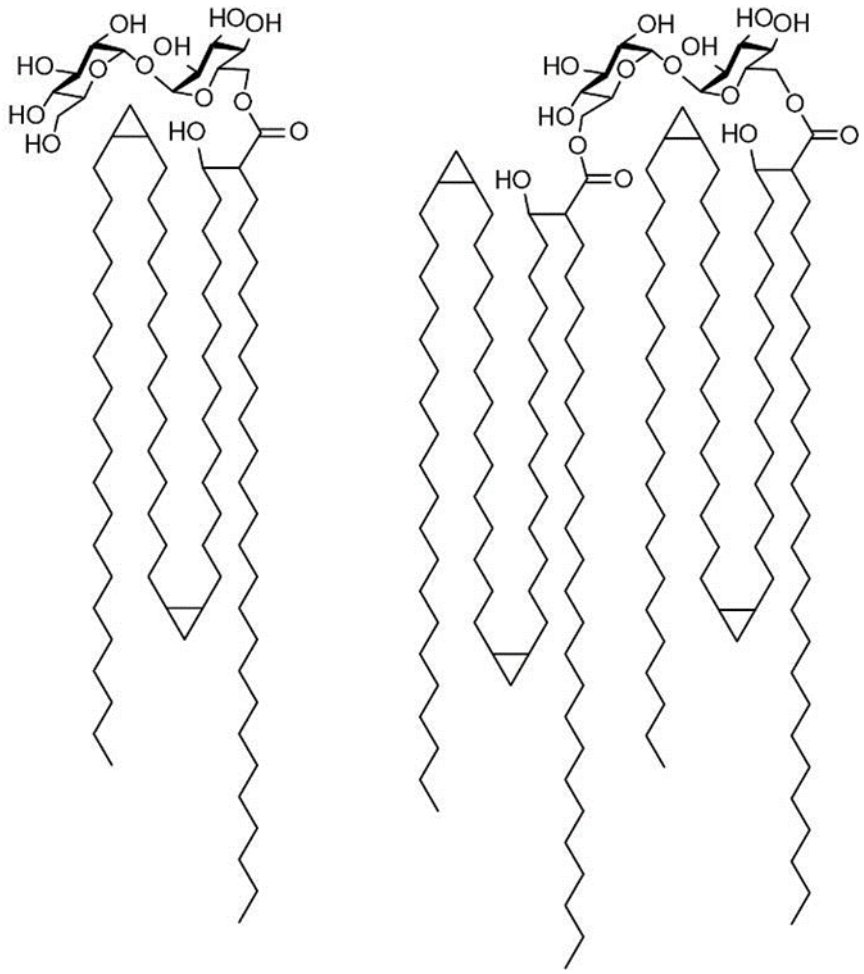

Figure 1.7 Chemical structures for trehalose monomycolate (TMM), left and trehalose dimycolate (TDM), right, of *M. tuberculosis* (Adapted from Marrakchi *et al*., (2014)

Another important biochemical process in *Mtb* involves the formation of granulomas within the host, forming lesions in the lungs for the pathogen to survive. This activity is associated with TDM in mycobacteria (Hsu *et al.*, 2011, Nazarova *et al*., 2011, Hunter *et al*., 2006).

1.10.3.3 Associated cell wall glycolipids

Treatment of mycobacterial infections have been a very difficult task due to the different lipid components within the cell envelope that contributes to the dry weight of *Mtb* (Sinsimer *et al*., 2008). For the organism to suppress the host immune system and survive within its host, cell wall components such as phthiocerol dimycocerosate (PDIM), phenolic glycolipid (PGL) and the sulpholipids (SL) are actively involved in this process (Figure 1.8 and 1.9) (Astarie-Dequeker *et al*., 2009). Clumping in cultures prepared from mycobacteria is as a result of PDIM, which is an apolar wax present within the *Mtb* cell wall (Brennan, 2003, Brennan and Nikaido, 1995). This wax has 34 carbons on which are attached two methyl branched mycocerosic acids with each acid having 34 carbons. The PDIM is associated with virulence in *Mtb* (Brennan, 2003, Astarie-Dequeker *et al*., 2009). Molecular characterisation of the PDIM produced from *Mtb* has shown that mutants that could not produce PDIM has reduced virulence in mice with an increased cell wall permeability (Camacho *et al*., 2001). Extension of the PDIM molecule produces phenolic glycolipid (PGL) which is found in *M. cannetti*. The PGL is derived via a phenolic trisaccharide constituent composed of a 2,3,4-tri-O-methyl-α-1-Fucp-(1→3)-α-1-Rhap-(1→3)-2-O-methyl-α-1-Rhap (Kaur *et al*., 2009, Reed *et al.*, 2004). The ability of the PGL to suppress Th1 immune response succeeded in increased virulence on mice and rabbits injected with *Mycobacterium sp*. (Tsenova *et al*., 2005, Reed *et al.*, 2004, Manca *et al*., 2001). Fusion of phagosomes with lysozymes can occur through the interaction with the catalytic site of the lysosomal hydrolases within the host macrophage. This fusion can be prevented through the action of the acyltrehaloes of *Mtb* and sulpholipid-1, DAT, TAT, PAT, TMM and TDM (Goren *et al*., 1976, Kato and Goren, 1974).

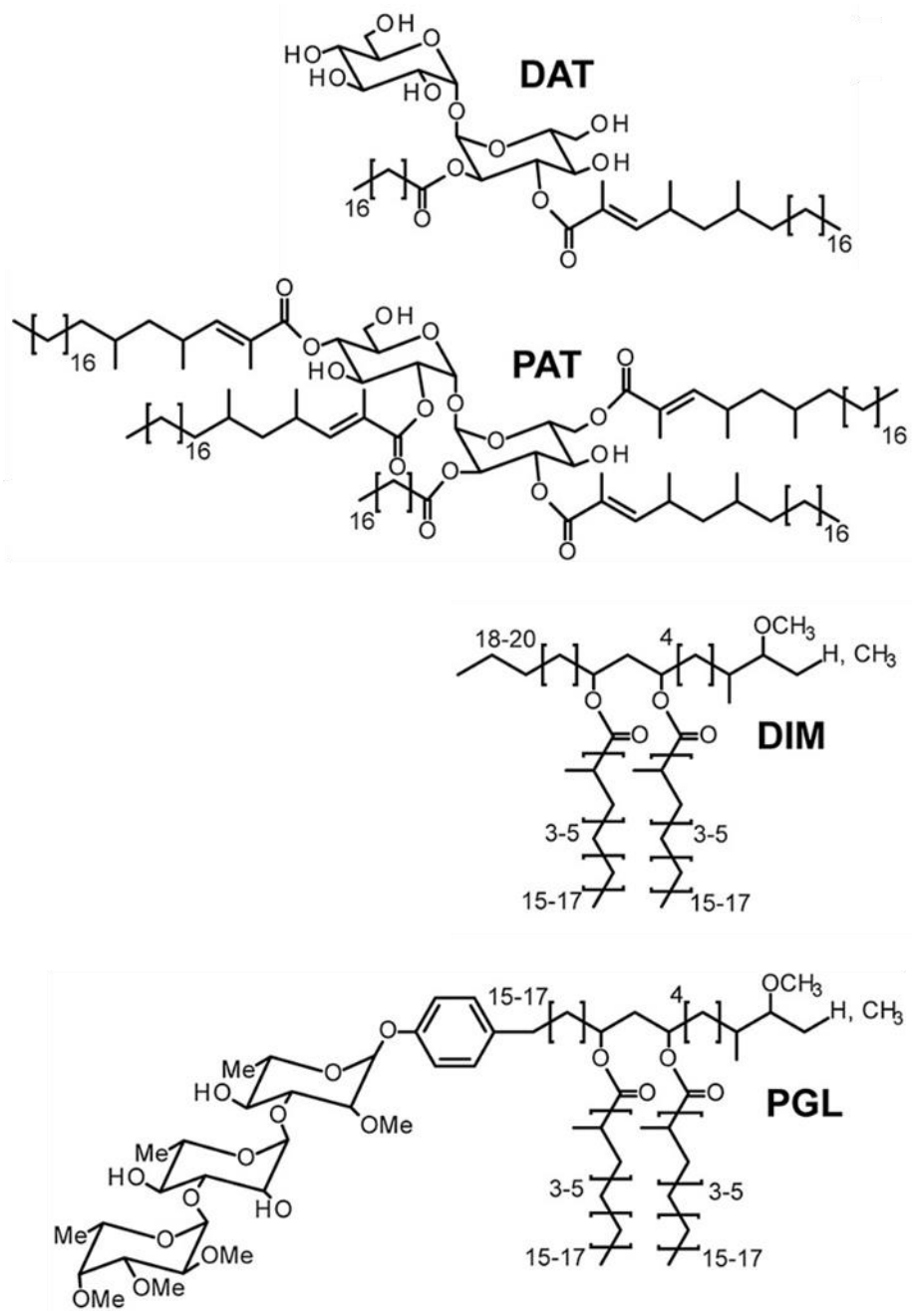

Figure 1.8 Chemical structure of DAT/PAT, DIM and PGL produced by *M. tuberculosis*
(Adapted from Jackson *et al*., 2014)

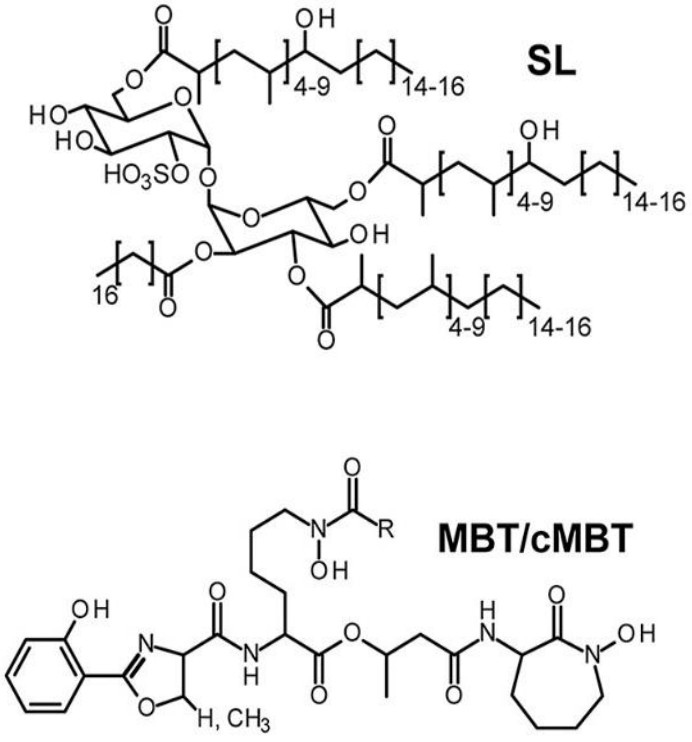

Figure 1.9 Chemical structure of SL, MBT/cMBT produced by *M. tuberculosis* (Adapted from Jackson *et al*., 2014)

These molecules also take part in modulating oxidative response and cytokine secretion (Brozna *et al*., 1991, Zhang *et al*., 1988).

The various components that make up the cell envelope in mycobacteria provide an impermeable barrier surrounding the cell. Therefore, the synthesis and acquisition of nutrients to produce these complex lipids are essential to the survival of the pathogen within the host. On such nutrient is the key biological co-factor biotin that plays a fundamental role in cell wall synthesis of *Mtb*.

1.11 Biochemistry of biotin in microorganisms

Biotin, Vitamin H or Vitamin B7, is an essential enzyme co-factor belonging to the group of B-complex vitamins. All organisms require biotin for growth and development, plants and most prokaryotes synthesize this essential component, while higher eukaryotes like animals obtain it from the food they eat (Berg *et al.*, 1995, Strzelczyk *et al*., 2001). Biotin is primarily used as a carrier for CO_2 and is involved in pyruvate carboxylase reactions where it is covalently attached to an amino group of a lysine residue in the enzyme (Chapman-Smith *et al*., 1994). Biotin is an essential co-factor in amino acid and long chain fatty acid biosynthesis (Strzelczyk *et al*., 2001). Some organisms have biotin analogs such as oxobiotin and selenobiotin having similar activity to biotin, whilst other homologs are converted to biotin *in situ* (Chapman-Smith *et al*., 1994, Strzelczyk *et al*., 2001).

1.12 Structure of biotin

There are three chiral carbon atoms in biotin molecule where the orientations of R and S of hydrogen atoms and pentanoic substituent can be found with respect to hydrothiophene ring. This means that 8 different isomers can be formed. There may be an increase in the number of biotin conformers to 32, provided the non-polarity seen in the two NH groups is considered. There is a slight non-planarity effect exhibited by the two NH groups seen in crystal biotin structure (DeTitta *et al*., 1976) (Figure 1.10).

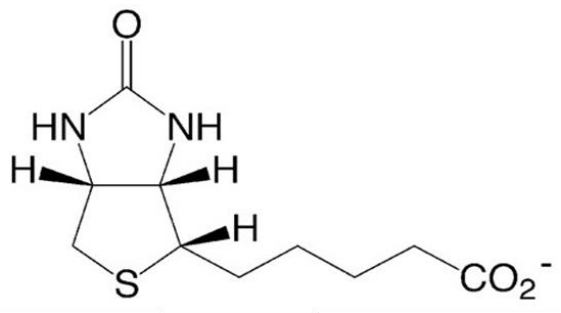

Figure 1.10 **The chiral carbons of biotin.** This gives R and S orientations of hydrogen atoms, while the NH groups are non-planer. (Adapted from DeTitta *et al*., 1976)

Studies on the crystallographic state of biotin showed that the asymmetric carbons have relative stereochemistry (DeTitta *et al*., 1976) (Figure 1.10). Biotin carboxylation mechanism was investigated by preparing a bis-*p*-bromoanilide derivative in biotin methyl ester-methyl chloroformate. After a crystallographic assay, the ureido 1'-N nitrogen was discovered to be the primary site for carboxylation reaction. An earlier work suggested that a dimethyl ester in carboxybiotin produced during a diazomethane trapping experiments had identical properties with the major product. When the anomalous dispersion properties of 1'N-carboxybiotin bis-*p*-bromoanilide were measured, the correct configuration of biotin was determined (DeTitta *et al*., 1976, Bonnemere *et al*., 1965, Trotter and Hamilton, 1966).

Biotin has six different centres in its molecule, the three oxygen, the two nitrogen and a sulphur atom. This implies that protonated biotin can result to six isomeric families, with each family compared to the biotin side chain that can be extended or folded (Fraschetti *et al*., 2015, Zhang et al., 2006, Strzelczyk *et al*., 2001). A rotation that is centred on carbon-carbon bonds in valeryl chain would give several conformers in each of the six families (Fraschetti *et al*., 2015).

1.12.1 Ureido ring

The ureido ring, which also includes the carbonyl oxygen, is primarily planar in biotin. There is a deviation of 0.03Å to the ureido atomic positions from the plane fit. Distances and angles between bonds within the ring are also planar, conforming to those observed in ethylenethiourea. The bond length in ureido carbonyl is 1.25Å, longer than the average 1.21Å observed in most stress depressants. In the same vein, distances between carbonyl carbon-nitrogen bonds are 1.34Å on the average, shorter than 1.37Å observed in most stress depressants and approach the 1.33Å urea C-N bond value. The ureido carbonyl bond lengthening and carbonyl C-C bond shortening is of great significance considering that the C=O and C-N bond values for standard deviation are quite small. The oxygen from the ureido carbonyl is strongly attached to a hydrogen bond (Caron and Donohue, 1969, Craven *et al*., 1973, Wheatley, 1953).

1.12.2 Tetrahydrothiophene ring

An interesting feature of the biotin molecule is the presence of a tetrahydrothiophene ring, an envelope shaped structure with 0.87Å sulphur atom fit to the plane positions of the four carbon atoms. A derivation of 0.02Å is observed for both C3 and C4 for this plane. The four-atom plane, C2-C3-C4-C5 and the three-atom plane C5-S-C2, intersects through a dihedral angle of 42.4°. Studies on the C-S bond lengths of the tetrahydrothiophene ring shows that the bond lengths are within the range of C-S bond lengths seen in thioether bonds of the methyl thioribopyranosides. The C-S-C bond angle in biotin is about 4° shorter than in tetrahydroselenophene iodine complex (DeTitta *et al*., 1976, Girling and Jeffrey, 1974, Hope and McCullough, 1964).

1.12.3 Symmetry of the 2'-keto-3, 4-imidazolidotetrahydrothiophene moiety

The biotin molecule possesses a 2'-keto-3,4-imidazolidotetrahydrothiophene moiety which is a bicycle ring system having a mirror symmetry that passes through the sulphur and carbonyl carbon, normal to the C3-C4 bond. Six atoms of the ureido portion and four carbon atoms of the tetrahydrothiophene ring usually meet at an angle of 122° where C3 and C4 are common to both. Endo configuration of the bicyclic ring of the tetrahydrothiophene moiety is achieved through the sulphur atom, while the exo-configuration of the sulphur atom shifts the valeryl C6 methylene group closer to the N3 nitrogen (Rohrer *et al.,* 1979).

1.12.4 Valeryl chain

Looking at the all *trans* conformation of valeryl chain of biotin, it is seen as a series of severe convolutions. The carbon-2 carbon-6 carbon-7 (C2-C6-C7) bond angle is 117.2° which is different from other bond distances and angles that are within normal ranges. The difference in the bond angle observed in C2-C6-C7 could be as a result of a close sulphur-carbon 7 (S-C7) non-bonded contact which is shorter than the van der Walls radii of the sulphur methylene. However, the C7 does not twist about the C2-C6 bond away from the sulphur atom and the S-C8 non-bonded contact is shorter than the S-C7 contact. Closeness between the valeryl C6 and the ureido N3 prevents contact to the side of the ureido ring that precedes the valeryl chain. A deviation of 0.01Å from the plane by a carboxylic carbon atom, from a planar carboxylic acid group can be explained by the positions of O10 and C9 (DeTitta *et al*., 1976, Pitzer 1960).

1.12.5 Hydrogen bonding in biotin

Neighbouring carboxylic acid group in combination with ureido N1 and N2 form a hydrogen bond ring [---O2'-C2'-N1'H---O10=C10-O10H---]. A carbonyl oxygen forms a three-dimensional bond with a hydrogen from its neighbouring N3-H group. This hydrogen bonding does not involve the sulphur atom since it is protonated in strong acid. Here, there are no sulphur-sulphur non-bonded conditions since such conditions are smaller than the overall Van der Walls radii. There is a strong hydrogen bond existing between O2'---O10 with a bond distance of 2.54Å (Olah and White, 2003; Pitzer, 1960).

1.13 Biotin synthesis

De novo biotin synthesis is exhibited by many microorganisms and by plants and fungi (Cronan and Lin, 2011). However, mammals obtain biotin from their intestinal micro flora, dietary sources and recycling (Said, 2008). Since biotin is not synthesised in mammals, the absence of a metabolic pathway provides a viable prospect for antibiotic discovery. In mycobacteria, there is no any defined biotin biosynthetic pathway. In the current biotin biosynthetic pathway (Figure 1.11), pimeloyl-thioester is converted to biotin through the activity of four enzymes, BioF, BioA, BioD and BioB.

The late steps proteins of biotin synthesis, BioA, BioB, BioD and BioF, have been well studied to the structural level in *E. coli* and *Bacillus subtilis*, whereas BioC and BioH, which are early steps enzymes, were much more poorly studied or understood. Since *E. coli* readily make use of each of the late step intermediates, sequence of steps in the late pathway was readily deduced (Cronan, 2014).

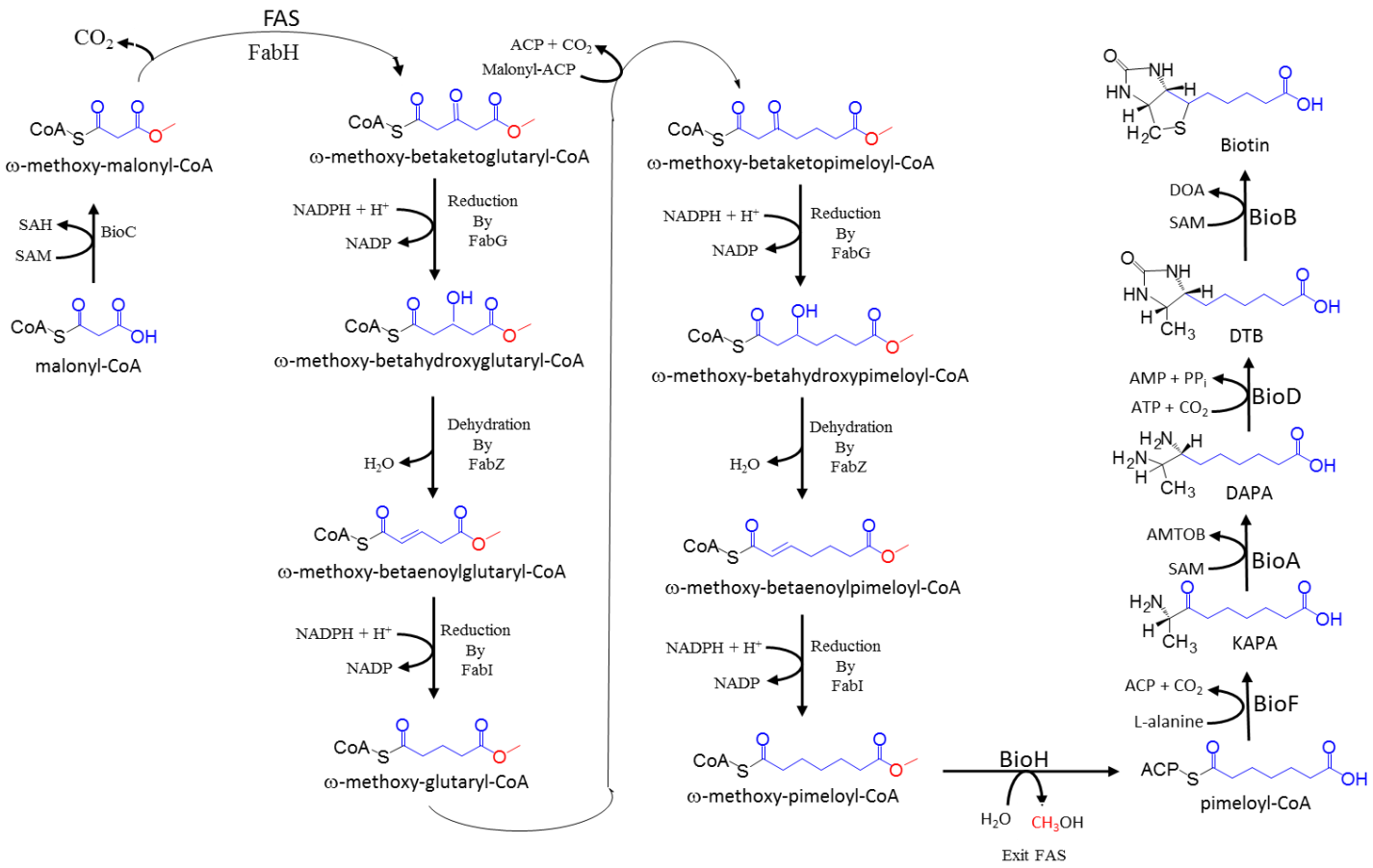

Figure 1.11 Current proposed pathway of biotin synthesis in *E. coli*. The primer molecule malonyl-CoA is methylated by BioC at its ω-carboxyl group. The resultant ω-methoxy-malonyl-CoA methyl ester hijacks the fatty acid biosynthetic pathway and act as a priming unit, instead of the acetyl-CoA in fatty acid synthesis which gives rise pimeloyl-ACP methyl ester. Pimeloyl-ACP is formed when BioH cleaves to the ester to prevent further elongation and the product is utilised by BioF to make KAPA (7-keto-8-amino pelargonic acid) that starts biotin synthesis. KAPA is catalysed by BioA to form DAPA (7,8-diaminopelargonic acid) which is further catalysed by BioD to form dethiobiotin (DTB) before biotin is finally formed through the enzyme BioB (Adapted from Lin *et al*., 2010).

New insights into the mechanism of biotin synthesis in *E. coli* have shown that a methyltransferase, BioC, transfers biotin precursor into the fatty acid synthesis pathway. An esterase, BioH, then facilitates the escape of pimeloyl-thioester so that BioF can act on it to synthesise KAPA, and the reaction continues to form biotin (Lin *et al*., 2010) (Figure 1.11). BioC and BioH have been identified in many mycobacterial genomes. This suggests that the biotin biosynthetic pathway identified in *E. coli* can also be employed in all mycobacterial species where these enzymes were identified (Yu *et al*., 2011).

1.14 Biotin biosynthesis enzymes

Bicyclic ring assembly in biotin biosynthetic pathway is evolutionary conserved and all enzymes in the pathway share some near identical chemistry. Biotin synthesis is a four-step pathway where a pimelate thioester is first converted to KAPA (7-keto-8-aminopelargonic acid). The pathway then proceeds through other intermediates to form biotin. The enzymes involved in this synthesis are BioF, BioA, BioD and BioB (Alexeev *et al*., 1998, Ploux *et al*., 1992).

1.14.1 BioF

Cleavage of the ω-methoxy-pimeloyl-ACP ester by BioH ensures that no further elongation of the pimeloyl-ACP occurs so that it can be utilised by 7-keto-8-amino pelargonic acid (KAPA) synthase, BioF. According to the BioF crystal structure it is a pyridoxal phosphate-dependent homodimer and condenses alanine with pimeloyl-CoA to form KAPA (Figure 1.11). The enzyme is a two-domain protein where the crevice between the two domains attaches to a pyridoxal phosphate. This enzyme has been extensively studied using pimeloyl-CoA in *E. coli* with pimeloyl-ACP as the possible physiological substrate (Alexeev *et al*., 1998, Ploux *et al*., 1992).

1.14.2 BioA

The 7,8-diaminopelargonic acid (DAPA) aminotransferase, BioA, is responsible for catalysing the transamination of the BioF product KAPA to DAPA. Its amino donor is considered as a non-standard amino acid but is a highly activated amino acid since S-adenosyl-2-oxo-4-thiomethyl butyrate (SAM) requires 3 ATP equivalents for its synthesis. Degradation of the deaminated form of BioA derived from SAM occurs *in vivo* where 3 ATP equivalents are consumed in a transamination reaction. A very good rationale for the tight regulation of biotin synthesis can be explained from the choice of this amino donor (Käck *et al.*, 1999).

1.14.3 BioD

Dethiobiotin synthase or DTBs (BioD) is different in terms of its catalytic action compared to the preceding enzymes. BioD catalyses the formation of the ureido moiety of biotin. The reaction is ATP-dependent where dethiobiotin is formed from DAPA and CO_2. There is an unusual second partial reaction where ϒ-phosphoryl moiety of ATP is transferred to carbamate oxygen, resulting in a mixed anhydride. This activates the carbamate. Finally, the N-8 nitrogen of DAPA attacks carbamoyl oxygen of the anhydride to release a phosphate group then form the ureido ring of DTB (Sandalova *et al*., 1999, Käck *et al*., 1998).

1.14.4 BioB

The last step of biotin synthesis involves the biotin synthase, BioB, is the most difficult step in the reaction cycle. A sulphur atom is inserted into a DTB resulting in thiophane ring of biotin. For this reaction to take place DTB, SAM, NADPH, BioB, Flavodoxin and

Flavodoxin reductase are all needed to achieve this task. BioB is understood to be in a large family of proteins catalysing very difficult reactions that can only be accessed by radical chemistry.

This occurs when there is a reductive cleavage of SAM, resulting on a deoxyadenosyl radical (DOA) and methionine. The DOA then cleaves to a C-H bond giving rise to a carbon radical that ensures the reaction continues (Cronan, 2014, Birch *et al*., 1995, Ifuku *et al*., 1994) (Figure 1.12).

Three major steps are involved in biotin synthase reaction; these are SAM-dependent abstractions of H from DTB, derivation of sulphur atom from $[2Fe\text{-}2S]^{2+}$ cluster, and a regeneration of an active enzyme. It is proposed that an electron is transferred from a reduced Flavodoxin to a SAM sulfonium through a $[4Fe\text{-}4S]^{2+}$ cluster. This produces a methionine and a 5'-deoxyadenosyl radical used for the C-H bond cleavage and abstraction of a hydrogen atom from the C9 methyl group of DTB. A sulphur atom is inserted at C6 and C9 of DTB, resulting in a tetrathiophene ring with a sacrifice of a $[2Fe\text{-}2S]^{2+}$ cluster (Ugulava, 2001, Escalettes *et al*., 1999).

Biotin synthase become inactive the moment the $[2Fe\text{-}2S]^{2+}$ is sacrificed and this is the reason behind the reports about the enzyme catalysing a single turnover per subunit *in vitro*. Multiple turnovers can be achieved by the reconstitution of the $[2Fe\text{-}2S]^{2+}$ cluster in the reaction cycle where *in vivo* biotin synthase can have up to 20 turnovers in the presence of Fe-S cluster assembly systems. Biotin synthase requires a partial unfolding to regenerate in the presence of HscA, a chaperone that renders biotin synthase susceptible to proteolysis and degradation (Farrar *et al*., 2010, Reyda *et al*., 2009)

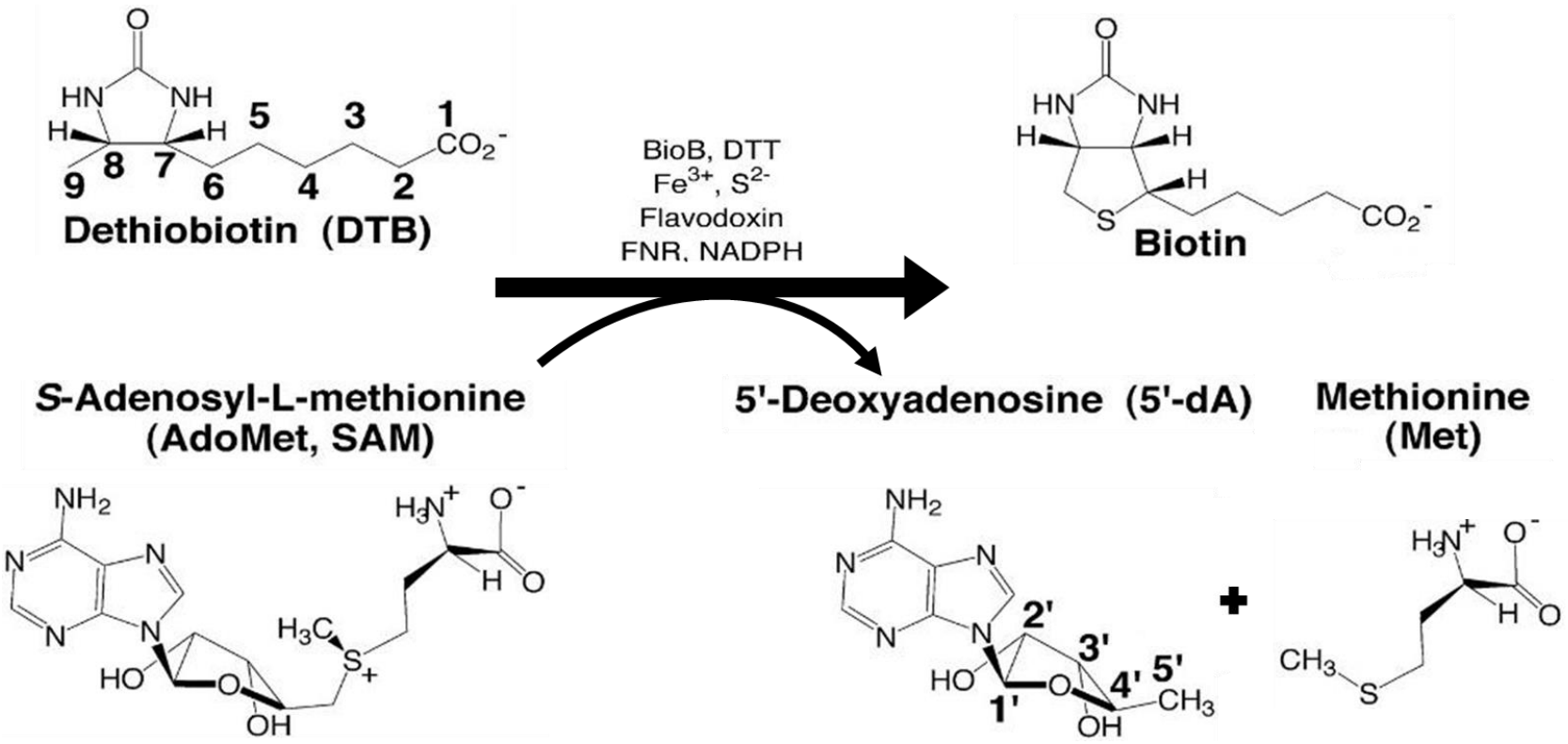

Figure 1.12 Dethiobiotin to biotin synthetic pathway catalysed by BioB (Adapted from Berkovitch *et al*., 2004)

1.15 Biotin transport in mycobacteria

Literature strongly suggests that *Mtb* primary source of biotin is via *de novo* biosynthesis (Lin *et al*., 2010). The bacilli do not possess an atypical biotin transport system to scavenge biotin from exogenous sources. Many other bacteria do possess this ability by utilizing a biotin transport protein (Salaemae *et al*., 2011). The most characterized example is BioY (Rodionov *et al*., 2009). This transporter works with an energy coupling system to actively move biotin across the bacterial cell membrane in an ATP-dependent manner (Rodionov *et al*., 2009, Hebbeln *et al*., 2007). Genome annotation studies have failed to identify homologues of *bioY* in the *Mtb* genome (Hebbeln *et al*., 2007, Rodionov *et al*., 2002). This supports the observation for the requirement for *de novo* biotin synthesis which is further reinforced by the chemical inhibition of the biotin biosynthetic enzymes show to impede growth of *Mtb in vitro*. This has been investigated using two natural compounds isolated from culture filtrates of *Streptomyces* species, namely amiclenomycin and actithiazic acid (Okami *et al*., 1974, Ogata *et al*., 1973). The BioA inhibitor, amiclenomycin (Figure 1.13), is a narrow-spectrum antibiotic with activity against *Mycobacterium* sp., but not other bacteria or fungi that can scavenge exogenous biotin (Kitahara *et al*., 1975).

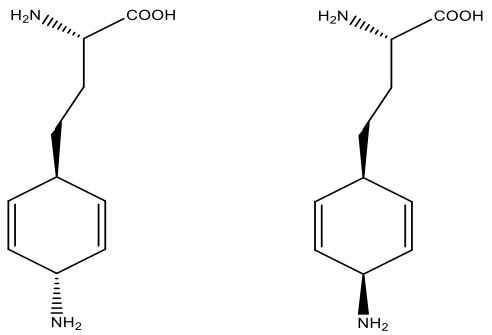

Figure 1.13 Structure of *cis* (right) and *trans* (left) amiclenomycin (Adapted from Sandmark *et al*., 2002)

Its anti-TB activity can be reversed by high concentrations of external biotin, above 0.01 μg/mL (Mann *et al*., 2005, Sandmark *et al*., 2002), which is at least 10-fold greater than the concentration found in normal human plasma (Mock and Malik, 1992). This implies that the water-soluble biotin might enter through the bacilli membrane using mechanisms that are not yet identified, but only in supra-physiological concentrations of the nutrient. Similarly, the BioA inhibitor actithiazic acid also displays narrow spectrum activity against Mycobacteria (Ogata *et al*., 1973). Together, the restricted antibiotic spectrum is consistent with the genetic studies demonstrating *de novo* biotin biosynthesis is essential in *Mtb* but not in other eubacteria (Salaemae *et al*., 2011).

In other organisms such as *C. glutamicum*, biotin production and transport is key to the development of the organism. A practical biotin bioassay system for facilitating strain improvement was developed (Ikeda *et al*., 2013). The key to this development is the finding that the disruption of *bioY* enhances the biotin requirement of *C. glutamicum* cells by almost 3 orders of magnitude. This study demonstrated the application of the *bioY* mutant to a biotin bioassay system. With respect to biotin uptake, multiple systems are suggested to exist in prokaryotes, including the BioYMN system, which is considered to constitute tripartite transporters containing ATP-binding cassettes (Hebbeln *et al*., 2007). *C. glutamicum* also has *bioYMN* homologs, and the predicted functions of the gene products have recently been verified by transport assays with radiolabelled biotin (Schneider et al., 2012). However, attempts to disrupt the system failed, the phenotype of the disruptant remained unclear (Schneider *et al*., 2012). Although it could expect that the disruption of *bioY* in the organism would lead to an increase in the biotin requirement, the approximately 1,000-fold increase was beyond expectation. The BioY protein in prokaryotes is the central unit of the biotin transporter and mediates biotin uptake by itself, while BioM and BioN encode an ATPase and permease, respectively, of an ABC-

type transporter and are considered to be needed to convert the system into a high-affinity transporter (Hebbeln *et al*., 2007). Taking this into consideration, it seems reasonable to assume that the *bioY* disruption would result in a complete loss of the biotin uptake capability of the system even when the other two components, *bioMN*, remain. This means that a further increase in the biotin requirement would not be expected from the deletion of the whole *bioYMN* gene set from the genome. On the other hand, disruption of either or both *bioMN* genes instead of *bioY* is likely to increase the biotin requirement of the wild-type strain, considering their predicted roles in biotin uptake efficiency.

1.16 Biotin regulation and function within microorganisms

A clear insight into the regulatory activity of biotin within microorganisms can be seen from extensive studies with *E. coli* in which a biotin induced repressor A (BirA) plays a key role, but there are reports also of a BirA activity in mycobacteria (Purushothaman *et al*., 2008).

1.16.1 Biotinylation of enzymes

Most bacteria, including *Mtb* shows a rare form of post-translational modification of their proteins known as protein biotinylation. This is the covalent attachment of biotin co-factor on specific lysine residue on a biotin carboxyl carrier domain (BCCD) of specific biotin metabolic enzymes. This is made possible by recognising a sequence motif in the highly conserved structure (Sternicki *et al*., 2017). Important metabolic pathways such as lipogenesis, gluconeogenesis, amino acid metabolism and energy transduction depend on these biotin-dependent enzymes. Biotin protein ligase (BPL) is the sole enzyme responsible for modifying all biotin-dependent enzymes (Chapman-Smith and Cronan,

1999). There are two major classes of BPLs in microorganisms. These are class I BPL and class II BPL.

The class I BPLs is made up of an SH2-like catalytic domain with an ATP binding site, and an SH3-like C-terminal cap (Sternicki *et al*., 2017). Mycobacteria and thermophilic archaea possess class I BPL which catalyses post-translational biotinylation. The class II BPLs is found in *E. coli* and *S. aureus* and it is used for post-translational biotinylation and as a transcriptional repressor (Brown *et al*., 2004, Chapman-Smith and Cronan, 1999).

In *Mtb*, Fatty acid biosynthesis in mycobacteria involve the activity of acyl coenzyme A carboxylases (ACCs) which catalyses the first committed step of the process. This is made possible by the synthesis of monomeric malonyl-CoA building blocks (Duckworth *et al*., 2011). There are multiple ACCs encoded by *Mtb* for malonyl-CoA biosynthesis which are utilised in the synthesis of fatty acids, mycolic acids and methyl-branched lipids (Kurth *et al*., 2009, Gago *et al*., 2006, Portevin *et al*., 2005). The ACCs are made active by a biotin protein ligase (BPL) in *Mtb* where the biotin-carboxylase carrier protein (BCCP) domains of these proteins are post-translationally modified to an active biotinylated form encoded by a biotin induced repressor A (BirA) and referred to as *mt*BPL (Purushothaman *et al*., 2008). The transfer of a carboxyl group to an acyl CoA substrate is mediated by biotin as a co-factor. *mt*BPL is also important in fatty acid degradation, since the enzyme causes biotinylation of BCCP domain of pyruvate carboxylase, which plays a key role in transporting oxaloacetate to phosphoenolpyruvate carboxylase, an enzyme that is critical for mycobacterial pathogenesis (Marrero *et al*., 2010). *mt*BPL is therefore a regulator of lipid metabolism and serves as an attractive target for new anti-tubercular agents.

In *E. coli* and *S. aureus*, BirA serves as both a transcriptional repressor and the enzyme responsible for protein biotinylation. Protein biotinylation is achieved through a conserved, two-step reaction mechanism that is catalysed by biotin protein ligase (BPL) in all organisms. In the first partial reaction, biotin and ATP are required to form biotinyl-5′-AMP that serves as both the reaction intermediate for protein biotinylation and corepressor for transcriptional regulation. The BirA: biotinyl-5′-AMP (holo) enzyme can then adopt one of two different fates. When the cellular demand for biotin is low holo-BirA can dimerise and bind DNA where it functions as the transcriptional repressor of the biotin biosynthesis operon, thereby inhibiting the synthesis of more biotin. In contrast, in the presence of substrate requiring biotinylation the holo-BirA functions as a biotin ligase. Here BPL recognizes and binds to a biotin carboxyl carrier protein (BCCP) present in the receiving enzyme that contains the lysine residue targeted for biotinylation (Chapman-Smith *et al*., 1999). Protein biotinylation is an example of a post-translational modification that is performed with exquisite specificity. For example, the *E. coli* biotin ligase (BirA) modifies just one of the >4000 different proteins in the bacterial cell (Chapman-Smith and Cronan, 1999). Moreover, the biotin cofactor is covalently attached onto the side chain of one single, specific target lysine residue present in the active site of biotin-dependent enzymes. BPLs from a wide variety of species are able to modify BCCP from unrelated organisms (Polyak *et al*., 2001, Cronan and Wallace, 1995, León-Del-Rio *et al*., 1995), highlighting how highly conserved both the catalytic mechanism and the protein-protein interactions between enzyme and substrate have remained throughout evolution.

All BPLs contain a conserved 2-domain catalytic core responsible for biotinyl-5′-AMP synthesis and protein biotinylation (Pendini *et al*., 2008). The greatest divergence between the BPLs is in their N-terminal regions. Class I BPLs are composed only of the

conserved catalytic module that is required for protein biotinylation. Hence, these are mono functional enzymes. X-ray crystal structures of Class I BPLs have been reported for *Mtb* (Duckworth *et al*., 2011) and *Pyrococcus horikoshii* (Bagautdinov *et al*., 2005). In contrast, the Class II BPLs are truly bi-functional having both biotin ligase and transcriptional repressor activities due to an N-terminal DNA binding domain.

1.16.2 BioR as a protein regulator in biotin synthesis

BioR is an important protein involved in the regulation of biotin synthesis within organisms. However, BioR has not been reported in *Mtb*, but its biotin regulatory function in other organisms makes it a protein of interest. BioR belongs to the GntR family of transcription factor and is reported as a repressor against biotin metabolism in species of α-proteobacteria and in *Agrobacterium tumefaciens* (Feng *et al*. 2013). In *Paracoccus denitrificans,* BioR encode two homologues (BioR1 and BioR2) with six predictive BioR-recognisable sites. The two *bioR* homologues each has one site, whereas the two *bio* operons (*bioBFDAGC* and *bioYB*) each contains two tandem BioR boxes (Feng *et al*. 2015b). This suggests that the BioR-mediated biotin regulation in *Paracoccus denitrificans* has an unexpected complexity. A combined analysis of its phylogeny with GC percentage indicated a possibility that the *bioR*2 gene might be acquired by horizontal gene transfer (Feng *et al*. 2015b). The predicted BioR-binding sites are functional for the two BioR homologs, like the one observed in BioR site of *A. tumefaciens bioBFDAZ*. Analysis of the reporter system in *A. tumefaciens* containing a plasmid borne LacZ fusion reveals that the two homologs of *P. denitrificans* BioR are functional repressors for biotin metabolism (Feng *et al*. 2015b). Expression of *bioYB* operon encoding biotin transport/uptake system, BioY, was stimulated by the addition of exogenous biotin in *P. denitrificans*. This stimulation also inhibited the transcription

of the *bioBFDA*GC operon resembling the *de novo* biotin synthetic pathway. However, EMSA-based screening failed to demonstrate that the biotin-related metabolite is involved in BioR-DNA interplay (Feng *et al*. 2015b).

1.16.3 BioQ mediated gene expression

The genome of *Mycobacterium smegmatis*, which is a close relative of tuberculosis-causing *Mtb*, contain a BirA protein which should act as a repressor for biotin biosynthetic pathway. However, the BirA in *Mycobacterium smegmatis* lacked the DNA-binding activity, which suggests that an alternative regulator might compensate for this function (Tang *et al*., 2014). A newly identified protein, belonging to the TetR family of transcription factor called BioQ, has been identified in *Mycobacterium smegmatis* (Tang *et al*., 2014). This protein therefore performs the regulatory function in the organism. It was revealed that BioQ binds specifically to the promoter regions of *bioFD* and *bioQ/B* when electrophoretic mobility shift assays was done. Further DNase I foot-printing elucidated the BioQ-binding palindromes. Important residues critical for BioQ/ DNA binding were revealed when Site-directed mutagenesis was done. Also, expression of *bio* operons was repressed by exogenous addition of biotin, and this repression seemed to depend on the presence of BioQ protein (Tang *et al*., 2014). Therefore, it is believed that *M. smegmatis* BioQ is not only a negative auto-regulator but also a repressor for *bioFD* and *bioB* operons involved in the biotin biosynthesis pathway. Collectively, this finding defined the two-protein paradigm of BirA and BioQ, representing a new mechanism for bacterial biotin metabolism.

Also, in *C. glutamicum*, the biotin synthesis pathway is incomplete, thereby rendering the bacteria biotin auxotrophic. However, the expression of the *bio* genes is proposed to be controlled by BioQ. Although the TetR family of regulators has been well

characterized, none have previously been shown to regulate biotin synthesis (Ramos *et al*., 2005). Bioinformatic analysis of the *C. glutamicum* genome revealed co-localization of the *bioQ* coding region with the biotin biosynthetic genes (Brune *et al*., 2012). The presence of the BioQ recognition sequence in the promoter of the *bioQ* gene suggests auto-regulation of the transcription factor. In addition, the same regulatory sequence is also found upstream of the *bioY* which was highly expressed in *ΔbioQ* strains (Tang *et al.*, 2014). Increasing levels of biotin in the growth media resulted in decreasing expression of biotin biosynthesis genes bioF, bioD and bioB for the wild type bacteria whereas there was no significant change in the *ΔbioQ* strain. These findings underline the biotin sensing ability of BioQ.

1.17 Biotin dependent carboxylases in bacteria

There are many biotin-dependent carboxylases in bacterial systems include acetyl-CoA carboxylase (ACC), propionyl-CoA carboxylase (PCC), 3-methylcrotonyl-CoA carboxylase (MCC), geranyl-CoA carboxylase (GCC), pyruvate carboxylase (PC), and urea carboxylase (UC). Each enzyme contains a biotin carboxylase (BC), carboxyl transferase (CT) and biotin-carboxyl carrier protein (BCCP) component. These enzymes are widely distributed in nature and have important functions in fatty acid metabolism, amino acid metabolism, carbohydrate metabolism, polyketide biosynthesis, urea utilization, and other cellular processes. ACCs are also attractive targets for drug discovery against Type 2 diabetes, obesity, cancer, microbial infections, and other diseases, and the plastid ACC of grasses is the target of action of three classes of commercial herbicides. Deficiencies in the activities of PCC, MCC or PC are linked to serious diseases in humans (Tong, 2013). Our understanding of these enzymes has been greatly enhanced over the past few years by the crystal structures of the holoenzymes of

PCC, MCC, PC, and UC. The structures reveal unanticipated features in the architectures of the holoenzymes, including the presence of previously unrecognized domains, and provide a molecular basis for understanding their catalytic mechanism as well as the large collection of disease-causing mutations in PCC, MCC and PC (Tong, 2013). The CT components of the acyl-CoA carboxylases show sequence and structural conservation. The acyl-CoA substrate is recognized by a domain/subunit with the crotonase fold, and it may be speculated that this part of the CT component evolved from a primordial crotonase. This fold is capable of binding CoA esters, and it also provides an oxyanion hole, in the form of two main-chain amides, that stabilizes the enolate oxyanion of the acyl group during catalysis. Remarkably, the main-chain carbonyl of one of the oxyanion-hole residues recognizes the N6 amino group, and the main-chain amide of the following residue is hydrogen-bonded to the N1 atom of the adenine base of CoA. Biotin is recognized by a separate domain/subunit, but also within the crotonase fold. The equivalent oxyanion hole in this domain/subunit stabilizes the biotin enolate oxyanion during the CT reaction. It might be possible that the biotin-binding domain/subunit of CT arose through gene duplication of a crotonase enzyme and then evolved its specificity toward biotin (Tong, 2013).

1.18 Biotin deficiency in bacteria

Biotin deficiency generally results in the decrease of activity in biotin-dependant enzymes, which in turn affects all other pathways that makes use of intermediates directly associated to biotin-dependant enzymes. A loss of PC activity in gluconeogenesis results in pyruvate and lactate accumulation. There is also reduced rate of lipogenesis and abnormalities observed in fatty acid synthesis as a result of reduced activity of ACC (Arinze and Mistry, 1971).

It has been shown that biotin deficiency in *Lactobacillus arabinosus* reduced the rate of fixation of carbon dioxide and growth rate. Biotin deficiency is also associated with changes in fatty acid composition in *Lactobacillus plantarum* (Croom *et al*., 1964).

Deficiency of biotin also affect other metabolic pathways that are not directly involved with biotin since they are not inhibited *in vitro* by avidin. Direct and indirect effects of biotin deficiency bring about pathological changes in the affected organism such as reduced growth and repair (Broquist *et al*., 1951).

In *Mtb*, since biotin is synthesised *de novo*, its absence or deficiency directly affect the synthesis of several other carboxylase that are directly involved with the synthesis of the mycobacterial cell wall complex. Thus, deficiency of biotin can result to cell death.

1.19 Project Aims and objectives

This project aims to apply a two pronged approach to the identification of novel anti-tubercular targets and compounds. Firstly, a biochemistry section assessing the synthetic enzymes of pimelate biosynthesis in *Mtb*, and secondly a chemistry section that primarily focuses on the synthesis of isoxyl with SQ109 combination analogues. The specific aims and objectives of the project are as follows:

1. To identify and isolate the enzyme involved in methylation in pimelate biosynthesis in *Mtb* and perform biochemical studies on the enzyme. This will be achieved with the following objectives:

    - Identification of enzyme involved in methylation in pimelate biosynthesis in *Mtb* by computational analysis of publicly available biological databases.

    - Target gene cloned into expression vectors which will be used to transform *E. coli* or Mycobacterial expression strains in order to produce soluble recombinant protein.

    - Purification and biochemical studies of the recombinant protein to determine its enzyme activity. The studies would utilise a luminometer dependant reaction to determine the rate of product formation by the purified enzyme. Optimum temperature, pH, inhibitor, among other properties will be established with this technique.

2. To identify and isolate the enzymes involved in later stages of pimelate biosynthesis in *Mtb*. This will be achieved with the following objectives:

- Identification of enzymes involved in later stages in pimelate biosynthesis in *Mtb* by computational analysis of publicly available biological databases

- Target genes cloned into expression vectors which will be used to transform *E. coli* or Mycobacterial expression strains in order to produce soluble recombinant proteins.

- Purification and initiation of crystallographic studies of the recombinant proteins to determine enzyme structure.

3. To synthesise a series of isoxyl-SQ109 hybrid analogues and test their potency. This will be achieved with the following objectives:

    - The synthesis will involve modifications to the base structures and fragments of the two drugs (SQ109 and isoxyl) with known differing mechanisms of action. These would be incorporated to produce different analogues that would theoretically target multiple aspects of cell wall synthesis.

    - The effectiveness of the synthesized hybrid(s) will be evaluated by testing against the wild type strain of *Mtb* and against RIF and INH spontaneous resistant mutants. This would create a new potential lead that will be a multi-targeted compound with efficacy that rivals current TB treatments.

Chapter 2
Materials and methods

2 Material and methods

2.1 Growth media

This study utilised different media to facilitate the growth of bacterial and mycobacterial species (Table 2.1).

Table 2.1 Preparation of Growth Media.

Growth Media	Recipe (per 1 L)	Species	Comments
Bertani Broth (LB Broth)	10 g tryptone 5 g yeast extract 10 g sodium chloride	*E. coli*	
Lennox Broth	10 g tryptone 5 g yeast extract 10 g sodium chloride 1 g glucose	*E. coli*	
Luria Bertani Agar (LB Agar)	10 g tryptone 5 g yeast extract 10 g sodium chloride 15 g agar	*E. coli*	
Middlebrook 7H9 Broth (7H9 Broth)	21 g Middlebrook 7H9 broth powder (Difco) 2 mL glycerol 100 mL Middlebrook enrichment media (OADC) (BD Scientific)	*Mycobacterium*	Middlebrook 7H9 was autoclaved for 15 minutes prior to addition of 100 mL OADC
Middlebrook 7H11 Agar (7H11 Agar)	4.7 g Middlebrook 7H11 Agar powder (Difco) 5 mL glycerol 100 mL Middlebrook enrichment media (OADC) (BD Scientific)	*Mycobacterium*	Middlebrook 7H9 was autoclaved for 15 minutes prior to addition of 100 mL OADC

Unless otherwise stated all growth, media was prepared in 18.2 Ω ddH2O and autoclaved at 121ºC for 15 minutes. Where required, Tween 80 (Final concentration 0.02%) and antibiotics (Table 2.3) were added aseptically to autoclaved media once cooled to 55ºC. All recipes given in Table 2.1 are for 1 L volumes and all reagents were purchased from Sigma Aldrich unless otherwise stated.

2.2 Bacterial Strains and Growth Conditions

All bacterial strains used in this study are described in Table 2.2. The growth condition used has been described below.

2.2.1 Escherichia coli

E. coli XL10 Gold, C41 (DE3), C43 (DE3), C43 (DE3) pLYSs, B834 (DE3) pLYSs, HMS174 (DE3), BL21 pLYSs (DE3) and BL21 (DE3) cells were cultured on Luria Bertani (LB) agar (section 2.1) and incubated at 37ºC for 16 hours. Liquid cultures used LB broth followed by orbital incubation (200 rpm) at 37ºC for 16 hours. *E. coli* strains were maintained by combining mid-log phase culture with an equal volume of 80% (v/v) sterile glycerol and stored at -80ºC.

2.2.2 Mycobacterium tuberculosis

Mtb $mc^2$7000 strains were cultured on Middlebrook 7H11 agar (Section 2.1) and incubated at 37ºC for 4-5 weeks. Liquid cultures were grown in Middlebrook 7H9 broth (section 2.1) supplemented with pantothenate (24 μg/mL), casamino acids (0.01%), tween 80 (0.02%) and incubated at 37ºC at 200 rpm for 3-4 weeks. *Mtb* strains were

maintained by combining mid-log phase culture with an equal volume of 80% (v/v) sterile glycerol and stored at -80ºC.

Table 2.2 Bacterial strains used in this investigation

Species	Strain Code	Genotype	Comments
Escherichia coli	XL10 Gold	endA1 glnV44 recA1 thi-1 gyrA96 relA1 lac Hte Δ(mcrA)183 Δ(mcrCB-hsdSMR-mrr)173 tet^R F'[proAB $lacI^qZ$ΔM15 Tn10 (Tet^R Cm^R)]	Cloning Host (Stratagene)
Escherichia coli	C41 (DE3)	F– ompT gal dcm hsdSB(rB- mB-)(DE3)	Expression Host (Lucigen)
Escherichia coli	C43 (DE3)	F– ompT gal dcm hsdSB(rB- mB-)(DE3)	Expression Host (Lucigen)
Escherichia coli	C43 pLYSs (DE3)	F– ompT gal dcm hsdSB(rB- mB-)(DE3) pLysS (Cmr)	Expression Host (Lucigen)
Escherichia coli	BL21 (DE3)	*E. coli* str. B F– ompT gal dcm lon hsdSB(rB–mB–) λ(DE3 [lacI lacUV5-T7p07 ind1 sam7 nin5]) [malB+]K-12(λS)	Expression Host (Lucigen)
Escherichia coli	BL21 pLYSs (DE3)	*E. coli* str. B F– ompT gal dcm lon hsdSB(rB–mB–) λ(DE3 [lacI lacUV5-T7p07 ind1 sam7 nin5]) [malB+]K-12(λS) pLysS[T7p20 orip15A](CmR)	Expression Host (Lucigen)
Escherichia coli	B834 (DE3)	F- ompT hsdSB(rB- mB-) gal dcm met (DE3)	Expression Host (Merck)
Escherichia coli	HMS174 (DE3)	F- recA1 hsdR(rK12- mK12+) (DE3) (Rif R)	Expression Host
Mycobacterium tuberculosis	mc^27000	ΔRD1, ΔpanCD, ΔLeu	Albert Einstein Institute, New York, NY
Mycobacterium tuberculosis	AKB7001	WT, parental	as mc^27000, this study
Mycobacterium tuberculosis	AKB7002	RIF^R	as mc^27000, this study
Mycobacterium tuberculosis	AKB7003	RIF^R	as mc^27000, this study
Mycobacterium tuberculosis	AKB7005	RIF^R	as mc^27000, this study
Mycobacterium tuberculosis	AKB7009	RIF^R	as mc^27000, this study
Mycobacterium tuberculosis	AKB7020	INH^R	as mc^27000, this study
Mycobacterium tuberculosis	AKB7021	INH^R	as mc^27000, this study
Mycobacterium tuberculosis	AKB7025	INH^R	as mc^27000, this study
Mycobacterium tuberculosis	AKB7028	INH^R	as mc^27000, this study
Mycobacterium tuberculosis	AKB7031	$JJH110A^R$	as mc^27000, this study
Mycobacterium tuberculosis	AKB7032	$JJH110A^R$	as mc^27000, this study
Mycobacterium tuberculosis	AKB7033	$JJH110A^R$	as mc^27000, this study
Mycobacterium tuberculosis	AKB7034	$JJH110A^R$	as mc^27000, this study
Mycobacterium tuberculosis	AKB7035	$JJH110A^R$	as mc^27000, this study
Mycobacterium tuberculosis	AKB7036	$JJH110A^R$	as mc^27000, this study
Mycobacterium tuberculosis	AKB7037	$JJH110A^R$	as mc^27000, this study
Mycobacterium tuberculosis	AKB7038	$JJH110A^R$	as mc^27000, this study
Mycobacterium tuberculosis	AKB7039	$JJH110A^R$	as mc^27000, this study
Mycobacterium tuberculosis	AKB7040	$JJH110A^R$	as mc^27000, this study
Mycobacterium tuberculosis	AKB7041	$JJH110A^R$	as mc^27000, this study
Mycobacterium tuberculosis	AKB7042	$JJH110A^R$	as mc^27000, this study
Mycobacterium tuberculosis	AKB7062	WT, parental	as mc^27000, this study

2.2.3 Antibiotic Stocks and Selective Growth

Antibiotic stocks solution was prepared using sterile ddH2O (∑H_2O) except for chloramphenicol which was prepared in 100% ethanol, and test compounds which were prepared in dimethyl sulphur oxide (DMSO). Antibiotic stock solutions were sterilised by filtering through a 0.2 µm filter (Milli-Q) and were stored in 1 mL aliquots at -20ºC. Stock solutions were prepared to the concentration and used in the final concentration outlined in Table 2.3 depending on the species. Antibiotics were included in the growth medium for selective growth of bacteria containing plasmids as describe in Table 2.4.

Table 2.3 Stock antibiotic concentration for selective bacterial growth

Antibiotic	Stock concentration (mg/mL)	*Mycobacterium tuberculosis* final concentration (µg/mL)	*Escherichia coli* final concentration (µg/mL)
Ampicillin	100	-	100
Chloramphenicol	30	30	30
Hygromycin	50	50	200
Kanamycin	25	25	25

Table 2.4 Plasmids and selective markers

Plasmid	Genetype	Marker	Source
pUC18	oriColE1 MCS *bla*	Amp^R	Thermo
pEX-A258	oriColE1 MCS *bla* P_{lac}	Amp^R	Eurofins
pET23b	P_{lac}-T7, *bla*; High-copy-number, C-terminal His-tag expression vector	Amp^R	Novagen
pET28b	P_{lac}-T7, Km; High-copy-number, N or C-terminal His-tag expression vector	Kan^R	Novagen
pMIND	P_{tet}; High-copy-number, MCS	Kan^R, Hyg^R	AddGene
pHMR3	P_{tet}; High-copy-number, N or C-terminal His-tag expression vector	Kan^R	A. K. B.

2.2.4 Oligonucleotide Primer Design

All primers were designed to be at least 20 nucleotides in length with melting temperature above 45ºC at 50 mM sodium chloride and 250 mM primer concentration. The GC content of the primer was typically between 40% and 60%. Since mycobacterial DNA typically has a high GC content some primers were adapted by replacing the typical "GATCGATC" junk DNA sequence with a poly-A sequence, lowering the GC content and consequently, the melting temperature. Stretches of any one base, repetitive G's and C's were avoided, as were palindromic sequences. Wherever possible, primer pairs with complementary sequences were avoided to minimise primer dimer formation, though this occurred incidentally in some cases.

2.2.5 Primer Sequences

Oligonucleotide primers for PCR amplification of DNA fragments were designed in a 5'-3' orientation and purchased from Eurofins MWG Operon (Eurofins, Germany). Primers designed for amplification of mycobacterial genes from *Mtb H37Rv* gDNA are described in Table 2.5.

Table 2.5 DNA oligonucleotides used in this study

Primer Name		Sequence		Usage
Rv0089For	5'	AAAAAACATATGGATCAACCGTGGAACGCC	3'	pET28b, pHMR3
Rv0089Rev	5'	AAAAAAAAGCTTTTAGACGGGTGCGCGCCA	3'	pET28b, pHMR3
Rv1882cFor	5'	AAAAAACATATGAAAGCGATATTCATCACC	3'	pET28b, pHMR3
Rv1882cRev	5'	AAAAAAAAGCTTTTACTTCCGTTTTGGCTC	3'	pET28b, pHMR3
Rv2715For	5'	AAAAAACATATGACCGAGCGGAAGCGAAAT	3'	pET28b, pHMR3
Rv2715Rev	5'	AAAAAAAAGCTTTCAGGTAGCGCTGCGTTC	3'	pET28b, pHMR3
Rv3177For	5'	AAAAAACATATGCCCCAGAGACAGGCCGGC	3'	pET28b, pHMR3
Rv3177Rev	5'	AAAAAAAAGCTTTCACGACTCGAGAAACTG	3'	pET28b, pHMR3

2.2.6 PCR Primer Design

Oligonucleotide primer pairs for PCR were designed with three primary regions. Junk DNA sequences of 6-8 nucleotide bases were included to improve binding of restriction enzymes to the DNA for restriction digestion of PCR products. The appropriate restriction sequence was determined by selection of restriction enzymes which did not digest within the desired PCR products sequences, or within the intended vector except for the multiple cloning site, as determined by analysis with the New England Biolabs (NEB) Cutter V2.0 tool. Priming sequences of ~16 nucleotide bases were identified for the 5' and 3' ends of the intended PCR product sequence. Melting temperatures were determined using the NEB T_m tool server and primers were adapted to have equal melting temperatures. Oligonucleotide melting temperatures in the study were higher than typically found as a result of the high GC content of actinomycete genomes.

2.2.7 DNA Sequencing Primer Design

Sequencing of construct was carried out by GATC Biotech as described in Section 2.5. Primers were designed according to standard protocols to anneal approximately 50 bp of the target sequence.

2.3 Polymerase Chain Reaction (PCR)

2.3.1 Standard PCR

The standard PCR reaction was prepared on ice to a 50 µL reaction volume using vent DNA polymerase as described in Table 2.6. Unless otherwise stated, PCR reaction components were purchased from NEB. All PCR reactions were carried out using filter sterilised ΣH_2O. PCR reactions were optimised by the addition of varying combinations

of Mg^{2+} and DMSO according to Table 2.7. The reaction mixture was pulse centrifuged and thermal cycling carried out in a Bio-Rad thermocycler using the thermal cycle outlined in Table 2.8. Optimisation of the PCR reaction was carried out according to the requirements of the experiment. This investigation employs a two-step PCR thermal cycling for the amplification of DNA fragments from high GC templates using oligonucleotide primers with melting temperatures ~68ºC.

Table 2.6 Standard PCR reaction components

Component	Volume (µL)	[Final]
Vent DNA Polymerase	0.5	2 U
10x ThermoPol Buffer I	5	1x
dNTPs (25 mM)	1	0.5 mM
Template DNA	0.5	10 ng/µL
Forward Primer	1	2 pmol
Reverse Primer	1	2 pmol
DNase free ΣH2O (Sigma)	X (to 45.5 µL)	-

Table 2.7 PCR optimisation conditions

	Reaction Condition				
Component	**1**	**2**	**3**	**4**	**[Final]**
$MgSO_4$ (100 mM)	-	0.5 µL	-	0.5 µL	1 mM
DMSO (Molecular Grade)	-	-	4 µL	4 µL	8% (v/v)
DNase free $ΣH_2O$ (Sigma)	4.5 µL	4 µL	0.5 µL	-	To 4.5 µL

Table 2.8 Standard PCR thermal cycle. In addition to optimisation of the PCR reaction mixture, PCR was carried out at an extension temperature of 68ºC or 70ºC.

Step	Temperature (ºC)	Time	
Initial Denaturation	95	3 minutes	
Denature	95	30 seconds	35 cycles
Extension	68/70	1 minute per Kb	35 cycles
Final Extension	68/70	10 minutes	

2.3.2 Incremental PCR

PCR reactions were prepared as described in Table 2.6. Thermal cycling was carried out according to Table 2.9.

Table 2.9 Incremental PCR thermal cycle

Step	Temperature (ºC)	Time	
Initial Denaturation	95	3 minutes	
Denature	94	30 seconds	0-5 cycles
Annealing	62 ±6	30 seconds	
Extension	66 ±4	1 minute per Kb	
Denature	94	30 seconds	25-30 cycles
Annealing	64 ±6	30 seconds	
Extension	68 ±4	1 minute per Kb	
Final Extension	68 ±4	10 minutes	

2.3.3 Bulk PCR

Bulk PCR to facilitate purification of DNA fragments was carried out using the PCR conditions determined in the standard or incremental PCR protocol (Section 2.3.1 & 2.3.2). Three 50 µL reactions were prepared under identical conditions. The PCR products were then separated by agarose gel electrophoresis (Section 2.4) and the DNA fragments purified using QIAquick Gel Extraction Kit (Qiagen).

2.4 Agarose Gel Electrophoresis

Agarose gel electrophoresis was carried out using the BioRad horizontal gel electrophoresis system. Agarose was prepared to the appropriate concentration according to Table 2.10 by melting agarose into 1x Tris-Acetate EDTA (TAE) buffer, prepared from a 50x TAE stock solution (2 M Tris.HCl pH 7.5, 50 mM EDTA).

Table 2.10 Optimal agarose gel concentration and type for the separation of DNA fragments of specified size

Agarose Concentration (%)	Optimal DNA Fragment Size (bp)	
	Standard Agarose	Low Melting Point Agarose
0.5	700-25000	-
0.8	500-15000	8000-10000
1	250-12000	4000-8000
1.2	150-6000	3000-7000
1.5	80-4000	2000-4000
2	-	1000-3000
3	-	500-1000
4	-	100-500

10 µL DNA ladder was used as a molecular size marker (GeneRuler™ 1 Kb Plus DNA Ladder, NEB-2-log Marker, 50 bp DNA ladder). DNA samples were combined with 10 µL of 6x DNA loading buffer (0.25% (w/v) bromophenol blue, 0.25% (w/v) xylene cyanol, 30% (w/v) glycerol) and 25 µL loaded. The gel was run at 120 V for 45 minutes, until the bromophenol blue band had run approximately 70% down the length of the gel. The gel was stained in ethidium bromide (EtBr) solution (1 µg/mL) for 10 minutes and visualised using a UV transilluminator gel documentation system and the Quantity One computer package (Bio-Rad).

2.5 Sequencing

Plasmid samples were sent for sequencing by GATC Biotech. Sequencing primers were designed as described in Table 2.11. Sequencing primers ordered from Eurofins MWG Operon were prepared to 100 pmol/µL and were provided to GATC Biotech for use.

Table 2.11 Sequencing primers

Primer Name		Sequence		Usage
M13 Fwd	5'	GTAAAACGACGGCCAGTG	3'	pUC18, pHMR3
M13 Rev	5'	GGAAACAGCTATGACCATG	3'	pUC18, pHMR3
T7 Promoter	5'	TAATACGACTCACTATAGGG	3'	pET23b, pET28b
T7 Terminator	5'	TATGCTAGTTATTGCTCAG	3'	pET23b, pET28b
pET Upstream	5'	ATGCGTCCGGCGTAGA	3'	pET28b

2.6 Plasmid Maintenance

All plasmids used in this study were transformed into competent *E. coli* XL10 Gold cells by heat shock transformation as described in section 2.9.1. Plasmid constructs were maintained as glycerol stocks prepared by mixing equal volumes of *E. coli* culture containing the propagated plasmid and sterile glycerol (80% v/v) and stored at -80ºC. Plasmids were purified for use by streaking out glycerol stocks onto LB agar containing the relevant selective antibiotics (Table 2.3). Individual colonies were used for inoculation of LB broths containing the same antibiotics. Plasmid preparations were then carried out according to the QIAprep Spin Miniprep manufacturer's protocol. Plasmids were eluted in 50 µL DNase free ∑H_2O and stored at -20ºC.

2.7 Competent Cell Preparation

Competent cells were prepared as described below and stored at -80ºC for up to 3 months.

2.7.1 Chemically Competent *E. coli*

Cultures of *E. coli* (Table 2.2) were grown to mid-log phase (OD_{600} of 0.5) in LB broth supplemented with magnesium sulphate (2 mM). The cultures were placed on ice for 1 hour and centrifuged at 2,500 *x g* for 15 minutes at 4ºC, the supernatant was discarded.

Pellets were resuspended to 50% of the original volume in ice cold transformation buffer 1 (TBF1) (30 mM potassium acetate, 15 mM calcium chloride, 80 mM manganese chloride, 100 mM rubidium chloride, 15% (v/v) glycerol, pH 5.8) and incubated on ice. Cultures were incubated on ice for 1 hour and then centrifuged at 2,500 *x g* for 15 minutes at 4ºC, the supernatant was discarded. The pellets were resuspended to 5% of the original volume in ice cold transformation buffer 2 (TBF2) (5 mM 3-(N-morpholino) propanesulfonic acid, 4-morpholinepropanesulfonic acid (MOPS), 50 mM calcium chloride, 5 mM rubidium chloride, 15% (v/v) glycerol, pH 6.5) and incubated on ice for 30 minutes. 50 µL aliquots were flash frozen in liquid nitrogen and stored at -80ºC.

2.7.2 Electrocompetent *Mycobacterium*

Cultures of *M. smegmatis* mc^2155 and *Mtb* mc^27000 were grown to mid-log phase (OD_{600} of 0.5) in Middlebrook 7H9 broth as per Table 2.1 and supplemented with Tween 80 (0.02% w/v) and 5 mM magnesium sulphate. The cultures were placed on ice for 30 minutes and centrifuged at 2,500 *x g* for 15 minutes at 4ºC and the supernatant discarded. The pellets were resuspended in 50% of the original volume in ice cold glycerol (10% v/v). The procedure for washing the cells was repeated to a final suspension volume 5% of the original culture volume. Aliquots of 100 µL were flash frozen in liquid nitrogen and stored at -80ºC for use within 6 months.

2.8 Cloning procedures

Filter sterilised DNase free ΣH_2O (Sigma) (0.2 µm filter, Millipore) was used for all molecular biology reactions.

2.8.1 Insert and Vector Preparation

DNA fragments for plasmid insert were generated by PCR amplification from gDNA or from parental plasmid sources. Restriction sites were introduced as part of the oligonucleotide primers used for PCR amplification as described in Table 2.5. Purified DNA fragments and plasmids were prepared for ligation by restriction digestion. Restriction enzymes digestion reactions were performed according to the manufacturer's instructions (New England Biolabs). Typically, reactions were prepared as described in Table 2.12 and incubated at the required temperature for 2 hours.

Table 2.12 Standard restriction digestion mixture

Component	Volume (µL)
Restriction Enzyme I	1
Restriction Enzyme II	1
Buffer (NEBuffer 1-3 or cut smart)	2
Target DNA	10 (0.5 µg)
DNase free ΣH_2O (Sigma)	6
Final Volume	20

Reaction products were separated by agarose gel electrophoresis as described in Section 2.5 and purified using the QIAquick Gel Extraction Kit (Qiagen). Products were eluted in 50 µL ΣH_2O.

2.8.2 Ligation

Ligations were carried out using T4 DNA Ligase (New England Biolabs) according to the manufacturer's protocol. Typically, reactions were prepared as described in Table 2.13 and incubated at 16ºC for 16 hours.

Table 2.13 Standard ligation reaction mixture

Component	Volume
T4 DNA Ligase	1 µL
10x T4 DNA Ligase Buffer	2 µL
DNase free ΣH_2O (Sigma)	6 µL
Plasmid (Digested)	50 ng
Fragment (Digested)	3:1 Ratio
Final Volume	20 µL

Ligation reactions were transformed into competent cells prepared as described in Section 2.9.1 by heat shock transformation or by electroporation as described in section 2.9.2 followed by culturing on selective antibiotic agar (Table 2.1 and 2.3). Transformants were screened for plasmid insertion by plasmid purification and restriction digestion (Section 2.8.1).

2.9 Transformation

2.9.1 Heat-Shock Treatment

Chemically competent *E. coli* cells prepared as described in Section 2.7.1 were thawed on ice. Cells for transformation with pure plasmids were mixed with 1 µL (~1 µg) of the required plasmid in a microcentrifuge tube and were incubated on ice for 60 minutes. For transformation with plasmids constructed by ligation, the full volume of the ligation reaction was mixed with the defrosted cells. The mixture was heat shocked in a water bath at 42ºC for 1 minute, then returned to ice for 5 minutes. After addition of 200 µL LB broth, cells were incubated at 37ºC for 1 hour. The cells were then plated across LB agar plates containing the required antibiotic (Table 2.3) and incubated at 37ºC overnight or for a minimum of 16 hours.

2.9.2 Electroporation

Electrocompetent cells prepared as described in Section 2.7.2 were defrosted on ice. The cells were mixed with 1 µl (~1 µg) of plasmid in an ice cold 1 mm electroporation cuvette (Bio-Rad UK) and incubated on ice for 30 minutes. The cells were electroporated using a Bio-Rad Gene Pulser II (2500 kV, 600 Ω, 50 µF). Typical pulse lengths were over 13 ms. Relevant broth (200 µL) was added to electroporated *Mtb* $mc^2$7000 and *M. smegmatis* $mc^2$155 cells and incubated overnight at 37ºC. The cells were then plated on 7H11 agar plates containing the required antibiotic (Table 2.3) and supplements before incubation at 37ºC for 5-24 days.

2.10 Expression studies

Plasmid constructs were transformed into expression strains as in Section 2.9.1 or 2.9.2. Colonies from expression strains obtained from transformation plates were used to inoculate 5 mL LB broth cultures containing selective antibiotic followed by agitated culturing (200 rpm) for 16 hours or overnight at 37ºC. The grown culture was used to inoculate (1% v/v) 1 L of LB broth and incubated at 37ºC to an OD_{600} of 0.6. The expression was allowed to cool down, then induced with 1 mM isopropyl β-D-1-thiogalactopyranoside (IPTG) followed by agitated culturing (200 rpm) for 16 hours or overnight at 37ºC or 16ºC. The next day, bacterial cell cultures were harvested by centrifugation at 4ºC at 4,000 rpm. Bacterial pellets were collected and stored in -20ºC for further expression studies.

2.10.1 Cell lysis

Bacterial cell pellets were resuspended in lysis buffer (Table 2.14 and 2.15) and lysed by sonication at 60% amplitude for 15 seconds on, 30 seconds off for 6 cycles to obtain crude extracts. Lysed cells were centrifuged at 27,000 *x g* for 1 hour to obtain the clarified extracts.

Table 2.14 Lysis and equilibrium buffers for Rv0089/Rv1882c

Component	Lysis Buffer	Equilibrium Buffer
Tris.HCl pH 7.4	50 mM	50 mM
NaCl	500 mM	50 mM
Imidazole	50 mM	25 mM
Glycerol	10%	-
2-Mercaptoethanol	5 mM	-

Table 2.15 Lysis and equilibrium buffers for Rv2715/Rv3177

Component	Lysis Buffer	Equilibrium Buffer
Tris.HCl pH 9.0	50 mM	50 mM
NaCl	250 mM	50 mM
Imidazole	10 mM	50 mM
Glycerol	5%	-
L-arginine	100 mM	-

2.10.2 Immobilised metal affinity chromatography (IMAC) purification

Clarified recombinant protein preparations were used in IMAC nickel purification procedures. The HiTrap FF (GE Healthcare, USA) was equilibrated with the equilibrium buffer (Table 2.14 and 2.15) and the crude extract applied to the column. The column was washed with wash buffers made up of 50 mM Tris.HCl pH 7.4 or 9.0 (depending on the

protein), 50 mM NaCl. An imidazole salt concentration gradient made in the correct wash buffer was then applied to the column (5 mM, 10 mM, 25 mM, 50 mM, 75 mM, 100 mM, 150 mM, 200 mM, 300 mM, 500 mM) and finally 0.5 M EDTA. Washes were collected for analysis by SDS-PAGE.

2.11 SDS-PAGE

2.11.1 Gel casting (Mini-Protean 3 Gel Unit)

SDS polyacrylamide gel electrophoresis (SDS-PAGE) resolving gels were prepared to the required concentration as described in Table 2.16 and were cast in the gel casting assembly unit as per the manufacture's protocol. Gels were overlaid with isopropanol until solidified. The SDS-PAGE stacking gel was prepared as described in Table 2.17. After removing the isopropanol from resolving gels, the stacking gel mixture was applied over the top of the resolving gel and a 10-well comb inserted.

The set gels were placed into the gel cassette assembly unit and were submerged in 1x SDS running buffer, prepared from a 10x SDS running buffer stock solution (250 mM Tris.HCl pH 8.3, 1.9 M glycine, 1% (w/v) SDS).

Table 2.16 Resolving gel mix for the preparation of 2x SDS-PAGE gels (8 cm x 7.3 cm)

	Volume (mL)			
Component	**8%**	**10%**	**12%**	**14%**
Acrylamide	2	2.5	3	3.5
DNase free ΣH2O (Sigma)	5.5	5	4.5	4
SDS Resolving buffer (3 M Trizma base, 0.4% (w/v) SDS, pH 8.8)	2.5	2.5	2.5	2.5
N,N,N',N'-tetramethylethylenediamine (TEMED)	0.015	0.015	0.015	0.015
Ammonium persulphate (APS) (10% w/v)	0.075	0.075	0.075	0.075

Table 2.17 Stacking gel mix for the preparation of 2x SDS-PAGE gels (8 cm x 7.3 cm)

Component	Volume (mL)
Acrylamide	0.5
DNase free ΣH_2O (Sigma)	2.5
SDS Stacking buffer (0.5 M Trizma base, 0.4% (w/v) SDS, pH 6.8)	1
TEMED	0.015
APS (10% w/v)	0.045

2.11.2 Running SDS-PAGE

PageRuler^{TM} Plus Prestained Protein Ladder (5 µL) was used as a molecular weight marker. The protein sample (15 µL) was mixed with 5 µL 4x SDS loading buffer (200 mM Tris.HCl pH 6.8, 400 mM DTT, 8% (w/v) SDS, 40% (w/v) glycerol and 0.4% (w/v) bromophenol blue) and boiled at 100ºC for 5 minutes. Loaded gels were run at 20 mA per gel, plus an additional 5 mA, for 45 minutes, or until the blue dye reaches the bottom of the gel.

2.11.3 Gel staining and de-staining

Gels were submerged in 0.1% (w/v) Coomassie Brilliant Blue R-250 (50% (v/v) methanol, 10% (v/v) glacial acetic acid, 40% ddH_2O) for 30 minutes and transferred into a de-stain solution (40% (v/v) methanol, 10% (v/v) glacial acetic acid and 50% ddH_2O) for 1 hour, or until background stain was sufficiently removed.

2.11.4 Protein dialysis

Proteins were dialysed in dialysis buffer (50 mM Tris.HCl pH 7.4 or 9.0, 50 mM NaCl), depending on the protein, to remove excess imidazole. First dialysis was done overnight, followed by two additional changes of buffer for 2 hours each.

2.11.5 Concentration of protein

Dialysed protein was concentrated using Amicon® Ultra-4 10K Centrifugal filter. Protein was added into the filter tubes and centrifuged at 4,000 *x g* at 4ºC until the desired concentration is achieved.

2.12 Minimum inhibition concentration (MIC) determination

RIF, INH and JJH-110AA compounds were all prepared in dimethyl sulfoxide (DMSO). Ten milligrams per millilitre (10 mg/mL) was prepared as the initial stock solution. Part of the stock was further diluted to 1 mg/mL with the same DMSO. Sterilised Middlebrook 7H9 broth (100 µL), supplemented with 10% OADC, 0.5% (v/v) glycerol, 24 mg/ml pantothenate and 20% casamino acid, was added into the wells of the sterilised 96-well U-bottom plates from column 1-12 using a multichannel pipette, by carefully opening the plate half way to avoid contamination. Another 100 µL of the media was added to all the wells in column 1 only, making column 1 having a total of 200 µL of media. In A-D of column 12, 100 µL of the media was added to serve as a negative control. To column 1, the tested compounds were added in quadruplet, with the first 2 wells having a concentration of 1 mg/mL, while the remaining 2 had a concentration of 10 mg/mL. 2-fold serial dilutions were performed across the plate, making sure there was a total mix of the compounds in each well before transferring 100 µL to the next column. The dilution was done to the 11th column and the final 100 µL discarded along with the tips. Resulting in 100 µL of liquid medium and compound across the wells, except the negative control.

After growing the test organisms to an OD of 0.2, the bacterial cell suspension (inoculum) were diluted 1:25 in growth media and added to the 100 µL of liquid medium and compound in column 1-11 and to E-H of column 12 which represents a positive growth

control. Nothing was added further to A-D of column 12 to avoid invalidating the experiment. All plates were sealed with parafilm™ and incubated at 37ºC in an atmosphere of 5% CO_2 for 5 days. Aseptically prepared resazurin solution (0.2 % w/v), (15 µl) was added to each of the wells. The plates were re-incubated at 37ºC for 24 hours. Any well which turned pink indicated the ability of the test organism to utilise resazurin and therefore indicated growth.

2.13 Spontaneous resistant mutants' generation

Mtb was grown on Middlebrook 7H11 agar plates supplemented with 10% (v/v) OADC enrichment, 0.5% (v/v) glycerol, 24 mg/mL pantothenate (1:1000 dilutions) and 20% casamino acid (1:1000 dilutions). The organism was allowed to grow for 4 weeks at 37ºC. The minimum inhibitory concentration of the tested compounds [RIF, INH and JJH-110A] were determined on solid media first by plating out 10 µL of dilutions of 10^4, 10^3, 10^2 and 10^1 of mid log phase bacteria onto the agar plates with increasing concentrations of the compounds. Spontaneous resistant mutants of the *Mtb* $mc^2$7000 were generated by plating 10^8 mid log cells (A_{600nm} of 0.8-1.0) onto agar plates containing 2.5, 5.0 and 10 times the MIC of each compound and incubated for 4 weeks at 37ºC. Resistance from these compounds was confirmed by plating 10 µL of the spontaneous resistant mutants and the parental strain, grown in 7H9 media in the absence of compounds, onto agar plates containing 5 times the MIC of each compound.

2.14 Genomic DNA (gDNA) Preparation from *Mycobacterium tuberculosis*

Mid-log (OD 0.6-0.8) culture (25 mL) was harvested by centrifugation for 30 mins, at room temperature (20ºC) at 3,500 rpm. The supernatant was discarded, and pellets re-

suspended in 450 µL GTE-RNase buffer (200 µL RNase A + 20 mL GTE buffer) (GTE: 25 mM Tris pH 8, 10 mM ethylenediaminetetraacetic acid (EDTA) pH 8, 50 mM Glucose). 50 µL of lysozyme (from 10 mg/ml stock) was added and the resultant solution incubated overnight at 37ºC without shaking. The following day, 100 µL 10% sodium dodecyl sulphate (SDS) (10% w/v) was added and the resultant solution gently mixed by turning upside down 10 times. 20 µL Proteinase K (15 mg/mL stock) was also added and mixed gently. This was incubated at 55ºC for 3 hours. After the 3 hours, 10 µL RNase A from 10 mg/mL stock solution was added followed by an incubation period of 30 minutes at 37ºC without shaking. This was immediately followed by the addition of 200 µL 5 M sodium chloride ($NaCl_2$) and 1 mL Chloroform:Isoamyl alcohol 24:1 in quick succession and mixed briefly and the resulting mixture centrifuged at 13,000 rpm for 10 minutes to form a bi-phase. The upper aqueous layer was carefully transferred, avoiding interphase, into a clean microcentrifuge tube. 1 mL of Chloroform: Isoamyl alcohol 24:1 was added into the tube and spun for 13,000 rpm 5-10 minutes. The upper aqueous layer was removed again into another clean microcentrifuge tube and 0.7 volume (~700 µL) of ice-cold isopropanol added and gently mixed by inversion to precipitate gDNA. This was then centrifuged at 4ºC 13,000 rpm for 30 minutes (minimum) to pellet the gDNA. The supernatant was discarded, and the resultant cell pellets washed with 70% (w/v) ice cold ethanol by centrifuging at 4ºC 13,000 rpm for 30 minutes. Ethanol was discarded using a micropipette leaving the pellet to air dry for 15 minutes. Pellets were re-suspended in 50 µL DNase free ΣH_2O and gDNA Nano-dropped to check and record DNA concentration. Samples were stored at -20ºC for further analysis.

Chapter 3

Identification and molecular characterisation of ω-methyl-malonyl-transferase (BioC) in *Mtb*

3 Identification and molecular characterisation of ω-methyl-malonyl-transferase (BioC) in *Mtb*

3.1 Introduction

Many enzyme catalysed reactions, synthesise biomolecules and chemical groups using S-adenosylmethionine (SAM) as a substrate (Roje, 2006). Methyl group transfer by SAM is one of the most notable biochemical reactions aided by SAM-dependent methyl transferase. SAM is derived from two ubiquitous biological compounds, nucleotide adenosine and amino acid methionine, which were present in the early form of living cells and even before life existed (Waddell *et al*., 2000). Cellular organisms utilise different SAM enzymes in the synthesis of many essential metabolic intermediates.

Methylation of biochemical reactions by SAM leads to covalent modifications for substrates such as chloride, bromide, oxidized arsenic, iodine ions, rRNA, tRNA and other proteins, where methylation can regulate signal interactions between proteins and other macromolecules (Thomas *et al*., 2004, Hopper and Phizicky, 2003, Anantharaman *et al*., 2002, Kouzarides, 2002, Saxena *et al*., 1998, Wuosmaa and Hager, 1990). There are several other reactions that requires SAM apart from methylation transfer. Such reactions include amino alkyl, ribosyl, methylene, 5'deoxyadenosyl radical formation, SAM decarboxylation, *de novo* synthesis of SAM from adenosine and methionine. Several other interactions between SAM and non-enzymatic proteins have also been recorded where SAM effects a regulatory change in the effector proteins (Kozbial and Mushegian, 2005). In plants, SAM also acts as a precursor to reactions involving metal ion chelating compounds nicotinamide and phytosiderophores, biosynthesis of spermidine and as a precursor to the gaseous plant hormone ethylene. It also catalyses 5'-

deoxyadenosyl radicals utilised as intermediates in other reactions (Roje, 2006). Despite the knowledge on the different functions of SAM and the three-dimensional structure of the different classes of SAM-dependent enzymes, the existing relationship between SAM-binding domains in terms of structure, function and evolution, remains unclear.

Proteins and nucleic acid modification by post-translation, post-transcription and epigenetics are vital to the activity of proteins and nucleic acids. Enzymatic modifications, such as phosphorylation, acetylation and methylation have been identified as essential biochemical processes within organisms and enzymes involved in such processes and are excellent drug targets with some of the enzymes playing key roles in pathogenicity. Methyltransferases are a good example of such enzymes affecting cellular function and physiology by modulating the methylation of proteins and nucleic acids and altering epigenomes (Lu *et al*., 2012).

A complete pathway for biotin synthesis is not fully elucidated in any organism, especially the early stages of the pathway (Lin *et al*., 2010). The most established knowledge of this pathway has been characterised in *E. coli* (Lin *et al*., 2010) (Figure 3.2) and *Bacillus subtilis* (Bower *et al*., 1996). In these species pimelic acid, a seven carbon dicarboxylic acid has a thioester linkage to one of its carboxyl groups during its assembly with pimeloyl-CoA serving as a thiol moiety in fatty acid synthesis (Cegielski, 2010, Stok and De Voss, 2000). Progression of the pathway starting at the *de novo* synthesised pimeloyl-thioester, are well elucidated in almost all organisms that perform this synthesis. This synthesis requires atoms that come from disparate, acetate, alanine, CO_2, S-adenosylmethionine (SAM) and sulphide which give rise to the completed biotin molecule. SAM contributes the nitrogen atom adjacent to C-7 and the other nitrogen atom is contributed by alanine. The labelling pattern conforms with pimelic acid moiety

formation in which there is a head to tail incorporation of three intact acetate units as found in fatty acid synthesis and other acceptable pathways from tryptophan, lysine, diaminopimelic acid and elongation of 2-oxoglutarate (Ifuku *et al.*, 1994, Sanyal *et al.*, 1994). The ^{13}C labelling analysis ensures that the free pimelic acid is completely eliminated in biotin biosynthesis. This is possible because the carboxyl groups of pimelic acid cannot be identified stereo-chemically and as such C-1 and C-7 carbon atoms of biotin would have similar labelling pattern, if the free pimelic acid is an intermediate (Figure 3.1). Therefore one of the carboxyl groups covalently links to another moiety of the pimelate so the pimelate can be assembled with a thioester most likely serving as the linkage (Cronan, 2014, Ifuku *et al.*, 1994, Sanyal *et al.*, 1994).

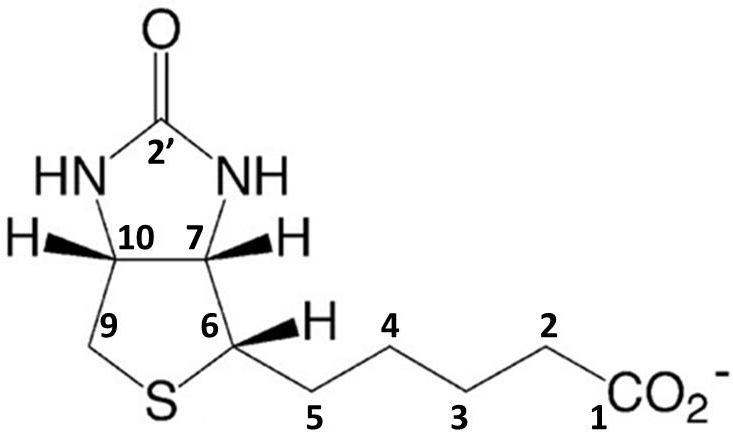

Figure 3.1 Schematic representation of ^{13}C labelling of biotin

The early steps of biotin synthesis have recently been deduced, while the late steps were elucidated many years ago (Figure 3.2). This is evident in the fact that the late steps proteins of biotin synthesis, BioA, BioB, BioD and BioF, have been well studied to the structural level, whereas BioC and BioH, which are early steps enzymes, are poorly studied or understood. Since *E. coli* readily makes use of each of the late step

intermediates, sequence of steps in the late pathway were readily deduced (Cronan, 2014). The functions of BioC and BioH however were not made clear for a further 50 years.

BioC acts on malonyl-CoA (or glutaryl-CoA) in which a free carboxyl group is converted to its methyl ester, then transferred to a methyl group from SAM (Figure 3.2). This methylation of malonyl CoA at its ω-carboxyl group cancels the net charge on the carboxyl groups then provide a methyl carbon that mimics the methyl of the normal acyl chains and the SAM loses its methyl group to form S-adenosyl-L-homocysteine (SAH). The malonyl-CoA acts as biotin precursor and enters the fatty acid biosynthetic pathway (FAS) as the biotin primer. Depending on the start substrate, the malonyl-CoA undergoes series of cycles in the FAS to form ω-methoxy-pimeloyl-ACP. The methyl ester on the ω-methoxy-pimeloyl-ACP is then cleaved by BioH to form pimeloyl-ACP, the biotin synthesis precursor. Therefore, BioH demethylates the pimeloyl-ACP methyl ester and frees the carboxylic group that eventually attach biotin to the metabolic enzymes where it performs its key metabolic roles (Figure 3.2) (Cronan, 2014, Cegielski, 2010, Chapman-Smith and Cronan, 1999).

Several studies have demonstrated an essential role of biotin biosynthesis in the growth and survival of several microorganisms, including mycobacteria within macrophages. Deletion of BioA involved in *de novo* biotin biosynthesis in *Mtb* (*Mtb*Δ*bioA*) was demonstrated to be highly attenuated in macrophage studies (Ikeda *et al*., 2017). Therefore, the essentiality of this core metabolite defines biotin synthesis as a viable target for novel anti-tubercular agents.

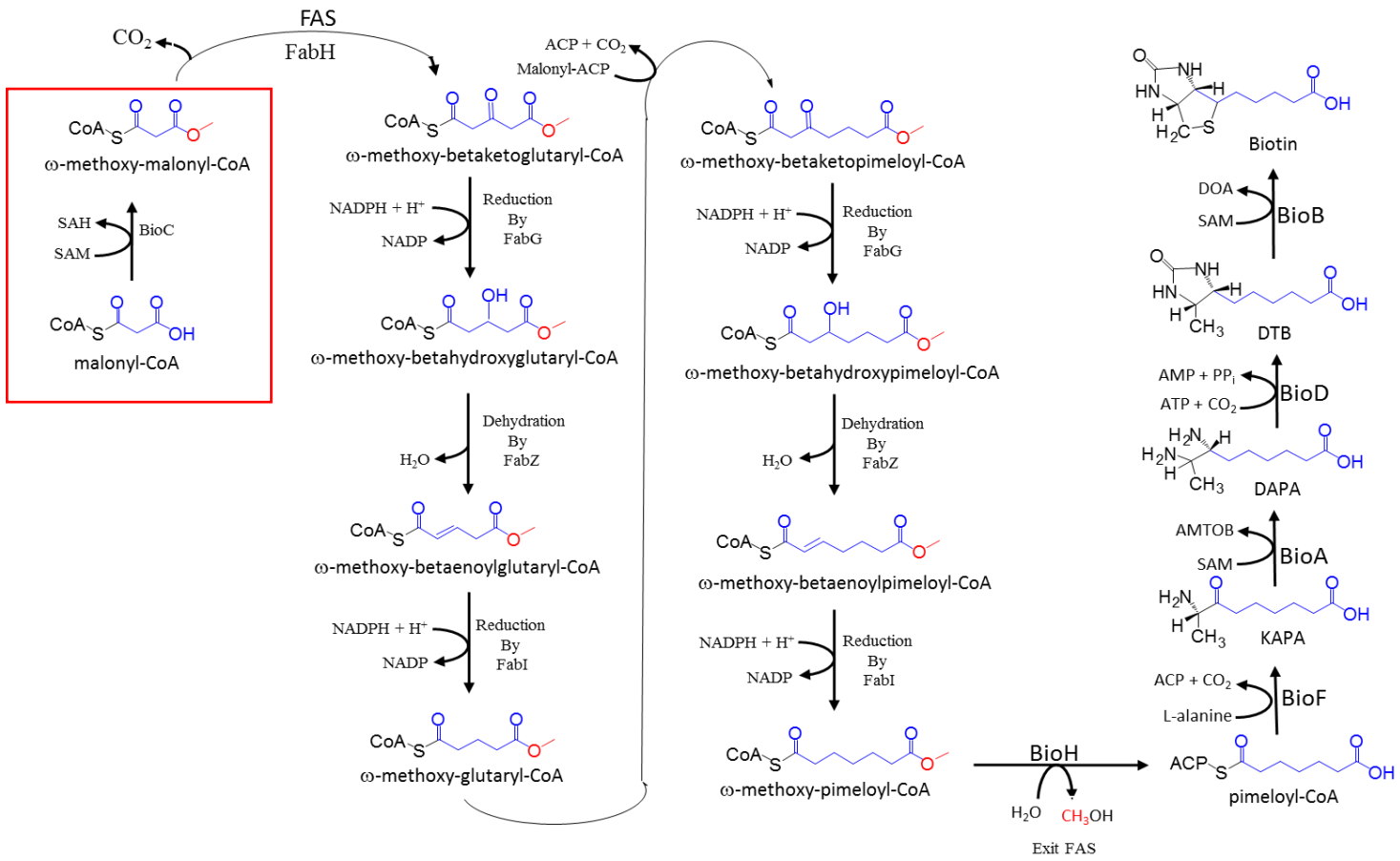

Figure 3.2 Current proposed pathway of biotin synthesis in *E. coli*. The primer molecule malonyl-CoA is methylated by BioC at its ω-carboxyl group. The resultant ω-methoxy-malonyl-CoA methyl ester hijacks the fatty acid biosynthetic pathway and act as a priming unit, instead of the acetyl-CoA in fatty acid synthesis which gives rise pimeloyl-ACP methyl ester. Pimeloyl-ACP is formed when BioH cleaves to the ester to prevent further elongation and the product is utilised by BioF to make KAPA (7-keto-8-amino pelargonic acid) that starts biotin synthesis. KAPA is catalysed by BioA to form DAPA (7,8-diaminopelargonic acid) which is further catalysed by BioD to form dethiobiotin (DTB) before biotin is finally formed through the enzyme BioB (Adapted from Lin *et al*., 2010).

3.2 Aims and objectives

The aims and objectives of this chapter are as follows:

1. The isolation and purification of recombinant *mt*BioC enzyme from *E. coli* expression strains. This will be achieved with the following objective:

    - *mt*BioC will be isolated and purified from different *E. coli* expression strains. Purification will involve the use of Immobilized Metal Affinity Chromatography (IMAC) that utilises Nickle charge His-trap columns (HiTrap FF, GE Healthcare).

2. To perform biochemical studies on *mt*BioC enzyme. This will be achieved through the following objectives:

    - Biochemical studies will be performed on *mt*BioC to determine its ability to utilise SAM as part of a methyl transferase reaction.

    - A special assay designed for methyl transferases will be utilised. This assay would be able to determine the optimum temperature of the enzyme, its optimum pH, its ability to utilise malonyl-CoA as a substrate, its ability to utilise different metal ions for its activity and the action of an inhibitor.

    - Perform enzyme kinetics (Michaelis-Menten) on purified *mt*BioC.

3.3 Methods

Recombinant protein bio-assaying was developed as part of this chapter and specific biochemical characterisation experiments are described in this section. The MTase-Glo™ Methyl transferase Assay (Cat# V7601, Promega, UK) was utilised to assess the production of SAH from the degradation of SAM by *mt*BioC.

3.3.1 SAH standard curve

A SAH standard curve was developed to quantify the conversion of SAM into SAH by the recombinant *mt*BioC. This assay created measurable correlation between luminescence and SAH concentrations. Standardised buffer mixes were used throughout the assay (Table 3.1). The assay was performed as per the manufacturer's protocol using the standard buffers.

Table 3.1 Buffers for SAH standard curve

[Start]		[Final]	mL Required 4x	mL Required 1x
1 M	Tris.HCl pH 7.4	100 mM	4	1
1 M	$MgCl_2$	20 mM	0.8	0.2
2 M	NaCl	100 mM	2	0.5
	ΣH2O		3.2	8.3
	Final volume		10	10

The luminescent signal generated by the MTase-Glo™ Methyl transferase Assay is proportional to SAH concentration. To correlate luminescence and SAH concentration, SAH standard curve was generated (0 µM to 10 µM) using either raw luminescence (i.e., luminescence without subtracting background) or background-subtracted luminescence. SAH standards were used to generate a standard curve by plotting luminescence (Y axis) against SAH concentration (X axis) and generate a linear regression graph. The linear

equation calculated from the SAH concentrations can then be used to calculate the concentration of SAH in a sample.

3.3.2 SAM assay *mt*BioC protein concentration determination

All reactions were performed in triplicate. Master Mix set ups were utilised to ensure parity across all the assays and hopefully reduce possible errors (Table 3.2).

Table 3.2 Master Mix for standard curve (40 assays)

[Start]		[Final]	µL Required	Master Mix
1 M	Tris.HCl pH 7.4	100 mM	1	40
1 mM	SAM	10 µm	0.1	4
1 M	$MgCl_2$	20 mM	0.4	16
2 M	NaCl	100 mM	0.5	20
10 mM	Malonyl-CoA	100 µM	0.2	8
	ΣH2O		7.8	312
	Final volume		10	400

Using a 96-well plate, 150 µL of the *mt*BioC was added to H1, while 75 µL of 1x buffer was added to H2-H12. The protein was titrated across the plate (H column) in a 2:1 dilution in 1x buffer (Table 3.1) by transferring 75 µL across the wells and discarding at column 11, leaving column 12 as negative control. 10 µL of the protein titration was transferred to each well in A, B and C, i.e. H1 into A1, B1, and C1 and repeated for H2 through to H12.

All SAM dependent assays followed the subsequent protocol; 10 µL of the master mix (Table 3.2) was added to each assay well and the resultant mixture incubated at 37ºC for 30 minutes. A 10x MTase-Glo reagent (stored at -80ºC) was diluted 2:1 in sigma water ($ΣH_2O$) and 5 µL added to all reaction wells. The reaction was centrifuged at room temperature for 1 minute at 1,000 rpm, then incubated at room temperature for 30 minutes.

A 25 µL MTase-Glo detection reagent was added to all assay wells and centrifuged at room temperature for 1 minute at 1,000 *x g* and incubated at room temperature for a further 30 minutes. Light production was measured using a luminometer (UMIstar® Omega microplate reader, BMG LABTECH).

3.3.3 Biochemical characterisation assay of *mt*BioC

The specificity of *mt*BioC methyl transferase was determined using glutaryl-CoA (100 µM), malonyl-CoA (1000 µM – 1 µM), and sinefugin (1000 µM – 1 µM) as an inhibitor. All experiments were set up in triplicates. The reactions were incubated at 37ºC for 30 minutes. SAH production was assayed as per Section 3.3.1.

A pH titration was performed to find the optimum pH that gives maximum *mt*BioC SAH production. Sodium acetate was analysed at pH of 4.0, 4.5 and 5.0. Sodium phosphate was analysed at pH of 5.5, 6.0, 6.5 and 7.0, while the Trizma base was analysed at 7.5, 8.0, 8.5 and 9.0 pH. The master mix was amended to use the relevant buffer, analysis was performed in triplicate. The plate was set up as previous assays, with 10 µl of the protein and assessed for SAH production as per Section 3.3.2.

The metal ion dependency of *mt*BioC was analysed in Trizma base at pH 7.4. The ion dependency was tested with EDTA and in Na, K, Mg, Mn, Zn, Cu, Ca, Ni and Fe. EDTA and the ions were analysed at a concentration of 20 mM each. The master mix was amended to use the relevant buffer, analysis was performed in triplicate. The plate was set up as previous assays, with 10 µl of the protein and assessed for SAH production as per Section 3.3.2.

3.3.4 Determination of K_m and V_{max}

The K_m and V_{max} values of the enzyme were also determined. First, the rate of catalysis (reaction velocity) was measured experimentally as set up in section 3.3.1. The

concentration of the substrate, glutaryl-CoA, was measured as set up in section 3.3.3. The velocity, V, of the reaction was determined at different concentrations of the substrate [S] (malonyl-CoA). The K_m (Michaelis-Menten constant) and Vmax values were determined using the Michaelis-Menten equation:

$$V = \frac{V_{max}[S]}{K_m + [S]}$$

The Michaelis-Menten equation was rearranged to give the Hanes-Woolf equation:

$$\frac{[S]}{V} = \frac{1}{V_{max}} \cdot \frac{[S] + K_m}{V_{max}}$$

Thus, using the Hanes-Woolf equation, plotting the ratio of the initial substrate concentration [S] to the velocity, V, against [S] will give a straight line graph that is used to determine K_m and V_{max}.

3.3.5 Trypsin digest method

The protein band was excised with a scalpel and the band cut into 1x1 to 2x2 mm pieces. Pieces were placed into a clean receiver tube and 200 µl of destaining solution (made up of 80 mg NH_4HCO_3, 20 mL acetonitrile and 20 mL ddH_2O, all stored at 4 °C for 2 months) was added to the gel pieces. This was incubated at 37 °C for 30 minutes with shaking. The stain was discarded and the staining and destining repeated. A 30 µL reducing buffer (3.3 µL Tris[2-carboxyethyl] phosphine, 30 µL digestion buffer [10 mg NH_4HCO_3, 5 mL ddH_2O - final concentration of 25 mM], with a final concentration of 50 mM) was added to the tube containing the sample and incubated at 60 °C for 10 minutes. The sample was allowed to cool and the reducing buffer was discarded. 30 µL of alkylation buffer (7 mg Iodoacetamide, 70 µL water, making 5X stock with final concentration of 500 mM. Dilute 7 µL of the stock with 28 µL of digestion buffer to get final alkylation buffer) was added to the tube and incubated in a dark room at room temperature for 1 hour. The alkylation buffer was removed and discarded and the sample washed with 200 µL destining buffer.

The tube containing the mixture was incubated at 37°C for 15 minutes with shaking. Destain was removed and discarded and the previous step with the alkylation buffer repeated. 50 µL of acetonitrile was added to shrink the gel pieces. This was incubated for 15 minutes at room temperature. The acetonitrile was carefully removed and gel pieces allowed to air-dry for 5-10 minutes. Swell the tube by adding 10 µL activated trypsin (dilute 1 µL of trypsin working solution [5 µL hydrated trypsin stock] with 9 µL digestion buffer, final concentration 10 ng/µL) and incubate at room temperature for 15 minutes. 25 µL of digestion buffer is added to the tube and incubated at 30°C overnight with shaking. The digestion mixture was removed and placed in a clean tube ready for electrospray ionization mass spectrometry.

3.4 Results and Discussion

The most probable candidate for BioC function in *Mtb* was identified using UniProtKB - P12999 (BIOC_ECOLI) protein sequence and the BLASTP function on the Tuberculist web server to identify possible candidates - (http://genolist.pasteur.fr/TubercuList/genome.cgi).

	Bit Score	E Value
M. tuberculosis H37Rv|Rv0089|Rv0089 POSSIBLE METHYLTRANSFERASE	59	1e-11
M. tuberculosis H37Rv|Rv1405c|Rv1405c PUTATIVE METHYLTRANSFERASE	46	8e-07
M. tuberculosis H37Rv|Rv3342|Rv3342 POSSIBLE METHYLTRANSFERASE	45	1e-06
M. tuberculosis H37Rv|Rv0558|menH PROBABLE UBIQUINONE/MENAQUINON	44	3e-06
M. tuberculosis H37Rv|Rv3038c|Rv3038c CONSERVED HYPOTHETICAL	43	9e-06

Rv0089 showed the highest degree of similarity. Sequence alignment showed that Rv0089 has 47 % similarity and 36 % identity to *ec*BioC (Figure 3.3).

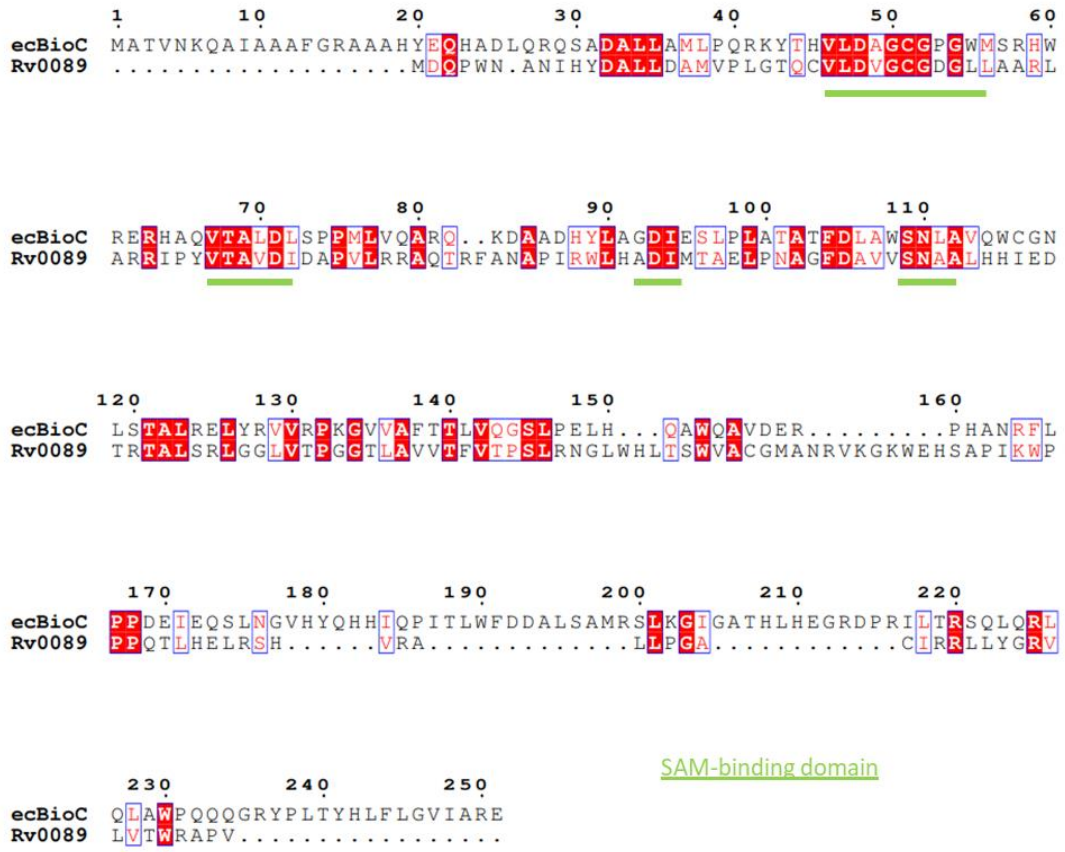

Figure 3.3 Protein Clustal Omega alignment of the most likely BioC candidate in *Mtb* versus the *E. coli* BioC homolog.

3.5 PCR amplification of *mt*BioC

DNA sequence of *mt*BioC *rv0089* (Tuberculist) were utilised to design PCR primers (forward 5' aaaaaacatatggatcaaccgtggaacgcc 3'; reverse 5' aaaaaaaggcctttagacgggtgcgcgcc 3') designed to introduce 5' *Nde*I and 3' *Hind*III restriction sites (underlined) that would allow subsequent cloning of the gene of interest into pET28b and pHMR3 expression vectors.

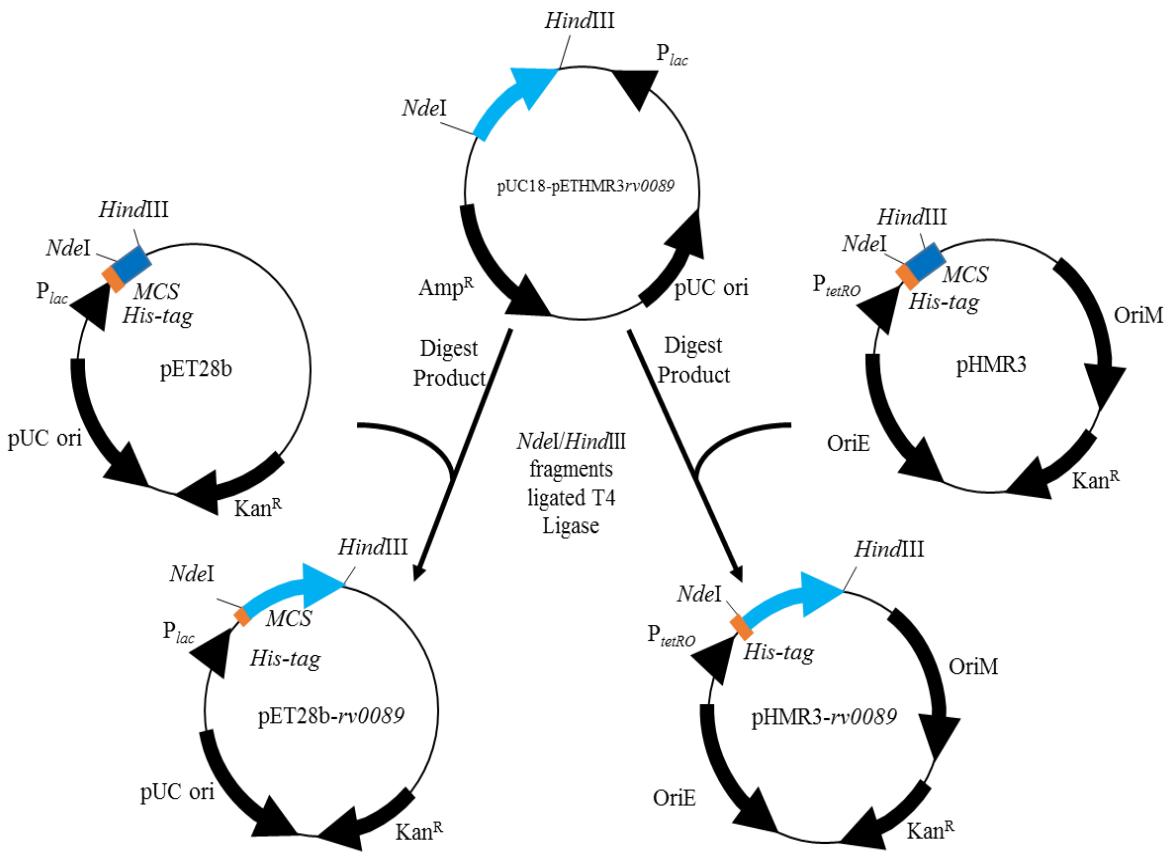

Figure 3.4 **Schematic representation of the *rv0089* expression plasmid construction.** Plasmid map construction of pET28-rv0089 and pHMR3-rv0089. In both cases the rv0089 gene was amplified and cloned into kanamycin resistant pET28b vector and *E. coli* shuttled pHMR3 vector, both digested with *Nde*I/*Hind*III

The genomic DNA template was prepared from *Mtb* H37Rv and used for DNA amplification. PCR optimisation protocols were performed as outlined in Section 2.3.1 (Figure 3.5). The presence of a DNA fragment was observed with the predicted 594 bp amplicon corresponding to the *rv0089* gene.

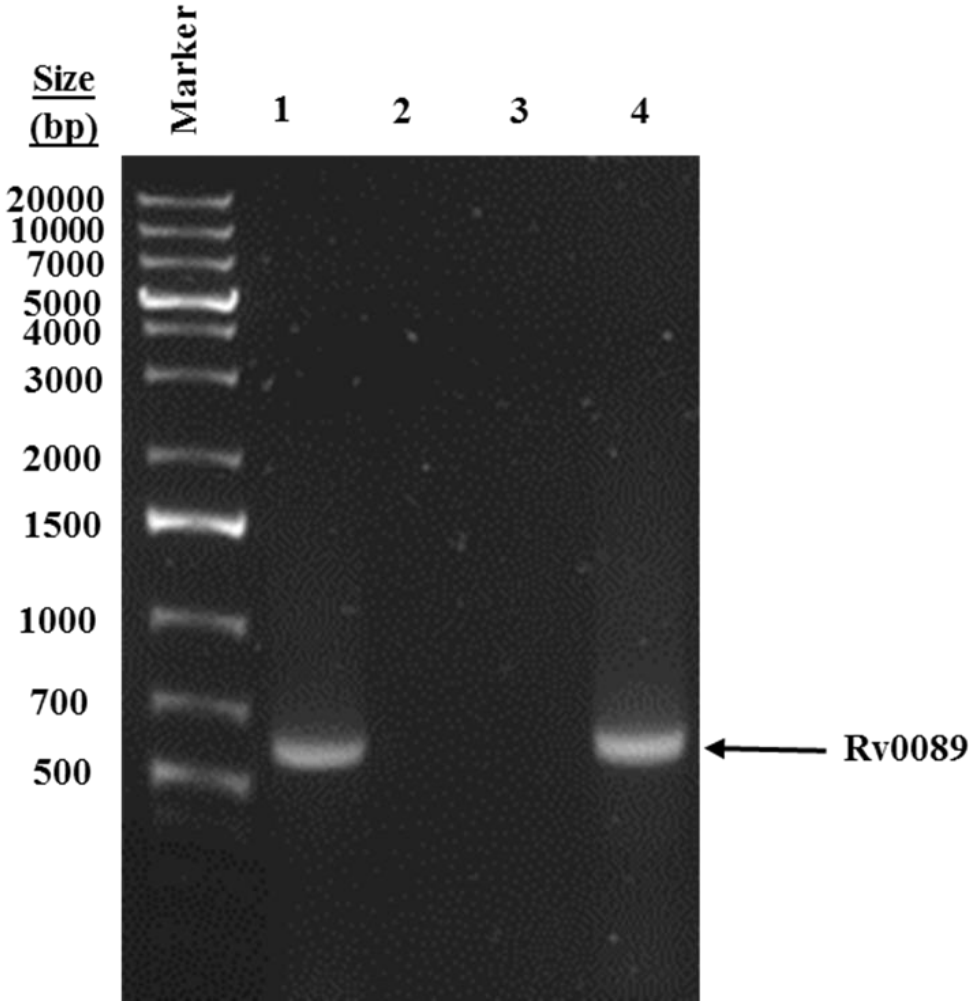

Figure 3.5 **Agarose gel electrophoresis of PCR optimisation for *rv0089*.** This resulted in a visible band of the right size 594 bp; GeneRuler 1 Kb Plus marker

Condition 4 (Table 2.7) was therefore used as the optimal PCR conditions for the amplification of the DNA sequence where the Vent^{TM} DNA polymerase buffer was supplement with 1 mM $MgSO_4$ and 8% DMSO. The *rv0089* was amplified by bulk PCR and purified from agarose for further use by QIAquick Gel Extraction.

The purified DNA fragment was ligated using T4 ligase (Section 2.8.2) into *Sma*I-cut pUC18 and the mixture used to transform *E. coli* TOP10; this was repeated a number of times but no visible transformants were observed. It was concluded after a series of test transformations that the cell line was highly inefficient and as a result the decision was made to utilise $CaCl_2$ competent *E. coli* XL10 Gold as a replacement in this procedure. This resulted in the successful observation of visible colonies after 16 hour incubation at 37ºC. Blue/white screening analysis was performed on the resulting pUC18-*rv0089* ligation. The 594 bp amplicon corresponding to the *rv0089* gene was successfully cloned into pUC18 which was confirmed by restriction digest of the purified plasmid from white colonies (Figure 3.6).

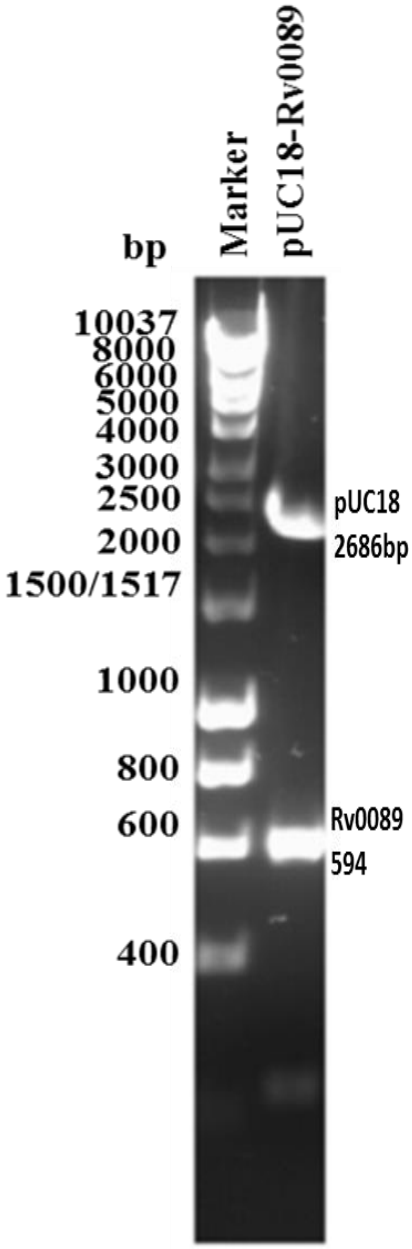

Figure 3.6 Double digest *Nde*I/*Hind*III restriction enzyme screening of pUC18 construct containing *rv0089*

The resulting plasmid was sequenced by Sanger sequencing using standard pUC18 primers at GATC (*www.gatc-biotech.com)*. The sequencing results showed that the cloned fragment was *rv0089* with the correct predicted sequence and restriction sites (Figure 3.7).

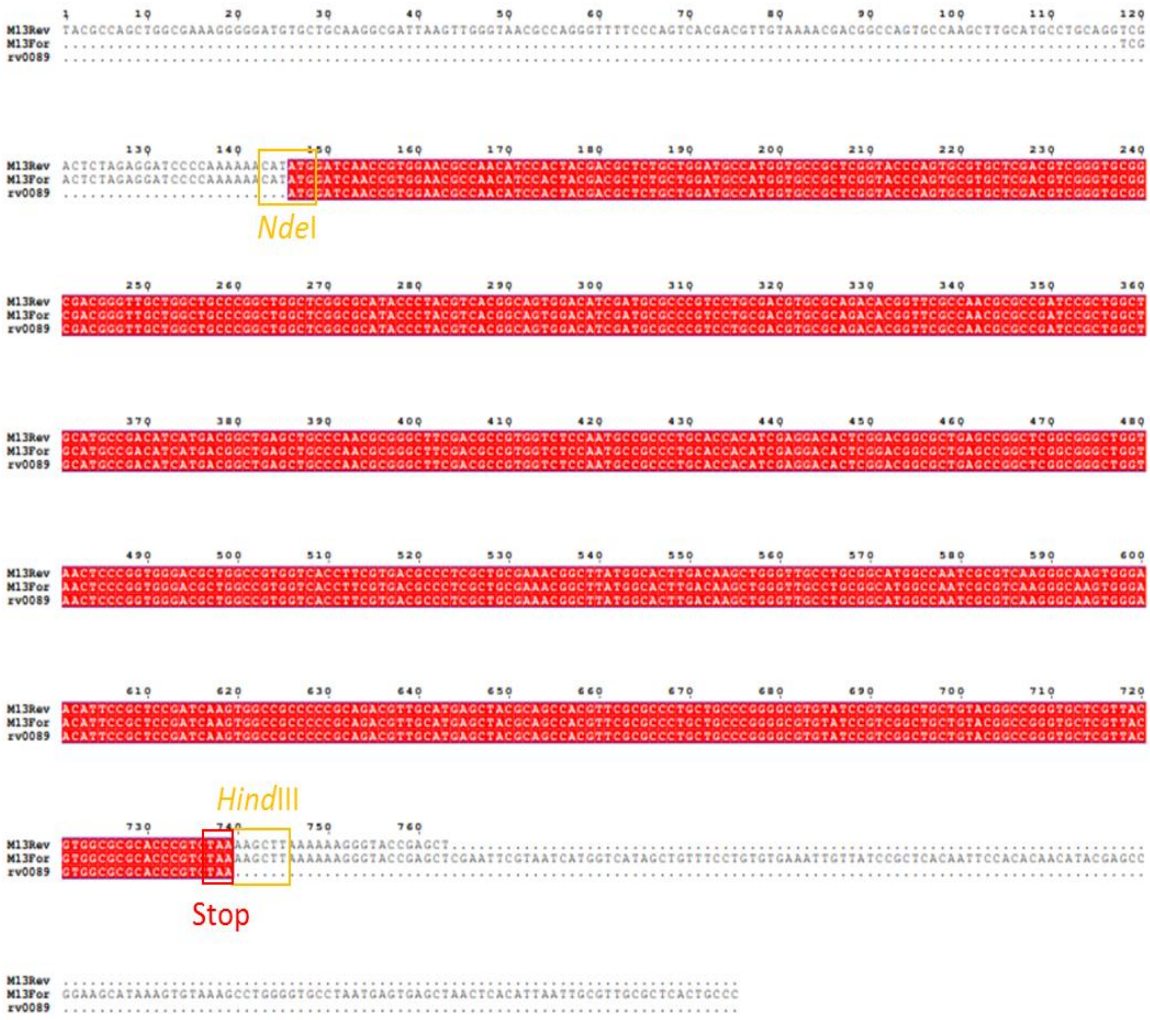

Figure 3.7 **Sequencing alignment of pUC18-*rv0089*.** *Nde*I and *Hind*III restriction sites are indicated.

This fragment was then sub-cloned into pET28b and pET23a (*E. coli* expression vectors) and pHMR3 (a mycobacterial expression vector). Briefly, the sequenced pUC18 plasmid were digested with *Nde*I and *Hind*III and ligated into similarly cut pET28b and pHMR3. Screening of valid constructs was performed by restriction digest (Figure 3.8). Plasmids with the correct restriction pattern were sent for confirmatory sequencing via GATC. Figure 3.9 and 3.10 shows the sequencing results of rv0089 pET28b and pHMR3 constructs, respectively, against the genomic sequence.

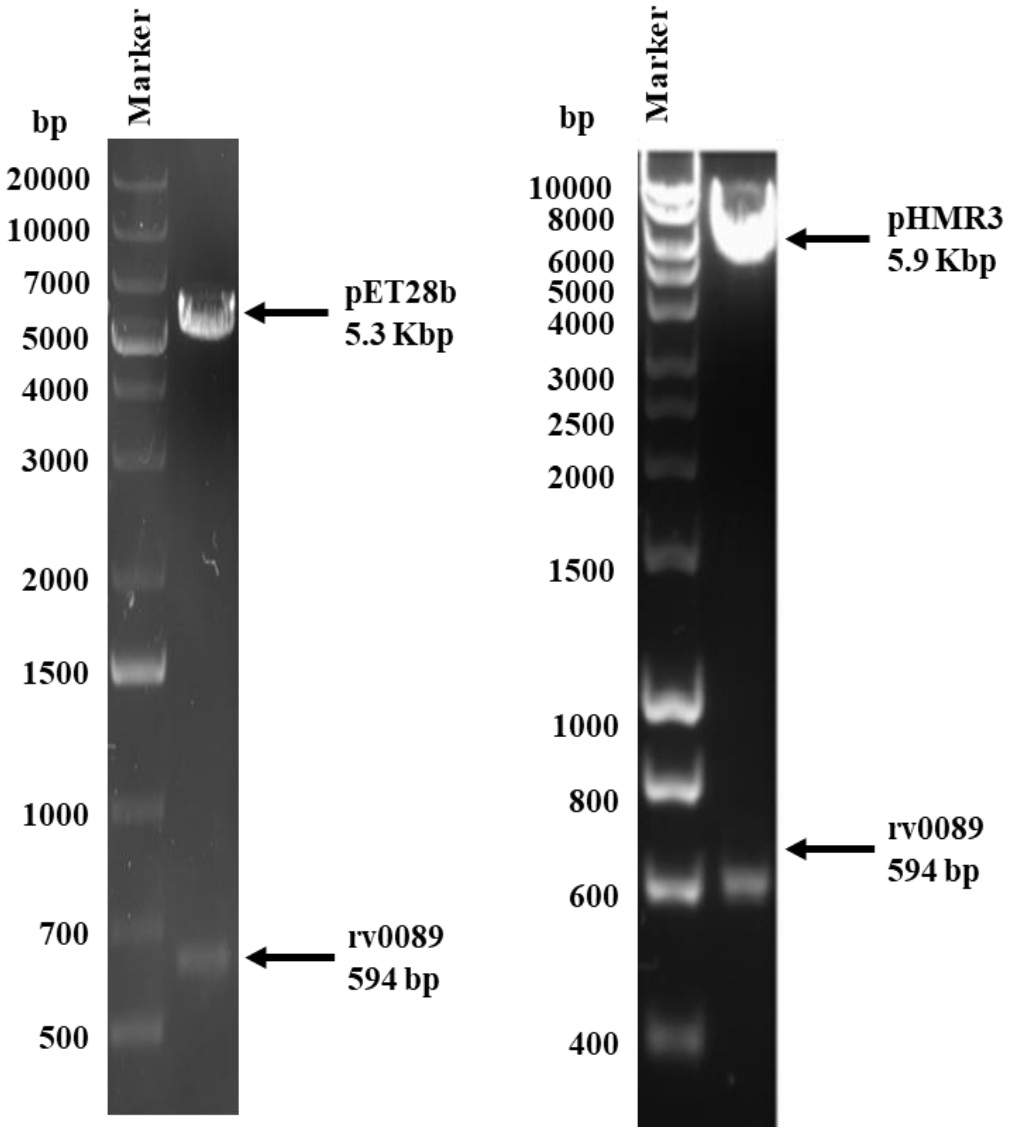

Figure 3.8 ***Nde*I and *Hind*III screening double digest of pET28b and pHMR3–*rv0089* constructs.**

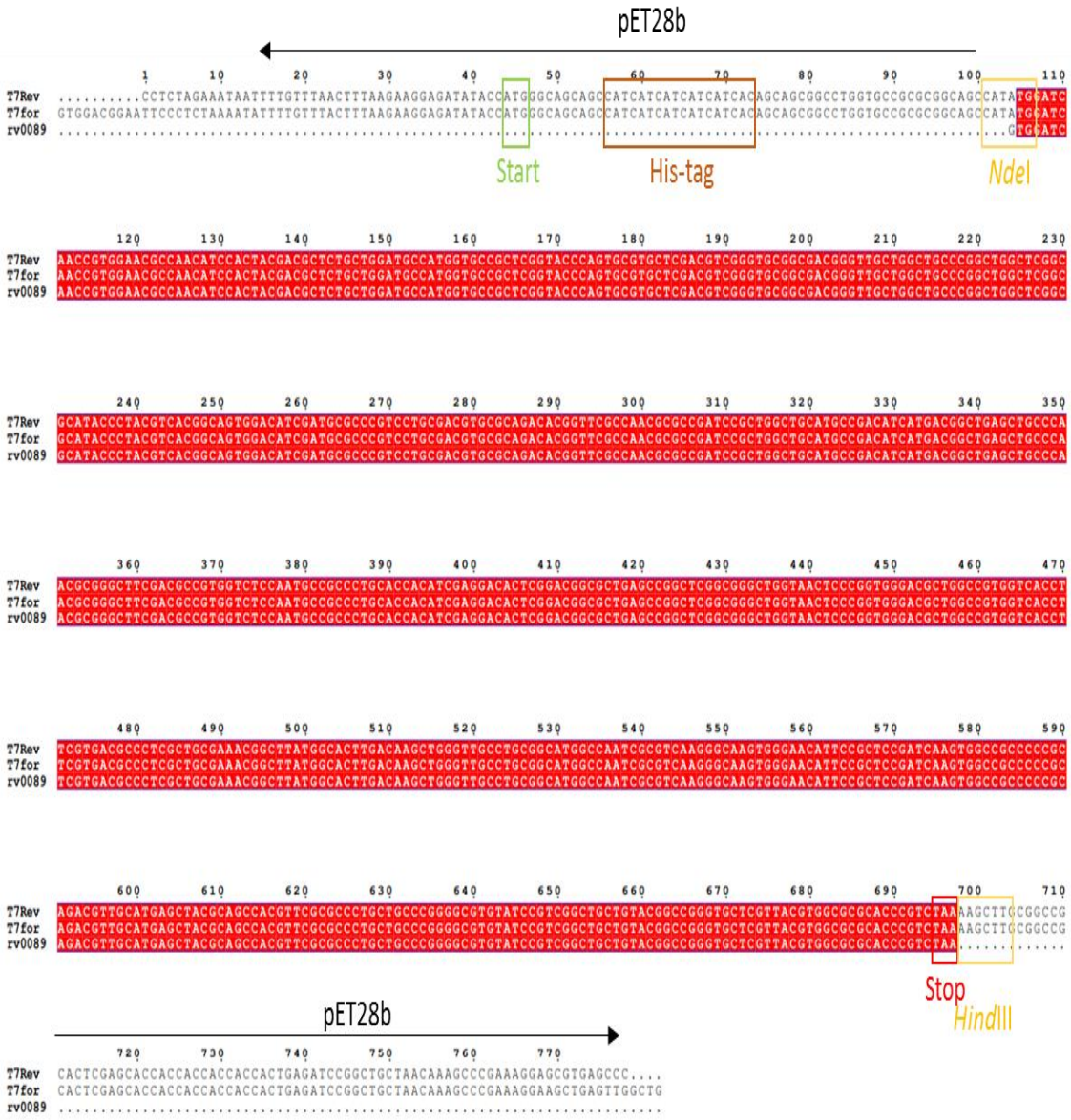

Figure 3.9 **Sequencing analysis of pET28b–rv0089** indicating both the start and stop codons. Cloning restriction sites are indicated**.**

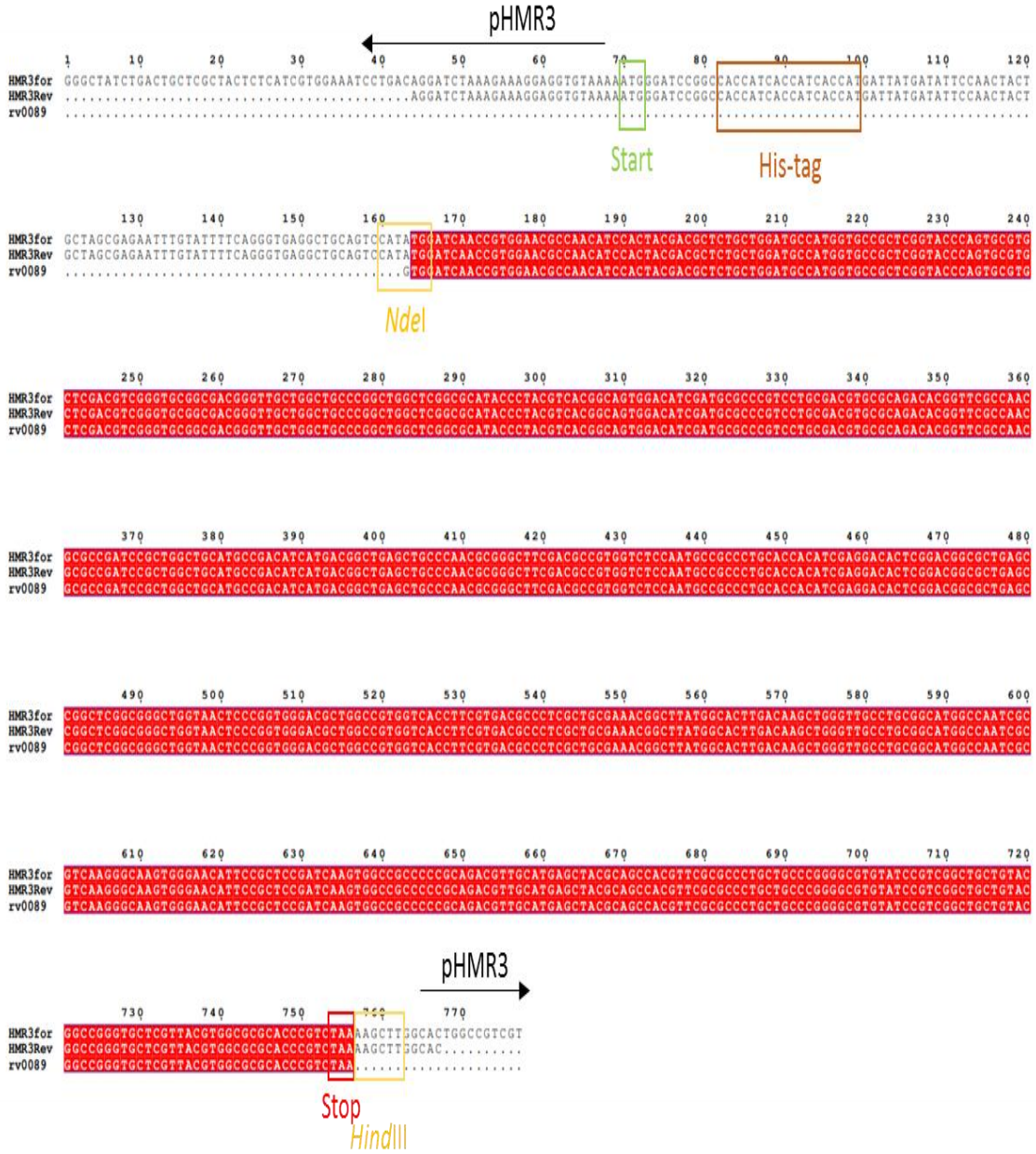

Figure 3.10 **Sequencing analysis of pHMR3–rv0089** indicating both start and stop codons. Cloning restriction sites are indicated

3.6 Expression of *mt*BioC

The resulting pET28b-*rv0089* plasmid was used to transform *E. coli* C41 DE3 to enable protein expression and purification analysis. The pHMR3 constructs was used to transform mycobacterial expression hosts by electroporation (*Mtb* mc^{2}7000 and *Mycobacterium smegmatis* mc^{2}155). The *E. coli* expression study using 100 mL cultures

showed that the *mt*BioC protein was expressed at 16ºC, 16 hrs, 1 mM IPTG once grown to an OD_{600nm} of 0.6. Briefly, *E. coli* C41 DE3 pET28b- *rv0089* cells were cultured in an orbital incubator to OD_{600nm} of 0.6 and induced with various concentrations of IPTG. The cells were harvested by centrifugation and resuspended in buffer (50 mM Tris.HCl, 50 mM NaCl, pH 7.4) lysed by sonication and samples taken as the crude extract. The remaining suspension was centrifuged at 27,000 x g for 1 hour to clarify the sample. The supernatant and the crude extract sample were analysed by SDS-PAGE (12%) (Figure 3.11).

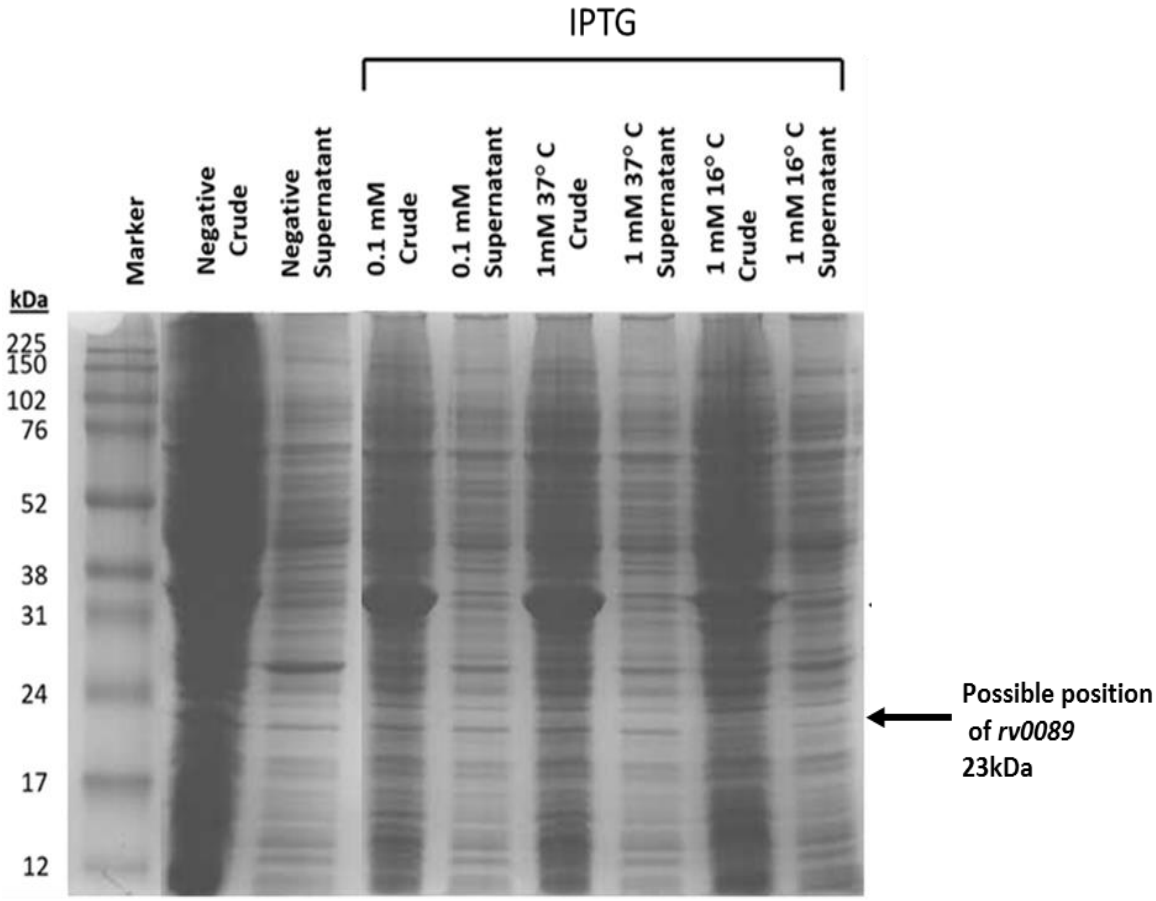

Figure 3.11 SDS-PAGE analysis of *mt*BioC expression studies in *E. coli* C41 DE3. The expression was done at 0.1 mM and 1 mM concentrations of imidazole and at 37ºC and 16 ^{O}C. Both crude and supernatants seem to contain the protein.

Recombinant protein can be observed in the crude and supernatant samples in all the different concentrations of IPTG and different temperatures used (Figure 3.11). However,

since a soluble supernatant fraction of 16ºC, 16 hrs, and 1 mM IPTG is shown to be one of the best conditions for protein expression, this condition was utilised in the scale up experiment in a bid to purify the recombinant protein. 1 L cultures were grown under the same conditions and lysed and clarified in the same manner. Clarified supernatants were then applied to Immobilized Metal Affinity Chromatography (IMAC). Nickle charge His-trap columns (HiTrap FF, GE Healthcare) were washed and charged as per the manufacturers' protocols followed by the application of supernatant. A crude imidazole concentration gradient was employed in an attempt to investigate the binding of the proteins (Figure 3.12). The purification was not particularly successful and warrants further investigation.

As part of efforts to further purify the protein, it was realised that the addition of phenylmethylsulfonyl fluoride (PMSF) initially added in the lysis buffer might have aggregated the protein, since PMSF strongly inhibits some proteins involved in the fatty acid biosynthetic pathway in *E. coli* (example, BioH) (Sanishvili et al., 2003). PMSF binds specifically to the active site of a serine residue in proteases and creates a hyperactive environment around the serine residue so that the PMSF does not affect the activity of any other serine residue in the protein. This then led to the exclusion of PMSF in the lysis buffer and a new attempt to express the protein was put in place. Expression and purification of the recombinant Rv0089 was performed as per the previous method. A 1L culture of lysed and clarified protein was applied to Nickle charge His-trap column and washed with different concentrations of wash buffer containing imidazole. A concentration gradient was created and analysed through SDS-PAGE. The expression and purification using a different lysis buffer did not give the required result. It was concluded that different expression strains should be utilised to test their expression ability.

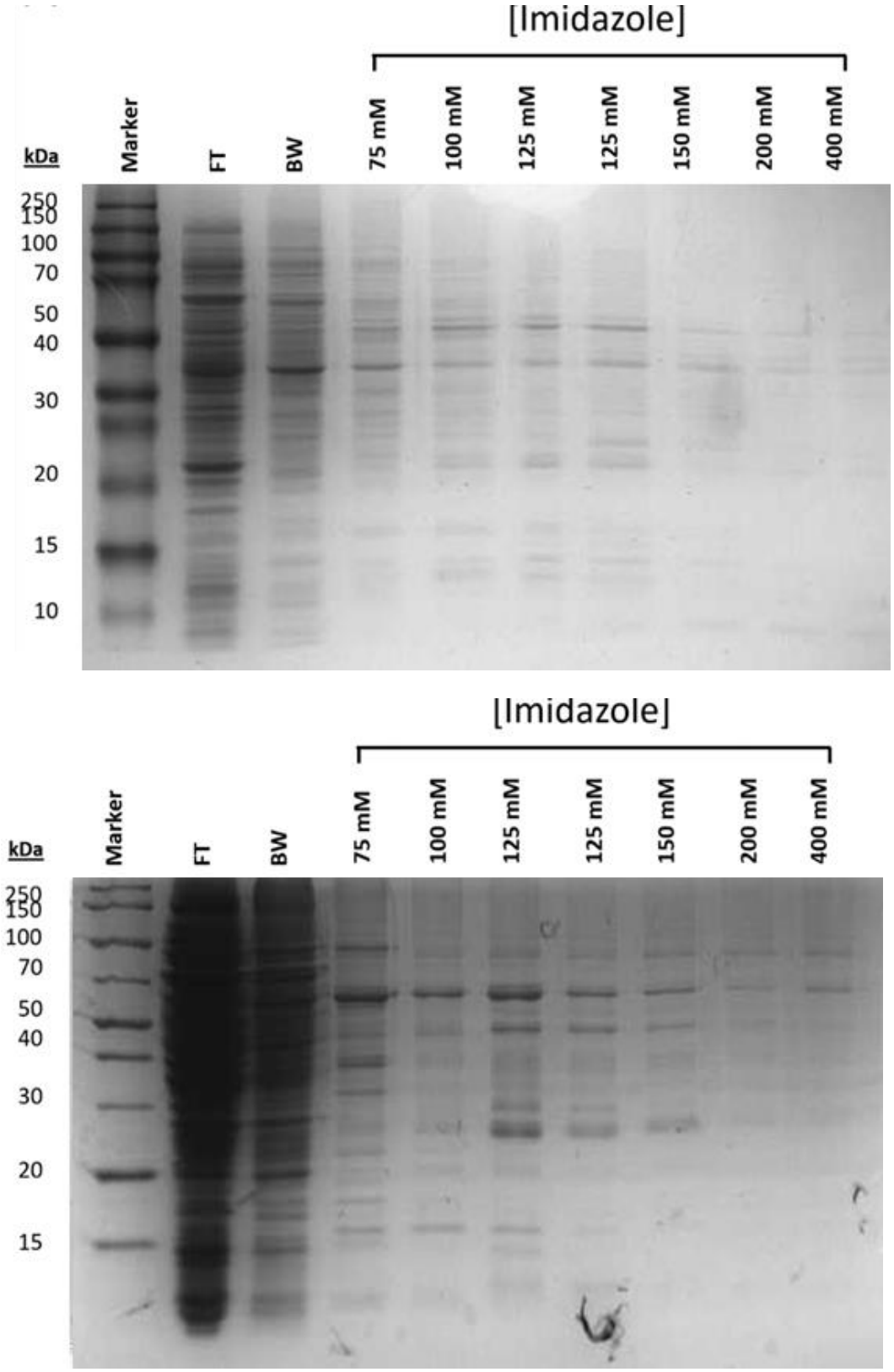

Figure 3.12 **SDS-PAGE analysis of *mt*BioC partial purification via IMAC in *E. coli* C41 DE3.** The expression and purification was not successful as there were no visible bands of expressed protein of the correct molecular weight.

3.6.1 Transformation and expression in various *E. coli* expression hosts

pET28-*rv0089* vector was used to transform seven different *E. coli* expression strains for recombinant protein expression and purification as described in sections 2.10.1 and 2.10.2. The expression strains used were *E. coli* BL21 (DE3) (Figure 3.13), BL21 (DE3) pLysS (Figure 3.14), C43 (DE3) (Figure 3.15), C43 (DE3) pLysS (Figure 3.16), C41 (DE3) (Figure 3.17), HMS174 (DE3) pLysS (Figure 3.18) and B834 (DE3) pLysS (Figure 3.19). Expression studies were performed on all strains and assessed as per section 2.10. Recombinant protein expression was assessed by SDS PAGE.

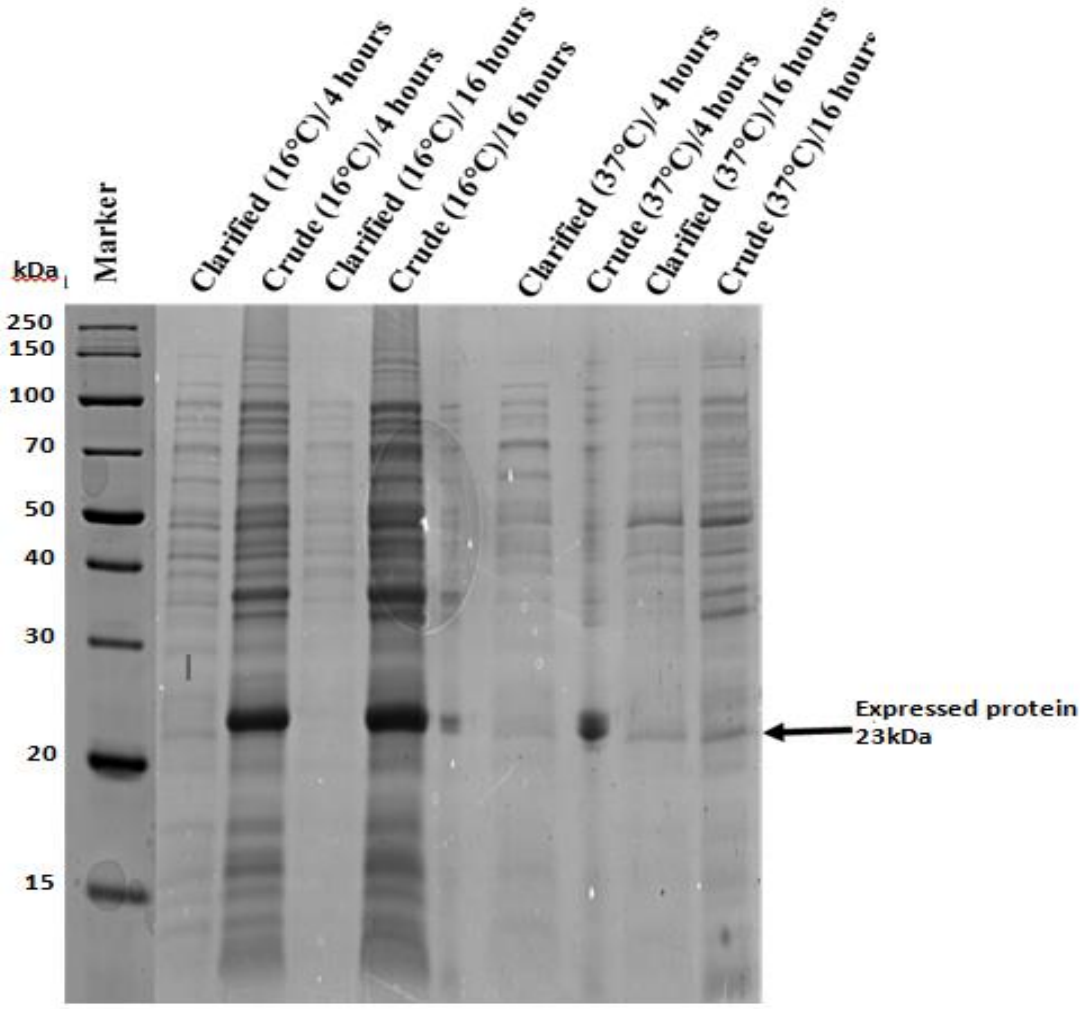

Figure 3.13 **SDS-PAGE analysis of *mt*BioC expression in *E. coli* BL21 (DE3) using crude and clarified extracts.** The result indicates that there was a minimal level of expression of a recombinant protein of the required molecular weight**.**

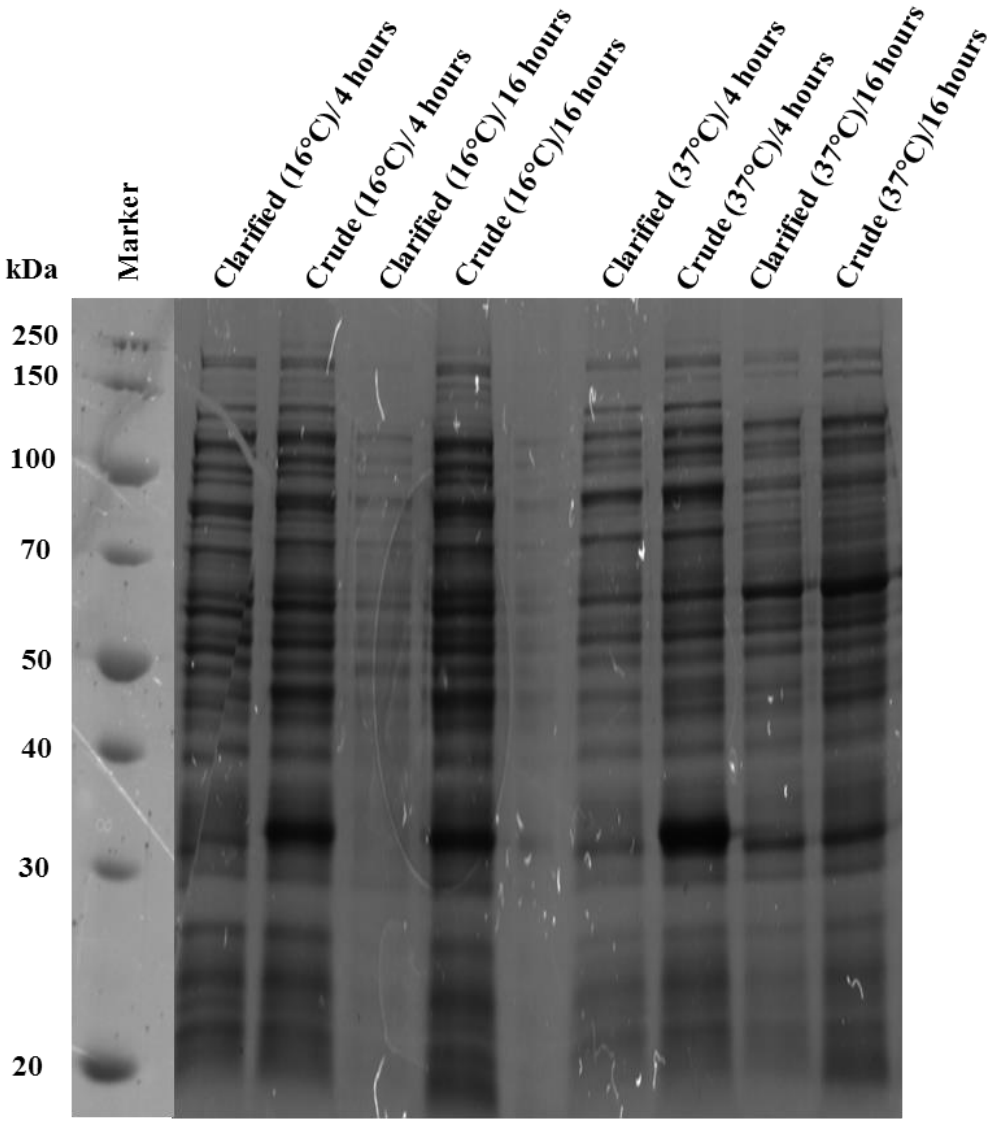

Figure 3.14 **SDS-PAGE analysis of *mt*BioC expression in *E. coli* BL21 (DE3) pLysS using crude and clarified extracts.** The result indicates that there was no clear expression of a recombinant protein of the required molecular weight.

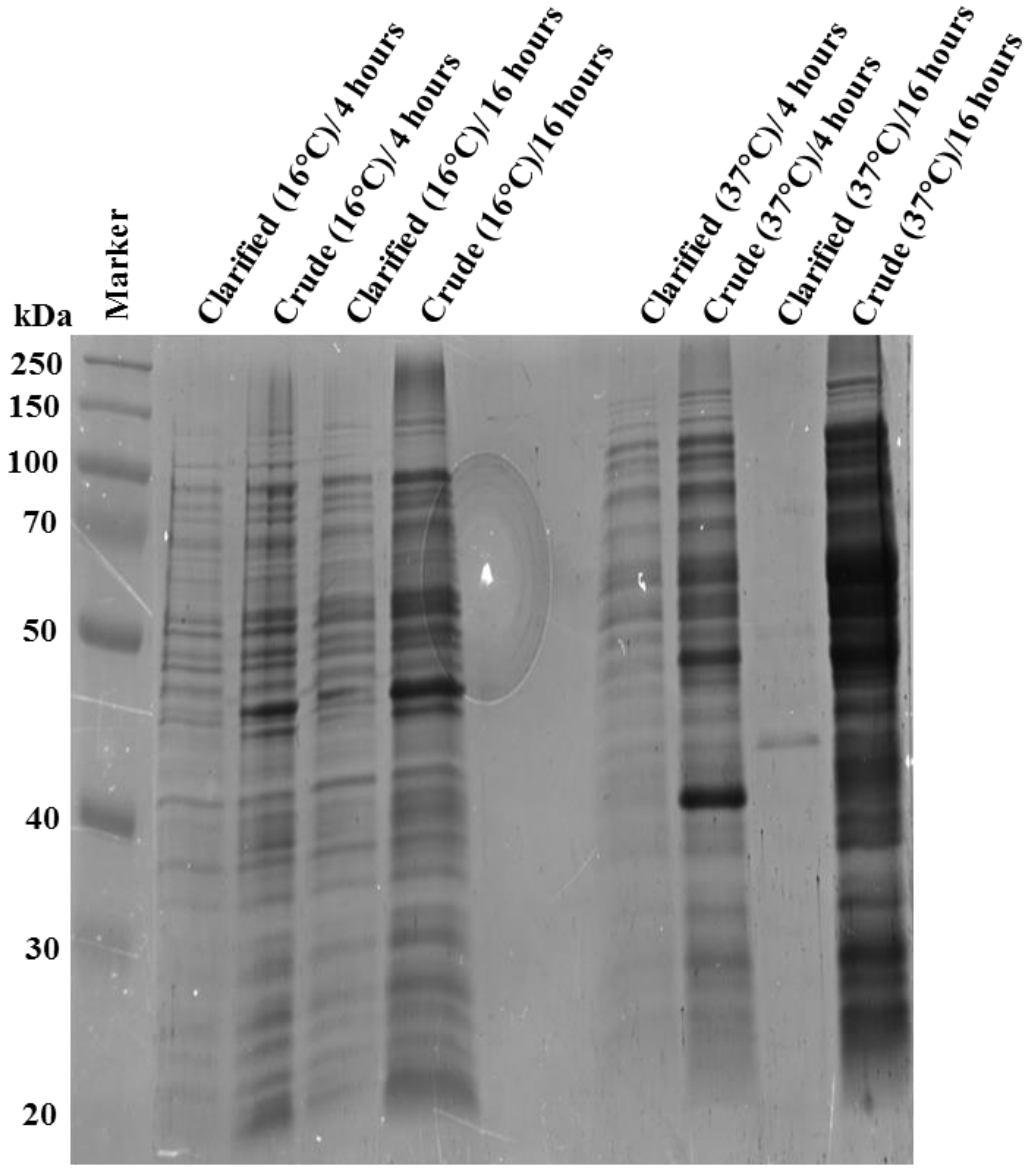

Figure 3.15 **SDS-PAGE analysis of *mt*BioC expression in *E. coli* C43 (DE3) using crude and clarified extracts.** The result indicates that there was no clear expression of a recombinant protein of the required molecular weight.

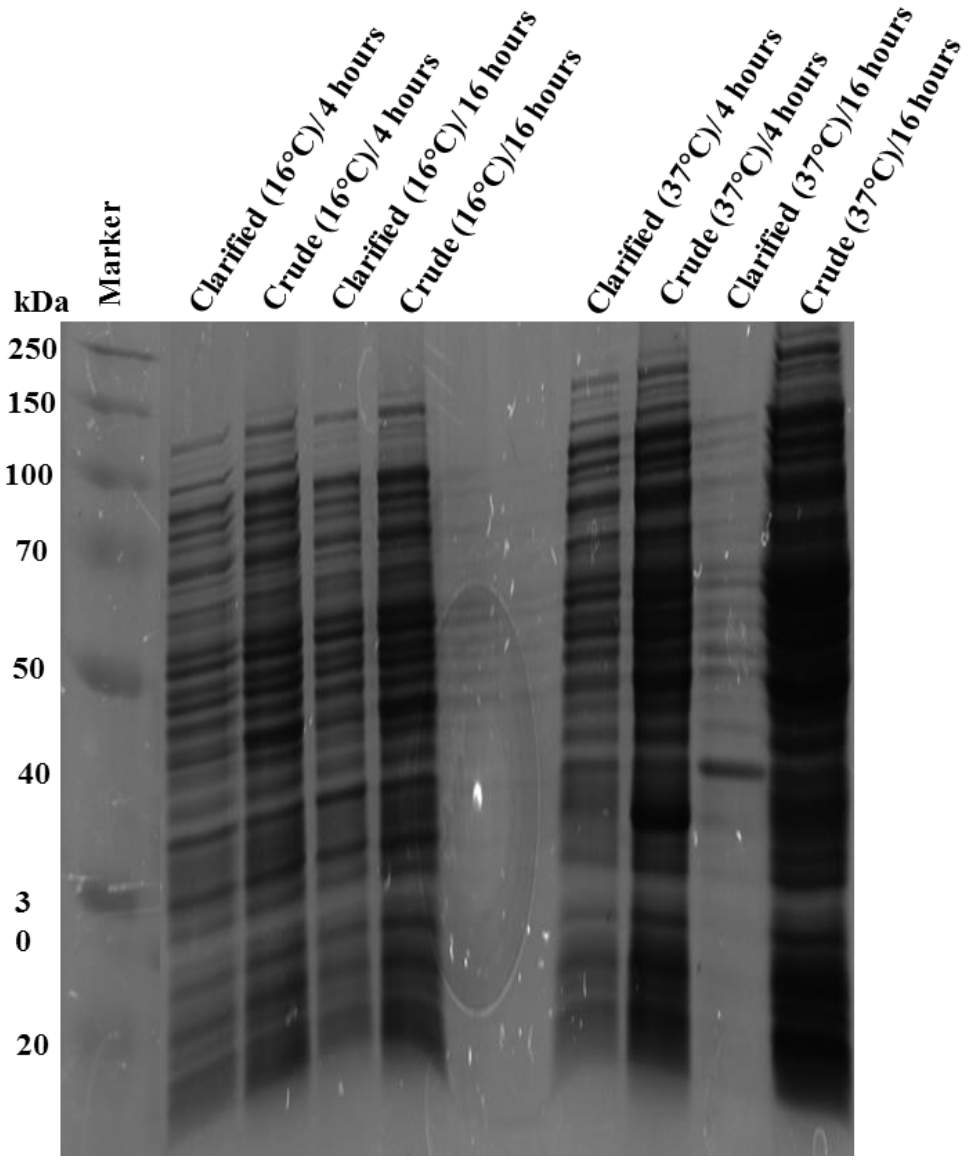

Figure 3.16 **SDS-PAGE analysis of *mt*BioC expression in *E. coli* C43 (DE3) pLysS using crude and clarified extracts.** The result indicates that there was no clear expression of a recombinant protein of the required molecular weight.

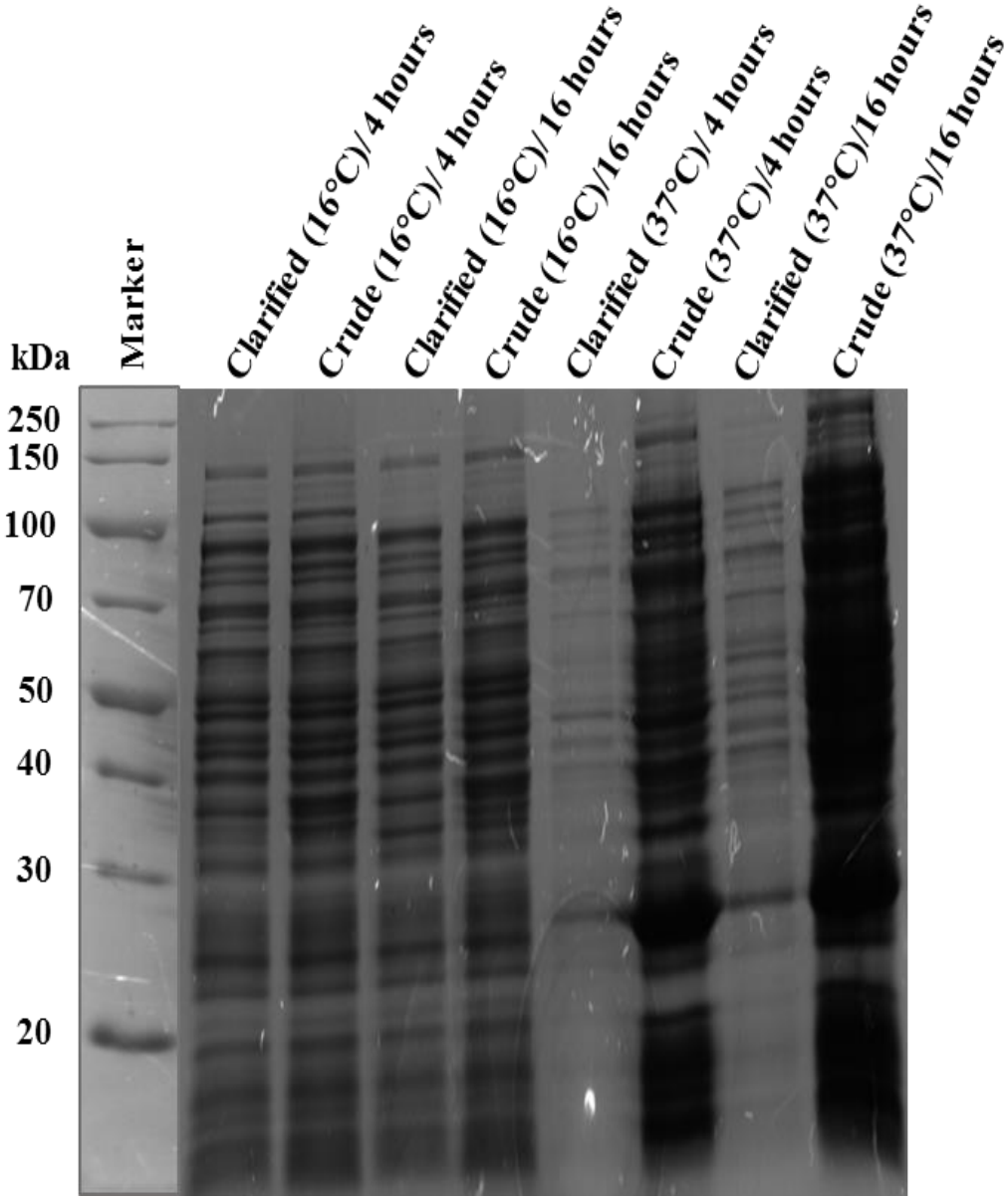

Figure 3.17 **SDS-PAGE analysis of *mt*BioC expression in *E. coli* C41 DE3 using crude and clarified extracts.** The result indicates that there was no clear expression of a recombinant protein of the required molecular weight.

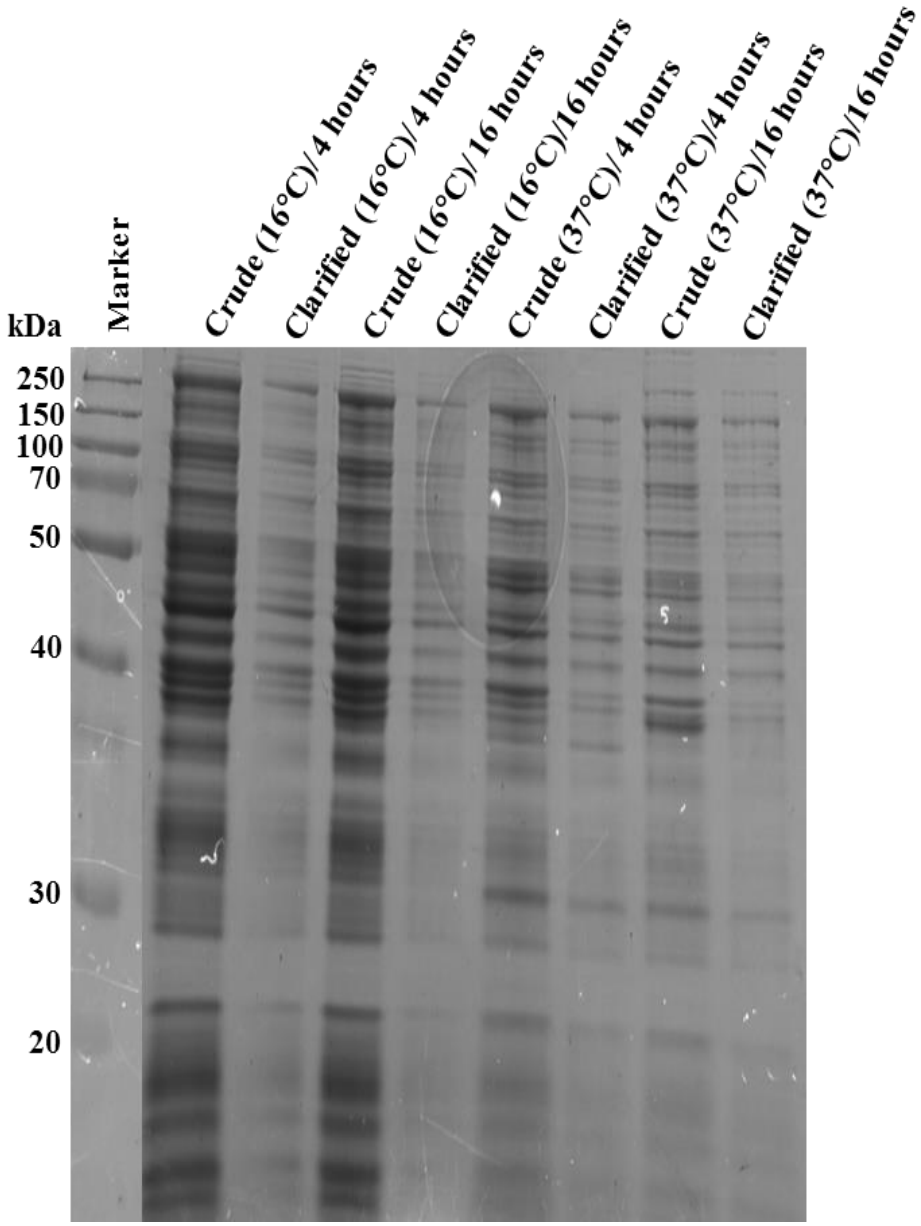

Figure 3.18 **SDS-PAGE analysis of *mt*BioC expression in *E. coli* HMS174 (DE3) pLysS using crude and clarified extracts.** The result indicates that there was no clear expression of a recombinant protein of the required molecular weight.

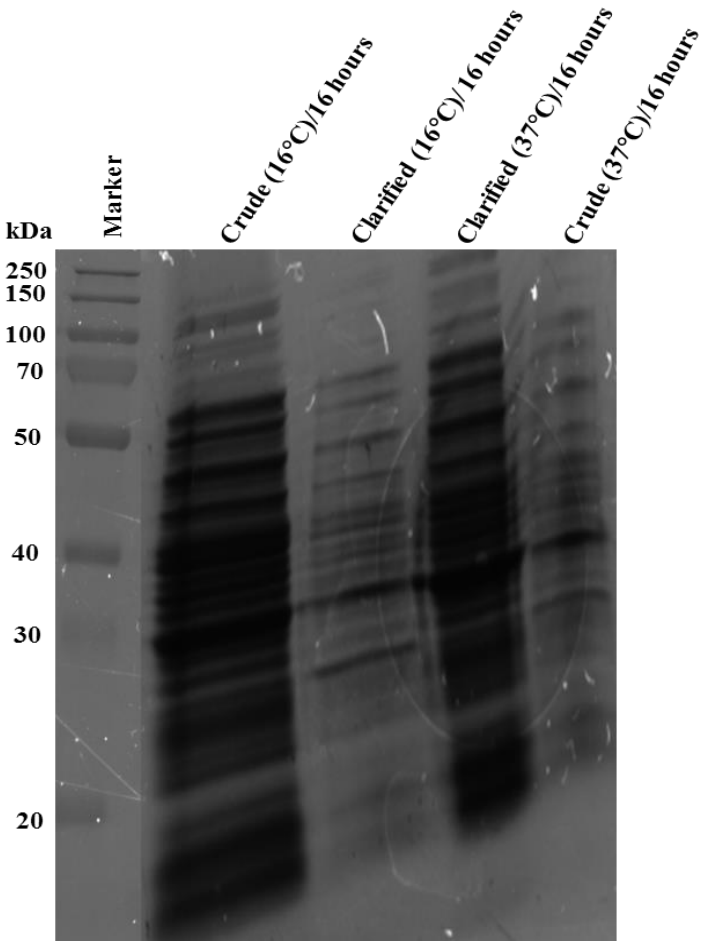

Figure 3.19 **SDS-PAGE analysis of *mt*BioC expression in *E. coli* B834 (DE3) pLysS using crude and clarified extracts.** The result indicates that there was no clear expression of a recombinant protein of the required molecular weight.

From the SDS PAGE analyses of the protein expressed in the 7 different strains of *E. coli*, it was clear that the BL21 (DE3) is the strain that showed great promise in expressing the protein. Extracts from this strain were therefore utilised in the purification studies via IMAC and SDS PAGE (Figure 3.20).

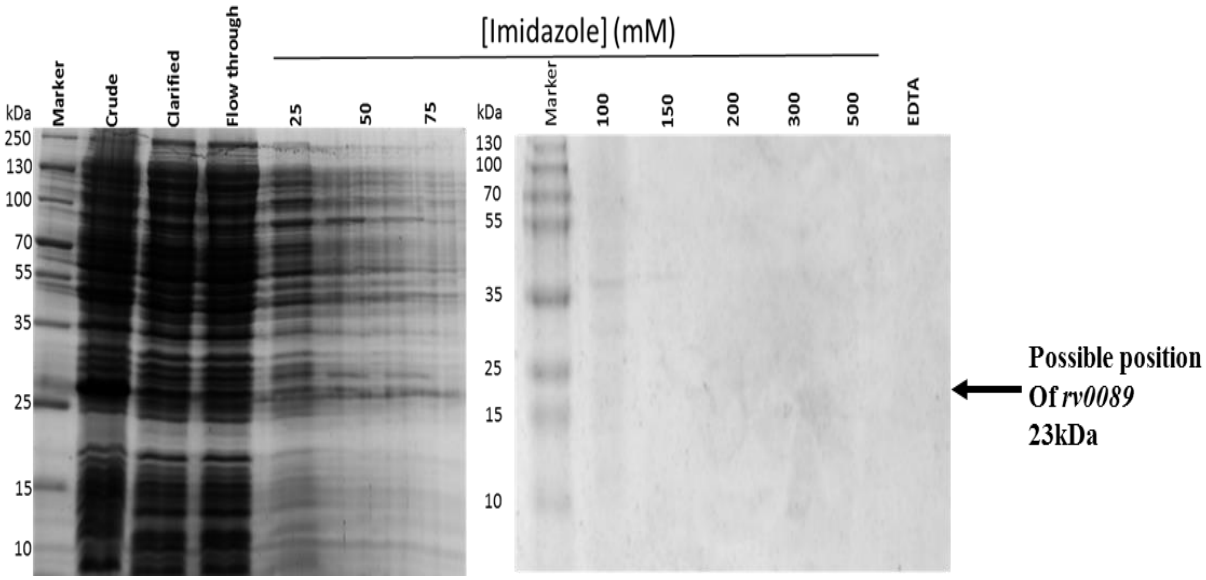

Figure 3.20 **12% SDS-PAGE analysis of *mt*BioC *E. coli* BL21 (DE3) expressed recombinant protein purification via IMAC.** The protein was scaled to a litre and purified. After imidazole elution no clear recombinant protein was purified.

Expression analysis of the protein in the BL21 (DE3) strain showed minimal amount of protein expressed (Figure 3.13) and several attempts to further scale it did not produce any significant change in the amount of expressed protein (Figure 3.20). It was concluded that another option to be explored was the optimisation of the DNA sequence for *E. coli* expression.

3.6.2 Codon optimisation

*mt*BioC (Rv0089) protein sequence was optimised using the MWG optimisation server. Protein sequences were transcribed to ensure the correct *mt*BioC sequence would be translated. The optimised sequence for *E. coli* expression was purchased from MWG biotech containing the relevant cloning restriction sites (Figure 3.21).

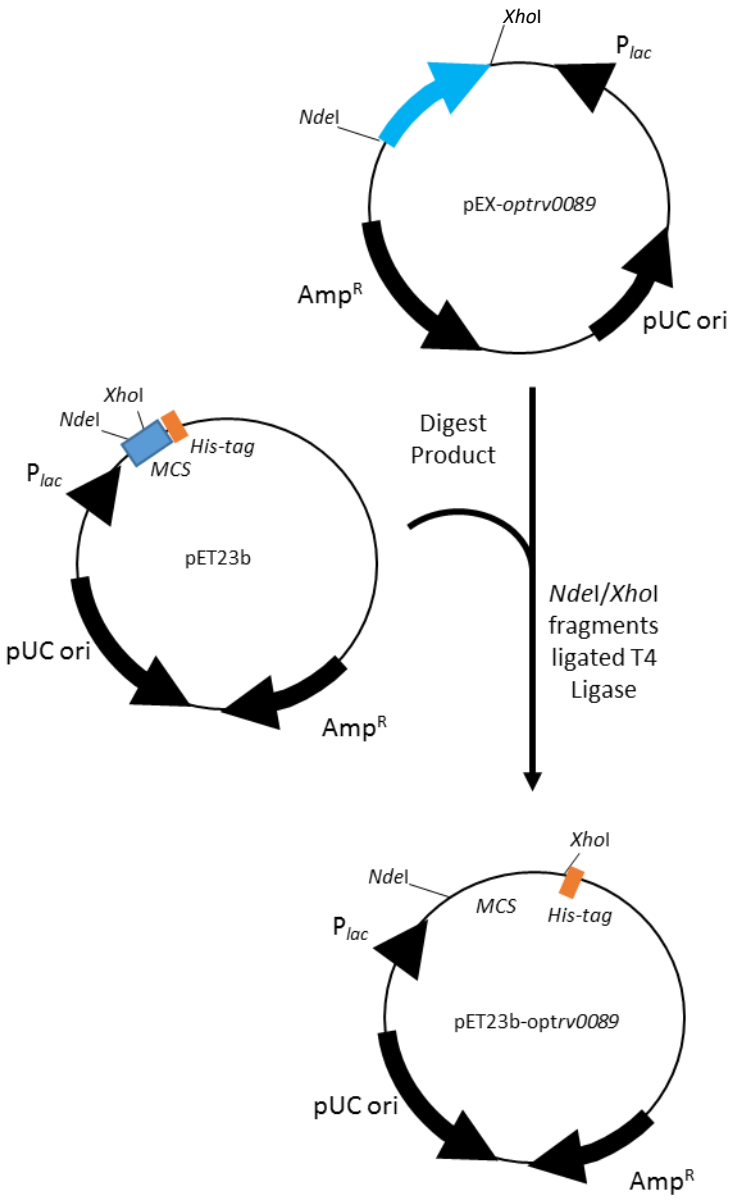

Figure 3.21 Schematic representation of the *optrv0089* expression plasmid construction. Plasmid map construction of pET23-rv0089; digested with *Nde*I/*Xho*I

The *Nde*I/*Xho*I digest fragment from the pEX construct was purified and ligated into similarly cut pET23b using T4 ligase (Section 2.8.2) and the mixture used to transform *E. coli* XL10-Gold. The 594 bp amplicon corresponding to the *optrv0089* gene was successfully cloned into pET23b which was confirmed by restriction digest of the purified plasmid (Figure 3.22).

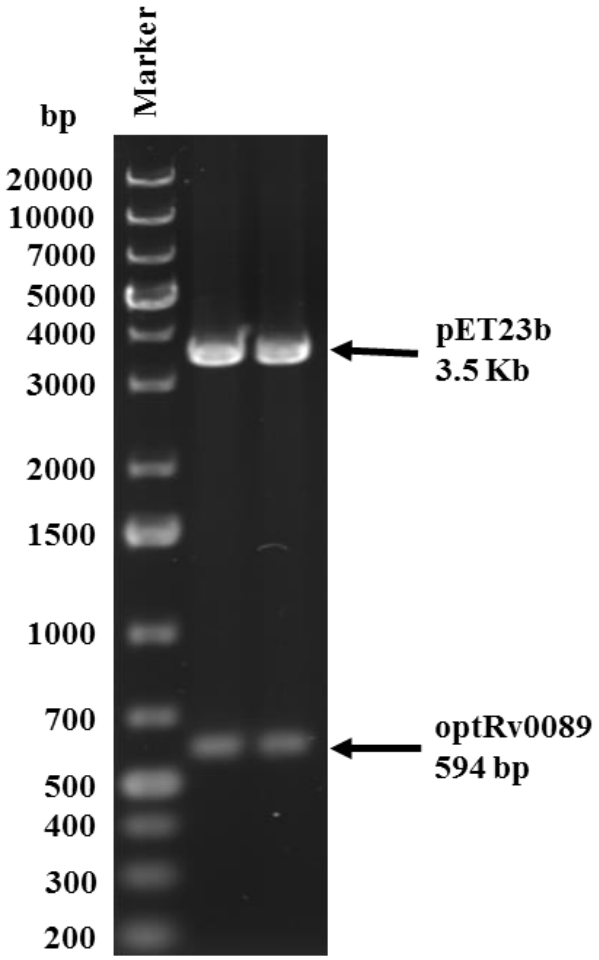

Figure 3.22 Double digest *Nde*I/*Xho*I restriction enzyme screening of pET23b construct containing *optrv0089;* 3.5 kb pET23 vector and 0.594 kb *optrv0089*; marker, GeneRuler 1 kb plus DNA ladder

The resulting plasmid was sequenced by Sanger sequencing using standard pET primers at GATC (www.gatc-biotech.com) (Figure 3.23).

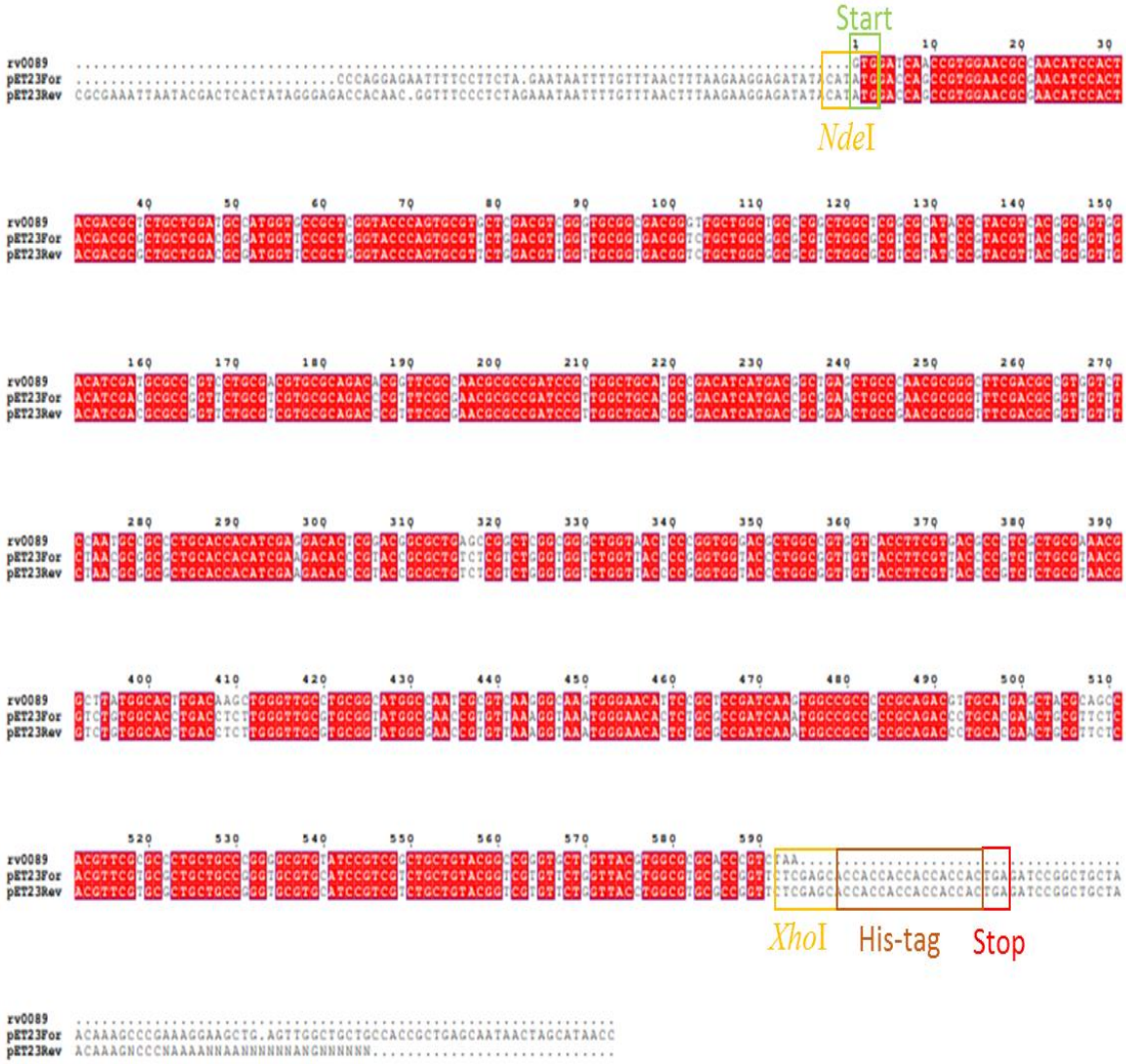

Figure 3.23 Sequencing analysis of pET23b–opt*rv0089* showing both the start and stop codons (Primers used; standard T7 promoter and T7 terminator)

The resulting DNA sequence was translated and the protein sequence was confirmed to be the same as the wild-type *mt*BioC.

3.6.3 Optimised-*Mt*BioC expression and purification

E. coli codon optimised *mt*BioC pET23b construct was used to transform the *E. coli* expression strain BL21 (DE3) as this gave the best expression in the previous study. Broth cultures containing ampicillin (Amp^{100}) were incubated at 37ºC overnight. The following

day 1 % inoculum was used to inoculate 1 litre LB broth with Amp^{100} followed by orbital incubation at 37ºC to an OD_{600} of 0.6. The culture was allowed to cool, then 1 mM Isopropyl β-D-1-thiogalactopyranoside (IPTG) was added and further incubated at 16ºC overnight. The following day the culture was harvested at 4000 rpm at 4ºC for 10 minutes and cell pellets stored at -20ºC for future use. 1 L cultures were lysed and clarified as per previous experiments. Clarified supernatants were then applied to Immobilized Metal Affinity Chromatography (IMAC). Nickle charge His-trap columns (HiTrap FF, GE Healthcare) were washed and charged as per the manufacturers' protocols followed by the application of supernatant. A crude imidazole concentration gradient was employed to investigate the binding of the proteins (Figure 3.24)

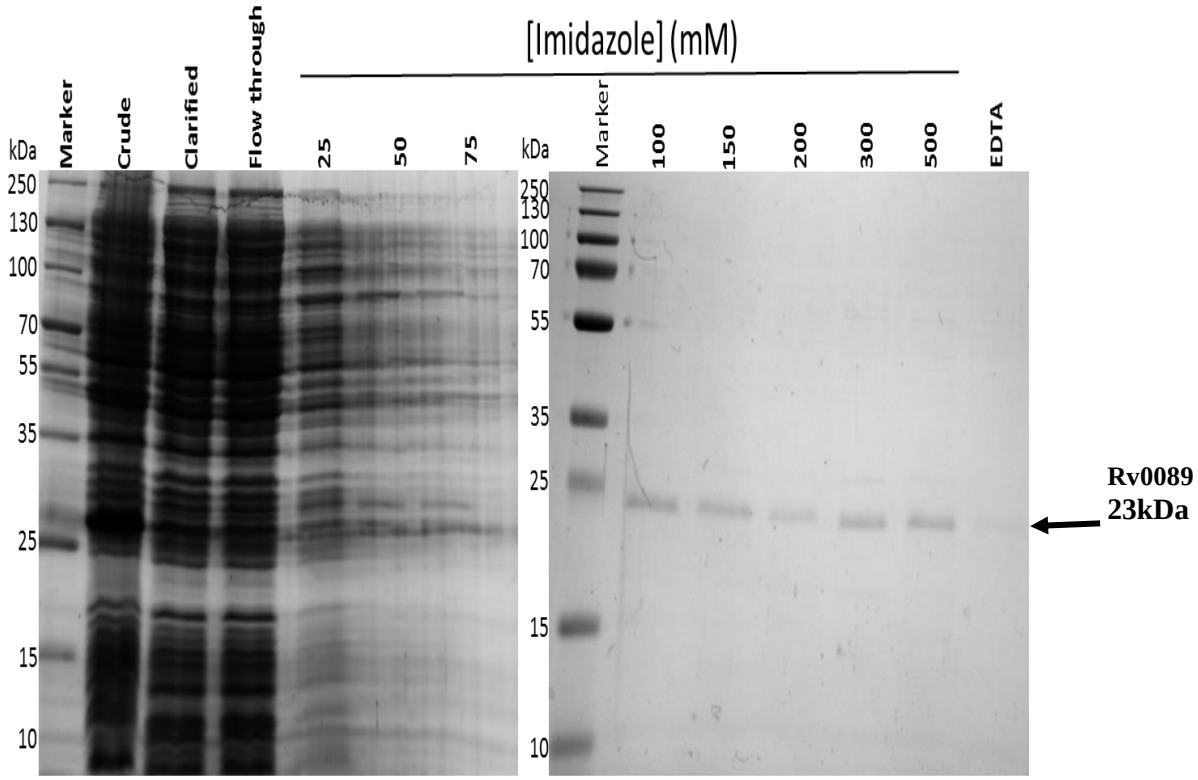

Figure 3.24 **SDS-PAGE analysis of codon optimised *mt*BioC purification by IMAC chromatography.** PageRuler plus prestained protein Marker. Protein samples were separated on a 12 % gel. *mt*BioC was eluted between at 100 mM and 500 mM concentrations of imidazole. The protein is 23 kDa in size.

3.6.4 Trypsin digest result

Results of the trypsin digest from the electrospray ionisation mass spectrometry gave a score of 1023 with a mass of 23,814 which is approximately the mass of the protein (23 kDa). The result also showed that there were a total of 67 matches and 44 of them were recorded as significant matches (65.7%). There were 9 sequences of the protein with 7 of them significant. The result therefore indicated that the protein is an uncharacterised methyl transferase and an *Mtb* homolog of Rv0089.

3.6.5 Protein dialysis

Eluted protein fraction was dialysed 3 times between intervals of 16 hours, 2 hours and 1 hour, using 50 mM Tris and 50 mM $NaCl_2$ pH 8. Dialysed protein was concentrated using Amicon® Ultra-4 10K Centrifugal filters by centrifuging at 4,000 *x g* at 4ºC until the desired concentration is achieved. This concentrated protein was also analysed by SDS-PAGE (Figure 3.25).

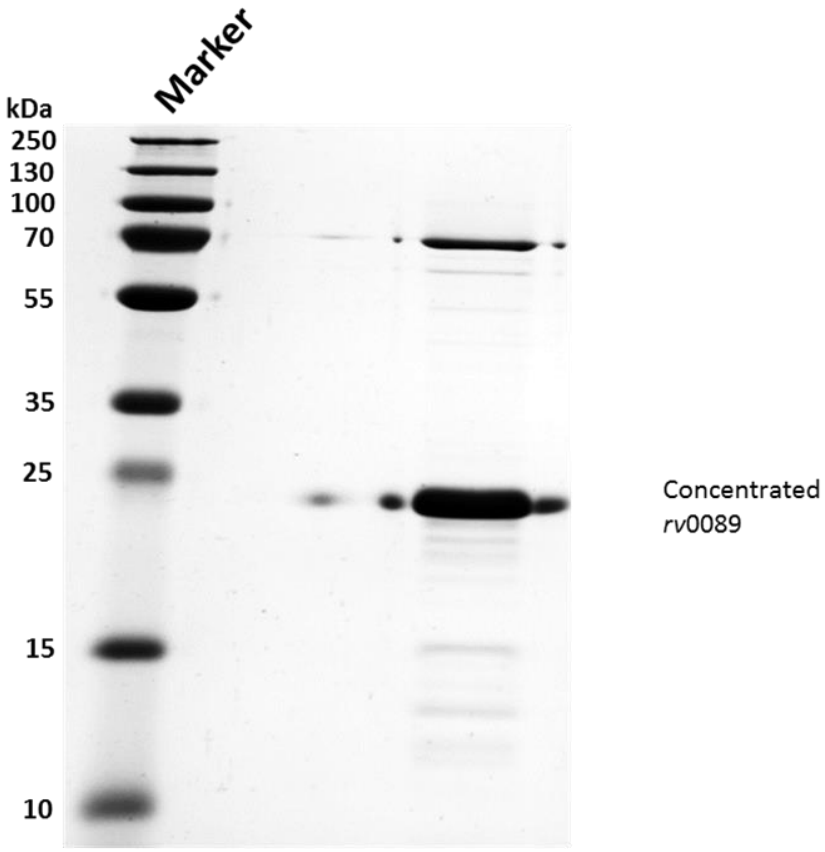

Figure 3.25 Concentrated recombinant Rv0089 – *mt*BioC

To further identify the presence of *mt*BioC, a trypsin digest was performed on the gel. This is a method of identifying the enzyme by analysing the pattern of peptide bonds obtained through a mass spectrometer, when trypsin cleaves to lysine and arginine residues of the protein. The data obtained (Section 3.6.4) confirmed the presence of *mt*BioC.

The initial project focus was to purify enough protein to perform biochemical characterisation and crystallography trials. Unfortunately, even though scaling up experiments were performed the level of protein required to set up the crystallography trials was not achieved.

3.6.6 Methyl transferase assay

*mt*BioC is an *O*-methyltransferase that methylates a free carboxyl group of either malonyl-CoA or malonyl-acyl carrier protein as with the *E. coli* BioC (Lin and Cronan, 2012). This assay utilises the ability of the enzyme to transfer a methyl group from SAM to a malonyl-CoA acceptor by monitoring the formation of the reaction product, SAH. The SAH generated is converted to ADP which is further converted to ATP. Luminescence is measured by a plate-reader luminometer (Figure 3.26). This provides the basis for measuring different conditions affecting the protein.

Figure 3.26 Schematic of SAM dependent assay developed for *mt*BioC

The assay was utilised to assess the biochemical properties of *mt*BioC and measure the effects of protein concentration, substrate concentration, substrate specificity, pH, temperature and inhibition by a known SAM inhibitor.

Initially the protein concentration effects were assessed to establish protein activity relative to concentration (Figure 3.27). As the protein concentration increased there was a proportional increase in SAH production. Highest activity was recorded with an increase of protein concentration of 800 µg/ml.

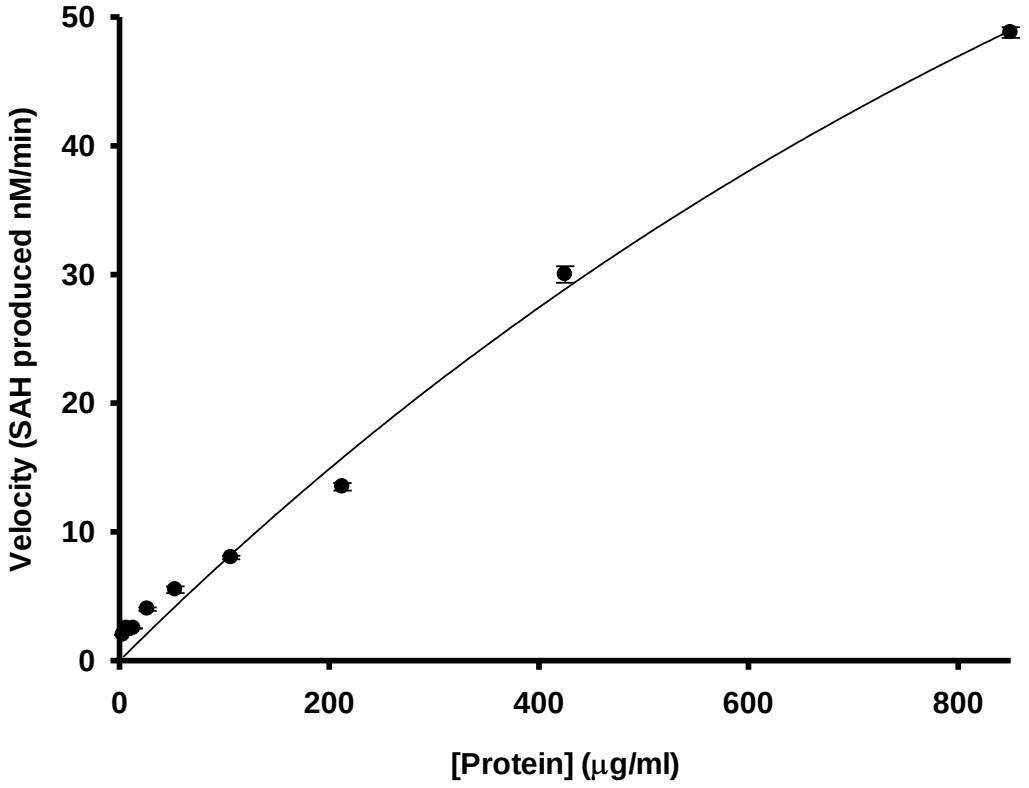

Figure 3.27 **Analysis of the activity of *mt*BioC by the amount of SAH produced.** As the protein concentration increased there is a proportional increase in SAH production in a SAM dependent luminescence assay.

As the suspected primary substrate, a malonyl-CoA concentration analysis was determined for 50 μg of *mt*BioC as described in Section 3.3.3. Malonyl-CoA acts as a BioC methyl acceptor and as expected a higher turnover of SAH was proportional to increasing amounts of malonyl-CoA (Figure 3.28). At 1000 nM the assay looked to be saturated giving approximately 12 nM/min of SAH produced.

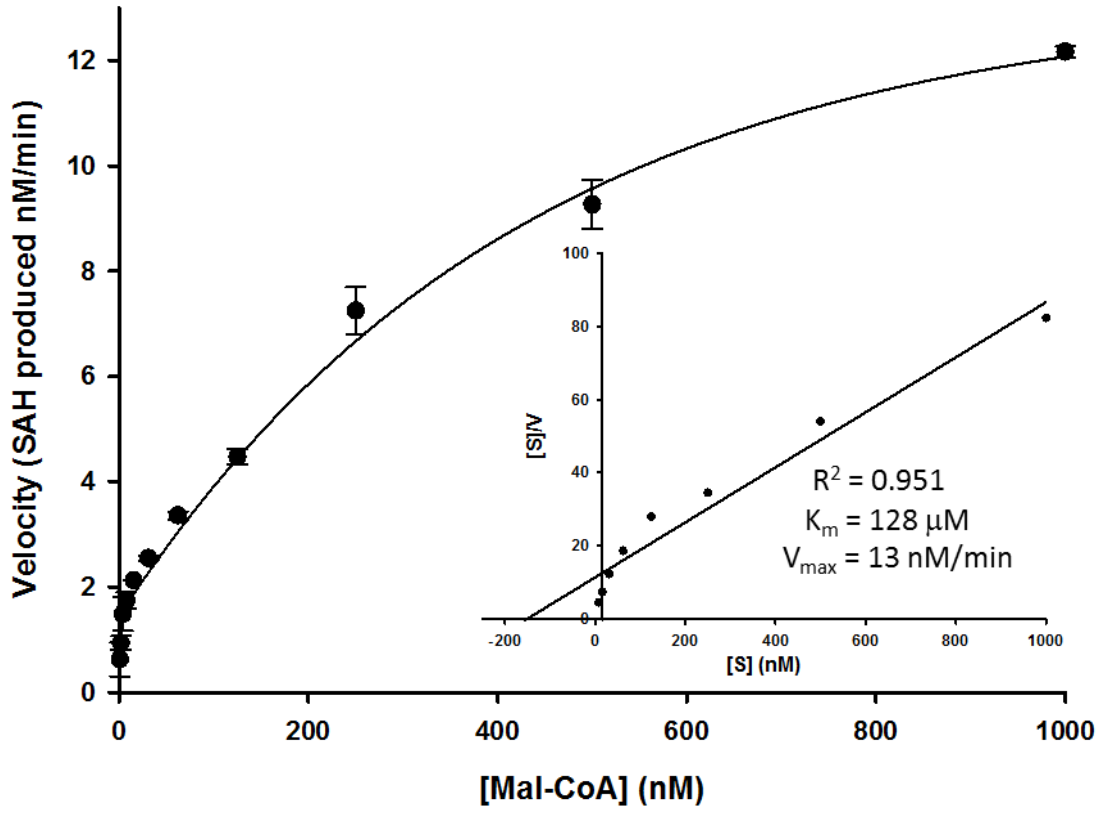

Figure 3.28 The effects of Malonyl-CoA concentration on SAH production by *mt*BioC in SAM dependent luminescence assay. Insert is a Hanes Plot indicating a relationship between [S] and V.

From figure 3.28, a relationship between [S] and [V] was established. A Michaelis-Menten kinetics was thereby used to deduce the Michaelis-Menten constant, K_m, which is the concentration of the substrate (malonyl-CoA) that would allow the enzyme to achieve half V_{max}. K_m was determined to be 128 µM and V_{max} also determined to be 13 nM/min. The insert on the graph (Figure 3.28) is a Hanes plot.

Substrate specificity analysis was limited to malonyl-CoA and glutaryl-CoA due to the availability of substrates. *mt*BioC was able to utilise both acceptor substrates in the SAM dependent assay but showed a preference for malonyl-CoA over glutaryl-CoA as a substrate (Figure 3.29). The preference for malonyl-CoA as the primary substrate further supports the evidence that Rv0089 is the *mt*BioC as predicted.

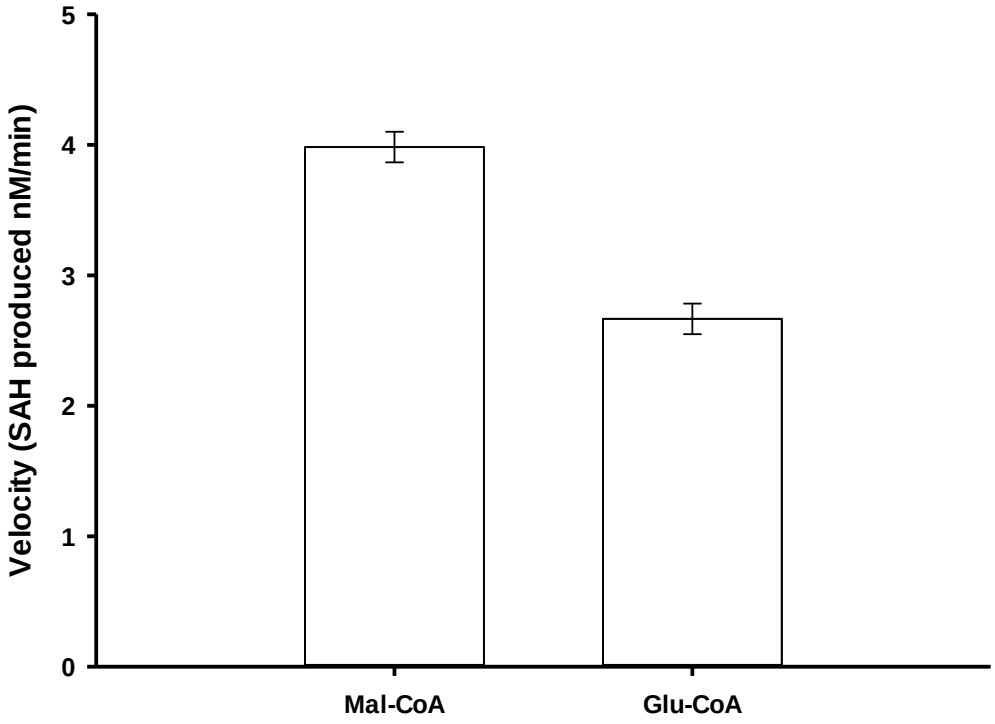

Figure 3.29 Comparism between the methyl accepting ability of malonyl-CoA and glutaryl-CoA by *mt*BioC in a SAM dependent luminescence assay

Other physiochemical properties assessed in the *mt*BioC SAM dependent luminescence assay were pH (Figure 3.30), metal ion co-factor presence (Figure 3.31) and temperature (Figure 3.32).

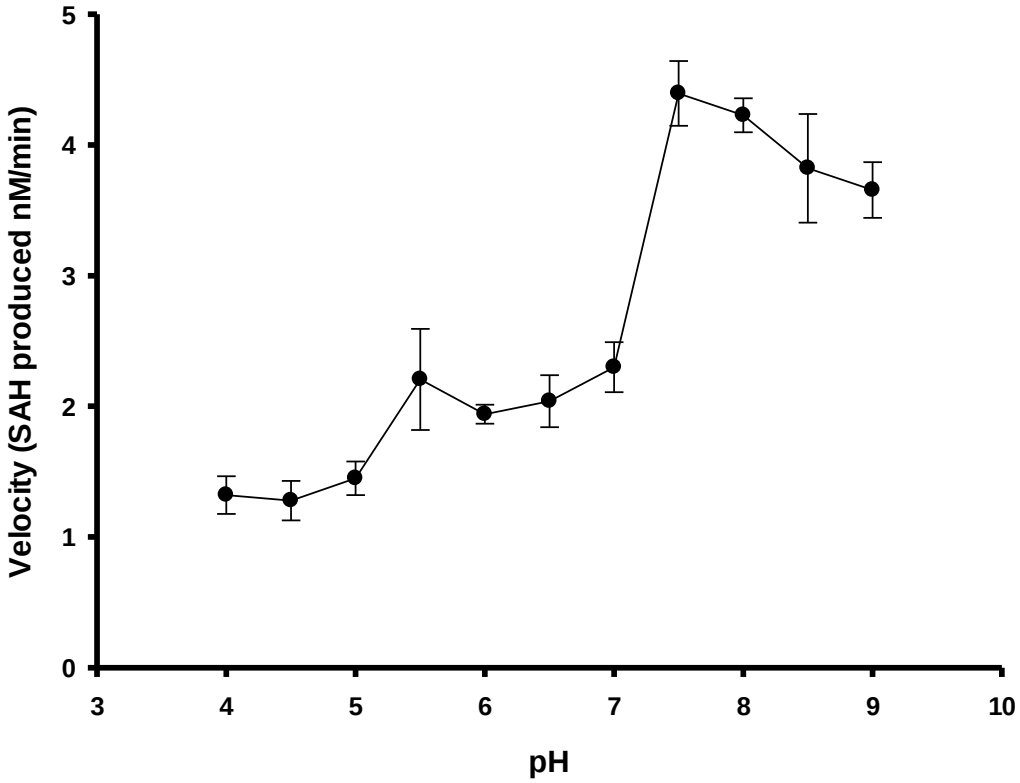

Figure 3.30 The effects of pH on SAH production by *mt*BioC in a SAM dependent luminescence assay.

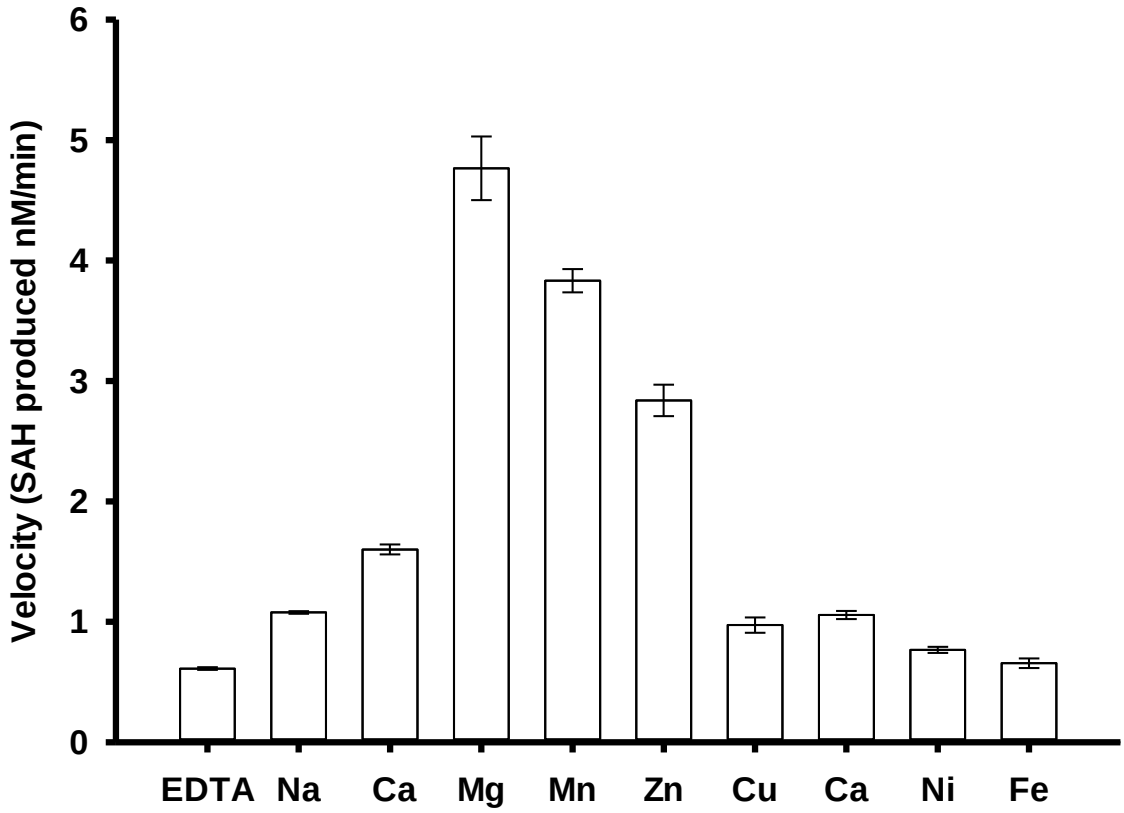

Figure 3.31 **Metal ion dependence on SAH production by *mt*BioC in a SAM dependent luminescence assay.** Mg^{2+} influenced the highest activity among the metal ions tested. EDTA abrogated activity

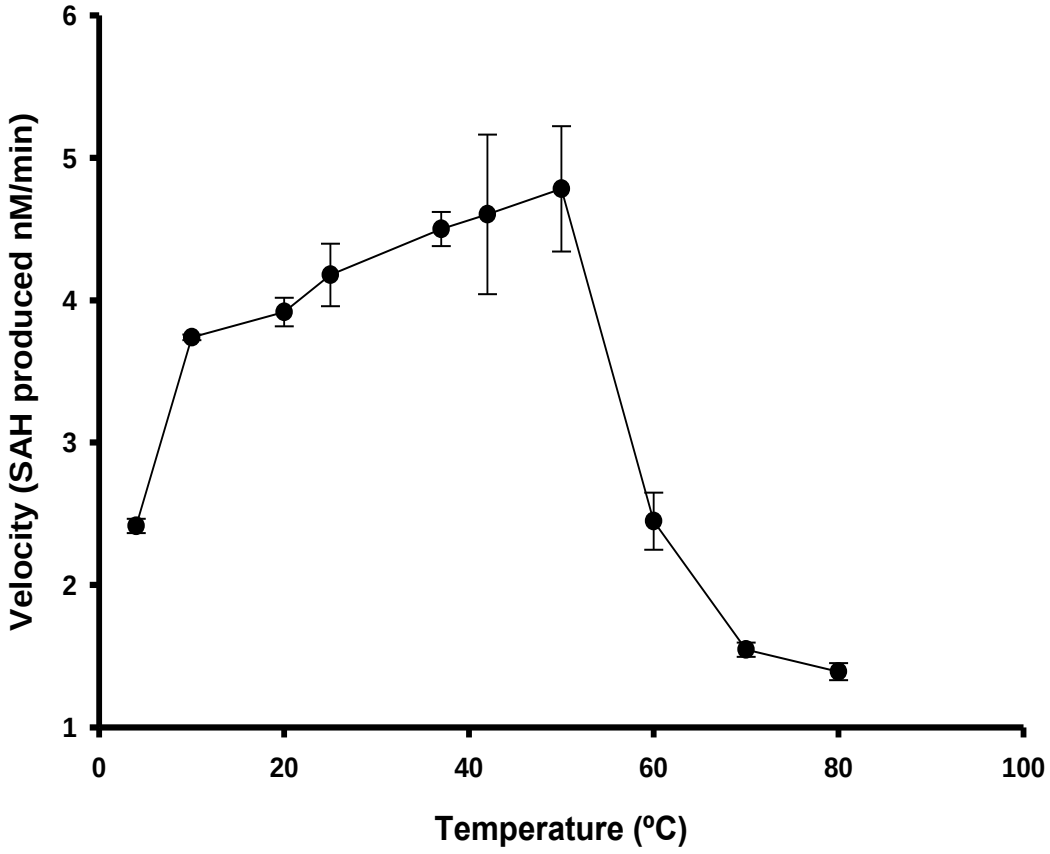

Figure 3.32 **Temperature optimisation on SAH production by *mt*BioC in a SAM dependent luminescence assay.**

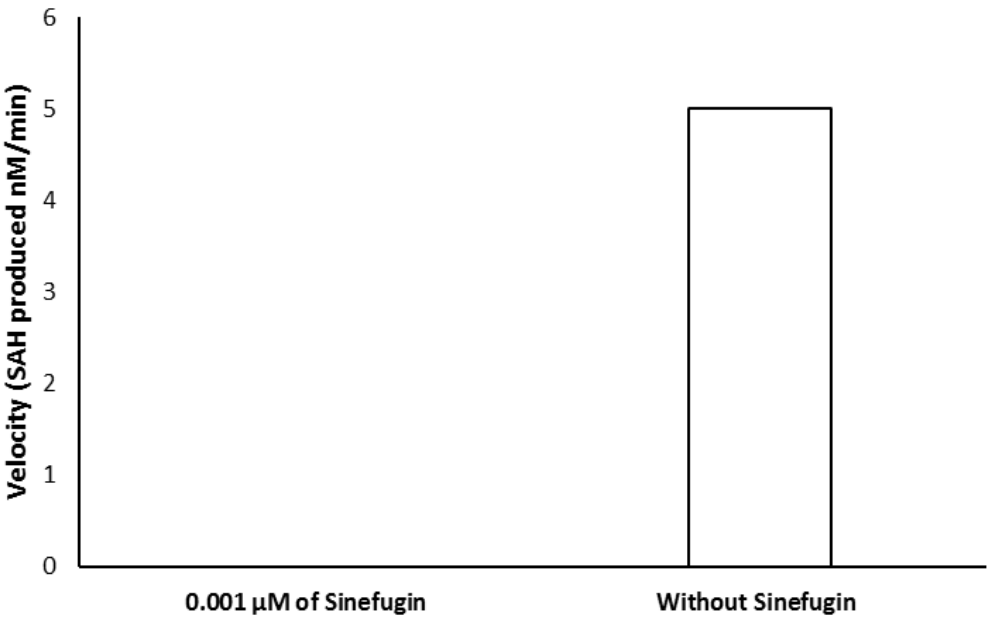

Figure 3.33 Effects of sinefugin on *mt*BioC. The inhibitor completely inhibited the enzyme activity at its lowest concentration of 0.001 µM

The results indicate that the optimal pH for *mt*BioC is pH~7.5 under the physiological conditions tested within the assay (Figure 3.30). There was a significant increase in activity of *mt*BioC when different metal ions or EDTA were added to the reaction as set up in Section 3.3.3. Mg^{2+}, Mn^{2+} and Zn^{2+} enhanced *mt*BioC activity more than other ions tested (Figure 3.31), with Mg^{2+} enhancing the highest activity in *mt*BioC. The results suggest that the enzyme requires the presence of Mg^{2+}, Mn^{2+} or Zn^{2+} for full activity and that the other ions are not suitable for this protein.

The optimal temperature range of the enzyme was observed to be between 37ºC and 50ºC. Temperature had a significant effect on the activity of the enzyme as expected. It was evident by the loss in activity at temperatures above 50ºC (Figure 3.32) that the enzyme was becoming denatured. Finally, Sinefugin, a known SAM inhibitor was tested in the *mt*BioC assay. The results of this test showed that the inhibitor completely inhibits the enzyme at the lowest concentration (0.001 µM) tested destroying all biochemical activity (Figure 3.33).

3.7 Discussion

Initial protein production experiments utilising a pET28b expression vector did not give the required results as little to no soluble protein was produced. Attempts to purify the protein using various *E. coli* expression strains including BL21(DE3), BL21(DE3) pLysS, C43(DE3), C43(DE3) pLysS, C41(DE3), HMS174(DE3) pLysS and B834(DE3) pLysS were not successful. Sequence analysis confirmed that there were no issues with the pET28b-*rv0089* construct, and the variety of *E. coli* strains used suggests an issue with the protein expression itself. Large quantities of protein were observed in the crude extracts but not the clarified indicating that there was a solubility issue and most of the recombinant protein was lost during this stage. As the main goal of these experiments was to perform crystallographic analysis refolding was ruled out. Mild denaturing conditions were assessed (1 M Urea and 2 M Guanidine hydrochloride) but to no avail with no change being observed in the recovery of recombinant protein.

A breakthrough came through codon optimisation and a change of expression vector. The use of pET23b in *E. coli* BL21 (DE3) enabled the purification of soluble recombinant Rv0089 *mt*BioC. This strain has a high transformation efficiency with a routine T7 expression factor (DE3). Additionally, it is also deficient in the cellular proteases Lon and OmpT which will reduce the level of degradation of recombinant protein expression (Chung *et al*., 1989, Phillips *et al*., 1984).

With *mt*BioC's shared identity of approximately 36% protein sequence and 47% similar to the *E. coli* BioC homolog, it could be envisaged that the organism shouldn't struggle to express the protein, but this wasn't the case. A large assortment of expression constructs, growth conditions, and host cells failed to give soluble *E. coli* BioC (Lin and Cronan, 2012) and the same recalcitrant behaviour as *E. coli* BioC was observed with homologues from *Kurthia* species, *Pseudomonas putida*, and *Chlorobium tepidum* which

were shown to be highly toxic to *E. coli* and could not be expressed to high levels (Lin and Cronan, 2012). The only amenable BioC homologue found to be expresable and purifiable is that of *Bacillus cereus* ATCC10987. The *B. cereus* bio operon is unidirectional and encodes homologues of all of the *E. coli* bio enzymes, although the sequence of *B. cereus* BioC shares only 26.5% identity with *E. coli* BioC. Before now, direct BioC activity methylation assay was not possible due to its inactive and insoluble nature, but this work proved that *mt*BioC can be both active and soluble and possible to conduct *mt*BioC methyl transfer assays. Notwithstanding this protein was stable and active throughout the assay and storage.

When the ability of malonyl-CoA as a substrate was tested, the enzyme showed good methyl acceptor ability (Figure 3.28). In a separate study (Lin and Cronan, 2012) malonyl-CoA methylation occurred, but at higher concentration utilised in the *mt*BioC assays. This supports the findings in this research where increase in methylation is also due to increase in malonyl-CoA concentration. Comparison between malonyl-CoA and glutaryl-CoA also revealed methylation activity by both substrates (Figure 3.29). Malonyl-CoA was found to be a better substrate that glutaryl-CoA. Malonyl-CoA is among the substrates that likely substitutes acetyl-CoA in BioC methylation reaction (Lin et al., 2010), hence the reason for its preference in *mt*BioC methylation. BioC methylation of malonyl moieties linked to either ACP or CoA has never been clear, with acyl-CoAs acting as reasonable *in vitro* analogues of acyl-ACPs because both are acidic in nature and share a similar 4'-phosphopantetheine group (Borgaro *et al*., 2011, Bennett *et al*., 2009).

The pH value influences reactions in such a way that it affects the shapes of both the enzyme and its complementary substrate active site. Changes in pH affects enzyme activity where extreme high or low pH results in complete loss in enzyme activity. The optimum pH value is the point at which the enzyme is most active and each enzyme has

greatest stability (Bennett *et al*., 1970). *mt*BioC pH profile was determined and it was equivalent to within the range of 7.2-7.5. During its purification, the enzyme was soluble in Tris buffer pH 7.4. The isoelectric point (pI) of *mt*BioC is 8.44, therefore its activity should be assayed in a pH value that is at least a unit away from its pI. Since pH 7.4 gives the best enzyme activity (Figure 3.30), it therefore suggests that the enzyme fulfils the condition for its pI and is consistent with a cytosolic protein.

Metal ions play a key role in enzyme activity through their oxidation-reduction capacity or by positioning and activating substrates on the active site of enzymes for reactions to occur. Some metal ions may act as 'superacids' and tend to become insensitive for pH changes (Guengerich, 2016). Enzymes select metals they use and can use as many metals as they can, but the presence of multiple metals results in differences in biological activity (Vashishtha et al., 2016). As enzymes show preference to certain metals, the fidelity of such metals continually decreases with use. The reasons for such selectivity are notably structural (Pence et al., 2009, Frank and Woodgate, 2007). Small differences among metals can be detected by proteins even when a metal is present at a higher concentration (Guengerich, 2016). The activity of enzymes is widely regulated through a metal ion complexation. This is key to the physiological requirement for enzyme stability and high catalytic activity (Gohara and Di Cera, 2016, Pfeiffer, 1954). *mt*BioC therefore showed the highest increase in methyl transfer when magnesium ions were used. Manganese and zinc ions also showed good activity when compared to each other (Figure 3.31). Therefore, the addition of metal ions or EDTA to this reaction showed a significant decrease in methyl transfer. This is contrary to what was observed when metal ions were added to a reaction involving *B. cereus* BioC where the addition had no significance on its BioC activity (Lin and Cronan, 2012). This difference in activity due to metal ion addition between *mt*BioC and *B. cereus* BioC could be as a result of structural differences between these proteins, although the *mt*BioC structure has not been determined yet.

Enzyme denaturation results due to its interaction with the aqueous environment. Its stability increases at a concentrated and dehydrated state and can be active after long periods at temperatures above 100ºC (Daniel and Danson, 2013). Rates of enzyme catalysed reactions increases with an increase in temperature. A 10ºC rise in temperature increases the activity of most enzymes by 50 to 100% (Bennett et al., 1970). Changes in enzymatic activity can be influenced by variations in reaction temperatures as small as 1 or 2 degrees which may result to a 10 or 20 % enhancement in activity (Martinek, 1969). Many enzymes are normally affected by high temperatures because an increase in temperature increases the rate of enzyme activity, but higher increases in temperature denatures proteins. Most optimal temperatures for enzyme activity are below 40ºC with any increase above that affecting enzyme activity (Pfeiffer, 1954). *mt*BioC showed its highest increase in activity at a temperature (50ºC) slightly above the usual temperature for optimal activity. The result suggests that this protein is highly stable and can be stored for reasonably longer periods.

The Michaelis-Menten constant, also known as K_m, is the concentration of the substrate that allows the enzyme to achieve half maximum velocity. This mean that the K_m is dependent on substrate concentration and it's a constant for a particular enzyme. It is a value that shows that 50% of the molecules of the enzyme are bound to the substrate molecules at a particular concentration. The K_m also shows the affinity of an enzyme to a particular substrate, whereby a decrease in K_m value mean the enzyme has a strong affinity to the substrate. The K_m value of an enzyme depend on a particular substrate and on conditions such as temperature and concentration of ion. An increase in the concentration of the substrate shows that there are more enzyme molecules working and 50% of the enzymes are attached to the substrate at half maximum velocity. The result from this experiment showed that the K_m value was low (128 µM), which mean the enzyme has a high affinity for the substrate and will require a lower concentration of the

substrate to achieve V_{max}. This is true, considering that BioC readily methylate malonyl-CoA as the starting substrate for pimelate biosynthesis.

SAH competitively inhibits SAM-dependent methyltransferases. SAH, a product of methyl transfer is expected to inhibit BioC depending on its concentration. A natural antibiotic isolated from *Streptomyces griseolus*, sinefugin, is another potent methyltransferase inhibitor (Lévy-Schil *et al*., 1993, Reich and Mashhoon, 1990). Sinefugin is a more potent inhibitor than SAH and presents as an electrostatic mimic of SAH (Borchardt *et al*., 1979). Even with the lowest concentration of sinefugin (0.001 µM) *mt*BioC activity was completely inhibited. It was observed from the background that the protein still had some activity even in the presence of the inhibitor, but the lowest concentration of the inhibitor does not allow for any clear observation.

3.8 Conclusion

The importance of biotin as an enzyme co-factor required by all organisms is very vital (Attwood and Wallace, 2002, Knowles, 1989). Two genes, *bioC* and *bioH* have been identified as two essential genes involved in biotin synthesis (Lin and Cronan, 2011). The dominant, but not the only pathway for the synthesis of biotin pimeloyl moiety in organisms is the BioC-BioH pathway. This pathway utilises a methylation and demethylation mechanism to produce a malonyl-CoA methyl ester to be used in biotin biosynthesis (Lin and Cronan, 2011). Among the 868 complete bacterial genomes currently available, annotated BioC homologues are present in 569 genomes, but some bacteria still do not have a recognisable encoded BioC homologue.

In the BioC-BioH pathway, the malonyl moiety is disguised and allows the chain to elongate and a subsequent elimination of an oxo-group by enzymes involved in fatty acid synthesis. This results in a pimeloyl moiety which is the carbon backbone for biotin. This

disguise facilitates synthesis in biotin biosynthesis, whereas the protective group prevents undesired reactions in organic synthesis (Lin and Cronan, 2011).

BioC was thought to have been involved in pimeloyl-CoA synthesis as an acyl carrier protein, where BioH obtains pimeloyl units from BioC and transfers it directly to CoA (Sanishvili *et al*., 2003). However, this proposal is no longer the case as BioC has recently been proposed to catalyse methyl group transfer from SAM to the ω-carboxyl group of malonyl thioester of either CoA or acyl carrier protein to form an *O*-methyl ester (Lin *et al*., 2010, White *et al*., 2005). Another study further suggested that malonyl-ACP is a better methyl acceptor substrate than malonyl-CoA, however in that study the malonyl-ACP was from *E. coli* whereas the BioC was from *B. cereus*. In this study, the methyl accepting ability of malonyl-ACP was not tested and therefore no comparison can be made on the methyl activity of malonyl-CoA and malonyl-ACP. However, both malonyl-CoA and glutaryl-CoA tests showed methyl transfer activity. The assay on *mt*BioC is important since previous assays were only done on *E. coli* BioC and *B. cereus* BioC in which malonyl-ACP was the preferred methyl acceptor substrate (Lin and Cronan, 2012). This suggests that the malonyl thioester of *Mtb* might be a better malonyl-CoA methyl acceptor than the *E. coli* BioC and *B. cereus* BioC. There was also a reasonable amount of methyl transfer when glutaryl-CoA was tested. This also suggests that the *mt*BioC can target both malonyl-CoA and glutaryl-CoA, two methyl substrates poorly targeted in *B. cereus*. This goes further to suggest that in *Mtb* malonyl-CoA methyl ester is the likely replacement of acetyl-CoA which is the substrate of 3-ketoacyl-ACP synthase III (FabH), an enzyme involved in the synthesis of new acyl chains (Heath and Rock, 2002). *mt*BioC must be reasonably active so it can compete with FabH (*mt*FabH) for malonyl-CoA/ACP. Over activity of *mt*BioC will result to too much conversion of malonyl-CoA/ACP to the methylated species which will block fatty acid synthesis in turn. There is therefore likely a tight control of BioC activity and expression. This is possible because the BioC gene in

both *E. coli* and *B. cereus* is co-transcribed with other genes along the fatty acid biosynthetic pathway, and its expression levels are coordinated. This ensures that BioC activity leads to a steady and low level production of malonyl-CoA/ACP methyl ester in a limiting methyl environment (Lin and Cronan, 2012). Also, increasing levels of BioC expression resulted in impaired growth in *E. coli* (Lévy-Schil *et al*., 1993). This increase in excess BioC resulted in redirection of flux distribution in primary metabolism or production of toxic BioC products.

This investigation shows that *Mtb* BioC has been identified, isolated and purified. Limited assay on this protein were carried out, but there is need for further purification and characterisation studies. The characterisation studies will further generate useful data good enough for molecular modelling and the data would be used to model inhibitors against the protein in a bid to finding a potent anti-tubercular drug and cure.

Chapter 4

Identification and molecular studies on BioH1, BioH2 and Rv1882c enzymes in *Mtb*

4 Pimelate Biosynthesis enzymes Rv3177 (mtBioH1), Rv2715 (mtBioH2) and Rv1882c (mtFabG)

4.1 Introduction

Central to the biosynthetic pathways of biotin is the precursor methyl pimelate. Studies in *E. coli* have shown that methyl-pimelate is synthesized via a similar pathway to fatty acid biosynthesis. Initially, a priming unit, either glutaryl or malonyl-CoA, is methylated to form ω-methoxy-glutaryl-CoA or ω-methoxy-malonyl-CoA respectively. This SAM-dependent methylation reaction is performed by BioC, an enzyme in *E. coli* which has been shown to be the initial step in biotin synthesis (Figure 4.1). Due to the methylation of the ω-carboxylic acid group of the fatty acid this product can now be utilised in fatty acid biosynthesis (FAS) type reactions. After 1-2 cycles of FAS, depending on the start substrate the ω-methoxyl-fatty acid product is an ω-methoxy-pimeloyl-ACP.

In *E. coli*, BioH, a ω-methylesterase removes the methyl from the ω-methoxy-pimeloyl-ACP (Figure 4.1, enzyme in the lower red box) producing pimeloyl-ACP, the precursor to biotin synthesis. Both BioC and BioH are yet to be identified and characterised in *Mycobacterium*. It is also noteworthy that the Mycobacterial FAS-II system has significantly different substrate specificity to that of *E. coli* and it is speculated that a secondary FAS-II type pathway is required in *Mycobacterium*. To date all the other enzymes involved in this secondary ω-methoxyl-acyl-ACP FAS-II pathway are yet to be identified.

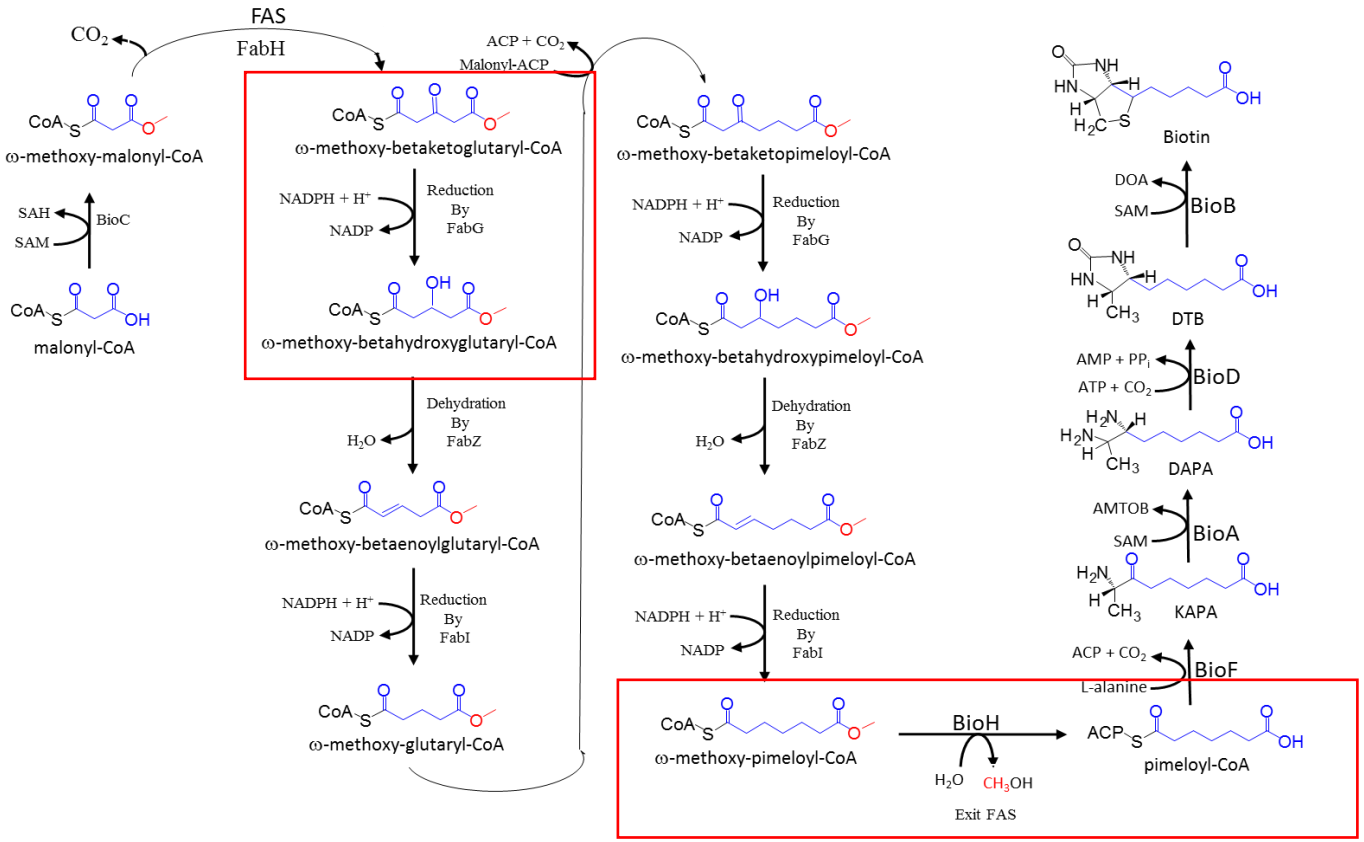

Figure 4.1 **Current proposed pathway of biotin synthesis in *E. coli*.** The primer molecule malonyl-CoA is methylated by BioC at its ω-carboxyl group. The resultant ω-methoxy-malonyl-CoA methyl ester hijacks the fatty acid biosynthetic pathway and act as a priming unit, instead of the acetyl-CoA in fatty acid synthesis which gives rise pimeloyl-ACP methyl ester. Pimeloyl-ACP is formed when BioH cleaves to the ester to prevent further elongation and the product is utilised by BioF to make KAPA (7-keto-8-amino pelargonic acid) that starts biotin synthesis. KAPA is catalysed by BioA to form DAPA (7,8-diaminopelargonic acid) which is further catalysed by BioD to form dethiobiotin (DTB) before biotin is finally formed through the enzyme BioB (Adapted from Lin *et al*., 2010).

Preliminary bioinformatics analysis using the *E. coli* BioH identified two candidate BioH enzymes in *Mtb*. The presence of two highly similar genes could indicate that the ω-methoxy-pimeloyl-ACP produced in Mycobacteria are utilised in two distinct biosynthetic pathways. Analyses of the biotin and mycobactin structures indicate that pimelate is a key constituent of both molecules. It is therefore hypothesised that these two candidate proteins are involved in this dual utilisation of ω-methoxy-pimeloyl-ACP products. Rv3177 has been annotated in this study as BioH1 as it is annotated in the genome as essential, whereas Rv2715, BioH2, is not (Sassetti *et al*., 2003).

Another enzyme involved in pimelate biosynthesis in *E. coli* is β-ketoacyl-acyl carrier protein (ACP) reductase (FabG) (Figure 4.1, indicated in the top red box). FabG is a ubiquitous enzyme that acts in type II fatty acid synthase (FAS-II) systems (White *et al*., 2005). FabG reduces β-ketoacyl-ACP to β-hydroxyacyl-ACP using the cofactor NADPH or NADH. FAS-II group of enzymes is made up of disassociated enzymes and each of the enzymes catalyses a specific reaction in which FabG plays a key role (Oppermann *et al*., 2003). The FAS-I on the other hand is made up of a single multi-enzyme protein complex that synthesizes lipids. The FabG proteins are classified under the broad family of short-chain dehydrogenase reductase (SDRs) involved in the catalysis of a wide spectrum of reactions (Oppermann *et al*., 2003). A recent study showed that there are some bacteria that can harbour multiple *fabG* encoding genes as found in *Ralstonia solanacearum* (Feng et al., 2015a). In *E. coli* there is only one gene coding for FabG (Lai and Cronan, 2004). FabG is involved in the *E. coli* biotin biosynthetic pathway where it reduces β-ketoglutaryl-ACP methyl ester into β-hydroxyglutaryl-ACP methyl ester which then feeds into the pathway as a substrate for subsequent products to be formed before biotin is finally synthesized (Lin *et al*., 2010).

In *Mtb*, cell wall biosynthesis is associated with several micronutrients and biochemical molecules. An important micronutrient critical to this important process in Mycobacteria is biotin. Also known as vitamin H or B7, biotin is an essential enzyme cofactor needed by all forms of life (Lin *et al*., 2010, Salaemae *et al*., 2011)

The discovery of biotin dates back to the 1940's, yet its detailed biosynthetic pathway is not completely clear in any organism (Arabolaza *et al*., 2010). Biotin dependant enzymes, such as pyruvate carboxylase (PC) and acyl-CoA carboxylase (ACC), catalyses the carboxylation of some acyl-CoA substrates, such as acetyl-CoA, propionyl-CoA and butyryl-CoA (Arabolaza *et al*., 2010, Gago *et al*., 2011). One of the major cellular products formed by this biotin-dependent biosynthetic process is malonyl-CoA. Malonyl-CoA is the major donor unit for both fatty acid biosynthesis and polyketide synthesis which receive these catalysed products as substrates enabling the synthesis of mycolic acids and multi-methyl-branched fatty acids present in the mycobacterial cell envelope (Salaemae *et al*., 2011, Kremer *et al*., 2002). Therefore, biotin is key to the survival of the organism, as it is used in the synthesis of cell wall components particularly the complex lipid components. Similarly, all the required nutrients needed by bacterial pathogens must be available in the surrounding host tissues.

4.2 Aims and objective

The aim of this study is to perform biochemical and biophysical characterisation of 3 novel proteins (Rv3177, Rv2715 and Rv1882c) in order to elucidate key enzymes involved in the initial stages of pimelate biosynthesis in *Mtb*. The specific aims of this chapter will involve:

1. Isolation and purification of *mt*BioH1 (Rv3177), *mt*BioH2 (Rv2715) and Rv1882c enzymes isolated from *E. coli* expression strains. This will be achieved through the following objective:

    - Isolation and purification of recombinant *mt*BioH1 (Rv3177), *mt*BioH2 (Rv2715) and Rv1882c from different *E. coli* expression strains. Purification will involve the use of Immobilized Metal Affinity Chromatography (IMAC) that utilises Nickle charge His-trap columns (HiTrap FF, GE Healthcare).

4.3 Results and Discussion

4.3.1 Gene identification

The most probable candidates for BioH function in *Mtb* was identified using the UniProtKB - P13001 (BIOH_ECOLI) protein sequence and the BLASTP function on the Tuberculist web server to identify possible candidates – (http://genolist.pasteur.fr/TubercuList/genome.cgi).

	Bit Score	E Value
M. tuberculosis H37Rv|Rv2715|Rv2715 POSSIBLE HYDROLASE	47	5e-07
M. tuberculosis H37Rv|Rv3177|Rv3177 POSSIBLE PEROXIDASE	44	4e-06
M. tuberculosis H37Rv|Rv0045c|Rv0045c POSSIBLE HYDROLASE	41	4e-05
M. tuberculosis H37Rv|Rv3569c|hsaD 4,9-DHSA hydrolase	41	5e-05
M. tuberculosis H37Rv|Rv3670|ephE POSSIBLE EPOXIDE HYDROLASE	39	3e-04
M. tuberculosis H37Rv|Rv0840c|pip PROB. PROLINE IMINOPEPTIDASE	38	4e-04

Rv2715 and Rv3177 showed the highest degree of similarity. Sequence alignment showed that Rv2715 and Rv3177 have 23% and 23% identity and 40% and 37% similarity to *ec*BioH, respectively. The *E. coli* and the mycobacterial BioH protein sequences were aligned using the multiple sequence alignment programme at the Clustal Omega (Figure 4.2).

Similarly, the mycobacterial biotin associated FabG was originally identified in *Mycobacterium marinum* (Yu et al., 2011). Bioinformatics analysis of *E. coli* and *M. marinum* FabG (MMAR_2770) identified only one candidate for FabG in *Mtb* which is Rv1882c (Figure 4.3).

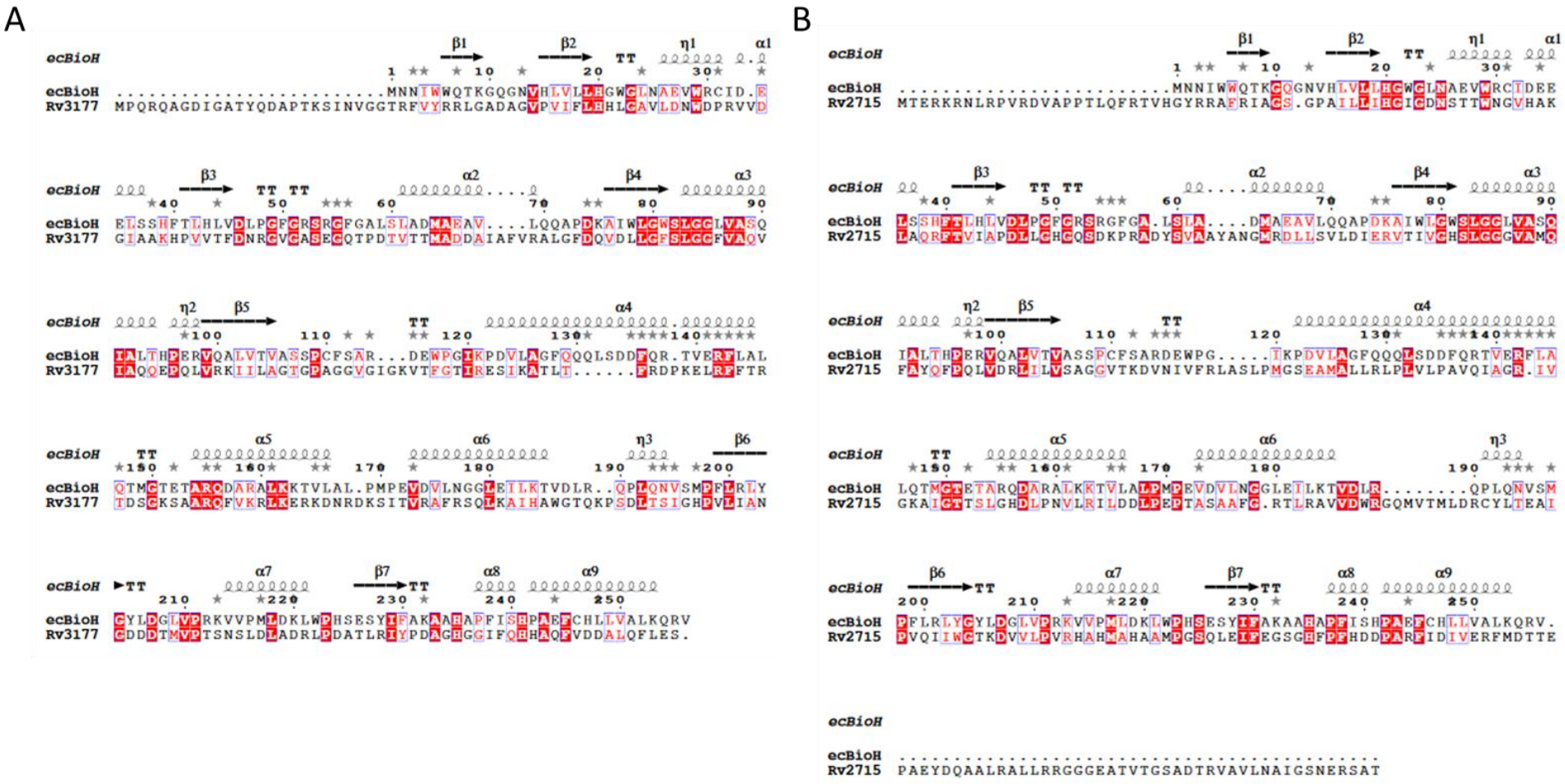

Figure 4.2 **Protein alignment of *E. coli* BioH (ecBioH) and Mycobacterial BioH1 (mtBioH1, Rv3177, (A)) and Mycobacterial BioH2 (mtBioH2, Rv2715, (B)) sequences.**

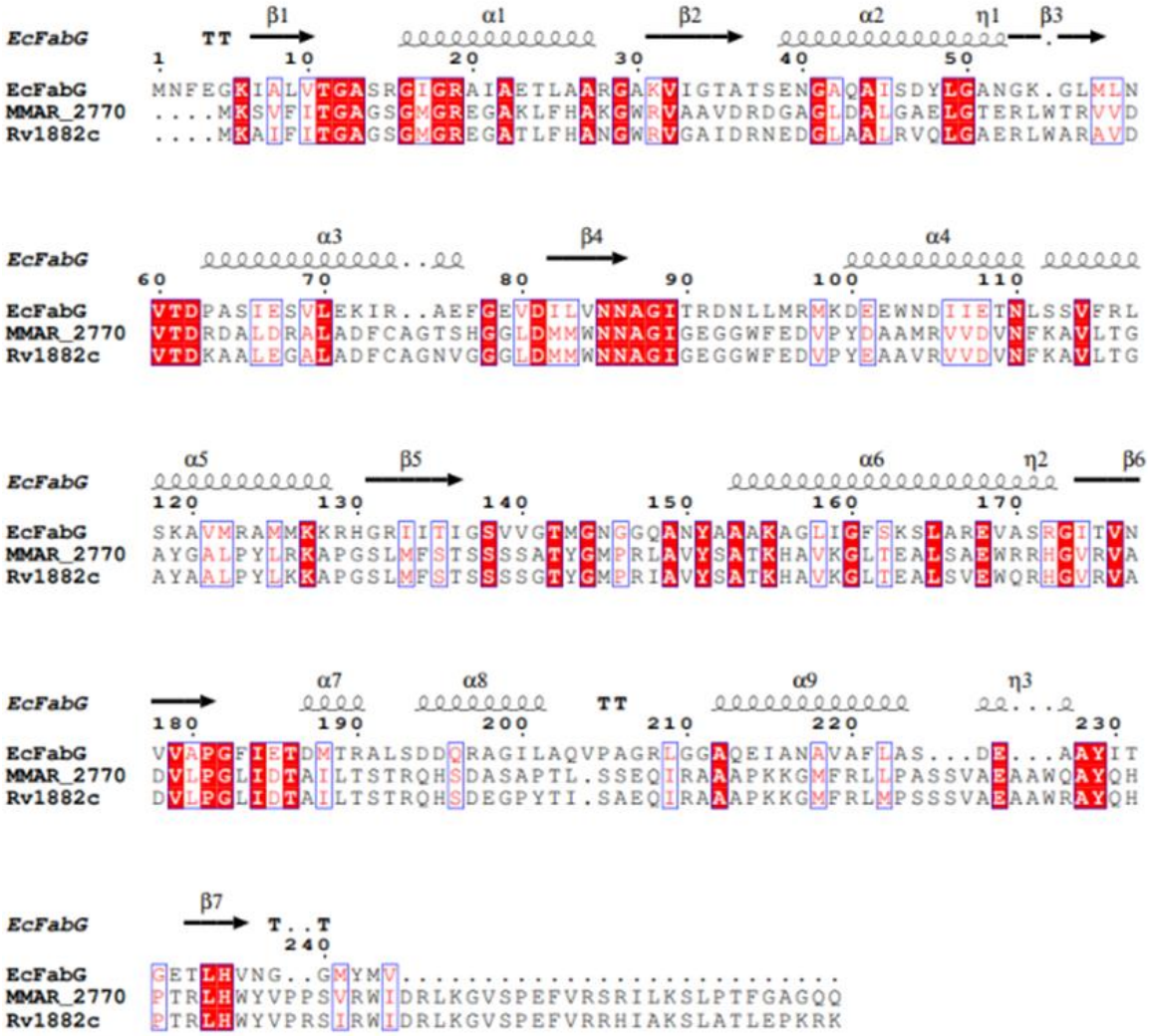

Figure 4.3 Protein alignment of *E. coli* FabG (ecBioH) and *M. marinum* FabG (MMAR_2770) and *Mtb* Rv1882c.

4.3.2 Polymerase Chain Reaction (PCR)

DNA sequence of *mt*BioH1, *rv3177*; *mt*BioH2, *rv2715* and *mt*FabG-Bio, *rv1882c*; were utilised to design PCR primers (Table 4.1) which would introduce 5' *Nde*I and a 3' *Hind*III restriction sites (underlined) that would allow subsequent cloning of the gene of interest into pET28b and pHMR3 expression vectors (Figure 4.4).

Table 4.1 Cloning primers for *mt*BioH1, rv3177; *mt*BioH2, rv2715 and *mt*FabGBio, rv1882c. Restriction sites are underlined.

Primer Name		Sequence		Usage
Rv1882cFor	5'	AAAAAACATATGAAAGCGATATTCATCACC	3'	pET28b, pHMR3
Rv1882cRev	5'	AAAAAAAAGCTTTTACTTCCGTTTTGGCTC	3'	pET28b, pHMR3
Rv2715For	5'	AAAAAACATATGACCGAGCGGAAGCGAAAT	3'	pET28b, pHMR3
Rv2715Rev	5'	AAAAAAAAGCTTTCAGGTAGCGCTGCGTTC	3'	pET28b, pHMR3
Rv3177For	5'	AAAAAACATATGCCCCAGAGACAGGCCGGC	3'	pET28b, pHMR3
Rv3177Rev	5'	AAAAAAAAGCTTTCACGACTCGAGAAACTG	3'	pET28b, pHMR3

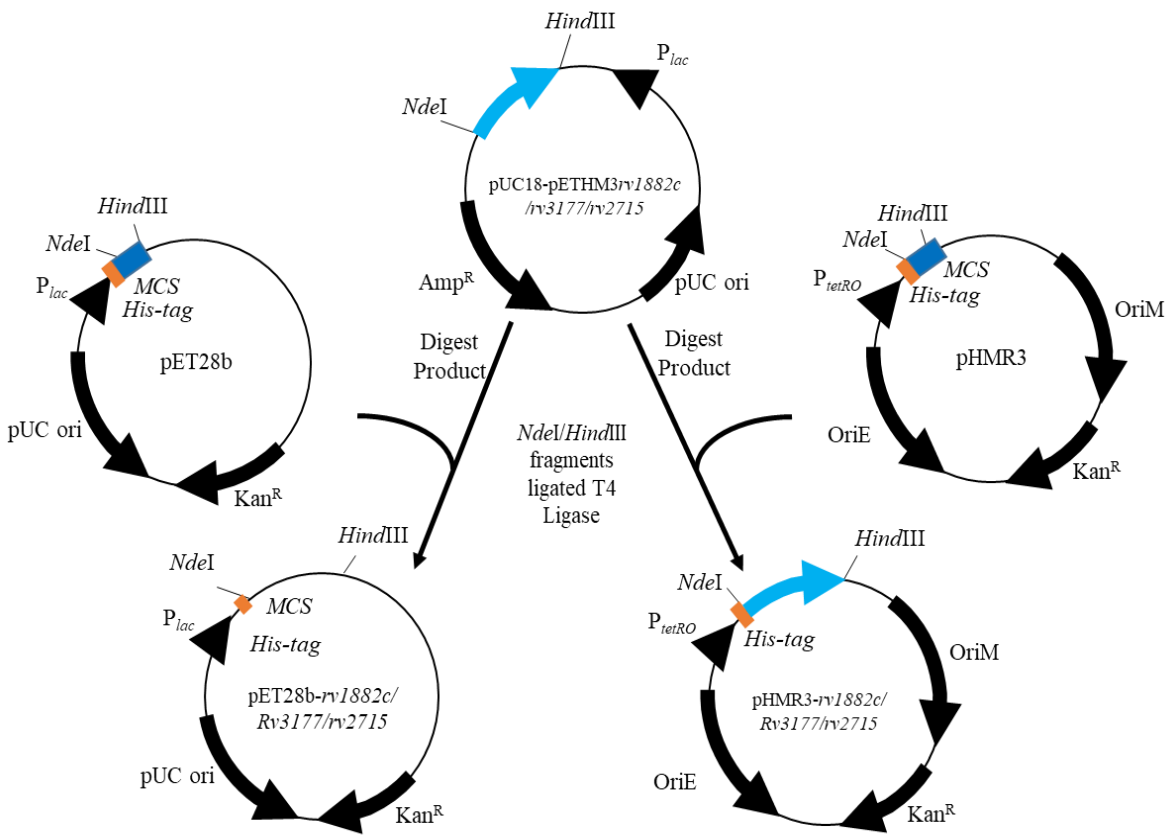

Figure 4.4 Schematic representation of the *rv3177, rv2715, rv1882c* expression plasmid construction. Plasmid map construction of pET28-rv0089 and pHMR3- *rv3177, rv2715, rv1882c*. In both cases the genes of interest were amplified and cloned into kanamycin resistant pET28b vector and the *E. coli* shuttled pHMR3 vector, both digested with *Nde*I/*Hind*III.

The genomic DNA template was prepared from *Mtb* H37Rv and used for DNA amplification. PCR optimisation protocols were performed as outlined in Section 2.3.1 (Figure 4.5). The presence of a DNA fragment was observed with the predicted 861 bp, 1,026 bp, 858 bp, amplicons corresponding to the *rv3177, rv2715, rv1882c* genes, respectively.

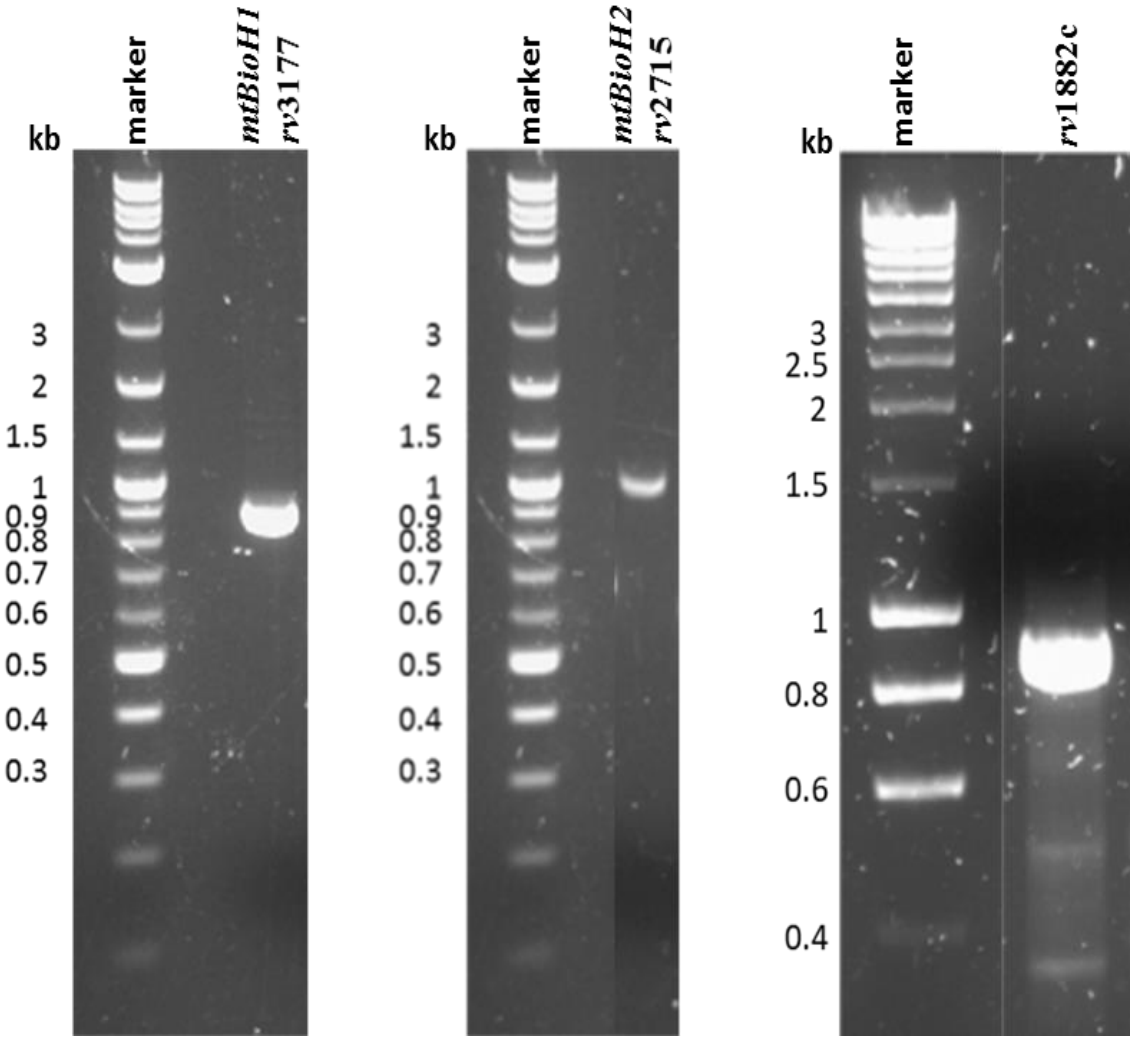

Figure 4.5 Agarose gel electrophoresis of PCR products for *rv3177, rv2715, rv1882c*

The *rv3177, rv2715, rv1882c* genes were amplified by bulk PCR and purified from agarose for further use by QIAquick Gel Extraction.

The purified DNA fragment was ligated using T4 ligase (Section 2.8.2) into *Sma*I-cut pUC18 and the mixture used to transform *E. coli* XL10 Gold. This resulted in the successful observation of visible colonies after 16 hour incubation at 37ºC. Blue/white screening analysis was performed on the resulting pUC18-*rv3177, -rv2715, -rv1882c* ligations. The correct size amplicons corresponding to the genes of interest were successfully cloned into pUC18 which was confirmed by restriction digest of the purified plasmid from white colonies (Figure 4.6).

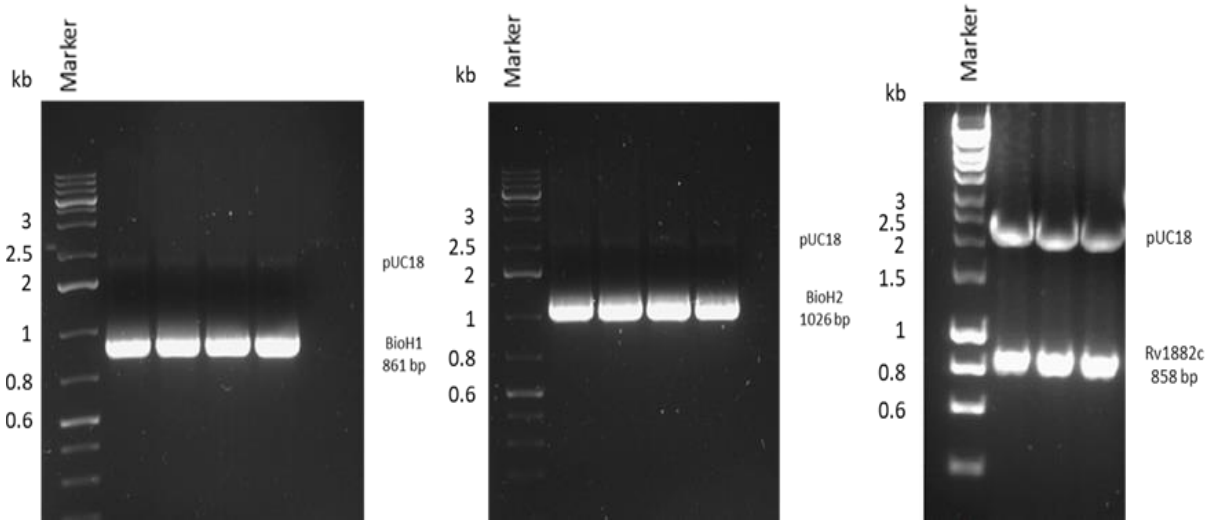

Figure 4.6 Double digest *Nde*I/*Hind*III restriction enzyme screening of pUC18-*rv3177, -rv2715, -rv1882c* constructs.

All amplicons were successfully cloned into pUC18 which was observed by restriction digest of the purified plasmid. Plasmids with the correct restriction pattern were sent for sequencing via GATC (www.gatc-biotech.com) (Figures 4.7, 4.8, 4.9).

Figure 4.7 Sequencing alignment of pUC18-*rv3177*. *Nde*I and *Hind*III restriction sites are indicated.

Figure 4.8 Sequencing alignment of pUC18-*rv2715*. *Nde*I and *Hind*III restriction sites are indicated.

Figure 4.9 Sequencing alignment of pUC18-*rv1882c*. *Nde*I and *Hind*III restriction sites are indicated.

These fragments were then sub-cloned into pET28b (*E. coli* expression vector) and pHMR3 (a mycobacterial expression vector). The sequenced pUC18 plasmid were digested with *Nde*I and *Hind*III and ligated into similarly cut pET28b and pHMR3. Screening of valid constructs was performed by restriction digest (Figure 4.10). Plasmids with the correct restriction pattern were sent for confirmatory sequencing via GATC.

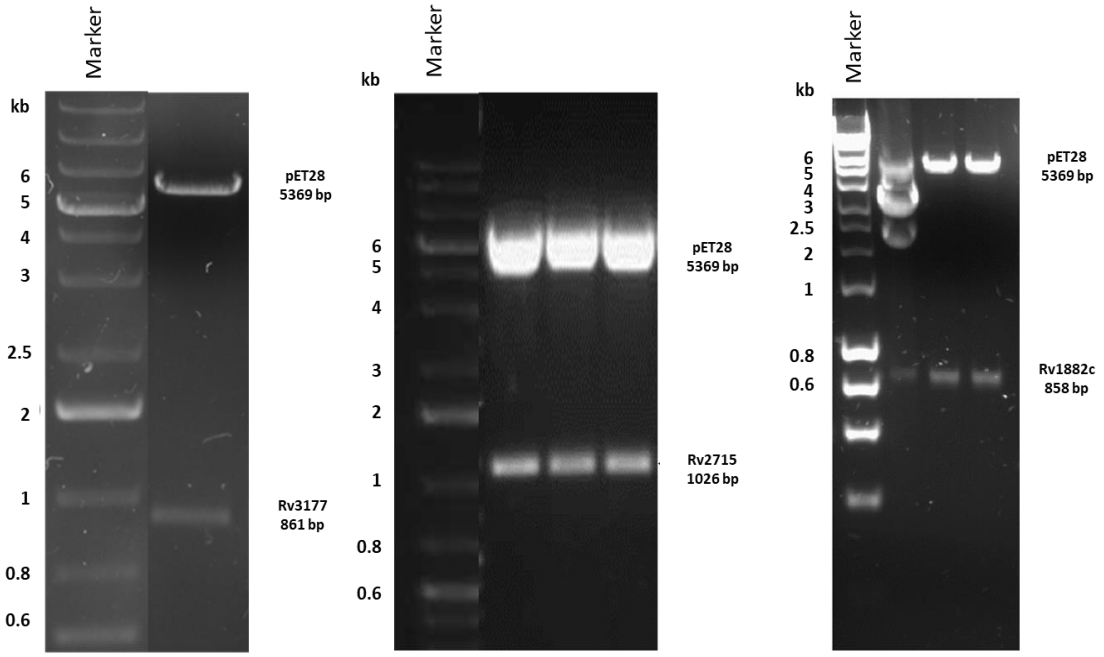

Figure 4.10 Screening double digest of pET28b constructs of *rv3177, rv2715* & *rv1882c*

The resulting plasmids were used to transform *E. coli* C41 DE3 to enable protein expression and purification analysis to be performed. Several attempts to express the genes into the expression strains did not work. Therefore, it was concluded that there was need for codon optimisation of the DNA sequence for better expression.

4.3.3 Codon optimisation

Rv3177, Rv2715 & Rv1882c protein sequence was optimised using the MWG optimisation server. Protein sequences were transcribed to ensure the correct sequence would be translated. The optimised sequence for *E. coli* expression was purchased from MWG biotech containing the relevant cloning restriction sites (Figure 4.11).

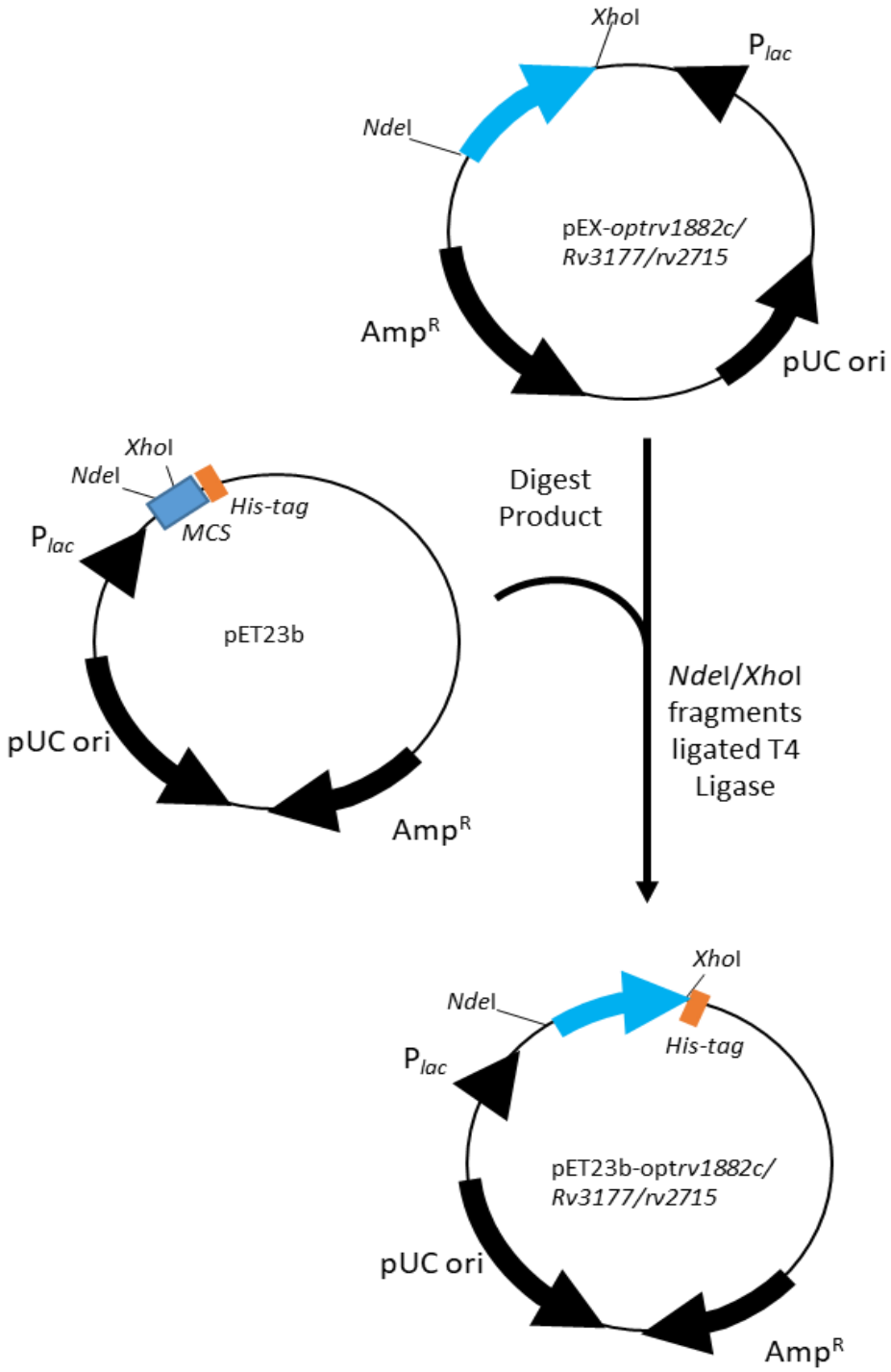

Figure 4.11 Schematic representation of the *optrv3177, rv2715* & *rv1882c* expression plasmid construction. Plasmid map construction of pET23-*rv3177, rv2715* & *rv1882c*; digested with *Nde*I/*Xho*I.

The *Nde*I/*Xho*I digest fragment from the pEX construct was purified and ligated into similarly cut pET23b using T4 ligase (Section 2.8.2) and the mixture used to transform *E. coli* XL10-Gold. The amplicon corresponding to the optimised *rv3177*, *rv2715* & *rv1882c* genes were successfully cloned into pET23b which was confirmed by restriction digest of the purified plasmid (Figure 4.12).

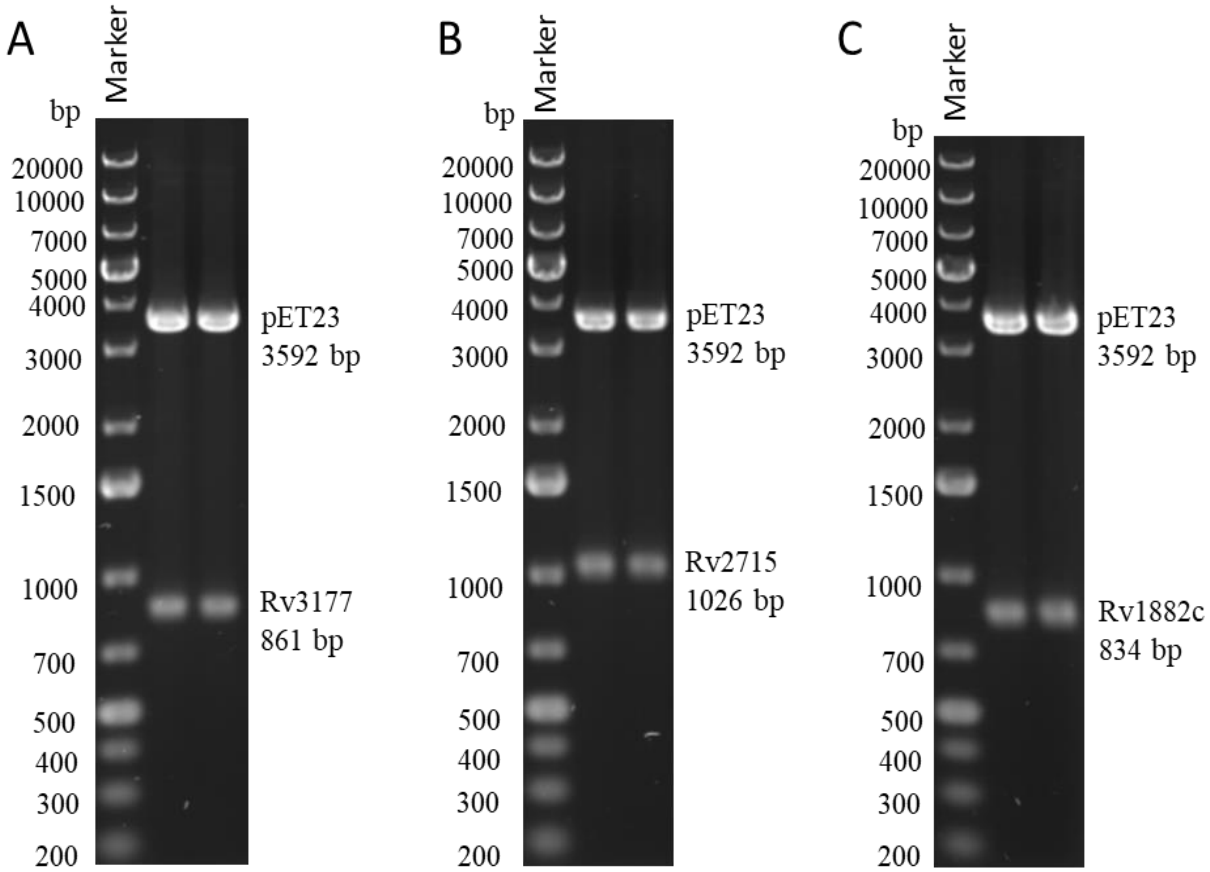

Figure 4.12 Screening of (A) pET23-Rv3177 (*mt*BioH1), (B) pET23-Rv2715 (*mt*BioH2) and (C) pET23-Rv1882c. Restriction digestion was done with *Nde*I/*Xho*I to produce two fragments in each case corresponding to 3.5 Kb pET23 vector and the corresponding proteins

The resulting plasmid was sequenced by Sanger sequencing using standard pET primers at GATC (www.gatc-biotech.com) (Figures 4.13, 4.14, 4.15).

Figure 4.13 Codon optimised pET23b-*rv3177* sequencing alignment.

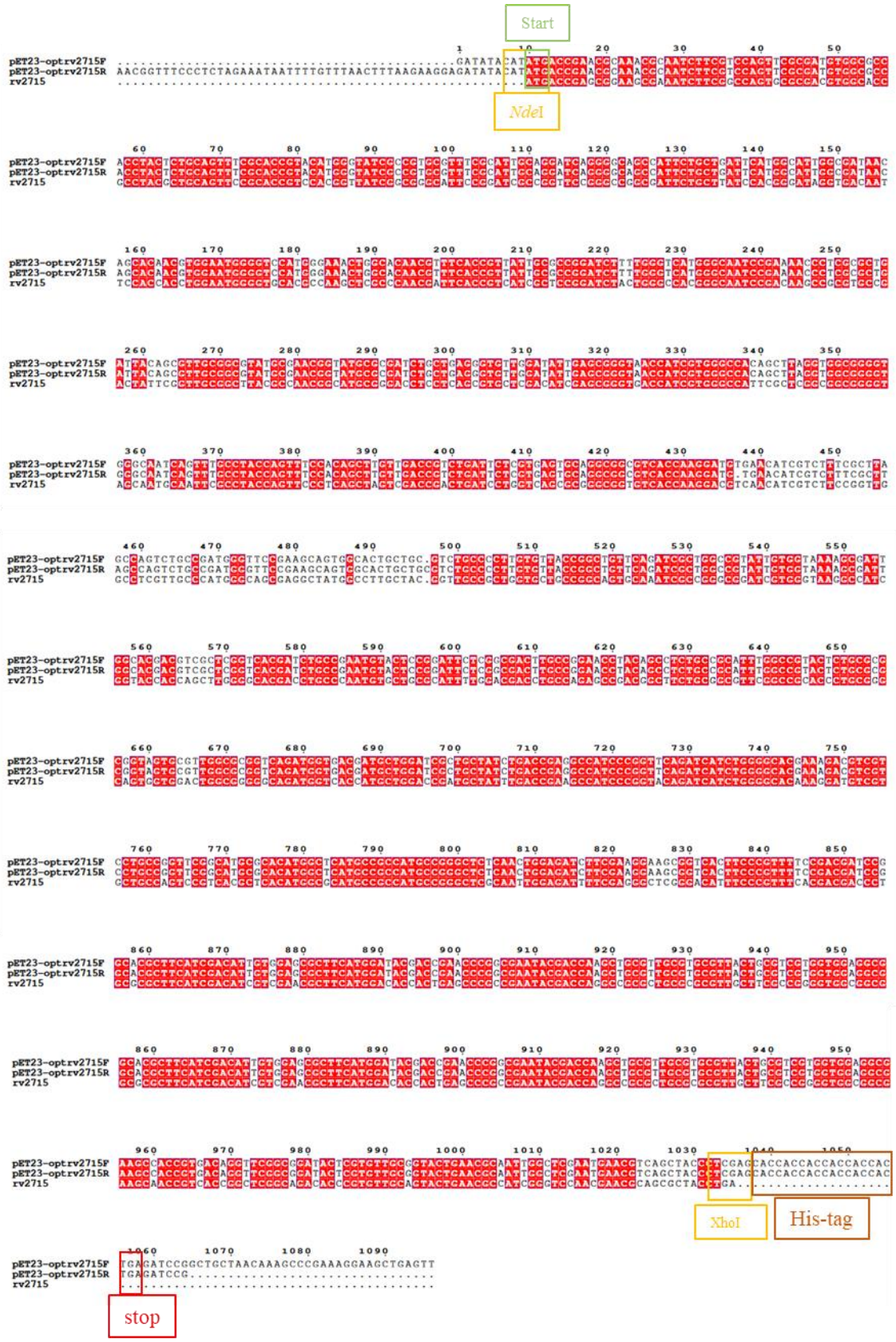

Figure 4.14 Codon optimised pET23b-*rv2715* sequencing alignment.

Figure 4.15 Codon optimised pET23b-*rv1882c* sequencing alignment.

4.4 Expression studies

The *E. coli* codon optimised pET23b constructs were used to transform *E. coli* BL21 (DE3) as this gave the best expression in previous studies. Broth cultures containing ampicillin (Amp^{100}) were incubated at 37ºC overnight. The following day 1% inoculum was used to inoculate 1 L LB broth with Amp^{100} followed by orbital incubation at 37ºC to an OD_{600} of 0.6. The culture was allowed to cool, then 1 mM isopropyl β-D-1-thiogalactopyranoside (IPTG) was added and further incubated at 16ºC overnight. The following day the culture was harvested at 4000 x *g* at 4ºC for 10 minutes and cell pellets stored at -20ºC for future use. 1 L cultures were lysed and clarified as per previous experiments. Clarified supernatants were then applied to Immobilized Metal Affinity Chromatography (IMAC). Nickle charge His-trap columns (HiTrap FF, GE Healthcare) were washed and charged as per the manufacturers' protocols followed by the application of supernatant. A crude imidazole concentration gradient was employed to investigate the binding of the proteins (Figures 4.16-4.18).

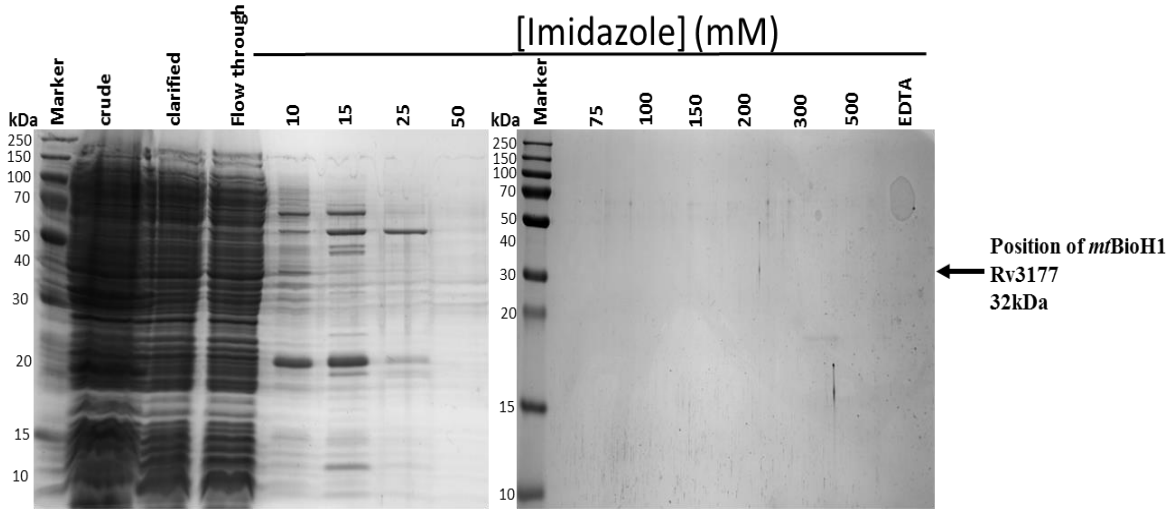

Figure 4.16 **12 % SDS-PAGE analysis of *mt*BioH1 from *M. tuberculosis*.** PageRuler Plus prestained protein ladder was used. There was no recombinant protein visible; mtBioH1 is 32 kDa.

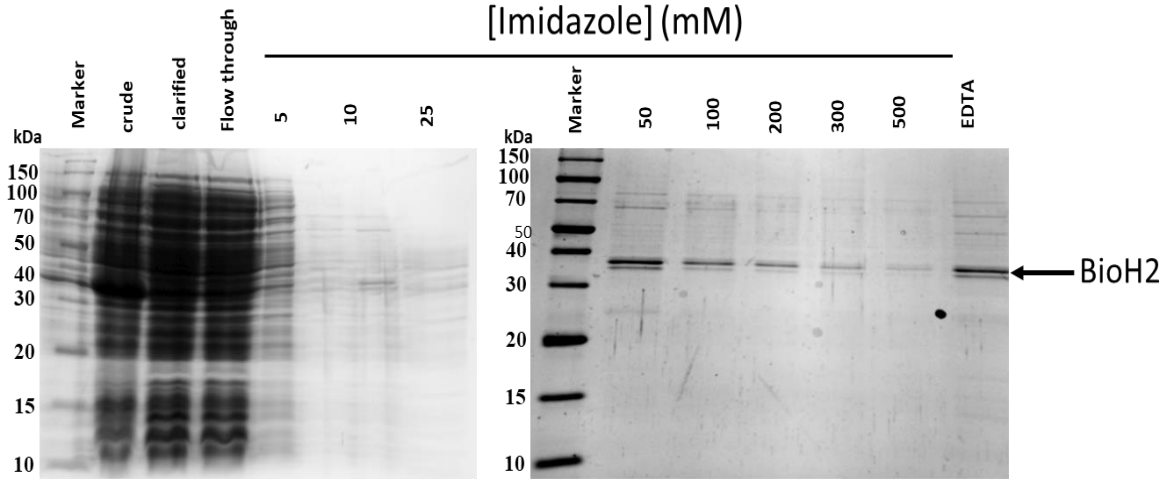

Figure 4.17 **12 % SDS-PAGE analysis of *mt*BioH2 from *M. tuberculosis.*** PageRuler Plus prestained protein ladder was used. *mt*BioH2 (38 kDa) eluted at concentrations of imidazole from 50 mM.

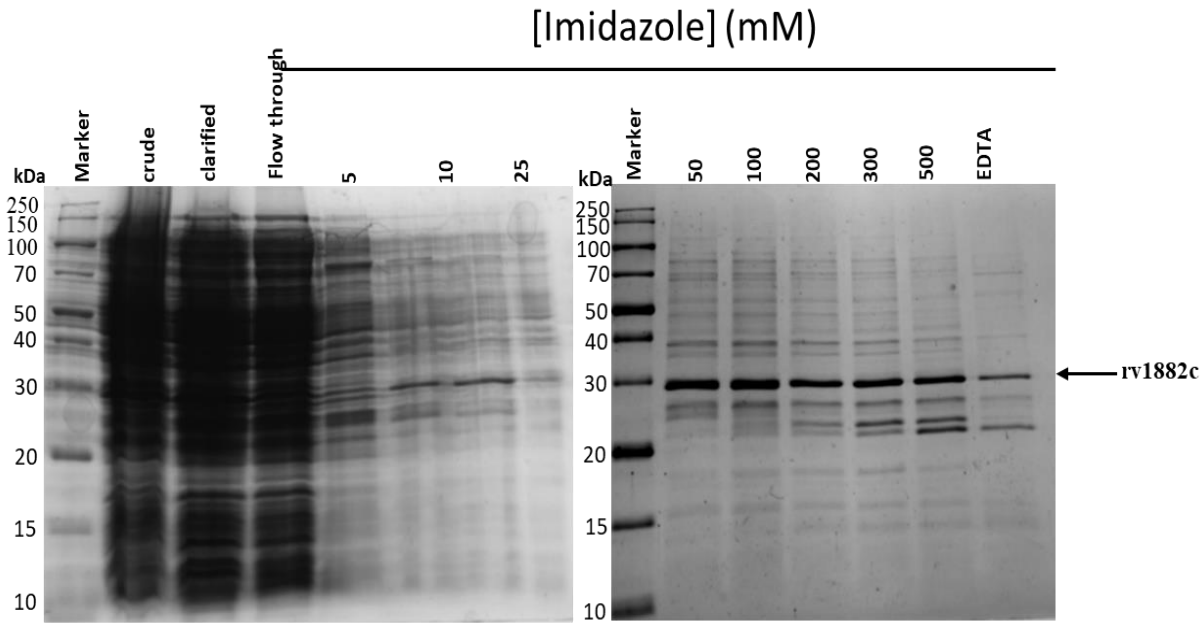

Figure 4.18 12 % SDS-PAGE analysis of Rv1882c from *M. tuberculosis*. PageRuler Plus prestained protein ladder was used. Rv1882c (30 kDa) eluted at concentrations of imidazole from 50 mM**.**

Expression of the three proteins did not go according to plan. The Rv1882c was purified and showed some expression, but further purification and concentration did not give a good concentration for any possible assay to be conducted. The attempts to purify recombinant *mt*BioH1 failed even when different expression strains were utilised. The *mt*BioH2 showed some level of expression, just like the Rv1882c, but it was also weak in concentration and could not be assayed or crystallized. Several expression strains were utilised to ensure better expressions of the proteins, but most of the strains used could not express the proteins.

4.5 Conclusion

The biotin biosynthetic pathway in *E. coli* has recently been elucidated with enzymes of the early stage becoming clearer (Lin *et al*., 2010). FabG and BioH are both involved in this early stage synthesis of pimelate. The pathway involves the synthesis of a pimelate moiety that acts as a substrate that feeds into the synthesis of biotin. The synthesis of the pimelate moiety has been described in only two organisms, *E. coli* having a BioC-BioH pathway and *Bacillus subtilis* with a BioI-BioW pathway (Lin and Cronan, 2011). In a bid to develop an understanding of pimelate biosynthetic pathway in *Mtb*, this work was designed to identify, purify and characterise the enzymes involved in the pathway. To date, there is no record of these enzymes being identified and characterised in *Mtb*. These enzymes were identified and partially purified, but the expression did not give a good yield for any biochemical study to be carried out. Further work is needed to optimise purification conditions and utilise new cell lines for better expression. This would lead to characterisation study through crystallisation and other biochemical analyses. These studies will form the basis for inhibitor design, were inhibitors are modelled into the crystal structures in a bid to develop drugs for effective control of tuberculosis disease.

Chapter 5

Synthesis and biological evaluation of Isoxyl-SQ109 hybrids as active inhibitors against *Mtb*

5 Isoxyl and SQ109 Derivatives

5.1 Introduction

An effective treatment of TB can be very challenging and requires accurate and early diagnosis to achieve maximum success (Zumla *et al*., 2013). For an effective treatment of drug-susceptible TB a six-month two-phase approach is required. This involves daily intake of RIF, INH, PZA and EMB for two months, then a four month administration of RIF and INH daily or three times a week for a complete eradication (BNF, 2016, North *et al*., 2014, Russell, 2004, Blanchard, 1996). The first phase ensures the minimisation of resistance, while the second phase ensures total eradication. Treatment results in a 95% success rate, though compliance to treatment has been a major problem through long treatment durations, high frequency dosing patterns and multiple tablet pill burdens (North *et al*., 2014, North *et al*., 2013, Finch, 2004). Resistance could be as a result of cell envelope permeability, bacterial drug efflux systems and drug modifying enzymes (Günther *et al*., 2016, BNF, 2016, Koul *et al*., 2011). Challenges to bacterial eradication are as a result of poor compliance, co-morbid patient complications and inadequate access to medicines in developing countries (Sullivan and Amor, 2016, Grzegorzewicz *et al*., 2014, North *et al*., 2013, Scherman *et al*., 2012, Koul *et al*., 2011, Takayama *et al*., 2005). Older drugs such as N-Geranyl-N'-(2-adamantyl)-ethane-1,2-diamine (SQ109) or Thiocarlide; 4,4'-diisoamyloxydiphenylthiourea (isoxyl) can be re-examined to provide an excellent lead for re-engineering that would lead to new drug series that may shorten the drug discovery pipeline (Mikušová and Ekins, 2017, Brown and Wright, 2016, Jones *et al*., 2016, Gopal and Dick, 2014). Isoxyl and SQ109 (Figure 5.1) are drugs implicated in the inhibition of the *Mtb* cell wall biosynthesis pathways.

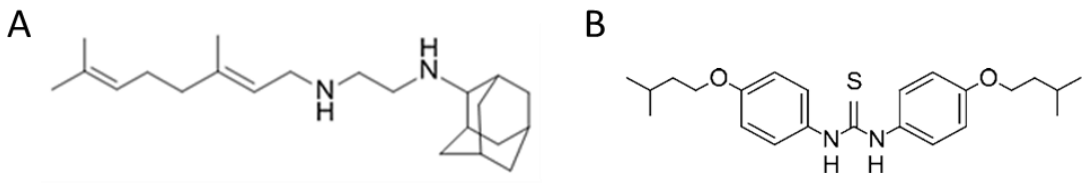

Figure 5.1 Structures of SQ109 (A) and Isoxyl (B)

Isoxyl was first used in the 1950s onwards, after its synthesis as an old second line TB treatment drug (Wang and Hickey, 2010, Liav *et al*., 2008). It was first used in combination with INH with greater success (Dover *et al*., 2007, Phetsuksiri *et al*., 1999), but its use was short-lived due to questions from clinical trial data, side effect profile and high frequency of resistant mutant species generated (Wang and Hickey, 2010, Janin, 2007, Emerson *et al*., 1969). The drug was also plagued with dissolution and bioavailability issues due to poor water solubility (Wang and Hickey, 2010, Crowle et al., 1963).

Isoxyl was first shown to inhibit mycolic acid synthesis in *M. bovis* and also a partial inhibition of the synthesis of shorter chain fatty acids (Winder *et al*., 1971). It was later confirmed that isoxyl targets mycolic acid synthesis earlier in the pathway, when the HadAB subunit of the hydratase in the FAS-II cycle is inhibited to prevent fatty acid elongation (Grzegorzewicz *et al*., 2014). The thiocarbonyl moiety of the isoxyl which is similar to thiacetazone is responsible for its activity (Dover *et al*., 2007, Korduláková *et al*., 2007). Another isoxyl target was recently identified as the membrane associated stearoyl-Coenzyme A (CoA) Δ9-desaturase DesA3 (Gannoun-Zaki *et al*., 2013, Phetsuksiri *et al*., 2003). Inhibition of this target inhibits other vital components of the mycobacterial membrane, such as oleic acid and tuberculostearic acid biosynthesis (Phetsuksiri *et al*., 2003).

SQ109 is another second generation anti-tubercular drug discovered as a safer and potent alternative TB drug to EMB (Li *et al*., 2014, Sacksteder *et al*., 2012, Onajole *et al*., 2011, Onajole *et al*., 2010). The drug is confirmed to have bactericidal action against MDR and XDR-TB. It also showed mycobacterial specificity, low spontaneous mutation rates, promising toxicity and acceptable pharmacokinetics (Sacksteder *et al*., 2012, Low, 2017, Protopopova *et al*., 2005). However, recent licensing of this drug from Sequella (a clinical-stage pharma company that develops new and better antibiotics) to Infectex (a pharma company that developed SQ109 for MDR-TB treatment) raised questions on its ethics for market approval because of the lack of a clear peer review drug data and inadequate registration trial sample sizes (80 patients) (Lessem, 2016). Another recent independent trial data led to the suspension of the drug as it failed to meet pre-specified efficacy thresholds (Boeree *et al*., 2017).

A mutation in the *mmpL3* gene was revealed as a result of sequencing of spontaneous resistant mutants with cross resistance to SQ109, implicating the role of MmpL3 in TDM depletion and TMM accumulation (Xu *et al*., 2017, Grzegorzewicz *et al*., 2012). The drug's ability to generate resistance mutants suggests that it is a multi-target inhibitor and has a multifaceted mode of action (Li *et al*., 2014).

Isoxyl was developed in an era where analogue chemistry was underutilised which could mean its full potential has not been utilised (Barry *et al*., 2000). The drug has also been identified to inhibit MDR-TB clinical isolates at a concentration of 1-10 µg/ml which gives a promising future evaluation (Phetsuksiri *et al*., 1999). Available technological advances through pulmonary aerosol delivery can now be used to tackle the problem of solubility complications (Wang and Hickey, 2010). There is also the possibility of a fast track accelerated drug approval since some positive aspects of it have already been

identified in the 1990s (Mahajan, 2013). On the other hand, SQ109 can be restructured since its mode of action is multifaceted outside the FAS system compared to other drugs.

This study therefore seeks to re-examine and redevelop isoxyl as an old forgotten drug that is highly potent and multi-targeted *Mtb* cell wall inhibitor. The study will involve the modification of SQ109 with its known mechanism of action to be incorporated into the isoxyl to produce a superior hybridised compound which would target multiple aspects of *Mtb* cell wall synthesis.

5.2 Aims and objectives

This study utilises the structures of isoxyl and SQ109 by synthesising analogues as potential inhibitors of *Mtb*. The specific aims of the study are:

1. To synthesise a series of analogues that hybridise the structures of isoxyl with SQ109 in order to identify a lead compound with a good inhibitory activity against *Mtb*. This can be achieved through the following objective:

    - Synthesis will involve the modification to the base structures and fragments of the two drugs (isoxyl and SQ109) with known differing mechanisms of action

2. To evaluate the effectiveness of the synthesised compounds against *Mtb*. This will be achieved through the following objective:

    - The effectiveness of the synthesized compounds will be evaluated by testing against the wild type strain of *Mtb* and against RIF and INH spontaneous resistant mutants. This would create a new lead compound that is multi-targeted with efficacy that rivals current TB treatments.

5.3 Materials and Methods

5.3.1 Synthesis of 3-(Adamant-1-yl)-1-[4-(3-Methylbutoxy)phenyl]thiourea

3-(Adamant-1-yl)-1-[4-(3-Methylbutoxy)phenyl]thiourea (JJH-17A) (Figure 5.2) is a known compound and its method of synthesis known established (Brown *et al*., 2011).

To a stirred solution of 1,1-thiocarbonyldiimidazole (0.651 g, 3.65 mmol, 2 equiv) in CH_3CN (3 mL) at -20ºC was added 4-(isopentyloxy)analine (0.327 g, 1.825 mmol, 1 equiv) and was stirred until all starting material was consumed by TLC (SiO_2, 2:1 Petrol (40-60ºC):EtOAc). Adamantidine hydrochloride (0.377 g, 2.01 mmol, 1.1 equiv) and DIPEA (0.350 mL, 2.01 mmol, 1.1 equiv) were added and the reaction stirred overnight at room temperature. Solvent was removed *in vacuo*, EtOAc (50 mL) and H_2O (50 mL) was added then transferred to a separatory funnel and layers separated. The EtOAc layer was washed with HCl (3 x 50 mL, 0.1 M), sat $NaHCO_3$ (50 mL), H_2O (50 mL), sat NaCl (50 mL), dried over an $MgSO_4$ and the solvent removed *in vacuo* to give a light brown pale crystalline solid (0.801 g, 84.90 %). Mpt 35.4-38ºC; IR ν_{max} (cm^{-1}) 3345 (N-H), 3200 (N-H), 2956 (C-H), 2853 (C-H), 2117 (C=S); ^{1}H NMR (400 MHz; $CDCl_3$): δ_H 0.95 (d, *J* = 6.0 Hz, CH(C**H**$_3$)$_2$, 6H), 1.66 (m, AdC**H**$_2$ & C**H**$_2$CH(CH$_3$)$_2$, 8H), 1.83 (m, C**H**(CH$_3$)$_2$, 1H), 1.97 (m, AdC**H**$_2$, 6H), 2.08 (m, AdC**H**, 3H), 3.95 (t, *J* = 6.0 Hz, C**H**$_2$O, 2H), 6.88 (d, *J* = 9.0 Hz, ArC-**H**, 2H), 7.08 (d, *J* = 9.0 Hz, ArC-**H**, 2H); ^{13}C NMR (100 MHz; $CDCl_3$): δ_C 22.57 ((**C**H$_3$)$_2$), 25.04 ((CH$_3$)$_2$**C**H), 29.22 (Ad**C**-H), 29.58 (Ad**C**-H), 35.54 (Ad**C**H$_2$), 36.27 (Ad**C**H$_2$), 37.89 ((CH$_3$)$_2$CH**C**H$_2$), 41.57 (Ad**C**H$_2$), 43.77 (Ad**C**H$_2$), 54.48 (Adq**C**-NH), 66.70 (**C**H$_2$O), 115.72 (Ar**C**H), 127.59 (Ar**C**H), 128.70 (Arq**CN**), 158.33 (Arq**C**-O), 179.13 (**C**=S).

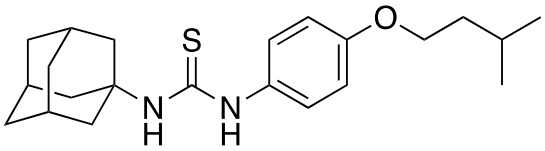

Figure 5.2 Chemical structure of 3-(Adamant-1-yl)-1-[4-(3- Methylbutoxy) phenyl]thiourea (JJH-17A)

5.3.2 Synthesis of 4-[(3-Methylbut-2-en-1-yl)oxy]aniline

The compound (Figure 5.3) was synthesised as follows: 1-((3-Methylbut-2-en-1-yl)oxy)-4-nitrobenzene (1.00 g, 4.84 mmol, 1 equiv), iron powder (1.87 g, 33.78 mmol , 7 equiv), MeOH (10 mL) and AcOH (2 mL) were refluxed for 150 minutes and then filtered through Celite® and solvents were removed *in vacuo*. Chromatography (SiO_2, 2:1 Petrol (40-60ºC) gave the product as a brown liquid 0.255 g (29.73 %); IR ν_{max} (cm^{-1}) 3365 (N-H), 3315 (N-H), 3019 (Ar C-H), 2972 (Al C-H), 2909, 2874 (Al C-H); ^{1}H NMR (400 MHz; $CDCl_3$): δ_H 1.66 (s, CH_3, 3H), 1.73 (s, CH_3, 3H), 3.39 (s, NH_2, 2H), 4.36 (d, *J* = 6.7 Hz , O**C**H_2, 2H), 5.44 (t, *J* = 6.7 Hz,C**H**C(CH_3)$_2$, 1H), 6.59 (d, *J* = 9.1, ArC-**H**, 2H), 6.72 (d, *J* = 9.1, ArC-**H**, 2H). ^{13}C NMR (100 MHz; $CDCl_3$): δ_C 18.18 (**C**H_3), 25.85 (**C**H_3), 65.41 (O**C**H_2), 115.82 (Ar**C**), 116.50 (Ar**C**), 120.16 (**C**HC(CH_3)$_2$), 137.73 (**C**(CH_3)$_2$), 139.76 (Ar-**C**-NH_2) 152.14 (**C**=O) (Brown *et al*., 2011).

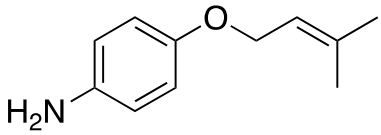

Figure 5.3 Chemical structure of 4-[(3-Methylbut-2-en-1-yl)oxy]aniline

5.3.3 Synthesis of 3-(Adamantan-1-yl)-1-(4-[(3-methylbut-2-en-1-yl)oxy]phenyl) thiourea (JJH-110AA)

This compound (Figure 5.4) was synthesized as follows: To a stirred solution of 1,1-thiocarbonyldiimidazole (0.397 g, 2.074 mmol, 2 equiv) in CH_3CN (2 mL) at -20ºC was added 4-[(3-methylbut-2-en-1-yl)oxy]aniline (0.184 g, 1.037 mmol, 1 equiv) and was stirred until all starting material was consumed by TLC (SiO_2, 2:1 Petrol (40-60ºC):EtOAc). Adamantidine hydrochloride (0.214 g, 1.14 mmol, 1.1 equiv) and DIPEA (0.199 mL, 1.14 mmol, 1.1 equiv) were added and the reaction stirred overnight at room temperature. Solvent was removed *in vacuo*, EtOAc (50 mL) and H_2O (50 mL) was added then transferred to a separatory funnel and layers separated. The EtOAc layer was washed with HCl (50 mL, 0.1 M), sat $NaHCO_3$ (50 mL), H_2O (50 mL), sat NaCl (50 mL), dried over an $MgSO_4$ and the solvent removed *in vacuo*. Chromatography (SiO_2, 4:1 Petrol (40-60ºC) gave a pale brown/sandy crystalline solid. (0.134 g, 34.88%). Mpt 118-125ºC; IR ν_{max} (cm^{-1}) 3352 (N-H), 3205 (N-H), 3023 (ArC-H), 2909 (Al C-H), 2853 (C-H stretch), 2060 (C=S); ^{1}H NMR (400 MHz; $CDCl_3$): δ_H 1.67 (m, AdC**H**$_2$, 3H), 1.75 (s, C**H**$_3$, 3H), 1.81 (s, C**H**$_3$, 3H), 1.99 (m, AdC**H**$_2$, 6H), 2.13 (m, AdC**H**, 6H), 4.51 (d, *J* = 6.0 Hz, OC**H**$_2$, 2H), 5.47 (t, *J* = 6.0 Hz, OCH$_2$C**H**, 1H), 6.92 (d, *J* = 9.0 Hz, ArC-**H**, 2H), 7.26 (d, *J* = 9.0 Hz, ArC-**H**, 2H); ^{13}C NMR (100 MHz; $CDCl_3$): δ_C 18.60 (**C**H$_3$), 25.63 (**C**H$_3$), 29.22 (Ad), 35.25 (Ad**C**H), 43.75 (Ad**C**H$_2$), 58.58 (Adq**C**-NH), 65.05 (O**C**H$_2$), 115.42 (Ar**C**H), 119.32 ((CH$_3$)$_2$C**C**H), 127.52 (Ar**C**H), 129.70 (Ar-q**C**NH), 138.62 ((CH$_3$)$_2$**C**), 158.01 (Arq**C**O), 181.00 (**C**=S) (Brown *et al*., 2011).

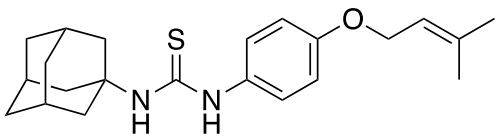

Figure 5.4 Chemical structure of 3-(Adamantan-1-yl)-1-(4-[(3-methylbut-2-en-1-yl)oxy]phenyl) thiourea (JJH-110AA)

5.3.4 Synthesis of 1-(Adamantan-2-yl)-3-(4-((3-methylbut-2-en-1-yl)oxy)phenyl) thiourea (JJH-III-051A)

This compound (Figure 5.5) was synthesized as follows: To a stirred solution of 1,1-thiocarbonyldiimidazole (0.886 g, 4.976 mmol, 2 equiv) in CH_3CN (5 mL) at -20ºC was added 4-[(3-methylbut-2-en-1-yl)oxy]aniline (0.441 g, 2.488 mmol, 1 equiv) and was stirred until all starting material was consumed by TLC (SiO_2, 2:1 Petrol (40-60ºC):EtOAc). 2-Adamantylamine hydrochloride (0.512 g, 2.737 mmol, 1.1 equiv) and Et_3N (0.347 mL, 2.488 mmol, 1 equiv) were added and the reaction stirred overnight at room temperature. Solvent was removed *in vacuo*, EtOAc (50 mL) and H_2O (50 mL) was added then transferred to a separatory funnel and layers separated. The EtOAc layer was washed with HCl (50 mL, 0.1 M), sat $NaHCO_3$ (50 mL), H_2O (50 mL), sat NaCl (50 mL), dried over an $MgSO_4$ and the solvent removed *in vacuo*. Chromatography (SiO_2, 4:1 Petrol (40-60ºC) gave a brown crystalline solid (0.512 g, 55.54 %); IR ν_{max} (cm^{-1}) 3350 (N-H), 3155 (N-H), 3050 (ArC-H), 2905 (Al C-H), 2851 (C-H stretch), 2060 (C=S); ^1H NMR (400 MHz; $CDCl_3$): δ_H 1.60 (m, AdC**H**$_2$, 3H), 1.73 (s, C**H**$_3$, 3H), 1.78 (s, C**H**$_3$, 3H), 1.81 (m, AdC**H**$_2$, 6H), 2.04 (m, AdC**H**, 6H), 4.51 (d, *J* = 6.0 Hz, OC**H**$_2$, 2H), 5.48 (t, *J* = 6.0 Hz, OCH_2C**H**, 1H), 6.95 (d, *J* = 9.0 Hz, ArC-**H**, 2H), 7.16 (d, *J* = 9.0 Hz, ArC-**H**, 2H); ^{13}C NMR (100 MHz; $CDCl_3$): δ_C 18.25 (**C**H_3), 25.83 (**C**H_3), 26.99 (Ad**C**H), 31.58 (Ad**C**H), 32.38 (Ad**C**H_2), 36.91 (Ad**C**H_2), 37.40 (Ad**C**H_2), 60.40 (Adq**C**-NH), 65.12 (O**C**H_2), 116.07 (Ar**C**H), 119.16 ($(CH_3)_2$C**C**H), 127.34 (Ar**C**H), 128.61 (Ar-q**C**NH), 138.69 ($(CH_3)_2$**C**), 158.09 (Arq**C**O), 179.58 (**C**=S).

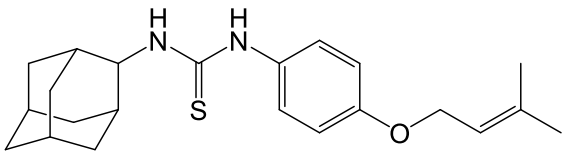

Figure 5.5 Chemical structure of 1-(Adamantan-2-yl)-3-(4-((3-methylbut-2-en-1-yl)oxy)phenyl) thiourea (JJH-III-051AA)

5.3.5 Synthesis of 1-(adamantan-1-yl)-3-(4-((3-methylbut-2-en-1-yl)oxy)phenyl) urea (JJH-III-039A)

This compound (Figure 5.6) was synthesized as follows: Adamantyl isocyanide (0.772 g, 4.354 mmol, 1.5 equiv) was added to the amine (0.500 g, 3.90 mmol, 1 equiv) in THF (10 mL) and stirred overnight at room temperature. H_2O (30 mL) and EtOAc (30 mL) and the mixture transferred to a separatory funnel and the two layers separated. The EtOAc layer was washed with HCl (30 mL, 0.1 M), sat $NaHCO_3$ (30 mL), H_2O (30 mL), sat NaCl (30 mL), dried over an $MgSO_4$ and the solvent removed *in vacuo* to give a pale tan solid (0.840g, 81.71%). Mpt 165-168ºC; IR ν_{max} 3354 (NH), 3302 (NH), 3050 (Ar C-H), 2903 (Al C-H), 2848 (Al C-H), 1644 (C=O); ^{1}H NMR (300 MHz; $CDCl_3$): δ_H 1.68 (m, AdC**H**$_2$, 3H), 1.76 (s, C**H**$_3$, 3H), 1.82 (s, C**H**$_3$, 3H), 1.98 (m, AdC**H**$_2$, 6H), 2.08 (m, AdC**H**, 6H), 4.49 (d, *J* = 6.0 Hz, OC**H**$_2$, 2H), 5.47 (m, OCH$_2$C**H**, 1H), 6.89 (d, *J* = 9.0 Hz, ArC-**H**, 2H), 7.16 (d, *J* = 9.0 Hz, ArC-**H**, 2H); ^{13}C NMR (75 MHz; $CDCl_3$): δ_C 18.20 (**C**H$_3$), 22.84 (**C**H$_3$), 29.54 (Ad**C**H), 36.42 (Ad**C**H$_2$), 42.27 (Ad**C**H$_2$), 51.09 (Adq**C**-NH), 65.08 (O**C**H$_2$), 115.27 (Ar**C**H), 119.67 ((CH$_3$)$_2$C**C**H), 123.65 (Ar**C**H), 131.21 (Ar-q**C**NH), 138.21 ((CH$_3$)$_2$**C**), 155.59 (Arq**C**O, **C**=O).

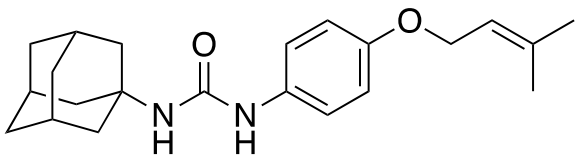

Figure 5.6 Chemical structure of 1-(adamantan-1-yl)-3-(4-((3-methylbut-2-en-1-yl)oxy)phenyl) urea (JJH-III-039A)

5.3.6 Synthesis of 1-cyclohexyl-3-(4-((3-methylbut-2-en-1-yl)oxy)phenyl) thiourea (JJH-III-052A)

To a stirred solution of 1,1-thiocarbonyldiimidazole (0.663 g, 3.72 mmol, 2 equiv) in CH_3CN (5 mL) at -20ºC was added 4-[(3-methylbut-2-en-1-yl)oxy]aniline (0.330 g, 1.86 mmol, 1 equiv) and was stirred until all starting material was consumed by TLC (SiO_2, 2:1 Petrol (40-60ºC):EtOAc). Cyclohexylamine (0.236 mL, 2.048 mmol, 1.1 equiv) and Et_3N (0.26 mL, 1.86 mmol, 1 equiv) were added and the reaction stirred overnight at room temperature. Solvent was removed *in vacuo*, EtOAc (30 mL) and H_2O (30 mL) was added then transferred to a separatory funnel and layers separated. The EtOAc layer was washed with HCl (30 mL, 0.1 M), sat $NaHCO_3$ (30 mL), H_2O (30 mL), sat NaCl (30 mL), dried over an $MgSO_4$ and the solvent removed *in vacuo*. Chromatography (SiO_2, 4:1 Petrol (40-60ºC) gave a brown crystalline solid (0.283 g, 35.92 %). Mpt 47-50ºC; IR ν_{max} 3350 (NH), 3155 (NH), 3050 (Ar C-H), 2905 (Al C-H), 2852 (Al C-H), 2060 (C=S); ^{1}H NMR (300 MHz, $CDCl_3$) δ_H 1.06 (m, Hex-C**H**$_2$, 4H), 1.36 (m, Hex-C**H**$_2$, 2H), 1.60 (m, Hex-C**H**$_2$, 4H), 1.74 (s, C**H**$_3$, 3H), 1.80 (s, C**H**$_3$, 3H), 2.03 (m, Hex-C**H**-NH, 1H), 4.49 (d, *J* = 6.0 Hz, OC**H**$_2$, 2H), 5.45 (m, OCH$_2$C**H**, 1H), 6.91 (d, *J* = 9.0, ArC-**H**, 2H), 7.12 (d, *J* = 9.0 Hz, ArC-**H**, 2H); ^{13}C NMR (75 MHz; $CDCl_3$): δ_C 18.25 (**C**H$_3$), 25.72 (Hex**C**H$_2$), 25.43 (Hex**C**H$_2$), 25.86 (**C**H$_3$), 32.64 (Hex**C**H$_2$) 53.93 (Hex**C**HNH), 65.08 (O**C**H$_2$), 115.99 (Ar**C**H), 119.13 ((CH$_3$)$_2$C**C**H), 127.54 (Ar**C**H), 128.30 (Ar-q**C**NH), 138.84 ((CH$_3$)$_2$**C**), 158.15 (Arq**C**O), 179.75 (**C**=S) (Onajole *et al*., 2010).

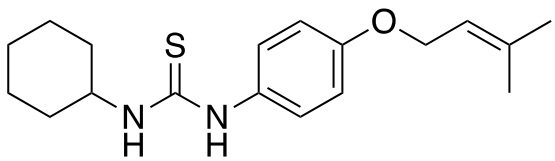

Figure 5.7 Chemical structure of 1-cyclohexyl-3-(4-((3-methylbut-2-en-1-yl)oxy)phenyl) thiourea (JJH-III-052A)

5.3.7 Analogue of JJH-110AA [JJH-III-040A and JJH-III-043A (SQ109 Analogue)]

The compounds (Figures 5.8 - 5.9) were synthesized as per literature methods (Onajole *et al*., 2010).

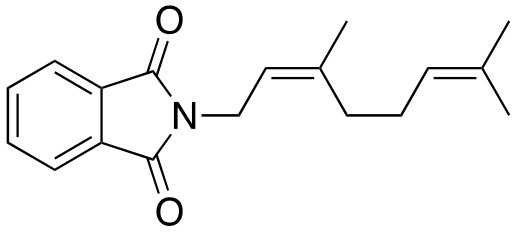

Figure 5.8 Chemical structure of (E)-2-(3,7-dimethylocta-2,6-dien-1-yl)isoindoline-1,3-dione (JJH-III-040A)

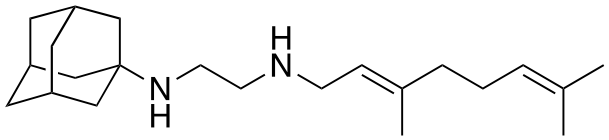

Figure 5.9 Chemical structure of N-(adamantan-1-yl)-N-((E)-3,7-dimethylocta-2,6-dien-1-yl)ethane-1,2-diamine (JJH-III-043A, SQ109 Analogue)

Table 5.1 showing synthesised compounds and structures

Synthesized Compounds from Isoxyl and SQ109	Structure
JJH-017A	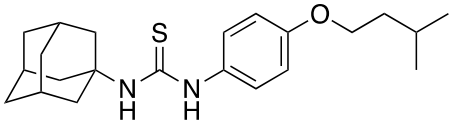
JJH-III-110A	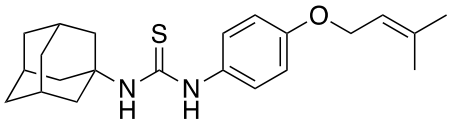
JJH-III-051A	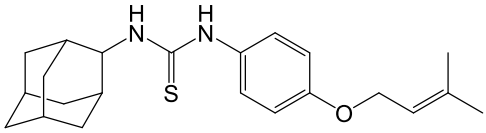
JJH-III-039A	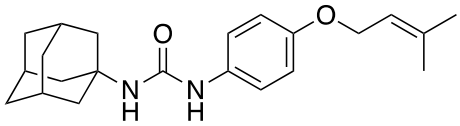
JJH-III-052A	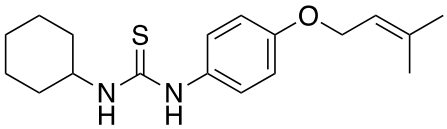
JJH-III-040A	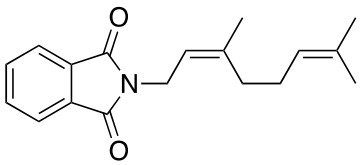
JJH-III-043A	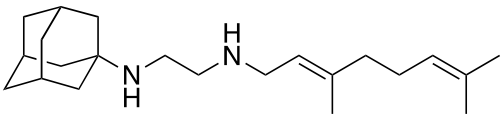

5.4 Results and discussion

In order to assess the overall potential of our isoxyl-SQ109 analogues there was a requirement to generate single resistant mutants of *Mtb* against both INH and RIF. These mutants were generated as per normal protocols as described in Section 2.13. Selected mutants were grown and tested against a broad spectrum of anti-tubercular agents (Table 5.1). Four mutants of RIFR (AKB7002, AKB7003, AKB7005, AKB7009) and INHR (AKB7020, AKB7021, AKB7025, AKB7028) were selected to screen the novel compounds against.

The isoxyl-SQ109 analogues showed varied activity against the wild-type and mutant strains of *Mtb*. The MIC result showed that among the synthesized or modified compounds, the JJH-110A showed the best activity (Table 5.2) with all of the mutants susceptible to the compound at a concentration of 0.120 µg/mL. Modifications of the JJH-110A that produced the various analogues were done on its various components which includes the isoprenyl chain, methoxy chain, the cyclohexane ring and the adamantyl ring. The different analogues produced from these modifications were meant to determine which part of the compound is essential for its activity against *Mtb*. This limited study didn't afford any clear results due to the small number of analogues tested. With a larger analogue library, it would have been possible to perform a structure activity relationship but from the limited data obtained it was evident that the adamantyl and isoprenyl combinations were required to achieve full activity.

Table 5.2 Minimum inhibitory concentration (MIC) of Isoxyl-SQ109 hybrid analogues and controls. MIC was measured in µg/mL.

		***Mtb* Strain MIC (µg/mL)**									
	Structure	mc^{2}7000	AKB7001	AKB7002	AKB7003	AKB7005	AKB7009	AKB7020	AKB7021	AKB7025	AKB7028
Phenotype		RIF^S, INH^S	RIF^S, INH^S	RIF^R, INH^S	RIF^R, INH^S	RIF^R, INH^S	RIF^R, INH^S	RIF^S, INH^R	RIF^S, INH^R	RIF^S, INH^R	RIF^S, INH^R
INH		0.1	0.1	0.1	0.1	0.1	0.1	>32	>32	>32	>32
RIF		0.03	0.03	12.8	4	0.8	0.4	0.03	0.03	0.03	0.03
EMB		0.5	0.5	0.5	0.5	0.5	0.5	0.5	0.5	0.5	0.5
Isoxyl	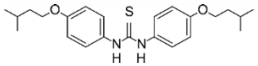	0.25	0.25	0.25	0.25	0.25	0.25	0.25	0.25	0.25	0.25
JJH-017A	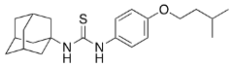	4	4	4	4	4	4	4	4	4	4
JJH-110A	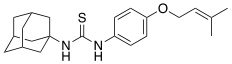	0.12	0.12	0.12	0.12	0.12	0.12	0.12	0.12	0.12	0.12
JJH-039A	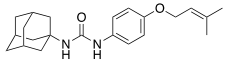	1	1	1	1	1	1	1	1	1	1
JJH-040A	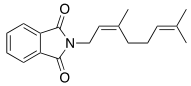	64	64	64	64	64	64	64	64	64	64
JJH-043A	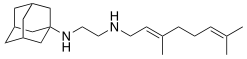	0.48	0.48	0.48	0.48	0.48	0.48	0.48	0.48	0.48	0.48
JJH-051A	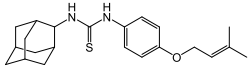	4	4	4	4	4	4	4	4	4	4
JJH-052A	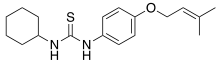	16	16	16	16	16	16	16	16	16	16

The results against the singly drug resistant *Mtb* strains indicated that the mutants remained susceptible to the JJH-110A. In comparison, JJH-110A was more active than its parental drugs (SQ109 and Isoxyl) against all strains (Table 5.3). Again, the mutants were susceptible to the JJH-110A at an MIC of 0.120 µg/mL. It was more potent than SQ109 (0.48 µg/mL) and Isoxyl (0.24 µg/mL). The mutants were susceptible to other antibiotics at a higher concentration, except RIF where most of the mutants were susceptible at between 0.008-0.06 µg/mL and INH where most of the mutants were susceptible at 0.015-0.03 µg/mL.

JJH-110A and other antibiotics were also tested against JJH-110A spontaneous mutants generated and the wild type (Table 5.4). The result indicated that mutants developed against JJH-110A were also resistant to the parental drugs, indicating a possible similar mode of action against *Mtb*. The JJH-110A mutants were susceptible to the JJH-110A at MIC of between 0.1-1.0 µg/mL which is also similar to the susceptibility of the mutants to RIF and INH. AKB7038 was susceptible to all the antibiotics and to the JJH-110A at an almost equal concentration (0.5 µg/mL).

MIC tests carried out on all compounds and antibiotics showed good inhibition against *Mtb* $mc^2$7000 and its spontaneous generated mutants. There were some variations in the level of resistance against JJH-110A in the mutant strains. The potency of the JJH-110A was of interest because it rivals the potency of SQ109 (0.48 µg/mL) and isoxyl (0.24 µg/mL), two drugs from which it was derived and was almost equivalent to INH (0.1 µg/mL).

Table 5.3 **MIC determination of the JJH-110A and other antibiotics on RIF^R and INH^R mutants and in combination.** MIC was measured in µg/mL.

		***Mtb* Strain MIC (µg/mL)**									
	Structure	mc^{2}7000	AKB7001	AKB7002	AKB7003	AKB7005	AKB7009	AKB7020	AKB7021	AKB7025	AKB7028
Phenotype		RIF^S, INH^S	RIF^S, INH^S	RIF^R, INH^S	RIF^R, INH^S	RIF^R, INH^S	RIF^R, INH^S	RIF^S, INH^R	RIF^S, INH^R	RIF^S, INH^R	RIF^S, INH^R
INH		0.03	0.03	0.03	0.015	0.015	0.015	>32	-	>32	>32
RIF		0.06	0.03	12.8	1	2	0.05	0.008	-	0.008	0.03
EMB		4	8	4	4	4	8	8	-	8	8
Isoxyl	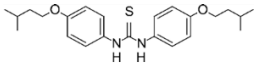	0.241	0.241	0.241	0.241	0.241	0.241	0.241	-	0.06	0.12
JJH-110A	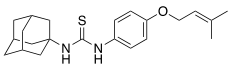	0.12	0.241	0.12	0.12	0.12	0.12	0.241	-	0.015	0.12
SQ109	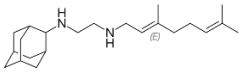	0.481	0.481	0.481	0.481	0.481	0.481	0.481	-	0.481	0.481
RIF+JJH-110A	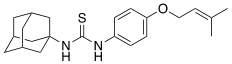	0.025	0.025	12.8	1	2	0.025	0.025	-	0.025	0.025
INH+JJH-110A	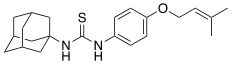	0.025	0.025	0.013	0.013	0.013	0.025	4	-	8	4

Table 5.4 **MIC determination of JJH-110A and other antibiotics against JJH-110A spontaneous *Mtb* mutants.** MIC was measured in µg/ml.

		***Mtb* Strain MIC (µg/mL)**											
	Structure	mc^{2}7000	AKB7031	AKB7032	AKB7033	AKB7034	AKB7035	AKB7036	AKB7037	AKB7038	AKB7039	AKB7041	AKB7042
Phenotype			JJH-110A^R	JJH-110A^R	JJH-110A^R	JJH-110A^R	JJH-110A^R	JJH-110A^R	JJH-110A^R	JJH-110A^R	JJH-110A^R	JJH-110A^R	JJH-110A^R
INH		0.03	0.03	0.03	0.03	0.03	0.03	0.015	0.03	0.03	0.03	0.03	0.03
RIF		0.06	0.06	0.06	0.06	0.06	0.06	0.06	0.015	0.06	0.06	0.06	0.06
EMB		4	4	4	8	8	8	8	8	0.5	8	8	8
Isoxyl	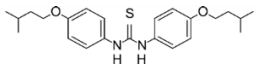	0.12	0.06	0.5	0.5	1	1	1	0.5	0.5	0.5	1	0.24
JJH-110A	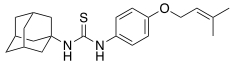	0.12	2	0.5	1	1	1	1	1	0.5	0.5	2	0.241
SQ109	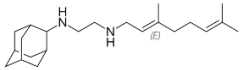	0.5	0.03	0.5	0.5	0.5	1	1	1	1	1	1	0.5

Previously, there have been a number of molecule modifications to both isoxyl and SQ109 leading to new compound series (Li *et al*., 2015, Brown et al., 2011, Onajole *et al*., 2010, Barry *et al*., 2000, Phetsuksiri *et al*., 1999). Also, information about thiourea structural activity relationship (SAR) that generates new compounds is also available (Bielenica *et al*., 2015, North *et al*., 2013, Scherman *et al.*, 2012, Brown *et al*., 2011).

The synthesis of the compound with the addition of a prenyl group offers some inhibitory advantage. A prenyl moiety incorporation may activate an action that is different to isoxyl, although this conclusion requires further proof. It is likely that the addition of the prenyl which gives an aliphatic side chain of approximately C4 length confers inhibitory property against *Mtb* (Bhowruth *et al*., 2006). Other studies have utilised prenyl functionality in synthesizing unsymmetrical compounds of urea series, but achieved a lesser *Mtb* inhibition of 5.2 µg/mL (Velappan *et al*., 2017). Incorporation of the urea as opposed to thiourea core may be as a result of their lower prenyl MIC. These active molecules derived from urea have shown good anti-tubercular activity (North *et al*., 2013, Scherman *et al*., 2012, Brown *et al*., 2011). The urea motif mimics a natural substance that binds to the *Mtb* in epoxide hydrolase inhibition (Biswal *et al*., 2008). An isoxyl activation by an ethionamide activator (EthA) is thought to produce a urea derivative (Korduláková *et al*., 2007). Therefore, investigation into this moiety in anti-tubercular design is not surprising. Also, integration of urea into isoxyl proved to be detrimental in Mtb where the MIC was increased to 10,000% when tested (Brown *et al*., 2011). This could be as a result of the inability of the urea to react with the cys61 residue of HadA of *Mtb* (Grzegorzewicz *et al*., 2014). It is therefore possible that a thiourea substitution may lead to more active analogues than urea incorporated isoxyl compounds.

The inhibition of *Mtb* due to prenyl group incorporation may give rise to a new mechanism of action. This deduction can be explained when considering the synthesized compound decaprenylphosphoryl-D-arabinose (DPA) which is similar to the Isoprenyl (Abdel-Magid, 2015). The DPA is an integral part of the cell wall arabinan synthesis pathway through a catalytic activity of decaprenylphosphoryl-D-ribose (DPR) epimerase (Zumla *et al*., 2013). DPR epimerase therefore became a potential drug target with 1,3-benzothiazin-4-ones (BTZ) and dinitrobenzamide derivatives targeting it (Manina *et al*., 2010).

The incorporation of an adamantyl group also proved advantageous for inhibition. The cyclohexane ring of the adamantyl is most likely as a result of its 'grease ball' classification and its ability to raise LogP (average 3.1 Log units) into druggable ranges (Kumar *et al*., 2015a, Liu *et al*., 2011, Lamoureux and Artavia, 2010). Penetration through the *Mtb* cell wall is achieved by raising the LogP which allows the compound to pass through the *Mtb* waxy, thick and highly lipophilic cell wall, thus giving way to aid specific delivery to target binding sites (Barry *et al*., 2000). This implies that the addition of adamantyl to isoxyl derivatives increases hydrophobicity and can be attributed to the improved activity (Barry *et al*., 2000).

Adamantyl is also a stearic bulk which makes it an ion channel perturbed that can disrupt transmembrane flux (Liu et al., 2011, Lamoureux and Artavia, 2010, Geldenhuys *et al*., 2005). This ability blocks MmpL3 and the compound prevents TMM translocation and hence mycolic acid intercalation (Tahlan *et al*., 2012). Again, since expression and overproduction of efflux pump is unregulated in MDR-TB to aid antibiotic expulsion, the bacteria's resistance mechanism can be targeted (Askoura *et al*., 2011). The adamantyl stearic bulk advantage which likely increased inhibition in this work supports the

deduction that bulk moieties such as alkyl and aryl substituents favour maximum *Mtb* activity (Brown *et al*., 2011). Adamantyl incorporation increased the compound's rigidity when compared to the parent molecule (Lamoureux and Artavia, 2010). This rigidity gives a better drug orientation, stability and provides a tighter active site binding (Wanka *et al*., 2013, Liu *et al*., 2011).

Geranyl addition also favours low MIC and less specificity than adamantyl inclusions. An important SQ109 SAR is made up of two isoprene units from geranyl (Kumar *et al*., 2015a). Extension of SQ109 geranyl side linker makes it withstand both elongation and increased saturation (Kumar *et al*., 2015b, Onajole *et al*., 2011, Onajole *et al*., 2010) which resulted to a more potent MIC against both H37Rv and XDR173 *Mtb* strains than SQ109 (Onajole *et al*., 2011, Onajole *et al*., 2010).

5.5 Conclusion

The structural activity relationship of the synthesized JJH-110A can be complicated, even though there has been a great success by the hybrid utilisation of the two anti-tubercular drugs. It is not clear whether or not the compound is utilising one, multiple or none of the mechanistic routes the parent drugs use. The hybridisation of isoxyl with SQ109 can form a new anti-tubercular lead. The study shows that old anti-tubercular drugs can be hybridised successfully with the concept relatively novel. This work is therefore at an early stage in a lengthy process of drug discovery, where the compound would have to go through a series of preclinical studies before its use in humans (Franzblau *et al*., 2012). Other work to be done include assessing the compound's toxicology that would predict its effect on mammalian cells (Barile, 2007). The compound can also be tested against other *Mtb* strains since H37Rv has sub lineages and other genetic strain alterations (Franzblau *et al*., 2012). It is also essential to establish the compound's mode of action since it is multi-targeted. This will start with a consideration of targets of the parental compounds and their appropriateness. Appearance of TDM and accumulation of TMM could suggest *MmpL3* target interaction (Tahlan *et al*., 2012). Both biochemical methods and genetic manipulations (deletion and expression) will throw more light on target elucidation (Sleno and Emili, 2008). Changes induced in the bacterial proteome as a result of the compound may be useful in target validation.

Chapter 6
Final Summary

6 Final Summary

The fatty acid biosynthetic pathway in *Mtb* is central to the survival of the organism due to its involvement in the synthesis of cell envelope mycolic acid which play a key role in virulence and resistance to antibiotics (Barry *et al*., 1998). Characterisation of the enzymes involved in the mycolic acid synthesis pathway have been identified as excellent targets for anti-tubercular drug development. Therefore, the synthesis of biotin, a co-factor required by the mycolic acid enzymes, and its priming substrate pimelate are valid targets for anti-tubercular development.

The enzymes involved in pimelate biosynthesis have been identified in *E. coli* (Lin *et al*., 2010) and in *B. subtilis* (Lin and Cronan, 2011), but little is known about the majority of the enzymes and its synthesis in *Mtb*. Identifying key enzymes involved in pimelate biosynthesis would therefore provide new targets for TB treatments. The critical nature of some of these enzymes and their essentiality to the survival of the organism would aid drug development strategies especially in the wake of the recent upsurge in MDR and XDR-TB prevalence worldwide (WHO, 2009, Dye, 2006).

This investigation was designed primarily to look into approaches that would provide an effective anti-tubercular drug. Two approaches were considered; the structure-based approach to anti-tubercular drug and the ligand-based approach. The two approaches would provide novel means by which anti-tubercular drug targets are identified and inhibitors designed against them. The structure-based approach in this study successfully identified four pimelate biosynthetic enzymes in *Mtb; rv0089, rv1882c, rv3177* and *rv2715*. Some of the enzymes were purified and biochemical assay performed on one. The ligand-based approach to anti-tubercular drug saw the emergence of a lead compound which is a hybrid of isoxyl and SQ109, combining a new drug with an old forgotten anti-tuberculosis drugs due to its toxicity.

The *mt*BioC identified in this work was purified and assayed to determine its activity. Initially, several attempts to purify the protein produce little to no purifiable recombinant protein, therefore as result codon optimised techniques were employed. This optimisation made it possible to isolate and purify the protein in an expression strain containing a DE3 lysogen that expresses T7 RNA polymerase. The *mt*BioC showed some level of activity when methyl transferase assays were conducted. The protein showed activity in response to changes in pH, temperature, metal ion dependence, malonyl-CoA, glutaryl-CoA, and an inhibitor. It is therefore postulated that the *mt*BioC initiates the pimelate biosynthesis in *Mtb* since it has been proven to be a SAM-dependent methyltransferase as with other BioC's found in other bacteria.

Rv1882c is another protein identified and purified from this research, although its purification level was not high enough to allow for further studies to be performed. Its purification was made possible due to codon optimisation after several attempts failed. Changes in growth condition and buffer optimisation were unable to improve the purification results due to such low concentrations and therefore it could not be used for biochemical and crystallographic studies. Rv1882c is expected to reduce one of the products of pimelate biosynthesis, 3-ketoglutaryl-ACP methyl ester to 3-hydroxyglutaryl-ACP methyl ester. Inability to better purify the enzyme and obtain a good concentration could not allow this aim to be proven.

Two potential BioH enzymes were identified and were hereby referred to as *mt*BioH1 and *mt*BioH2. Just as with the other previous enzymes, initial purification of these enzymes by direct cloning of gene and expression did not work. Both *mt*BioH1 and *mt*BioH2 were codon optimised for *E. coli* and all buffers optimised. This enabled successful cloning and expression of *mt*BioH2. Several attempts to express the *mt*BioH1 even with the codon optimisation and change in expression strains and buffer conditions did not produce recombinant protein. The expression and purification of the *mt*BioH2 gave a good level

of protein, but the concentration of this protein was not good enough for any possible assay or crystallographic studies. This affected the extent at which the protein was to be analysed.

The BioH enzyme is postulated to demethylate the methyl group at the ω- position added by the BioC so as to produce the pimeloyl moiety. This happens at the beginning of the biotin biosynthetic pathway, where fatty acid biosynthesis pathway is hijacked by the biotin biosynthetic enzymes. The pimeloyl moiety produced is utilised by the biotin biosynthetic enzymes as a substrate and channelled into the synthesis of biotin.

Analysis of *Mtb* and its mycobactin structure indicates a possible pimelate structure similar to that synthesised *de novo* in the biotin pathway. In order to survive within the host macrophage *Mtb* requires mycobactin to obtain key metals required for its survival within the host. Therefore, the organism uses these extracellular siderophores to capture iron from the environment for their survival within the host. Since the mycobactin structure has a pimelate attached to it, it is hereby postulated that the two candidate BioHs identified from this work are utilised for biotin and mycobactin synthesis. The biotin catalysed BioH is hereby referred to as BioH1, while the mycobactin catalysed enzyme is referred to as BioH2. In this work the two proteins are referred to as *mt*BioH1 and *mt*BioH2 for biotin and mycobactin synthesis, respectively.

The ligand-based approach to anti-tubercular drug discovery used in this study identified a lead compound JJH110A as a potent compound against *Mtb*. This compound was as a result of hybridising isoxyl and SQ109 which are two old TB drugs. The investigation showed that the two drugs can be effectively hybridised to form a new anti-tubercular lead. Analogues of the synthesised JJH110A had low inhibitory ability as none of them could rival the inhibitory activity of the lead compound. The study shows that old anti-

tubercular drug structures can be re-examined and hybridized to discover new drug leads.

6.1 Future work

This project is just the initiation of the studies required to characterise these enzymes included in this thesis. There will be a considerable amount of further work to be done on the two approaches to drug discovery. The setbacks encountered during the purifications of *mt*BioC, *mt*BioH1 (Rv3177), *mt*BioH2 (Rv2715) and Rv1882c will require appropriate addressing with alternative strategies, ideas and methods to overcome these limitations.

E. coli is the preferred organism for expressing recombinant proteins in microorganisms because the organism has a well-established system that is safe and inexpensive to grow. It also allows large variety of vectors to be used on this organism. Therefore, different *E. coli* expression strains, other than the ones used, should be exploited. Strains containing *trp* and *tac* promoters will be utilised. The *trp* promoter is a group of genes that transcribes or codes for the components used in tryptophan production. It is used to regulate the genes for tryptophan synthesis by stopping the expression of the genes when tryptophan is present. The *tac* vector uses a combination of *trp* and *lac* operons and commonly used for controlled expression of foreign genes at high levels in *E. coli* and *P. pastoris*. They direct transcription that is 7 times more efficient than its parental lacUV promoter (Peranen *et al*., 1996). These will give further options for expression and allows for easy purification of the proteins.

Other expression strains not utilised in the study that uses a combination of T7 express and *lysY/lg* genes could be utilised to give a better expression. The LysY is a T7 lysozyme variant that lack amidase activity. This makes the cells less susceptible to lysis during induction and can still be able to inhibit T7 RNA polymerase. It allows for a minimised

basal expression of the target gene without inhibiting IPTG induced expression. This gene is encoded on a single copy miniF plasmid that does not require antibiotic selection (Peranen *et al*., 1996).

A yeast expression system is another viable option that will further be used to allow for easy purification of the proteins. It is a eukaryotic expression system that is suitable for a large scale manufacture and purification of recombinant proteins in eukaryotes and in bacteria. This system gives a high yield with high productivity in a chemically defined media that allows for easy genetic manipulation. *Saccharomyces cerevisiae* and *Pichia pastoris* are the two strain systems commonly utilised in yeast expression system. These strains are durable with stable production ability, easy to scale up proteins and cost effective (Baghban *et al*., 2019). The yeast express the protein of interest through extracellularly secretion directly into the expression medium and the cells removed by centrifugation while the supernatant is analysed for protein.

Yeast strains containing MET_{17} promoter encoding a homocysteine synthase (Liu et al., 2012) will be used. This will go in line with the ability of *mt*BioC to easily convert malonyl-CoA into its methoxy form, utilising S-adenosyl methionine (SAM) into S-adenosyl homocysteine (SAH) in the reaction process. Other yeast strains containing a POX_2 promoter encoding an acyl-CoA oxidase 2 (Zeng *et al*., 2018) will also be utilised. This will facilitate the utilisation of substrates containing acyl-CoAs in the process.

In addition to this, mycobacterial expression strains such as *M. smegmatis* will further be analysed and used to express the protein, since it is a close relative and non-pathogenic strain. Also, initial observations showed that *Streptomyces lividans* (*S. lividans*) could make use of the *Mycobacterium bovis* (*M. bovis*) BCG translational signals, suggesting its use as an expression host for mycobacterial genes (Kieser *et al*., 1986). These

mycobacterial strains will be investigated as additional options for protein expression but are considerably harder to manipulate and grow and therefore may not be a valid option.

Other pET vectors in *E. coli* and the pSUM shuttle vectors used in both *E. coli* and mycobacteria will also be utilised. These vectors allow purification in *E. coli* and can also be used in mycobacterial organisms for protein expression and purification.

The pBAD system is another vector system that will be used. This system makes use of tightly regulated expression with a dose-dependent induction. It also give high protein yields and makes detection and purification of expressed protein easy (Peranen *et al*., 1996).

Further purifications will involve the use of size exclusion chromatography to remove impurities to obtain pure recombinant proteins of the correct molecular weight. This will allow for a more accurate biochemical study and better data. A better protein expression and purification will allow for crystallographic studies to be initiated.

In 5 years from now, it is envisaged that all proteins will be well purified and biochemical studies completed. Crystal structures of these proteins will also be developed within this period. The development of crystal structures will allow the use of pharmacophore modelling technique to design novel inhibitors to the proteins. These will be tested *in vitro* to determine their anti-tubercular activity. Fragment based library screening in the developed assay could then afford opportunities to take these inhibitors towards clinical trials and further the development of potential *Mtb* drugs.

Novel synthesised compounds require a series of preclinical studies before use in humans. Therefore, this study merely forms a very early stage in a lengthy process of drug discovery. Initial follow up on the synthesised hybrid compound would thus include acute assessment of the compound's toxicology, enabling prediction of the compound's adverse effect likelihood on mammalian cells. This will be achieved in the next 5 years.

Toxicity prediction could be undertaken via MTT calorimetry to quantify the amount of viable cell counts on the basis of tetrazolium salt reduction in the presence of compound. Changing the REMA assay variables could also yield more data. For instance, the compounds could be tested against other strains of *Mtb* given that there are H37Rv sub-lineages and genetic strain alterations. Activity examination against the virulent *Mtb* strain would also be required. In 7 years from now these novel compounds could be developed into an anti-tubercular drug, with clinical trials initiated.

Therefore, the major outcomes of this thesis have initiated a number of schemes of work that should aid the development of the next generation of anti-tubercular agents.

References

7 References

Abdel-Magid, A. F. (2015). Decaprenylphosphoryl-β-d-ribose 2′-epimerase 1 (DprE1): A novel therapeutic target for the treatment of tuberculosis. *ACS Med Chem Lett.,* 6(4), 373-374.

Abreu, C., Rocha-Pereira, N., Sarmento, A., & Magro, F. (2015). Nocardia infections among immunomodulated inflammatory bowel disease patients: a review. *World J Gastroenterol.,* 21(21), 6491.

Adegboye, M. F., & Babalola, O. O. (2012). Taxonomy and ecology of antibiotic producing actinomycetes. *Afr. J. Agric. Res.,* 7(15), 2255-2261.

Alderwick, L. J., Lloyd, G. S., Ghadbane, H., May, J. W., Bhatt, A., Eggeling, L., Fütterer, K., & Besra, G. S. (2011). The C-terminal domain of the arabinosyltransferase *Mycobacterium tuberculosis* EmbC is a lectin-like carbohydrate binding module. *PLoS Pathog.,* 7(2), e1001299.

Alexeev, D., Alexeeva, M., Baxter, R. L., Campopiano, D. J., Webster, S. P., & Sawyer, L. (1998). The crystal structure of 8-amino-7-oxononanoate synthase: a bacterial PLP-dependent, acyl-CoA-condensing enzyme. *J Mol Biol.,* 284(2), 401-419.

Anantharaman, V., Koonin, E. V., & Aravind, L. (2002). Comparative genomics and evolution of proteins involved in RNA metabolism. *Nucleic Acids Res.,* 30(7), 1427-1464.

Arabolaza, A., Shillito, M. E., Lin, T., Diacovich, L., Melgar, M., Pham, H., Amick, D., Gramajo, H., & Tsai, S. (2010). Crystal structures and mutational analyses of acyl-CoA carboxylase β subunit of *Streptomyces coelicolor*. *Biochemistry,* 49(34), 7367-7376.

Arinze, J. C., & Mistry, S. P. (1971). Activities of some biotin enzymes and certain aspects of gluconeo-genesis during biotin deficiency. *Comp Biochem and Physiol.,* 38(2), 285-294.

Askoura, M., Mattawa, W., Abujamel, T., & Taher, I. (2011). Efflux pump inhibitors (EPIs) as new antimicrobial agents against *Pseudomonas aeruginosa*. *Libyan J M.,* 6(1), 5870.

Astarie-Dequeker, C., Le Guyader, L., Malaga, W., Seaphanh, F., Chalut, C., Lopez, A., & Guilhot, C. (2009). Phthiocerol dimycocerosates of *M. tuberculosis* participate in macrophage invasion by inducing changes in the organization of plasma membrane lipids. *PLoS Pathogens,* 5(2), e1000289.

Attwood, P. V., & Wallace, J. C. (2002). Chemical and catalytic mechanisms of carboxyl transfer reactions in biotin-dependent enzymes. *Acc Chem Res.,* 35(2), 113-120.

Bagautdinov, B., Kuroishi, C., Sugahara, M., & Kunishima, N. (2005). Crystal structures of biotin protein ligase from *Pyrococcus horikoshii* OT3 and its complexes: structural basis of biotin activation. *J Mol Biol.,* 353(2), 322-333.

Baghban, R., Farajnia, S., Rajabibazl, M., Ghasemi, Y., Mafi, A. A., Hoseinpoor, R., Rahbarnia, L., & Aria, M. (2019). Yeast expression systems: overview and recent advances. *Mol biotechnol.,* 61(5), 365-384.

Barile, F. A. (2007). Principles of toxicology testing. *CRC Press*, 1-362.

Barkan, D., Hedhli, D., Yan, H., Huygen, K., & Glickman, M. S. (2012). *Mycobacterium tuberculosis* lacking all mycolic acid cyclopropanation is viable but highly attenuated and hyperinflammatory in mice. *Infect Immun.,* 80(6), 1958-1968.

Barreto, M. L., Pereira, S. M., & Ferreira, A. A. (2006). BCG vaccine: efficacy and indications for vaccination and revaccination. *J Pediatr (Rio J).* 82(3), s45-s54.

Barry, C. E., Lee, R. E., Mdluli, K., Sampson, A. E., Schroeder, B. G., Slayden, R. A., & Yuan, Y. (1998). Mycolic acids: structure, biosynthesis and physiological functions. *Prog Lipid Res.,* 37(2), 143-179.

Barry, C. E., Slayden, R. A., Sampson, A. E., & Lee, R. E. (2000). Use of genomics and combinatorial chemistry in the development of new antimycobacterial drugs. *Biochem Pharmacol.,* 59(3), 221-231.

Beard, P. M., Daniels, M. J., Henderson, D., Pirie, A., Rudge, K., Buxton, D., Rhind, S., Greig, A., Hutchings, M. R., & McKendrick, I. (2001). *Paratuberculosis* infection of nonruminant wildlife in Scotland. *J Clin Microbiol.,* 39(4), 1517-1521.

Behling, C. A., Perez, R. L., Kidd, M. R., Staton, G. W., & Hunter, R. L. (1993). Induction of pulmonary granulomas, macrophage procoagulant activity, and tumor necrosis factor-alpha by trehalose glycolipids. *Ann Clin & Lab Sci.,* 23(4), 256-266.

Behr, M. A. (2004). Tuberculosis due to multiple strains: a concern for the patient? A concern for tuberculosis control? *Am J Respir Crit Care Med.,* 169(5), 554-555.

Bell, K. S., Philp, J. C., Aw, D. W. J., & Christofi, N. (1998). The genus *Rhodococcus*. *J Appl Microbiol.,* 85(2), 195-210.

Bennett, B. D. (1970). *Modern topics in biochemistry: structure and function of biological molecules.*: Macmillan.

Bennett, B. D., Kimball, E. H., Gao, M., Osterhout, R., Van Dien, S. J., & Rabinowitz, J. D. (2009). Absolute metabolite concentrations and implied enzyme active site occupancy in *Escherichia coli*. *Nat Chem Biol.,* 5(8), 593.

Bentley, S. D., Chater, K. F., Cerdeno-Tarraga, A. M., Challis, G. L., Thomson, N. R., James, K. D., Harris, D. E., Quail, M. A., Kieser, H., & Harper, D. (2002). Complete genome sequence of the model actinomycete *Streptomyces coelicolor* A3 (2). *Nature,* 417(6885), 141.

Bentley, S. D., Maiwald, M., Murphy, L. D., Pallen, M. J., Yeats, C. A., Dover, L. G., Norbertczak, H. T., Besra, G. S., Quail, M. A., & Harris, D. E. (2003). Sequencing and analysis of the genome of the Whipple's disease bacterium *Tropheryma whipplei*. *Lancet,* 361(9358), 637-644.

Berdy, J. (2005). Bioactive microbial metabolites. *J Antibiot (Tokyo).* 58(1), 1.

Berg, J. M., Tymoczko, J. L., & Stryer, L. (1995). *Biochemistry* (J. Gatto Jr. Ed. 7th ed.): W. H. Freeman and Company.

Berkovitch, F., Nicolet, Y., Wan, J. T., Jarrett, J. T., & Drennan, C. L. (2004). Crystal structure of biotin synthase, an S-adenosylmethionine-dependent radical enzyme. *Science,* 303(5654), 76-79.

Bernard, K. (2012). The genus Corynebacterium and other medically relevant coryneform-like bacteria. *J clin microbiol.,* 50(10), 3152-3158.

Bevilacqua, L., Ovidi, M., Di Mattia, E., Trovatelli, L. D., & Canganella, F. (2003). Screening of *Bifidobacterium* strains isolated from human faeces for antagonistic activities against potentially bacterial pathogens. *Microbiol Res.,* 158(2), 179-185.

Bhowruth, V., Brown, A. K., Reynolds, R. C., Coxon, G. D., Mackay, S. P., Minnikin, D. E., & Besra, G. S. (2006). Symmetrical and unsymmetrical analogues of isoxyl; active agents against *Mycobacterium tuberculosis*. *Bioorg Med Chem Lett.,* 16(18), 4743-4747.

Bielenica, A., Stefańska, J., Stępień, K., Napiórkowska, A., Augustynowicz-Kopeć, E., Sanna, G., Madeddu, S., Boi, S., Giliberti, G., & Wrzosek, M. (2015). Synthesis, cytotoxicity and antimicrobial activity of thiourea derivatives incorporating 3-(trifluoromethyl) phenyl moiety. *Eur J Med Chem.,* 101, 111-125.

Birch, H. L., Alderwick, L. J., Bhatt, A., Rittmann, D., Krumbach, K., Bai, Y., Lowary, T. L., Eggeling, L., & Besra, G. S. (2008). Biosynthesis of mycobacterial arabinogalactan: identification of a novel α (1→ 3) arabinofuranosyltransferase. *Mol Microbiol.,* 69(5), 1191-1206.

Birch, H. L., Fuhrmann, M., & Shaw, N. M. (1995). Biotin synthase from *Escherichia coli*, an investigation of the low molecular weight and protein components required for activity *in vitro*. *J Biol Chem.,* 270(32), 19158-19165.

Biswal, B. K., Morisseau, C., Garen, G., Cherney, M. M., Garen, C., Niu, C., Hammock, B. D., & James, M. N. G. (2008). The molecular structure of epoxide hydrolase B from *Mycobacterium tuberculosis* and its complex with a urea-based inhibitor. *J Mol Biol.,* 381(4), 897-912.

Blanchard, J. S. (1996). Molecular mechanisms of drug resistance in *Mycobacterium tuberculosis*. *Annu Rev Biochem.,* 65(1), 215-239.

Bloom, B. R., & Godal, T. (1983). Selective primary health care: strategies for control of disease in the developing world. V. Leprosy. *Rev Infect Dis.,* 5(4), 765-780.

Blumberg, H. M., Burman, W. J., Chaisson, R. E., & Daley, C. L. (2003). American thoracic society/centers for disease control and prevention/infectious diseases society of America: treatment of tuberculosis. *Am J Respir Crit Care Med.,* 167(4), 603.

BNF. (2016). British National Formulary (online) London: BMJ Group and Pharmaceutical Press.

Boeree, M. J., Heinrich, N., Aarnoutse, R., Diacon, A. H., Dawson, R., Rehal, S., Kibiki, G. S., Churchyard, G., Sanne, I., & Ntinginya, N. E. (2017). High-dose rifampicin, moxifloxacin, and SQ109 for treating tuberculosis: a multi-arm, multi-stage randomised controlled trial. *Lancet Infect Dis.,* 17(1), 39-49.

Bonnemere, C., Hamilton, J. A., Steinrauf, L. K., & Knappe, J. (1965). Structure of the bis-*p*-bromoanilide of carbon dioxide biotin. *Biochemistry,* 4(2), 240-245.

Borchardt, R. T., Eiden, L. E., Wu, B., & Rutledge, C. O. (1979). Sinefungin, a potent inhibitor of S-adenosylmethionine: Protein O-methyltransferase. *Biochem Biophys Res Commun.,* 89(3), 919-924.

Borgaro, J. G., Chang, A., Machutta, C. A., Zhang, X., & Tonge, P. J. (2011). Substrate recognition by β-ketoacyl-ACP synthases. *Biochemistry,* 50(49), 10678-10686.

Bower, S., Perkins, J. B., Yocum, R. R., Howitt, C. L., Rahaim, P., & Pero, J. (1996). Cloning, sequencing, and characterization of the *Bacillus subtilis* biotin biosynthetic operon. *J Bacteriol.,* 178(14), 4122-4130.

Brennan, P. J. (2003). Structure, function, and biogenesis of the cell wall of *Mycobacterium tuberculosis*. *Tuberculosis (Edinb),* 83(1), 91-97.

Brennan, P. J., & Nikaido, H. (1995). The envelope of mycobacteria. *Annu Rev Biochem.,* 64(1), 29-63.

Briken, V., Porcelli, S. A., Besra, G. S., & Kremer, L. (2004). Mycobacterial lipoarabinomannan and related lipoglycans: from biogenesis to modulation of the immune response. *Mol Microbiol.,* 53(2), 391-403.

Broquist, H. P., & Snell, E. E. (1951). Biotin and bacterial growth. *J. Biol Chem.,* 188, 431-444.

Brosch, R., Gordon, S. V., Marmiesse, M., Brodin, P., Buchrieser, C., Eiglmeier, K., Garnier, T., Gutierrez, C., Hewinson, G., & Kremer, L. (2002). A new evolutionary scenario for the *Mycobacterium tuberculosis* complex. *Proc Natl Acad Sci.,* 99(6), 3684-3689.

Brown-Elliott, B. A., Brown, J. M., Conville, P. S., & Wallace, R. J. (2006). Clinical and laboratory features of the *Nocardia spp*. based on current molecular taxonomy. *Clin Microbiol Rev.,* 19(2), 259-282.

Brown, E. D., Cronan, J. E., Grøtli, M., & Beckett, D. (2004). The biotin repressor: modulation of allostery by corepressor analogs. *J Mol Biol.,* 337(4), 857-869.

Brown, E. D., North, E. J., Hurdle, J. G., Morisseau, C., Scarborough, J. S., Sun, D., Korduláková, J., Scherman, M. S., Jones, V., & Grzegorzewicz, A. E. (2011). The structure–activity relationship of urea derivatives as anti-tuberculosis agents. *Bioorg Med Chem.,* 19(18), 5585-5595.

Brown, E. D., & Wright, G. D. (2016). Antibacterial drug discovery in the resistance era. *Nature,* 529(7586), 336.

Brozna, J. P., Horan, M., Rademacher, J. M., Pabst, K. M., & Pabst, M. J. (1991). Monocyte responses to sulfatide from *Mycobacterium tuberculosis*: inhibition of priming for enhanced release of superoxide, associated with increased secretion of interleukin-1 and tumor necrosis factor alpha, and altered protein phosphorylation. *Infect Immun.,* 59(8), 2542-2548.

Brune, I., Götker, S., Schneider, J., Rodionov, D. A., & Tauch, A. (2012). Negative transcriptional control of biotin metabolism genes by the TetR-type regulator BioQ in biotin-auxotrophic *Corynebacterium glutamicum* ATCC 13032. *J Biotechnol.,* 159(3), 225-234.

Burian, J., Ramón-García, S., Howes, C. G., & Thompson, C. J. (2012). WhiB7, a transcriptional activator that coordinates physiology with intrinsic drug resistance in *Mycobacterium tuberculosis*. *Expert Rev Anti Infect Ther.,* 10(9), 1037-1047.

Camacho, L. R., Constant, P., Raynaud, C., Lanéelle, M., Triccas, J. A., Gicquel, B., Daffé, M., & Guilhot, C. (2001). Analysis of the phthiocerol dimycocerosate locus of *Mycobacterium tuberculosis* evidence that this lipid is involved in the cell wall permeability barrier. *J Biol Chem.,* 276(23), 19845-19854.

Caron, A., & Donohue, J. (1969). Redetermination of thermal motion and interatomic distances in urea. *Acta Cryst.,* 25(2), 404-404.

Cayabyab, M., Macovei, L., & Campos-Neto, A. (2012). Current and novel approaches to vaccine development against tuberculosis. *Front Cell Infect Microbiol.,* 2, 154.

Cegielski, J. P. (2010). Extensively drug-resistant tuberculosis: “there must be some kind of way out of here”. *Clin Infect Dis.,* 50(3), 195-200.

Chapman-Smith, A., & Cronan, J. E. (1999). The enzymatic biotinylation of proteins: a post-translational modification of exceptional specificity. *Trends Biochem Sci.,* 24(9), 359-363.

Chapman-Smith, A., Morris, T. W., Wallace, J. C., & Cronan, J. E. (1999). Molecular recognition in a post-translational modification of exceptional specificity mutants of the biotinylated domain of acetyl-CoA carboxylase defective in recognition by biotin protein ligase. *J Biol Chem.,* 274(3), 1449-1457.

Chapman-Smith, A., Turner, D. L., Cronan, J. E., Morris, T. W., & Wallace, J. C. (1994). Expression, biotinylation and purification of a biotin-domain peptide from the biotin carboxy carrier protein of *Escherichia coli* acetyl-CoA carboxylase. *Biochem J.,* 302(3), 881-887.

Chatterjee, D. (1997). The mycobacterial cell wall: structure, biosynthesis and sites of drug action. *Curr Opin Chem Biol.,* 1(4), 579-588.

Chatterjee, D., Hunter, S. W., McNeil, M., & Brennan, P. J. (1992). Lipoarabinomannan. Multiglycosylated form of the mycobacterial mannosylphosphatidylinositols. *J Biol Chem.,* 267(9), 6228-6233.

Chatterjee, D., & Khoo, K. (1998). Mycobacterial lipoarabinomannan: an extraordinary lipoheteroglycan with profound physiological effects. *Glycobiology,* 8(2), 113-120.

Chung, C. T., Niemela, S. L., & Miller, R. H. (1989). One-step preparation of competent *Escherichia coli*: transformation and storage of bacterial cells in the same solution. *Proc Natl Acad Sci.,* 86(7), 2172-2175.

Coco, W. M., Levinson, W. E., Crist, M. J., Hektor, H. J., Darzins, A., Pienkos, P. T., Squires, C. H., & Monticello, D. J. (2001). DNA shuffling method for generating highly recombined genes and evolved enzymes. *Nat Biotechnol.,* 19(4), 354.

Cooper, A. M. (2009). Cell-mediated immune responses in tuberculosis. *Ann Rev Immu.,* 27, 393-422.

Corbett, E. L., Watt, C. J., Walker, N., Maher, D., Williams, B. G., Raviglione, M. C., & Dye, C. (2003). The growing burden of tuberculosis: global trends and interactions with the HIV epidemic. *Arch Intern Med.,* 163(9), 1009-1021.

Craven, B. M., Cusatis, C., Gartland, G. L., & Vizzini, E. A. (1973). Hydrogen bonding effects on molecular structure: crystallographic studies of barbiturates. *J Mol Struc.,* 16(2), 331-342.

Cronan, J. E. (2014). Biotin and lipoic acid: synthesis, attachment, and regulation. *EcoSal Plus.,* 6(1), 0001-2012.

Cronan, J. E., & Lin, S. (2011). Synthesis of the α, ω-dicarboxylic acid precursor of biotin by the canonical fatty acid biosynthetic pathway. *Curr Opin Chem Biol.,* 15(3), 407-413.

Cronan, J. E., & Wallace, J. C. (1995). The gene encoding the biotin-apoprotein ligase of *Saccharomyces cerevisiae*. *FEMS Microbiol Lett.,* 130(2-3), 221-229.

Croom, J. A., McNeill, J. J., & Tove, S. B. (1964). Biotin deficiency and the fatty acids of certain biotin-requiring bacteria. *J Bacteriol.*, 88(2), 389-394.

Crowle, A. J., Mitchell, R. S., & Petty, T. L. (1963). The effectiveness of a thiocarbanilide (Isoxyl) as a therapeutic drug in mouse tuberculosis. *Am Rev Respir Dis.*, 88(5), 716-717.

Csukás, Z., Banizs, B., & Rozgonyi, F. (2004). Studies on the cytotoxic effects of *Propionibacterium acnes* strains isolated from cornea. *Microb Pathog.*, 36(3), 171-174.

Daffé, M., Brennan, P. J., & McNeil, M. (1990). Predominant structural features of the cell wall arabinogalactan of *Mycobacterium tuberculosis* as revealed through characterization of oligoglycosyl alditol fragments by gas chromatography/mass spectrometry and by ^{1}H and ^{13}C NMR analyses. *J Biol Chem.*, 265(12), 6734-6743.

Daley, C. L., Small, P. M., Schecter, G. F., Schoolnik, G. K., McAdam, R. A., Jacobs Jr, W. R., & Hopewell, P. C. (1992). An outbreak of tuberculosis with accelerated progression among persons infected with the Human Immunodeficiency Virus: an analysis using restriction-fragment—length polymorphisms. *N Engl J Med.*, 326(4), 231-235.

Daniel, R. M., & Danson, M. J. (2013). Temperature and the catalytic activity of enzymes: A fresh understanding. *FEBS Lett.*, 587(17), 2738-2743.

Davidson, L. A., Draper, P., & Minnikin, D. E. (1982). Studies on the mycolic acids from the walls of *Mycobacterium microti*. *J Gen Microbiol.*, 128(4), 823-828.

de Jong, B. C., Antonio, M., & Gagneux, S. (2010). *Mycobacterium africanum*—review of an important cause of human tuberculosis in West Africa. *PLoS Negl Trop Dis.*, 4(9), e744.

de Jong, B. C., Hill, P. C., Brookes, R. H., Otu, J. K., Peterson, K. L., Small, P. M., & Adegbola, R. A. (2005). *Mycobacterium africanum*: a new opportunistic pathogen in HIV infection? *Aids*, 19(15), 1714-1715.

De Rossi, E., Branzoni, M., Cantoni, R., Milano, A., Riccardi, G., & Ciferri, O. (1998). *mmr*, a *Mycobacterium tuberculosis* gene conferring resistance to small cationic dyes and inhibitors. *J Bacteriol.*, 180(22), 6068-6071.

Deb, C., Lee, C., Dubey, V. S., Daniel, J., Abomoelak, B., Sirakova, T. D., Pawar, S., Rogers, L., & Kolattukudy, P. E. (2009). A novel *in vitro* multiple-stress dormancy model for *Mycobacterium tuberculosis* generates a lipid-loaded, drug-tolerant, dormant pathogen. *Plos ONE*, 4(6), e6077.

Desnues, B., Al Moussawi, K., & Fenollar, F. (2010). New insights into Whipple's disease and *Tropheryma whipplei* infections. *Microbes Infect.*, 12(14-15), 1102-1110.

DeTitta, G. T., Edmonds, J. W., Stallings, W., & Donohue, J. (1976). Molecular structure of biotin. Results of two independent crystal structure investigations. *J Am Chem Soc.,* 98(7), 1920-1926.

Dheda, K., Booth, H., Huggett, F., Johnson, M. A., Zumla, A., & Rook, G. A. W. (2005). Lung remodeling in pulmonary tuberculosis. *J Infect Dis.,* 192(7), 1201-1210.

Dover, L. G., Alahari, A., Gratraud, P., Gomes, J. M., Bhowruth, V., Reynolds, R. C., Besra, G. S., & Kremer, L. (2007). EthA, a common activator of thiocarbamide-containing drugs acting on different mycobacterial targets. *Antimicrob Agents Chemother.,* 51(3), 1055-1063.

Dover, L. G., Cerdeno-Tárraga, A. M., Pallen, M. J., Parkhill, J., & Besra, G. S. (2004). Comparative cell wall core biosynthesis in the mycolated pathogens, *Mycobacterium tuberculosis* and *Corynebacterium diphtheriae*. *FEMS Microbiol Rev.,* 28(2), 225-250.

Dubnau, E., Chan, J., Raynaud, C., Mohan, V. P., Lanéelle, M., Yu, K., Quémard, A., Smith, I., & Daffé, M. (2000). Oxygenated mycolic acids are necessary for virulence of *Mycobacterium tuberculosis* in mice. *Mol Microbiol.,* 36(3), 630-637.

Duckworth, B. P., Geders, T. W., Tiwari, D., Boshoff, H. I., Sibbald, P. A., Barry, C. E., Schnappinger, D., Finzel, B. C., & Aldrich, C. C. (2011). Bisubstrate adenylation inhibitors of biotin protein ligase from *Mycobacterium tuberculosis*. *Chem Biol.,* 18(11), 1432-1441.

Dye, C. (2000). Tuberculosis 2000–2010: control, but not elimination. *Int J Tuberc Lung Dis.,* 4(12), S146-S152.

Dye, C. (2006). Global epidemiology of tuberculosis. *Lancet,* 367(9514), 938-940.

Dye, C. (2013). Making wider use of the world's most widely used vaccine: Bacille Calmette–Guérin revaccination reconsidered. *J R Soc Interface.,* 10(87), 20130365.

Edwards, D., & Kirkpatrick, C. H. (1986). The immunology of mycobacterial diseases. *Am Rev Respir Dis.,* 134(5), 1062-1071.

Embley, T. M., & Stackebrandt, E. (1994). The molecular phylogeny and systematics of the actinomycetes. *Annu Rev Microbiol.,* 48(1), 257-289.

Emerson, P. A., Lacey, B. W., & Breach, M. R. (1969). A bacteriological study of thiocarlide monotherapy. *Tubercle,* 50(3), 273-279.

Ernst, J. D. (2012). The immunological life cycle of tuberculosis. *Nature Rev Immu.,* 12(8), 581.

Escalettes, F., Florentin, D., Tse, B., Lesage, D., & Marquet, A. (1999). Biotin synthase mechanism: evidence for hydrogen transfer from the substrate into deoxyadenosine. *J. Am. Chem. Soc.,* 121(15), 3571-3578.

Espinal, M. A., Laszlo, A., Simonsen, L., Boulahbal, F., Kim, S. J., Reniero, A., Hoffner, S., Rieder, H. L., Binkin, N., & Dye, C. (2001). Global trends in resistance to antituberculosis drugs. *N Engl J Med.*, 344(17), 1294-1303.

Euzéby, J. P. (1997). List of bacterial names with standing in nomenclature: a folder available on the Internet. *Int J Syst Bacteriol.*, 47(2), 590-592.

Faller, M., Niederweis, M., & Schulz, G. E. (2004). The structure of a mycobacterial outer-membrane channel. *Science*, 303(5661), 1189-1192.

Farrar, C. E., Siu, K. K. W., Howell, P. L., & Jarrett, J. T. (2010). Biotin synthase exhibits burst kinetics and multiple turnovers in the absence of inhibition by products and product-related biomolecules. *Biochemistry*, 49(46), 9985-9996.

Feng, S., Ma, J., Yang, J., Hu, Z., Zhu, L., Bi, H., Sun, Y., & Wang, H. (2015a). *Ralstonia solanacearum* fatty acid composition is determined by interaction of two 3-ketoacyl-acyl carrier protein reductases encoded on separate replicons. *BMC Microbiol.*, 15(1), 223.

Feng, S. Y., Kumar, R., Ravcheev, D. A., & Zhang, H. (2015b). *Paracoccus denitrificans* possesses two BioR homologs having a role in regulation of biotin metabolism. *Microbiol Open*, 4(4), 644-659.

Feng, Y., Zhang, H., & Cronan, J. E. (2013). Profligate biotin synthesis in α-proteobacteria–a developing or degenerating regulatory system? *Mol Microbiol.*, 88(1), 77-92.

Fenton, M. J., Riley, L. W., & Schlesinger, L. S. (2005). *Receptor-mediated recognition of Mycobacterium tuberculosis by host cells.* (S. T. Cole Ed.). Tuberculosis and the tubercle bacillus: *American Soc. Microbiol.*

Figueroa-Munoz, J. I., & Ramon-Pardo, P. (2008). Tuberculosis control in vulnerable groups. *Bull World Health Organ.*, 86(9), 733-735.

Finch, R. (2004). *Clinical uses of antimicrobial drugs* (S. P. Denyer, Hodges, N.A., Gorman, S.P Ed. 7th ed.).

Flor de Lima, B., & Tavares, M. (2014). Risk factors for extensively drug-resistant tuberculosis: a review. *Clin Respir J.*, 8(1), 11-23.

Flynn, J. A., & Chan, J. (2001). Immunology of tuberculosis. *Annu Rev Immunol.*, 19, 93-129.

Frank, E. G., & Woodgate, R. (2007). Increased catalytic activity and altered fidelity of human DNA polymerase I in the presence of manganese. *J Biol Chem.*, 282(34), 24689-24696.

Franzblau, S. G., DeGroote, M. A., Cho, S. H., Andries, K., Nuermberger, E., Orme, I. M., Mdluli, K., Angulo-Barturen, I., Dick, T., & Dartois, V. (2012).

Comprehensive analysis of methods used for the evaluation of compounds against *Mycobacterium tuberculosis*. *Tuberculosis,* 92(6), 453-488.

Fraschetti, C., Filippi, A., Guarcini, L., Steinmetz, V., & Speranza, M. (2015). Structure and conformation of protonated d-(+)-biotin in the unsolvated state. *J Phys Chem B.,* 119(20), 6198-6203.

Fu, L. M., & Fu-Liu, C. S. (2002). Is *Mycobacterium tuberculosis* a closer relative to Gram positive or Gram negative bacterial pathogens? *Tuberculosis,* 82(2-3), 85-90.

Fukuda, T., Matsumura, T., Ato, M., Hamasaki, M., Nishiuchi, Y., Murakami, Y., Maeda, Y., Yoshimori, T., Matsumoto, S., & Kobayashi, K. (2013). Critical roles for lipomannan and lipoarabinomannan in cell wall integrity of mycobacteria and pathogenesis of tuberculosis. *MBio.,* 4(1), e00472-00412.

Gago, G., Diacovich, L., Arabolaza, A., Tsai, S., & Gramajo, H. (2011). Fatty acid biosynthesis in actinomycetes. *FEMS Microbiology Rev.,* 35(3), 475-497.

Gago, G., Kurth, D., Diacovich, L., Tsai, S., & Gramajo, H. (2006). Biochemical and structural characterization of an essential acyl coenzyme A carboxylase from *Mycobacterium tuberculosis*. *J Bacteriol.,* 188(2), 477-486.

Gandhi, N. R., Moll, A., Sturm, A. W., Pawinski, R., Govender, T., Lalloo, U., Zeller, K., Andrews, J., & Friedland, G. (2006). Extensively drug-resistant tuberculosis as a cause of death in patients co-infected with tuberculosis and HIV in a rural area of South Africa. *Lancet,* 368(9547), 1575-1580.

Gannoun-Zaki, L., Alibaud, L., & Kremer, L. (2013). Point mutations within the fatty acid synthase type II dehydratase components HadA or HadC contribute to isoxyl resistance in *Mycobacterium tuberculosis*. *Antimicrob Agents Chemother.,* 57(1), 629-632.

Gao, B., & Gupta, R. S. (2012). Phylogenetic framework and molecular signatures for the main clades of the phylum Actinobacteria. *Microbiol Mol Biol Rev.,* 76(1), 66-112.

Gebhardt, H., Meniche, X., Tropis, M., Krämer, R., Daffe, M., & Morbach, S. (2007). The key role of the mycolic acid content in the functionality of the cell wall permeability barrier in Corynebacterineae. *Microbiol.,* 153(5), 1424-1434.

Gehre, F., Otu, J. K., DeRiemer, K., de Sessions, P., Hibberd, M., Mulders, W., Corrah, T., de Jong, B. C., & Antonio, M. (2013). Deciphering the growth behaviour of *Mycobacterium africanum*. *PLoS Negl Trop Dis.,* 7(5), e2220.

Geldenhuys, W. J., Malan, S. F., Bloomquist, J. R., Marchand, A. P., & Van der Schyf, C. J. (2005). Pharmacology and structure-activity relationships of bioactive polycyclic cage compounds: a focus on pentacycloundecane derivatives. *Med Res Rev.,* 25(1), 21-48.

Geldmacher, C., Ngwenyama, N., Schuetz, A., Petrovas, C., Reither, K., Heeregrave, E. J., Casazza, J. P., Ambrozak, D. R., Louder, M., & Ampofo, W. (2010). Preferential infection and depletion of *Mycobacterium tuberculosis*–specific CD4 T cells after HIV-1 infection. *J Exp Med.,* 207(13), 2869-2881.

Gilleron, M., Bala, L., Brando, T., Vercellone, A., & Puzo, G. (2000). *Mycobacterium tuberculosis* H37Rv parietal and cellular lipoarabinomannans characterisation of the acyl- and glyco- forms. *J Biol Chem.,* 275(1), 677-684.

Girling, R. L., & Jeffrey, G. A. (1974). The crystal structures of methyl 1, 5-dithio-α-d-ribopyranoside quarterhydrate and methyl 1,5-dithio-β-d-ribopyranoside. *Acta Cryst.,* 30(2), 327-333.

Glickman, M. S., Cox, J. S., & Jacobs Jr, W. R. (2000). A novel mycolic acid cyclopropane synthetase is required for cording, persistence, and virulence of *Mycobacterium tuberculosis*. *Mol Cell,* 5(4), 717-727.

Godfrey-Faussett, P., & Stoker, N. G. (1992). Genetic 'fingerprinting'for clues to the pathogenesis of tuberculosis. *RSTMH.,* 86(5), 472-475.

Gohara, D. W., & Di Cera, E. (2016). Molecular mechanisms of enzyme activation by monovalent cations. *J Biol Chem.,* 291(40), 20840-20848.

Goodfellow, M., & Minnikin, D. E. (1985). *Chemical methods in bacterial systematics* (Vol. 30). London; Orlando: Academic Press.

Gopal, P., & Dick, T. (2014). Reactive dirty fragments: implications for tuberculosis drug discovery. *Curr Opin Microbiol.,* 21, 7-12.

Goren, M. B., Brokl, O., Roller, P., Fales, H. M., & Das, B. C. (1976). Sulfatides of *Mycobacterium tuberculosis*: the structure of the principal sulfatide (SL-I). *Biochemistry,* 15(13), 2728-2735.

Greene, C. E. (2006). Actinomycosis and nocardiosis. *Infect Dis Dog and Cat.,* 3, 451-461.

Grzegorzewicz, A. E., Eynard, N., Quémard, A., North, E. J., Margolis, A., Lindenberger, J. J., Jones, V., Korduláková, J., Brennan, P. J., & Lee, R. E. (2014). Covalent modification of the *Mycobacterium tuberculosis* FAS-II dehydratase by isoxyl and thiacetazone. *ACS Infect Dis.,* 1(2), 91-97.

Grzegorzewicz, A. E., Pham, H., Gundi, V. A. K. B., Scherman, M. S., North, E. J., Hess, T., Jones, V., Gruppo, V., Born, S. E. M., & Korduláková, J. (2012). Inhibition of mycolic acid transport across the *Mycobacterium tuberculosis* plasma membrane. *Nature Chem Biol.,* 8(4), 334.

Guengerich, F. P. (2016). Metals in biology 2016: Molecular basis of selection of metals by enzymes. *J Biol Chem.,* 291(40), 20838-20839.

Günther, G., Lange, C., Alexandru, S., Altet, N., Avsar, K., Bang, D., Barbuta, R., Bothamley, G., Ciobanu, A., & Crudu, V. (2016). Treatment outcomes in multidrug-resistant tuberculosis. *N Engl J Med.,* 375(11), 1103-1105.

Hadfield, T. L., McEvoy, P., Polotsky, Y., Tzinserling, V. A., & Yakovlev, A. A. (2000). The pathology of diphtheria. *J Infect Dis.,* 181(1), 116-120.

Hawken, M., Nunn, P., Godfrey-Faussett, P., McAdam, K., Morris, J., Odhiambo, J., Githui, W., Gilks, C., Gathua, S., & Brindle, R. (1993). Increased recurrence of tuberculosis in HIV-1-infected patients in Kenya. *Lancet,* 342(8867), 332-337.

Heath, R. J., & Rock, C. O. (2002). The Claisen condensation in biology. *Nat. Prod. Rep.,* 19(5), 581-596.

Hebbeln, P., Rodionov, D. A., Alfandega, A., & Eitinger, T. (2007). Biotin uptake in prokaryotes by solute transporters with an optional ATP-binding cassette-containing module. *Proc Natl Acad Sci.,* 104(8), 2909-2914.

Hermon-Taylor, J. (2009). *Mycobacterium avium subspecies paratuberculosis*, Crohn's disease and the Doomsday scenario. *Gut Pathog.,* 1(1), 15.

Hines, M. E., Kreeger, J. M., & Herron, A. J. (1995). Mycobacterial infections of animals: Pathology and pathogenesis. *Lab Anim Sci.,* 45, 334-351.

Hirsch, A. M., & Valdés, M. (2010). *Micromonospora*: an important microbe for biomedicine and potentially for biocontrol and biofuels. *Soil Biol Biochem.,* 42(4), 536-542.

Hoffmann, C., Leis, A., Niederweis, M., Plitzko, J. M., & Engelhardt, H. (2008). Disclosure of the mycobacterial outer membrane: cryo-electron tomography and vitreous sections reveal the lipid bilayer structure. *Proc Natl Acad Sci.,* 105(10), 3963-3967.

Hoft, D. F., Blazevic, A., Abate, G., Hanekom, W. A., Kaplan, G., Soler, J. H., Weichold, F., Geiter, L., Sadoff, J. C., & Horwitz, M. A. (2008). A new recombinant Bacille Calmette-Guerin vaccine safely induces significantly enhanced tuberculosis-specific immunity in human volunteers. *J Infect Dis.,* 198(10), 1491-1501.

Hoft, D. F., Blazevic, A., Stanley, J., Landry, B., Sizemore, D., Kpamegan, E., Gearhart, J., Scott, A., Kik, S., & Pau, M. G. (2012). A recombinant adenovirus expressing immunodominant TB antigens can significantly enhance BCG-induced human immunity. *Vaccine,* 30(12), 2098-2108.

Holt, J., Krieg, P., & Sneath, J. J. (1994). *Stanley and ST Williams*.

Hope, H., & McCullough, J. D. (1964). The crystal structure of the molecular complex of iodine with tetrahydroselenophene, $C_4H_8Se.I_2$. *Acta Cryst.,* 17(6), 712-718.

Hopper, A. K., & Phizicky, E. M. (2003). tRNA transfers to the limelight. *Genes Dev.,* 17(2), 162-180.

Hopwood, D. A. (2007). *Streptomyces in nature and medicine: the antibiotic makers*: Oxford University Press.

Horn, D. L., Hewlett, D., Haas, W. H., Butler, W. R., Alfalla, C., Tan, E., Levine, A., Nayak, A., & Opal, S. M. (1994). Superinfection with rifampin-isoniazid-streptomycin-ethambutol (RISE)-resistant tuberculosis in three patients with AIDS: confirmation by polymerase chain reaction fingerprinting. *Ann Intern Med.,* 121(2), 115-116.

Horsburgh, C. R., Feldman, S., & Ridzon, R. (2000). Practice guidelines for the treatment of tuberculosis. *Clinical Infect Dis.,* 31(3), 633-639.

Horwitz, M. A., Harth, G., Dillon, B. J., & Masleša-Galić, S. (2000). Recombinant Bacillus Calmette–Guérin (BCG) vaccines expressing the *Mycobacterium tuberculosis* 30-kDa major secretory protein induce greater protective immunity against tuberculosis than conventional BCG vaccines in a highly susceptible animal model. *Proc Natl Acad Sci.,* 97(25), 13853-13858.

Horwitz, M. A., Lee, B. W., Dillon, B. J., & Harth, G. (1995). Protective immunity against tuberculosis induced by vaccination with major extracellular proteins of *Mycobacterium tuberculosis*. *Proc Natl Acad Sci.,* 92(5), 1530-1534.

Hsu, F., Wohlmann, J., Turk, J., & Haas, A. (2011). Structural definition of trehalose 6-monomycolates and trehalose 6, 6'-dimycolates from the pathogen *Rhodococcus equi* by multiple-stage linear ion-trap mass spectrometry with electrospray ionization. *J Am Soc Mass Spectrom.,* 22(12), 2160-2170.

Hunter, R. L., Olsen, M., Jagannath, C., & Actor, J. K. (2006). Trehalose 6, 6′-dimycolate and lipid in the pathogenesis of caseating granulomas of tuberculosis in mice. *Am J Pathol.,* 168(4), 1249-1261.

Ifuku, O., Miyaoka, H., Koga, N., Kishimoto, J., Haze, S., Wachi, Y., & Kajiwara, M. (1994). Origin of carbon atoms of biotin. ^{13}C-NMR studies on biotin biosynthesis in *Escherichia coli*. *Eur J Biochem.,* 220(2), 585-591.

Ikeda, M., Miyamoto, A., Mutoh, S., Kitano, Y., Tajima, M., Shirakura, D., Takasaki, M., Mitsuhashi, S., & Takeno, S. (2013). Development of biotin-prototrophic and -hyperauxotrophic *Corynebacterium glutamicum* strains. *Appl Environ Microbiol.,* 79(15), 4586-4594.

Ikeda, M., Nagashima, T., Nakamura, E., Kato, R., Ohshita, M., Hayashi, M., & Takeno, S. (2017). *In vivo* roles of fatty acid biosynthesis enzymes in biosynthesis of biotin and alpha-lipoic acid in *Corynebacterium glutamicum*. *Appl Environ Microbiol.,* 83(19).

Ingham, E. (1999). The immunology of *Propionibacterium acnes* and acne. *Curr Opin Infect Dis.,* 12(3), 191-197.

Jackson, M. (2014). The mycobacterial cell envelope—lipids. *Cold Spring Harb Perspect Med.,* 4(10), a021105.

Jackson, M., Crick, D. C., & Brennan, P. J. (2000). Phosphatidylinositol is an essential phospholipid of mycobacteria. *J Biol Chem.,* 275(39), 30092-30099.

Janin, Y. L. (2007). Antituberculosis drugs: ten years of research. *Bioorg Med Chem.,* 15(7), 2479-2513.

Jarlier, V., Gutmann, L., & Nikaido, H. (1991). Interplay of cell wall barrier and beta-lactamase activity determines high resistance to beta-lactam antibiotics in *Mycobacterium chelonae*. *Antimicrob Agents Chemother.,* 35(9), 1937-1939.

Jones, J. A., Virga, K. G., Gumina, G., & Hevener, K. E. (2016). Recent advances in the rational design and optimization of antibacterial agents. *Medchemcomm.,* 7(9), 1694-1715.

Käck, H., Gibson, K. J., Lindqvist, Y., & Schneider, G. (1998). Snapshot of a phosphorylated substrate intermediate by kinetic crystallography. *Proc Natl Acad Sci.,* 95(10), 5495-5500.

Käck, H., Sandmark, J., Gibson, K. J., Schneider, G., & Lindqvist, Y. (1999). Crystal structure of diaminopelargonic acid synthase: evolutionary relationships between pyridoxal-5′-phosphate-dependent enzymes. *J Mol Biol.,* 291(4), 857-876.

Kana, B. D., & Mizrahi, V. (2010). Resuscitation-promoting factors as lytic enzymes for bacterial growth and signaling. *FEMS Immunol Med Microbiol.,* 58(1), 39-50.

Kaplan, G., Post, F. A., Moreira, A. L., Wainwright, H., Kreiswirth, B. N., Tanverdi, M., Mathema, B., Ramaswamy, S. V., Walther, G., & Steyn, L. M. (2003). *Mycobacterium tuberculosis* growth at the cavity surface: a microenvironment with failed immunity. *Infect Immun.,* 71(12), 7099-7108.

Kasik, J. E. (1965). The nature of mycobacterial penicillinase. *Am Rev Respir Dis.,* 91(1), 117-119.

Kasik, J. E., & Peacham, L. (1968). Properties of β-lactamases produced by three species of mycobacteria. *Biochem J.,* 107(5), 675-682.

Kato, M., & Goren, M. B. (1974). Synergistic action of cord factor and mycobacterial sulfatides on mitochondria. *Infect Immun.,* 10(4), 733-741.

Kaur, D., Guerin, M. E., Škovierová, H., Brennan, P. J., & Jackson, M. (2009). Biogenesis of the cell wall and other glycoconjugates of *Mycobacterium tuberculosis*. *Adv Appl Microbiol.,* 69, 23-78.

Khan, F. A., Minion, J., Pai, M., Royce, S., Burman, W. J., Harries, A. D., & Menzies, D. (2010). Treatment of active tuberculosis in HIV-coinfected patients: a systematic review and meta-analysis. *Clinical Infect Dis.,* 50(9), 1288-1299.

Kieser, T., Moss, M. T., Dale, J. W., & Hopwood, D. A. (1986). Cloning and expression of *Mycobacterium bovis* BCG DNA in" *Streptomyces lividans*". *J Bacteriol.,* 168(1), 72-80.

Kim, T. K., Thomas, S. M., Ho, M., Sharma, S., Reich, C. I., Frank, J. A., Yeater, K. M., Biggs, D. R., Nakamura, N., & Stumpf, R. (2009). Heterogeneity of vaginal microbial communities within individuals. *J Clin Microbiol.,* 47(4), 1181-1189.

Kitahara, T., Hotta, K., Yoshida, M., & Okami, Y. (1975). Biological studies on amiclenomycin. *J Antibiot (Tokyo).* 28(3), 215-221.

Klopper, M., Warren, R. M., Hayes, C., van Pittius, N. C. G., Streicher, E. M., Müller, B., Sirgel, F. A., Chabula-Nxiweni, M., Hoosain, E., & Coetzee, G. (2013). Emergence and spread of extensively and totally drug-resistant tuberculosis, South Africa. *Emerg Infect Dis.,* 19(3), 449.

Knowles, J. R. (1989). The mechanism of biotin-dependent enzymes. *Annual Rev Biochem.,* 58(1), 195-221.

Kordulakova, J., Gilleron, M., Mikušová, K., Puzo, G., Brennan, P. J., Gicquel, B., & Jackson, M. (2002). Definition of the first mannosylation step in phosphatidylinositol mannoside synthesis *pimA* is essential for growth of mycobacteria. *J Biol Chem.,* 277(35), 31335-31344.

Korduláková, J., Janin, Y. L., Liav, A., Barilone, N., Dos Vultos, T., Rauzier, J., Brennan, P. J., Gicquel, B., & Jackson, M. (2007). Isoxyl activation is required for bacteriostatic activity against *Mycobacterium tuberculosis*. *Antimicrob Agents Chemother.,* 51(11), 3824-3829.

Kothari, H., Rao, L. V. M., Vankayalapati, R., & Pendurthi, U. R. (2012). *Mycobacterium tuberculosis* infection and tissue factor expression in macrophages. *PloS ONE,* 7(9), e45700.

Koul, A., Arnoult, E., Lounis, N., Guillemont, J., & Andries, K. (2011). The challenge of new drug discovery for tuberculosis. *Nature,* 469(7331), 483.

Kouzarides, T. (2002). Histone methylation in transcriptional control. *Curr Opin Genet Dev.,* 12(2), 198-209.

Kowalski, K., Szewczyk, R., & Druszczyńska, M. (2012). Mycolic acids--potential biomarkers of opportunistic infections caused by bacteria of the suborder Corynebacterineae. *Postepy Hig Med Dosw.,* 66, 461-468.

Kozbial, P. Z., & Mushegian, A. R. (2005). Natural history of S-adenosylmethionine-binding proteins. *BMC Struc Biol.,* 5(1), 19.

Kremer, L., Dover, L. G., Carrère, S., Nampoothiri, K. M., Lesjean, S., Brown, A. K., Brennan, P. J., Minnikin, D. E., Locht, C., & Besra, G. S. (2002). Mycolic acid biosynthesis and enzymic characterization of the β-ketoacyl-ACP synthase A condensing enzyme from *Mycobacterium tuberculosis*. *Biochem J.,* 364(2), 423-430.

Kritski, A. L., Marques, M. J., Rabahi, M. F., Vieira, M. A., Werneck-Barroso, E., Carvalho, C. E., Andrade, G. N., Bravo-de-Souza, R., Andrade, L. M., & Gontijo, P. P. (1996). Transmission of tuberculosis to close contacts of patients with multidrug-resistant tuberculosis. *Am J Respir Crit Care Med.,* 153(1), 331-335.

Kumar, C. S., Kwong, H. C., Mah, S. H., Chia, T., Loh, W., Quah, C. K., Lim, G. K., Chandraju, S., & Fun, H. (2015a). Synthesis and crystallographic insight into the structural aspects of some novel adamantane-based ester derivatives. *Molecules,* 20(10), 18827-18846.

Kumar, D., Negi, B., & Rawat, D. S. (2015b). The anti-tuberculosis agents under development and the challenges ahead. *Future Med Chem.,* 7(15), 1981-2003.

Kurth, D. G., Gago, G. M., de la Iglesia, A., Lyonnet, B. B., Lin, T., Morbidoni, H. R., Tsai, S., & Gramajo, H. (2009). ACCase 6 is the essential acetyl-CoA carboxylase involved in fatty acid and mycolic acid biosynthesis in mycobacteria. *Microbiology,* 155(Pt 8), 2664.

Lai, C., & Cronan, J. E. (2004). Isolation and characterization of β-ketoacyl-acyl carrier protein reductase (fabG) mutants of *Escherichia coli* and *Salmonella enterica serovar Typhimurium*. *J Bacteriol.,* 186(6), 1869-1878.

Lamoureux, G., & Artavia, G. (2010). Use of the adamantane structure in medicinal chemistry. *Curr Med Chem.,* 17(26), 2967-2978.

Lavollay, M., Arthur, M., Fourgeaud, M., Dubost, L., Marie, A., Veziris, N., Blanot, D., Gutmann, L., & Mainardi, J. (2008). The peptidoglycan of stationary-phase *Mycobacterium tuberculosis* predominantly contains cross-links generated by L, D-transpeptidation. *J Bacteriol.,* 190(12), 4360-4366.

León-Del-Rio, A., Leclerc, D., Akerman, B., Wakamatsu, N., & Gravel, R. A. (1995). Isolation of a cDNA encoding human holocarboxylase synthetase by functional complementation of a biotin auxotroph of *Escherichia coli*. *Proc Natl Acad Sci.,* 92(10), 4626-4630.

Lerner, P. I. (1996). Nocardiosis. *Clinical infect dis.,* 891-903.

Lessem, E. (2016). The tuberculosis treatment pipeline: activity, but no answers. *2016 Pipeline Rep.,* 163.

Lévy-Schil, S., Debussche, L., Rigault, S., Soubrier, F., Bacchetta, F., Lagneaux, D., Schleuniger, J., Blanche, F., Crouzet, J., & Mayaux, J. (1993). Biotin biosynthetic pathway in recombinant strains of *Escherichia coli* overexpressing *bio* genes:

evidence for a limiting step upstream from KAPA. *Appl Microbiol Biotechnol.,* 38(6), 755-762.

Li, K., Schurig-Briccio, L. A., Feng, X., Upadhyay, A., Pujari, V., Lechartier, B., Fontes, F. L., Yang, H., Rao, G., & Zhu, W. (2014). Multitarget drug discovery for tuberculosis and other infectious diseases. *J Med Chem.,* 57(7), 3126-3139.

Li, K., Wang, Y., Yang, G., Byun, S., Rao, G., Shoen, C., Yang, H., Gulati, A., Crick, D. C., & Cynamon, M. (2015). Oxa, thia, heterocycle, and carborane analogues of SQ109: Bacterial and protozoal cell growth inhibitors. *ACS Infect Dis.,* 1(5), 215-221.

Liav, A., Angala, S. K., Brennan, P. J., & Jackson, M. (2008). ND-aldopentofuranosyl-N′-[*p*-(isoamyloxy) phenyl]-thiourea derivatives: potential anti-TB therapeutic agents. *Bioorg Med Chem Lett.,* 18(8), 2649-2651.

Lievin, V., Peiffer, I., Hudault, S., Rochat, F., Brassart, D., Neeser, J. R., & Servin, A. L. (2000). *Bifidobacterium* strains from resident infant human gastrointestinal microflora exert antimicrobial activity. *Gut,* 47(5), 646-652.

Lin, S., & Cronan, J. E. (2011). Closing in on complete pathways of biotin biosynthesis. *Mol Biosyst.,* 7(6), 1811-1821.

Lin, S., & Cronan, J. E. (2012). The BioC O-methyltransferase catalyzes methyl esterification of malonyl-acyl carrier protein, an essential step in biotin synthesis. *J Biol Chem.,* 287(44), 37010-37020.

Lin, S., Hanson, R. E., & Cronan, J. E. (2010). Biotin synthesis begins by hijacking the fatty acid synthetic pathway. *Nature Chem Biol.,* 6(9), 682.

Liu, J., Obando, D., Liao, V., Lifa, T., & Codd, R. (2011). The many faces of the adamantyl group in drug design. *Eur J Med Chem.,* 46(6), 1949-1963.

Liu, Z. I., Tyo, K. E., Martínez, J. L., Petranovic, D., & Nielsen, J. (2012). Different expression systems for production of recombinant proteins in *Saccharomyces cerevisiae*. *Biotechnol Bioen.,* 109(5), 1259-1268.

Lockwood, D. N. J. (2002). Leprosy elimination—a virtual phenomenon or a reality? *BMJ.,* 324(7352), 1516-1518.

Low, M. (2017). The tuberculosis treatment pipeline: a breakthrough year for the treatment of XDR-TB. *Pipeline report,* 129.

Mahajan, R. (2013). Bedaquiline: First FDA-approved tuberculosis drug in 40 years. *Int J Appl Basic Med Res.,* 3(1), 1.

Mahapatra, S., Scherman, H., Brennan, P. J., & Crick, D. C. (2005). N-glycolylation of the nucleotide precursors of peptidoglycan biosynthesis of *Mycobacterium spp*. is altered by drug treatment. *J Bacteriol.,* 187(7), 2341-2347.

Manca, C., Tsenova, L., Bergtold, A., Freeman, S., Tovey, M., Musser, J. M., Barry, C. E., Freedman, V. H., & Kaplan, G. (2001). Virulence of a *Mycobacterium tuberculosis* clinical isolate in mice is determined by failure to induce Th1 type immunity and is associated with induction of IFN-α/β. *Proc Natl Acad Sci.,* 98(10), 5752-5757.

Manina, G., R Pasca, M., Buroni, S., De Rossi, E., & Riccardi, G. (2010). Decaprenylphosphoryl-β-D-ribose 2'-epimerase from *Mycobacterium tuberculosis* is a magic drug target. *Curr Med Chem.,* 17(27), 3099-3108.

Mann, S., Marquet, A., & Ploux, O. (2005). Inhibition of 7, 8-diaminopelargonic acid aminotransferase by amiclenomycin and analogues. *Biochem Soc Trans.,* 33(4), 802-805.

Marrakchi, H., Laneelle, M., & Daffé, M. (2014). Mycolic acids: structures, biosynthesis, and beyond. *Chem Biol.,* 21(1), 67-85.

Marrero, J., Rhee, K. Y., Schnappinger, D., Pethe, K., & Ehrt, S. (2010). Gluconeogenic carbon flow of tricarboxylic acid cycle intermediates is critical for *Mycobacterium tuberculosis* to establish and maintain infection. *Proc Natl Acad Sci.,* 107(21), 9819-9824.

Martinek, R. (1969). Practical clinical enzymology. *J. Am. Med. Tech.,* 31(162), 2005-2007.

Mattos-Guaraldi, A. L., Sampaio, J. L. M., Santos, C. S., Pimenta, F. P., Pereira, G. A., Pacheco, L. G. C., Miyoshi, A., Azevedo, V., Moreira, L. O., & Gutierrez, F. L. (2008). First detection of *Corynebacterium ulcerans* producing a diphtheria-like toxin in a case of human with pulmonary infection in the Rio de Janeiro metropolitan area, Brazil. *Mem Inst Oswaldo Cruz.,* 103(4), 396-400.

McNeil, M. R., Robuck, K. G., Harter, M., & Brennan, P. J. (1994). Enzymatic evidence for the presence of a critical terminal hexa-arabinoside in the cell walls of *Mycobacterium tuberculosis*. *Glycobiology,* 4(2), 165-174.

McShane, H., Pathan, A. A., Sander, C. R., Keating, S. M., Gilbert, S. C., Huygen, K., Fletcher, H. A., & Hill, A. V. S. (2004). Recombinant modified vaccinia virus Ankara expressing antigen 85A boosts BCG-primed and naturally acquired antimycobacterial immunity in humans. *Nat Med.,* 10(11), 1240.

Meena, L. S. (2010). Survival mechanisms of pathogenic *Mycobacterium tuberculosis* H37Rv. *FEBS J.,* 277(11), 2416-2427.

Meltzer, M. S., Skillman, D. R., Gomatos, P. J., Kalter, D. C., & Gendelman, H. E. (1990). Role of mononuclear phagocytes in the pathogenesis of human immunodeficiency virus infection. *Annual Rev Immu.,* 8(1), 169-194.

Menard, J. P., Mazouni, C., Salem-Cherif, I., Fenollar, F., Raoult, D., Boubli, L., Gamerre, M., & Bretelle, F. (2010). High vaginal concentrations of *Atopobium*

vaginae and *Gardnerella vaginalis* in women undergoing preterm labor. *Obstet Gynecol.,* 115(1), 134-140.

Meyer, C. G., Scarisbrick, G., Niemann, S., Browne, E. N. L., Chinbuah, M. A., Gyapong, J., Osei, I., Owusu-Dabo, E., Kubica, T., Rüsch-Gerdes, S., Thye, T., & Horstmann, R. D. (2008). Pulmonary tuberculosis: Virulence of *Mycobacterium africanum* and relevance in HIV co-infection. *Tuberculosis,* 88(5), 482-489.

Middlebrook, G., Dubos, R. J., & Pierce, C. (1947). Virulence and morphological characteristics of mammalian tubercle bacilli. *J Exp Med.,* 86(2), 175-184.

Mikušová, K., & Ekins, S. (2017). Learning from the past for TB drug discovery in the future. *Drug discov today,* 22(3), 534-545.

Minnikin, D. E., Kremer, L., Dover, L. G., & Besra, G. S. (2002). The methyl-branched fortifications of *Mycobacterium tuberculosis*. *Chem Biol.,* 9(5), 545-553.

Minnikin, D. E., Lee, O., Wu, H. H. T., Nataraj, V., Donoghue, H. D., Ridell, M., Watanabe, M., Alderwick, L. J., Bhatt, A., & Besra, G. S. (2015). Pathophysiological implications of cell envelope structure in *Mycobacterium tuberculosis* and related taxa (pp. 145-175): Intech.

Mishra, M. N., & Daniels, L. (2013). Characterization of the MSMEG_2631 gene encoding a multidrug and toxic compound extrusion (MATE) family protein in *Mycobacterium smegmatis* and exploration of its polyspecific nature using biolog phenotype microarray. *J Bacteriol.,* 195(7), 1610-1621.

Mock, D. M., & Malik, M. I. (1992). Distribution of biotin in human plasma: most of the biotin is not bound to protein. *Am J Clin Nutr.,* 56(2), 427-432.

Nam, H. C., Whiting, D., Forouhi, N., Guariguata, L., Hambleton, I., & Li, R. (2013). IDF diabetes atlas. *Inter Diabetes Fed.,* 6, 34.

Nardell, E., McInnis, B., Thomas, B., & Weidhaas, S. (1986). Exogenous reinfection with tuberculosis in a shelter for the homeless. *N Engl J Med.,* 315(25), 1570-1575.

Nathanson, E., Gupta, R. S., Huamani, P., Leimane, V., Pasechnikov, A. D., Tupasi, T. E., Vink, K., Jaramillo, E., & Espinal, M. A. (2004). Adverse events in the treatment of multidrug-resistant tuberculosis: results from the DOTS-Plus initiative. *Int J Tuberc Lung Dis.,* 8(11), 1382-1384.

Nazarova, E. V., Shleeva, M. O., Morozova, N. S., Kudykina, Y. K., Vostroknutova, G. N., Ruzhitsky, A. O., Selishcheva, A. A., Sorokoumova, G. M., Shvets, V. I., & Kaprelyants, A. S. (2011). Role of lipid components in formation and reactivation of *Mycobacterium smegmatis* “nonculturable” cells. *Biochemistry (Moscow),* 76(6), 636-644.

Nguyen, L., & Thompson, C. J. (2006). Foundations of antibiotic resistance in bacterial physiology: the mycobacterial paradigm. *Trends Microbiol.,* 14(7), 304-312.

Noordeen, S. K., Bravo, L. L., & Sundaresan, T. K. (1992). Estimated number of leprosy cases in the world. *Bull World Health Organ.,* 70(1), 7.

North, E. J., Jackson, M., & Lee, R. (2014). New approaches to target the mycolic acid biosynthesis pathway for the development of tuberculosis therapeutics. *Curr Pharm Des.,* 20(27), 4357-4378.

North, E. J., Scherman, M. S., Bruhn, D. F., Scarborough, J. S., Maddox, M. M., Jones, V., Grzegorzewicz, A. E., Yang, L., Hess, T., & Morisseau, C. (2013). Design, synthesis and anti-tuberculosis activity of 1-adamantyl-3-heteroaryl ureas with improved *in vitro* pharmacokinetic properties. *Bioorg Med Chem Lett.,* 21(9), 2587-2599.

Ogata, K., Izumi, Y., & Tani, Y. (1973). The controlling action of actithiazic acid on the biosynthesis of biotin-vitamers by various microorganisms. *Agr. Bioi. Chem.,* 37(5), 1079-1085.

Okami, Y., Kitahara, T., Hamada, M., Naganawa, H., Kondo, S., Maeda, K., Takeuchi, T., & Umezawa, H. (1974). Studies on a new amino acid antibiotic, amiclenomycin. *J Antibiot (Tokyo).* 27(9), 656-664.

Olah, G. A., & White, A. M. (2003). Stable carbonium ions. LXIX: protonation of ureas, guanidines, and biotin in super acid solution *Across Conventional Lines: Selected Papers of George A Olah Volume 1* (pp. 373-377).

Onajole, O. K., Belewa, X. V., Coovadia, Y., Govender, T., Kruger, H. G., Maguire, G. E. M., Naidu, D., Somai, B., Singh, N., & Govender, P. (2011). SQ109 analogues as potential antimicrobial candidates. *Med Chem Res.,* 20(8), 1394-1401.

Onajole, O. K., Govender, P., van Helden, P. D., Kruger, H. G., Maguire, G. E. M., Wiid, I., & Govender, T. (2010). Synthesis and evaluation of SQ109 analogues as potential anti-tuberculosis candidates. *Eur J Med Chem.,* 45(5), 2075-2079.

Oppermann, U., Filling, C., Hult, M., Shafqat, N., Wu, X., Lindh, M., Shafqat, J., Nordling, E., Kallberg, Y., & Persson, B. (2003). Short-chain dehydrogenases/reductases (SDR): the 2002 update. *Chem Biol Interact.,* 143, 247-253.

Osset, J., Martin-Casabona, N., Bellver, P., Xairó, D., & Codina, G. (1995). 289-PA12 Recurrences of tuberculosis in HIV-related patients. Period 1985–1994. *Tuber Lung Dis.,* 76, 137.

Patel, N. R., Swan, K., Li, X., Tachado, S. D., & Koziel, H. (2009). Impaired *M. tuberculosis*-mediated apoptosis in alveolar macrophages from HIV+ persons: potential role of IL-10 and BCL-3. *J Leukoc Biol.,* 86(1), 53-60.

Patterson, J. H., Waller, R. F., Jeevarajah, D., Billman-Jacobe, H., & McConville, M. J. (2003). Mannose metabolism is required for mycobacterial growth. *Biochem J.,* 372(1), 77-86.

Paulsen, I. T., Brown, M. H., & Skurray, R. A. (1996). Proton-dependent multidrug efflux systems. *Microbiol. Mol. Biol. Rev.,* 60(4), 575-608.

Pendini, N. R., Bailey, L. M., Booker, G. W., Wilce, M. C., Wallace, J. C., & Polyak, S. W. (2008). Microbial biotin protein ligases aid in understanding holocarboxylase synthetase deficiency. *Biochim Biophys Acta.,* 1784(7-8), 973-982.

Peränen, J., Rikkonen, M., Hyvönen, M., & Kääriäinen, L. (1996). T7 vectors with a modified T7lac promoter for expression of proteins in *Escherichia coli*. *Anal biochem.,* 236(2), 371-373.

Petit, J. F., Adam, A., Wietzerbin-Falszpan, J., Lederer, E., & Ghuysen, J. (1969). Chemical structure of the cell wall of *Mycobacterium smegmatis*. I—Isolation and partial characterization of the peptidoglycan. *Biochem Biophys Res Commun.,* 35(4), 478-485.

Pfeiffer, J. (1954). *Enzymes, the physics and chemistry of life*: Simon & Schuster, New York.

Phetsuksiri, B., Baulard, A. R., Cooper, A. M., Minnikin, D. E., Douglas, J. D., Besra, G. S., & Brennan, P. J. (1999). Antimycobacterial activities of isoxyl and new derivatives through the inhibition of mycolic acid synthesis. *Antimicrob Agents Chemother.,* 43(5), 1042-1051.

Phetsuksiri, B., Jackson, M., Scherman, H., McNeil, M., Besra, G. S., Baulard, A. R., Slayden, R. A., DeBarber, A. E., Barry, C. E., & Baird, M. S. (2003). Unique mechanism of action of the thiourea drug isoxyl on *Mycobacterium tuberculosis*. *J Biol Chem.,* 278(52), 53123-53130.

Phillips, T. A., VanBogelen, R. A., & Neidhardt, F. C. (1984). *lon* gene product of *Escherichia coli* is a heat-shock protein. *J Bacteriol.,* 159(1), 283-287.

Phunpruch, S., Warit, S., Suksamran, R., Billamas, P., Jaitrong, S., Palittapongarnpim, P., & Prammananan, T. (2013). A role for 16S rRNA dimethyltransferase (*ksgA*) in intrinsic clarithromycin resistance in *Mycobacterium tuberculosis*. *Int J Antimicrob Agents.,* 41(6), 548-551.

Pisabarro, A. G., Prats, R., Vaquez, D., & Rodríguez-Tébar, A. (1986). Activity of penicillin-binding protein 3 from *Escherichia coli*. *J Bacteriol.,* 168(1), 199-206.

Pitzer, K. S. (1960). The nature of the chemical bond and the structure of molecules and crystals: an introduction to modern structural chemistry. *J. Am. Chem. Soc.,* 82(15), 4121-4121.

Ploux, O., Soularue, P., Marquet, A., Gloeckler, R., & Lemoine, Y. (1992). "Investigation of the first step of biotin biosynthesis in *Bacillus sphaericus*. Purification and characterization of the pimeloyl-CoA synthase, and uptake of pimelate." *Biochem J.* 287(3): 685-690.

Polyak, S. W., Chapman-Smith, A., Mulhern, T. D., Cronan, J. E., & Wallace, J. C. (2001). Mutational analysis of protein substrate presentation in the post-translational attachment of biotin to biotin domains. *J Biol Chem.*, 276(5), 3037-3045.

Portevin, D., de Sousa-D'Auria, C., Montrozier, H., Houssin, C., Stella, A., Lanéelle, M., Bardou, F., Guilhot, C., & Daffé, M. (2005). The Acyl-AMP ligase FadD32 and AccD4-containing acyl-CoA carboxylase are required for the yynthesis of mycolic acids and essential for mycobacterial growth Identification of the carboxylation product and determination of the acyl-Coa carboxylase components. *J Biol Chem.*, 280(10), 8862-8874.

Prescott, J. F. (1991). *Rhodococcus equi*: an animal and human pathogen. *Clin Microbiol Rev.*, 4(1), 20-34.

Protopopova, M., Hanrahan, C., Nikonenko, B., Samala, R., Chen, P., Gearhart, J., Einck, L., & Nacy, C. A. (2005). Identification of a new antitubercular drug candidate, SQ109, from a combinatorial library of 1, 2-ethylenediamines. *J Antimicrob Chemother.*, 56(5), 968-974.

Puech, V., Chami, M., Lemassu, A., Lanéelle, M., Schiffler, B., Gounon, P., Bayan, N., Benz, R., & Daffé, M. (2001). Structure of the cell envelope of corynebacteria: importance of the non-covalently bound lipids in the formation of the cell wall permeability barrier and fracture plane. *Microbiology*, 147(5), 1365-1382.

Purushothaman, S., Gupta, G., Srivastava, R., Ramu, V. G., & Surolia, A. (2008). Ligand specificity of group I biotin protein ligase of *Mycobacterium tuberculosis*. *PLoS ONE*, 3(5), e2320.

Ramos, J. L., Martínez-Bueno, M., Molina-Henares, A. J., Terán, W., Watanabe, K., Zhang, X., Gallegos, M. T., Brennan, R., & Tobes, R. (2005). The TetR family of transcriptional repressors. *Microbiol Mol Biol Rev.*, 69(2), 326-356.

Raoult, D., La Scola, B., Lecocq, P., Lepidi, H., & Fournier, P. (2001). Culture and immunological detection of *Tropheryma whippelii* from the duodenum of a patient with Whipple disease. *JAMA.*, 285(8), 1039-1043.

Rath, P., Saurel, O., Czaplicki, G., Tropis, M., Daffé, M., Ghazi, A., Demange, P., & Milon, A. (2013). Cord factor (trehalose 6, 6′-dimycolate) forms fully stable and non-permeable lipid bilayers required for a functional outer membrane. *Biochim Biophys Acta.*, 1828(9), 2173-2181.

Ravi, A., & Sunita, S. D. (2013). Global Tuberculosis Report 2012. *Australasian Med J.*, 6(2), 94.

Ray, A., Cot, M., Puzo, G., Gilleron, M., & Nigou, J. (2013). Bacterial cell wall macroamphiphiles: pathogen-/microbe-associated molecular patterns detected by mammalian innate immune system. *Biochimie*, 95(1), 33-42.

Raymond, J. B., Mahapatra, S., Crick, D. C., & Pavelka, M. S. (2005). Identification of the *namH* gene, encoding the hydroxylase responsible for the N-glycolylation of the mycobacterial peptidoglycan. *J Biol Chem.,* 280(1), 326-333.

Reed, M. B., Domenech, P., Manca, C., Su, H., Barczak, A. K., Kreiswirth, B. N., Kaplan, G., & Barry, C. E. (2004). A glycolipid of hypervirulent tuberculosis strains that inhibits the innate immune response. *Nature,* 431(7004), 84.

Reibel, F., Cambau, E., & Aubry, A. (2015). Update on the epidemiology, diagnosis, and treatment of leprosy. *Med Mal Infect.,* 45(9), 383-393.

Reich, N. O., & Mashhoon, N. (1990). Inhibition of *Eco*RI DNA methylase with cofactor analogs. *J Biol Chem.,* 265(15), 8966-8970.

Reyda, M. R., Fugate, C. J., & Jarrett, J. T. (2009). A complex between biotin synthase and the iron− sulfur cluster assembly chaperone HscA that enhances *in vivo* cluster assembly. *Biochemistry,* 48(45), 10782-10792.

Rezwan, M., Grau, T., Tschumi, A., & Sander, P. (2007). Lipoprotein synthesis in mycobacteria. *Microbiology,* 153(3), 652-658.

Ribeiro, M. G., Salerno, T., Mattos-Guaraldi, A. L., Camello, T. C. F., Langoni, H., Siqueira, A. K., Paes, A. C., Fernandes, M. C., & Lara, G. H. B. (2008). Nocardiosis: an overview and additional report of 28 cases in cattle and dogs. *Revista do Instituto de Medicina Tropical de São Paulo,* 50(3), 177-185.

Rodionov, D. A., Hebbeln, P., Eudes, A., Ter Beek, J., Rodionova, I. A., Erkens, G. B., Slotboom, D. J., Gelfand, M. S., Osterman, A. L., & Hanson, A. D. (2009). A novel class of modular transporters for vitamins in prokaryotes. *J Bacteriol.,* 191(1), 42-51.

Rodionov, D. A., Mironov, A. A., & Gelfand, M. S. (2002). Conservation of the biotin regulon and the BirA regulatory signal in Eubacteria and Archaea. *Genome Res.,* 12(10), 1507-1516.

Rodrigues, L. C., Diwan, V. K., & Wheeler, J. G. (1993). Protective effect of BCG against tuberculous meningitis and miliary tuberculosis: a meta-analysis. *Int J Epidemiol.,* 22(6), 1154-1158.

Rodrigues, L. C., Mangtani, P., & Abubakar, I. (2011). How does the level of BCG vaccine protection against tuberculosis fall over time? *BMJ.,* 343, d5974.

Rohrer, D. C., Duax, W. L., & Wolff, M. E. (1979). Conformational analysis of synthetic androgens. IV. 1, 2-seco-A-bisnor-5α-androstan-17β-ol acetate. *Steroids,* 34(5), 589-595.

Roje, S. (2006). S-Adenosyl-L-methionine: beyond the universal methyl group donor. *Phytochemistry,* 67(15), 1686-1698.

Rückert, C., Albersmeier, A., Winkler, A., & Tauch, A. (2015). Complete genome sequence of *Corynebacterium kutscheri* DSM 20755, a corynebacterial type strain with remarkably low G+C content of chromosomal DNA. *Genome Announc.,* 3(3), e00571-00515.

Russell, D. G. (2004). Types of antibiotics and synthetic antimicrobial agents. *Hugo and Russell's,* 152.

Russell, D. G. (2007). Who puts the tubercle in tuberculosis? *Nature Rev Microbiol.,* 5(1), 39.

Russell, D. G., Barry, C. E., & Flynn, J. L. (2010). Tuberculosis: what we don't know can, and does, hurt us. *Science,* 328(5980), 852-856.

Sacksteder, K. A., Protopopova, M., Barry, C. E., Andries, K., & Nacy, C. A. (2012). Discovery and development of SQ109: a new antitubercular drug with a novel mechanism of action. *Future Microbiol.,* 7(7), 823-837.

Said, H. M. (2008). Cell and molecular aspects of human intestinal biotin absorption. *J Nutr.,* 139(1), 158-162.

Saier, M. H., Paulsen, I. T., Sliwinski, M. K., Pao, S. S., Skurray, R. A., & Nikaido, H. (1998). Evolutionary origins of multidrug and drug-specific efflux pumps in bacteria. *FASEB J.,* 12(3), 265-274.

Saitoh, T., Yano, I., Kumazawa, Y., & Takimoto, H. (2012). Pulmonary TCR γδ T cells induce the early inflammation of granuloma formation by a glycolipid trehalose 6, 6′-dimycolate (TDM) isolated from *Mycobacterium tuberculosis*. *Immunopharmacol Immunotoxicol.,* 34(5), 815-823.

Salaemae, W., Azhar, A., Booker, G. W., & Polyak, S. W. (2011). Biotin biosynthesis in *Mycobacterium tuberculosis*: physiology, biochemistry and molecular intervention. *Protein Cell,* 2(9), 691-695.

Salem, M., Heydel, C., El-Sayed, A., Ahmed, S. A., Zschöck, M., & Baljer, G. (2013). *Mycobacterium avium* subspecies *paratuberculosis:* an insidious problem for the ruminant industry. *Trop Anim Health Prod.,* 45(2), 351-366.

Sandalova, T., Schneider, G., Käck, H., & Lindqvist, Y. (1999). Structure of dethiobiotin synthetase at 0.97 Å resolution. *Acta Crystallogr D Biol Crystallogr.,* 55(3), 610-624.

Sander, P., De Rossi, E., Böddinghaus, B., Cantoni, R., Branzoni, M., Böttger, E. C., Takiff, H., Rodriquez, R., Lopez, G., & Riccardi, G. (2000). Contribution of the multidrug efflux pump LfrA to innate mycobacterial drug resistance. *FEMS Microbiol Lett.,* 193(1), 19-23.

Sandmark, J., Mann, S., Marquet, A., & Schneider, G. (2002). Structural basis for the inhibition of the biosynthesis of biotin by the antibiotic amiclenomycin. *J Biol Chem.,* 277(45), 43352-43358.

Sanishvili, R., Yakunin, A. F., Laskowski, R. A., Skarina, T., Evdokimova, E., Doherty-Kirby, A., Lajoie, G. A., Thornton, J. M., Arrowsmith, C. H., & Savchenko, A. (2003). Integrating structure, bioinformatics and enzymology to discover function: BioH, a new carboxylesterase from *E. coli*. *J Biol Chem.*, 278(28), 26039-26045.

Sanyal, I., Lee, S. L., & Flint, D. H. (1994). Biosynthesis of pimeloyl-CoA, a biotin precursor in *Escherichia-coli*, follows a modified fatty-acid synthesis pathway ^{13}C-labeling studies. *J. Am. Chem. Soc.*, 116(6), 2637-2638.

Sasindran, S. J., & Torrelles, J. B. (2011). *Mycobacterium tuberculosis* infection and inflammation: what is beneficial for the host and for the bacterium? *Front Microbiol.*, 2(2), 1-16.

Sassetti, C. M., Boyd, D. H., & Rubin, E. J. (2003). Genes required for mycobacterial growth defined by high density mutagenesis. *Molecular Microbiol.*, 48(1), 77-84.

Saunders, B. M., & Cooper, A. M. (2000). Restraining mycobacteria: role of granulomas in mycobacterial infections. *Immunol Cell Biol.*, 78(4), 334-341.

Saxena, D., Aouad, S., Attieh, J., & Saini, H. S. (1998). Biochemical characterization of chloromethane emission from the wood-rotting fungus *Phellinus pomaceus*. *Appl Environ Microbiol.*, 64(8), 2831-2835.

Scherman, M. S., North, E. J., Jones, V., Hess, T. N., Grzegorzewicz, A. E., Kasagami, T., Kim, I., Merzlikin, O., Lenaerts, J., & Lee, R. E. (2012). Screening a library of 1600 adamantyl ureas for anti-*Mycobacterium tuberculosis* activity *in vitro* and for better physical chemical properties for bioavailability. *Bioorg Med Chem.*, 20(10), 3255-3262.

Schmalstieg, A. M., Srivastava, S., Belkaya, S., Deshpande, D., Meek, C., Leff, R., van Oers, N. S. C., & Gumbo, T. (2012). The antibiotic resistance arrow of time: efflux pump induction is a general first step in the evolution of mycobacterial drug resistance. *Antimicrob Agents Chemother.*, 56(9), 4806-4815.

Schneider, J., Peters-Wendisch, P., Stansen, K. C., Götker, S., Maximow, S., Krämer, R., & Wendisch, V. F. (2012). Characterization of the biotin uptake system encoded by the biotin-inducible *bioYMN* operon of *Corynebacterium glutamicum*. *BMC Microbiol.*, 12(1), 6.

Schroeder, E. K., de Souza, O. N., Santos, D. S., Blanchard, J. S., & Basso, L. A. (2002). Drugs that inhibit mycolic acid biosynthesis in *Mycobacterium tuberculosis*. *Curr Pharm Biotechnol.*, 3(3), 197-225.

Shafer, R. W., Singh, S. P., Larkin, C., & Small, P. M. (1995). Exogenous reinfection with multidrug-resistant *Mycobacterium tuberculosis* in an immunocompetent patient. *Tuber Lung Dis.*, 76(6), 575-577.

Shah, N. S., Wright, A., Bai, G., Barrera, L., Boulahbal, F., Martín-Casabona, N., Drobniewski, F., Gilpin, C., Havelková, M., & Lepe, R. (2007). Worldwide emergence of extensively drug-resistant tuberculosis. *Emerging Infect Dis.,* 13(3), 380.

Sinsimer, D., Huet, G., Manca, C., Tsenova, L., Koo, M., Kurepina, N., Kana, B. D., Mathema, B., Marras, S. A. E., & Kreiswirth, B. N. (2008). The phenolic glycolipid of *Mycobacterium tuberculosis* differentially modulates the early host cytokine response but does not in itself confer hypervirulence. *Infect Immun.,* 76(7), 3027-3036.

Sleno, L., & Emili, A. (2008). Proteomic methods for drug target discovery. *Curr Opin Chem Biol.,* 12(1), 46-54.

Small, P. M., Shafer, R. W., Hopewell, P. C., Singh, S. P., Murphy, M. J., Desmond, E., Sierra, M. F., & Schoolnik, G. K. (1993). Exogenous reinfection with multidrug-resistant *Mycobacterium tuberculosis* in patients with advanced HIV infection. *N Engl J Med.,* 328(16), 1137-1144.

Sonnenberg, P., Murray, J., Glynn, J. R., Shearer, S., Kambashi, B., & Godfrey-Faussett, P. (2001). HIV-1 and recurrence, relapse, and reinfection of tuberculosis after cure: a cohort study in South African mineworkers. *Lancet,* 358(9294), 1687-1693.

Sørensen, A. L., Nagai, S., Houen, G., Andersen, P., & Andersen, A. B. (1995). Purification and characterization of a low-molecular-mass T-cell antigen secreted by *Mycobacterium tuberculosis*. *Infect Immun.,* 63(5), 1710-1717.

Sternicki, L. M., Wegener, K. L., Bruning, J. B., Booker, G. W., & Polyak, S. W. (2017). Mechanisms governing precise protein biotinylation. *Trends Biochem Sci.,* 42(5), 383-394.

Stok, J. E., & De Voss, J. (2000). Expression, purification, and characterization of BioI: a carbon-carbon bond cleaving cytochrome P450 involved in biotin biosynthesis in *Bacillus subtilis*. *Arch Biochem Biophys.,* 384(2), 351-360.

Stoop, E. J. M., Mishra, A. K., Driessen, N. N., Stempvoort, G., Bouchier, P., Verboom, T., Leeuwen, L. M., Sparrius, M., Raadsen, S. A., & Zon, M. (2013). Mannan core branching of lipo (arabino) mannan is required for mycobacterial virulence in the context of innate immunity. *Cell Microbiol.,* 15(12), 2093-2108.

Strzelczyk, A. A., Dobrowolski, J. C., & Mazurek, A. P. (2001). On the conformation of the biotin molecule. *J Mol Struct.,* 541(1-3), 283-290.

Sullivan, T., & Amor, Y. B. (2016). Global introduction of new multidrug-resistant tuberculosis drugs—balancing regulation with urgent patient needs. *Emerg Infect Dis.,* 22(3).

Sutcliffe, I. C. (2010). A phylum level perspective on bacterial cell envelope architecture. *Trends Microbiol.,* 18(10), 464-470.

Tahlan, K., Wilson, R., Kastrinsky, D. B., Arora, K., Nair, V., Fischer, E., Barnes, S. W., Walker, J. R., Alland, D., & Barry, C. E. (2012). SQ109 targets MmpL3, a membrane transporter of trehalose monomycolate involved in mycolic acid donation to the cell wall core of *Mycobacterium tuberculosis*. *Antimicrob Agents Chemother.,* 56(4), 1797-1809.

Takayama, K., Wang, C., & Besra, G. S. (2005). Pathway to synthesis and processing of mycolic acids in *Mycobacterium tuberculosis*. *Clin Microbiol Rev.,* 18(1), 81-101.

Tang, Q., Li, X., Zou, T., Zhang, H., Wang, Y., Gao, R., Li, Z., He, J., & Feng, Y. (2014). *Mycobacterium smegmatis* BioQ defines a new regulatory network for biotin metabolism. *Mol Microbiol.,* 94(5), 1006-1023.

Tekaia, F., et al. (1999). Analysis of the proteome of Mycobacterium tuberculosis in silico. *Tuber Lung Dis*. 79(6): 329-342.

Thomas, D. J., Waters, S. B., & Styblo, M. (2004). Elucidating the pathway for arsenic methylation. *Toxicol Appl Pharmacol.,* 198(3), 319-326.

Tong, L. (2013). Structure and function of biotin-dependent carboxylases. *Cell Mol Life Sci.,* 70(5), 863-891.

Trotter, J., & Hamilton, J. A. (1966). The absolute configuration of biotin. *Biochemistry,* 5(2), 713-714.

Tsenova, L., Ellison, E., Harbacheuski, R., Moreira, A. L., Kurepina, N., Reed, M. B., Mathema, B., Barry, C. E., & Kaplan, G. (2005). Virulence of selected *Mycobacterium tuberculosis* clinical isolates in the rabbit model of meningitis is dependent on phenolic glycolipid produced by the bacilli. *J Infect Dis.,* 192(1), 98-106.

Turner, J. (2011). Growing old and immunity to bacteria *The Immune Response to Infection* (pp. 413-423): American Society of Microbiology.

Ugulava, N. B., Sacanell, C. J., & Jarrett, J. T. (2001). Spectroscopic changes during a single turnover of biotin synthase: destruction of a [2Fe-2S] cluster accompanies sulfur insertion. *Biochemistry,* 40(28), 8352-8358.

Ulrichs, T., & Kaufmann, S. H. E. (2006). New insights into the function of granulomas in human tuberculosis. *J Pathol.,* 208(2), 261-269.

Ulrichs, T., Kosmiadi, G. A., Jörg, S., Pradl, L., Titukhina, M., Mishenko, V., Gushina, N., & Kaufmann, S. H. E. (2005). Differential organization of the local immune response in patients with active cavitary tuberculosis or with nonprogressive tuberculoma. *J Infect Dis.,* 192(1), 89-97.

Van Pinxteren, L. A. H., Ravn, P., Agger, E. M., Pollock, J., & Andersen, P. (2000). Diagnosis of tuberculosis based on the two specific antigens ESAT-6 and CFP10. *Clin Diagn Lab Immunol.,* 7(2), 155-160.

van Pittius, N. C. G., Gamieldien, J., Hide, W., Brown, G. D., Siezen, R. J., & Beyers, A. D. (2001). The ESAT-6 gene cluster of *Mycobacterium tuberculosis* and other high G+C Gram-positive bacteria. *Genome Biol.,* 2(10), 1-18.

Vandal, O. H., Roberts, J. A., Odaira, T., Schnappinger, D., Nathan, C. F., & Ehrt, S. (2009). Acid-susceptible mutants of *Mycobacterium tuberculosis* share hypersusceptibility to cell wall and oxidative stress and to the host environment. *J Bacteriol.,* 191(2), 625-631.

Vashishtha, A. K., Wang, J., & Konigsberg, W. H. (2016). Different divalent cations alter the kinetics and fidelity of DNA polymerases. *J Biol Chem.,* 291(40), 20869-20875.

Velappan, A. B., Raja, M. R. C., Datta, D., Tsai, Y. T., Halloum, I., Wan, B., Kremer, L., Gramajo, H., Franzblau, S. G., & Mahapatra, S. K. (2017). Attenuation of *Mycobacterium* species through direct and macrophage mediated pathway by unsymmetrical diaryl urea. *Eur J Med Chem.,* 125, 825-841.

Velayati, A. A., Masjedi, M. R., Farnia, P., Tabarsi, P., Ghanavi, J., ZiaZarifi, A. H., & Hoffner, S. E. (2009). Emergence of new forms of totally drug-resistant tuberculosis bacilli: super extensively drug-resistant tuberculosis or totally drug-resistant strains in Iran. *Chest,* 136(2), 420-425.

Verbelen, C., Christiaens, N., Alsteens, D., Dupres, V., Baulard, A. R., & Dufrêne, Y. F. (2009). Molecular mapping of lipoarabinomannans on mycobacteria. *Langmuir.,* 25(8), 4324-4327.

Vergne, I., & Daffé, M. (1998). Interaction of mycobacterial glycolipids with host cells. *Front Biosci.,* 3, 865-876.

Verschoor, J. A., Baird, M. S., & Grooten, J. (2012). Towards understanding the functional diversity of cell wall mycolic acids of *Mycobacterium tuberculosis*. *Prog Lipid Res.,* 51(4), 325-339.

Waddell, T. G., Eilders, L. L., Patel, B. P., & Sims, M. (2000). Prebiotic methylation and the evolution of methyl transfer reactions in living cells. *Orig Life Evol Biosph.,* 30(6), 539-548.

Wang, C., & Hickey, A. J. (2010). Isoxyl aerosols for tuberculosis treatment: preparation and characterization of particles. *AAPS PharmSciTech.,* 11(2), 538-549.

Wang, J., Thorson, L., Stokes, R. W., Santosuosso, M., Huygen, K., Zganiacz, A., Hitt, M., & Xing, Z. (2004). Single mucosal, but not parenteral, immunization with recombinant adenoviral-based vaccine provides potent protection from pulmonary tuberculosis. *J Immunol.,* 173(10), 6357-6365.

Wanka, L., Iqbal, K., & Schreiner, P. R. (2013). The lipophilic bullet hits the targets: medicinal chemistry of adamantane derivatives. *Chem Rev.,* 113(5), 3516-3604.

Watve, M. G., Tickoo, R., Jog, M. M., & Bhole, B. D. (2001). How many antibiotics are produced by the genus *Streptomyces*? *Arch Microbiol.,* 176(5), 386-390.

Whalen, C. C., Zalwango, S., Chiunda, A., Malone, L., Eisenach, K., Joloba, M., Boom, W. H., & Mugerwa, R. (2011). Secondary attack rate of tuberculosis in urban households in Kampala, Uganda. *PloS ONE,* 6(2), e16137.

Wheatley, P. J. (1953). The structure of ethylenethiourea. *Acta Cryst.,* 6(5), 369-377.

White, S. W., Zheng, J., Zhang, Y., & Rock, C. O. (2005). The structural biology of type II fatty acid biosynthesis. *Annu. Rev. Biochem.,* 74, 791-831.

Whitman, W. B., Goodfellow, M., & Kämpfer, P. (2012). *Bergey's manual of systematic bacteriology: The Actinobacteria* (Vol. 5): Springer New York.

WHO. (2009). World Health Organization: Rapid advice: antiretroviral therapy for HIV infection in adults and adolescents-November 2009. 1-28.

WHO. (2013). World Health Organization: Global tuberculosis report 2013. 1-289.

WHO. (2016). World Health Organization: Global tuberculosis report 2016. 1-214.

WHO. (2017). World Health Organization: Global tuberculosis report 2017. 1-147.

WHO. (2018). World Health Organization: Global tuberculosis report 2018. 1-277.

Williams, S., Goodfellow, M., Alderson, G., Wellington, E., Sneath, P., & Sackin, M. (1983). Numerical classification of streptomyces and related genera. *Microbiology,* 129(6), 1743-1813.

Winder, F. G., Collins, P. B., & Whelan, D. (1971). Effects of ethionamide and isoxyl on mycolic acid synthesis in *Mycobacterium tuberculosis* BCG. *J Gen Microbiol.,* 66(3), 379-380.

Wirth, T., Hildebrand, F., Allix-Béguec, C., Wölbeling, F., Kubica, T., Kremer, K., van Soolingen, D., Rüsch-Gerdes, S., Locht, C., & Brisse, S. (2008). Origin, spread and demography of the *Mycobacterium tuberculosis* complex. *PLoS Pathog.,* 4(9), e1000160.

Wolucka, B. A., McNeil, M. R., de Hoffmann, E., Chojnacki, T., & Brennan, P. J. (1994). Recognition of the lipid intermediate for arabinogalactan/arabinomannan biosynthesis and its relation to the mode of action of ethambutol on mycobacteria. *J Biol Chem.,* 269(37), 23328-23335.

Wuosmaa, A. M., & Hager, L. P. (1990). Methyl chloride transferase: a carbocation route for biosynthesis of halometabolites. *Science,* 249(4965), 160-162.

Xu, Z., Meshcheryakov, V. A., Poce, G., & Chng, S. (2017). MmpL3 is the flippase for mycolic acids in mycobacteria. *Proc Natl Acad Sci.,* 114(30), 7993-7998.

Yamada, H., Bhatt, A., Danev, R., Fujiwara, N., Maeda, S., Mitarai, S., Chikamatsu, K., Aono, A., Nitta, K., & Jacobs, W. R. (2012). Non-acid-fastness in *Mycobacterium tuberculosis ΔkasB* mutant correlates with the cell envelope electron density. *Tuberculosis,* 92(4), 351-357.

Yang, Y., Shi, F., Tao, G., & Wang, X. (2012). Purification and structure analysis of mycolic acids in *Corynebacterium glutamicum*. *J Microbiol.,* 50(2), 235-240.

Yu, J., Niu, C., Wang, D., Li, M., Teo, W., Sun, G., Wang, J., Liu, J., & Gao, Q. (2011). MMAR_2770, a new enzyme involved in biotin biosynthesis, is essential for the growth of *Mycobacterium marinum* in macrophages and zebrafish. *Microbes Infect.,* 13(1), 33-41.

Yuan, Y., Lee, R. E., Besra, G. S., Belisle, J. T., & Barry, C. E. (1995). Identification of a gene involved in the biosynthesis of cyclopropanated mycolic acids in *Mycobacterium tuberculosis*. *Proc Natl Acad Sci.,* 92(14), 6630-6634.

Yuan, Y., Zhu, Y., Crane, D. D., & Barry, C. E. (1998). The effect of oxygenated mycolic acid composition on cell wall function and macrophage growth in *Mycobacterium tuberculosis*. *Mol Microbiol.,* 29(6), 1449-1458.

Zachariah, R., Bemelmans, M., Akesson, A., Gomani, P., Phiri, K., Isake, B., Van den Akker, T., Philips, M., Mwale, A., & Gausi, F. (2011). Reduced tuberculosis case notification associated with scaling up antiretroviral treatment in rural Malawi. *Int J Tuberc Lung Dis.,* 15(7), 933-937.

Zeng, S., Liu, H., Shi, T., Song, P., Ren, L., Huang, H., & Ji, X. (2018). Recent advances in metabolic engineering of *Yarrowia lipolytica* for lipid overproduction. *Eur. J. Lipid Sci. Technol.,* 120(3), 1700352.

Zhang, L., Goren, M. B., Holzer, T. J., & Andersen, B. R. (1988). Effect of *Mycobacterium tuberculosis*-derived sulfolipid I on human phagocytic cells. *Infect Immun.,* 56(11), 2876-2883.

Zhang, L., Li, H., Hu, X., & Han, S. (2006). 1-NH proton of biotin is not always more active than 3-NH proton. *Chem Phy Lett.,* 421(4-6), 334-337.

Zhi, X., Li, W., & Stackebrandt, E. (2009). An update of the structure and 16S rRNA gene sequence-based definition of higher ranks of the class Actinobacteria, with the proposal of two new suborders and four new families and emended descriptions of the existing higher taxa. *Int J Syst Evol Microbiol.,* 59(3), 589-608.

Zink, A., Reischl, U., Wolf, H., Nerlich, A., & Miller, R. (2001). *Corynebacterium* in ancient Egypt. *Medical His.,* 45(2), 267-272.

Zuber, B., Chami, M., Houssin, C., Dubochet, J., Griffiths, G., & Daffé, M. (2008). Direct visualization of the outer membrane of mycobacteria and corynebacteria in their native state. *J Bacteriol.,* 190(16), 5672-5680.

Zumla, A., Nahid, P., & Cole, S. T. (2013). Advances in the development of new tuberculosis drugs and treatment regimens. *Nat Rev Drug Discov.*, 12(5), 388.

Appendices

8 Appendices

8.1 ^{13}C NMR SPECTRUM (100 MHZ; CDCL3) of JJH-017A

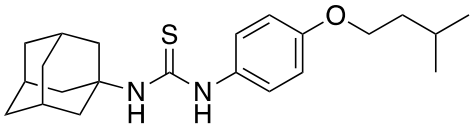

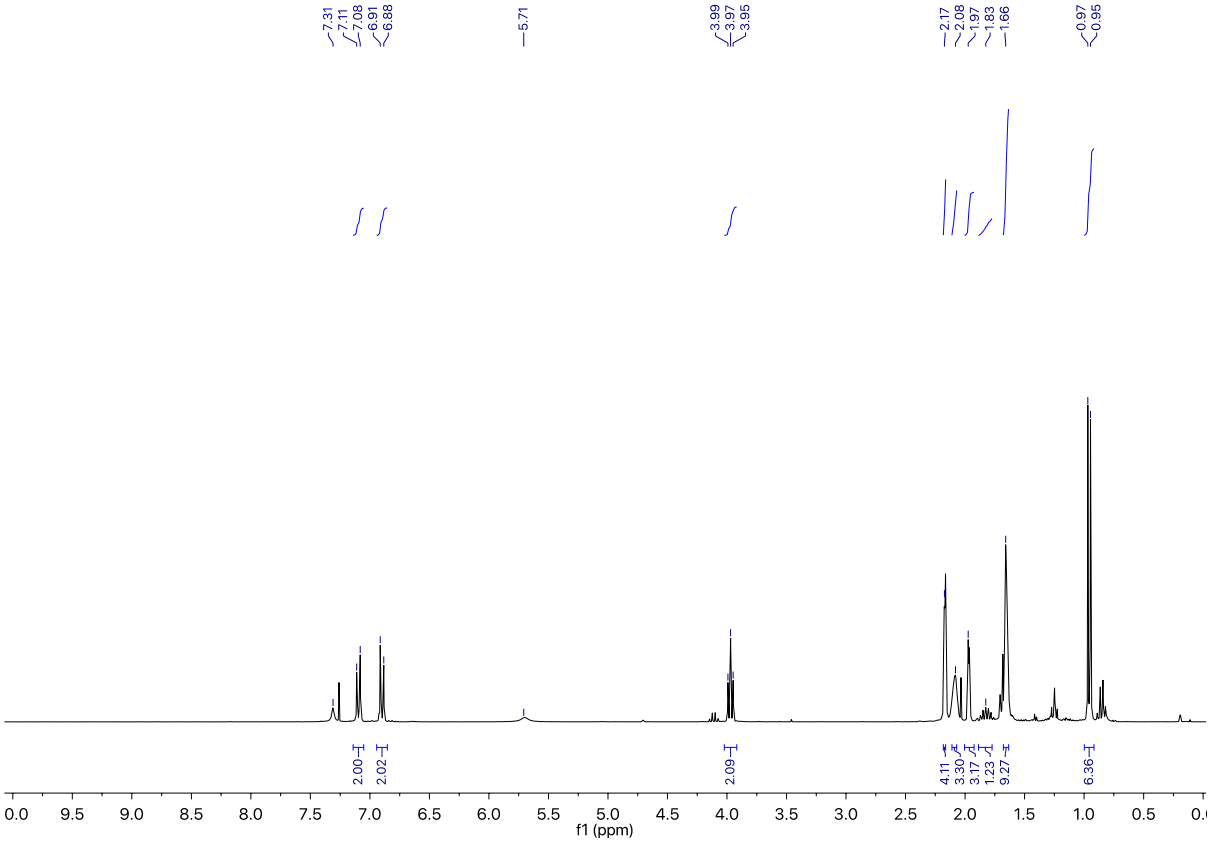

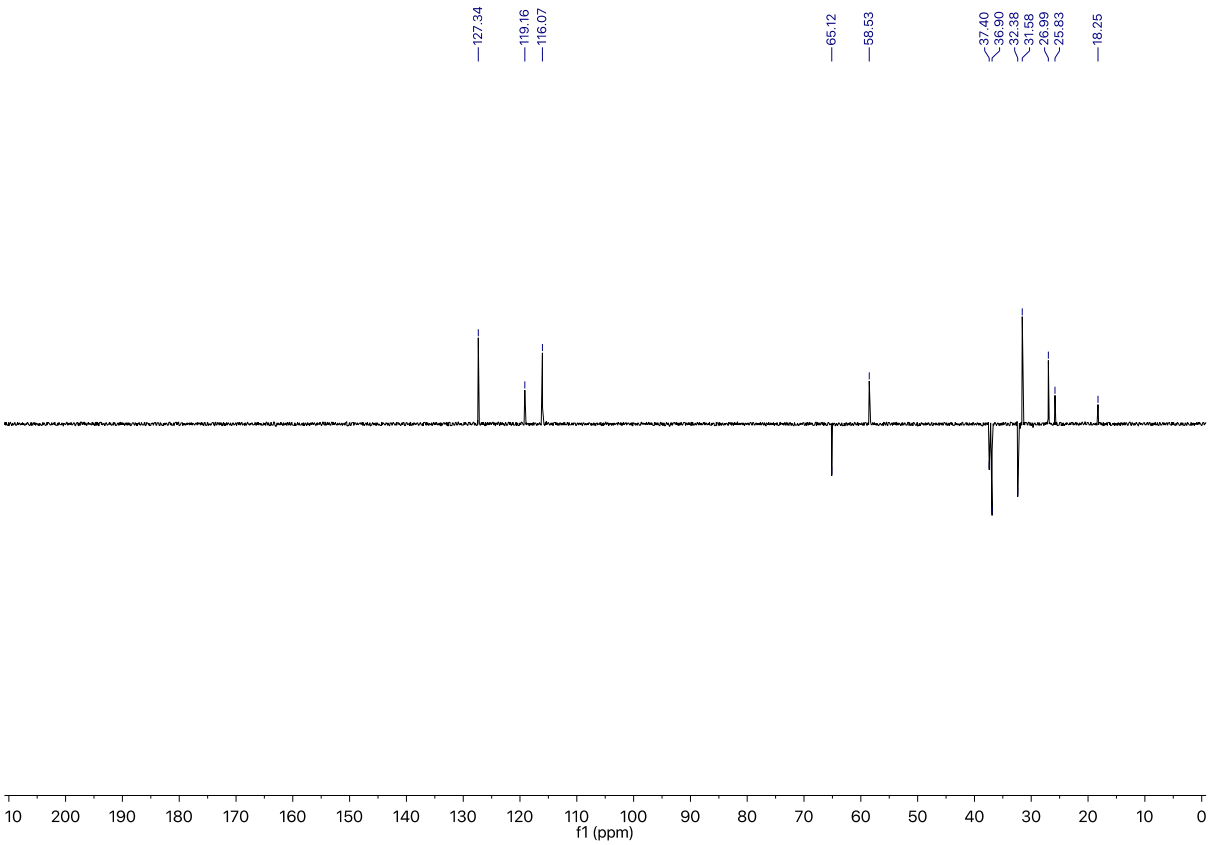
127.34
119.16
116.07
65.12
58.53
37.40
36.90
32.38
31.58
26.99
25.83
18.25
10 200 190 180 170 160 150 140 130 120 110 100 90 80 70 60 50 40 30 20 10 0
f1 (ppm)

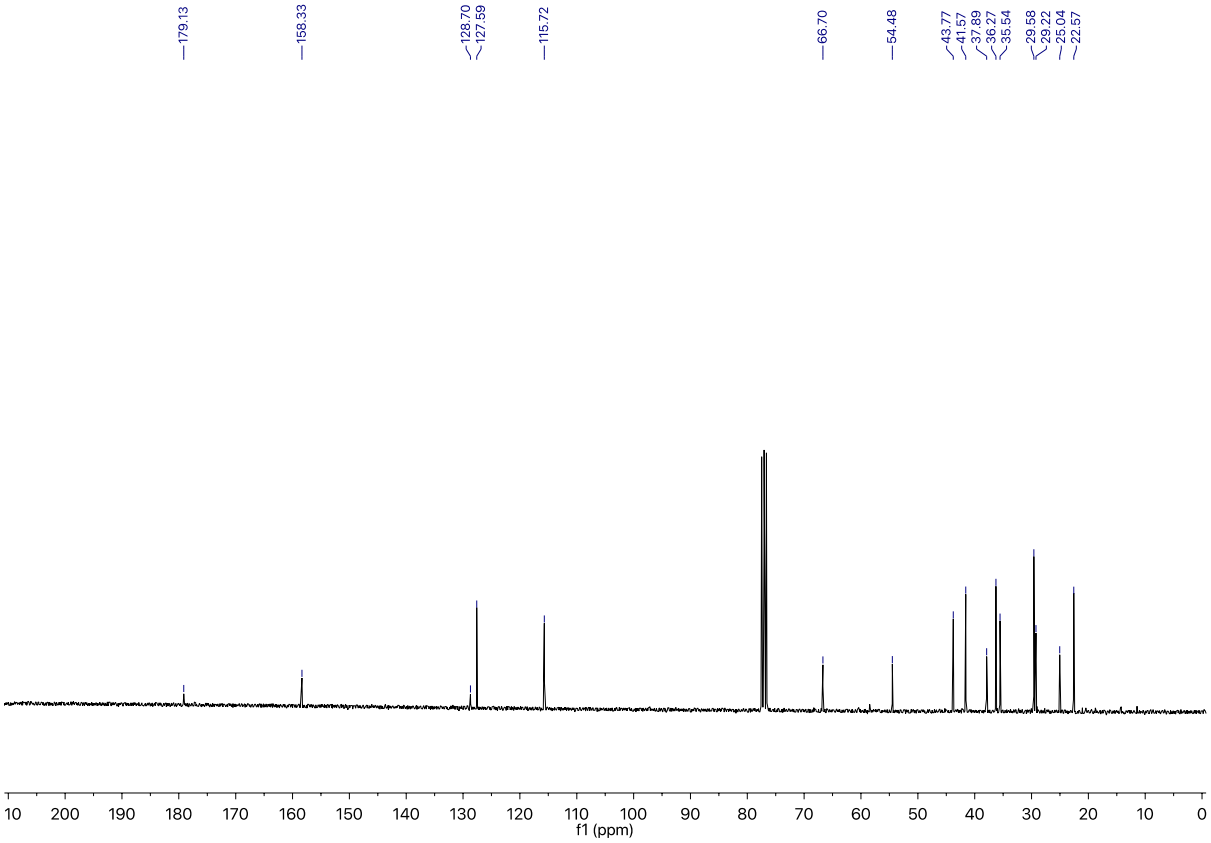
179.13
158.33
128.70
127.59
115.72
66.70
54.48
43.77
41.57
37.89
36.27
35.54
29.58
29.22
25.04
22.57
10 200 190 180 170 160 150 140 130 120 110 100 90 80 70 60 50 40 30 20 10 0
f1 (ppm)

8.2 ^{13}C NMR SPECTRUM (100 MHZ; CDCL3) of JJH-III-110A

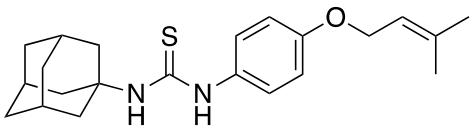

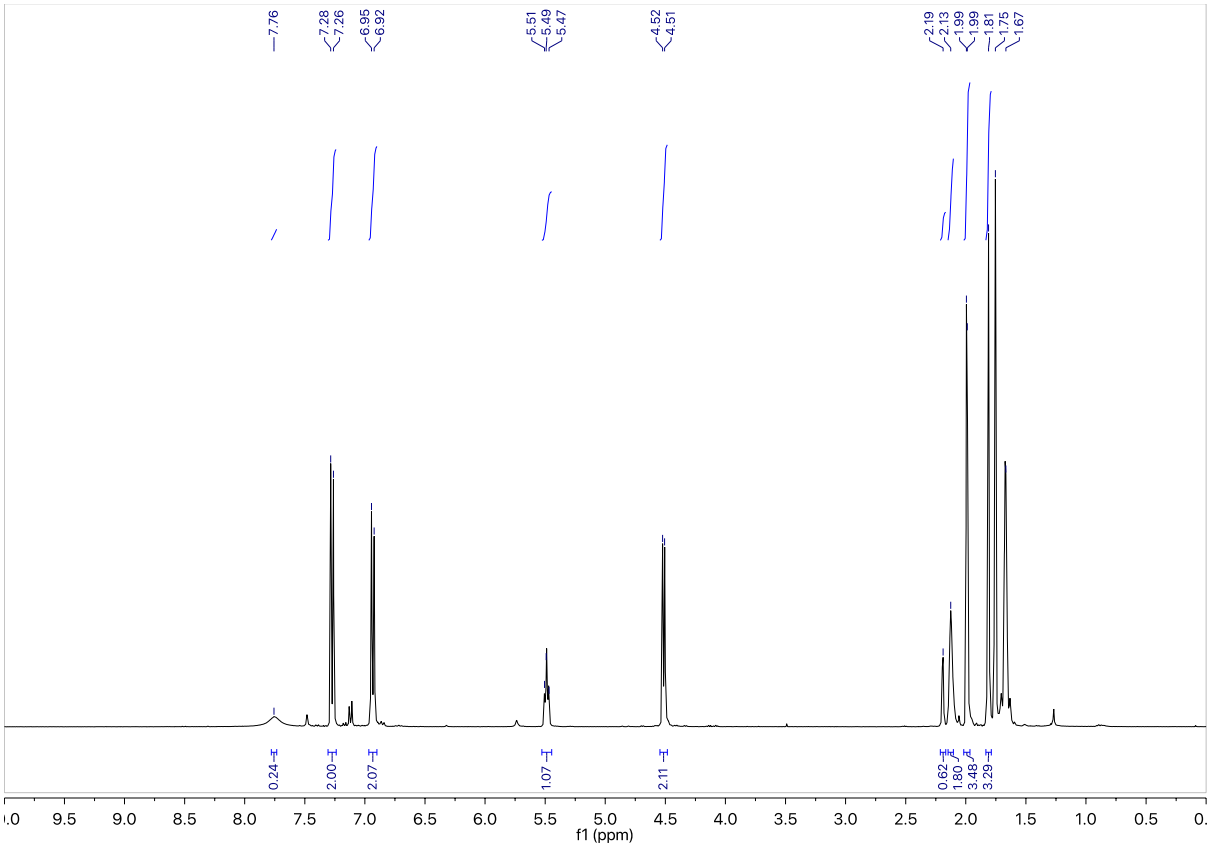

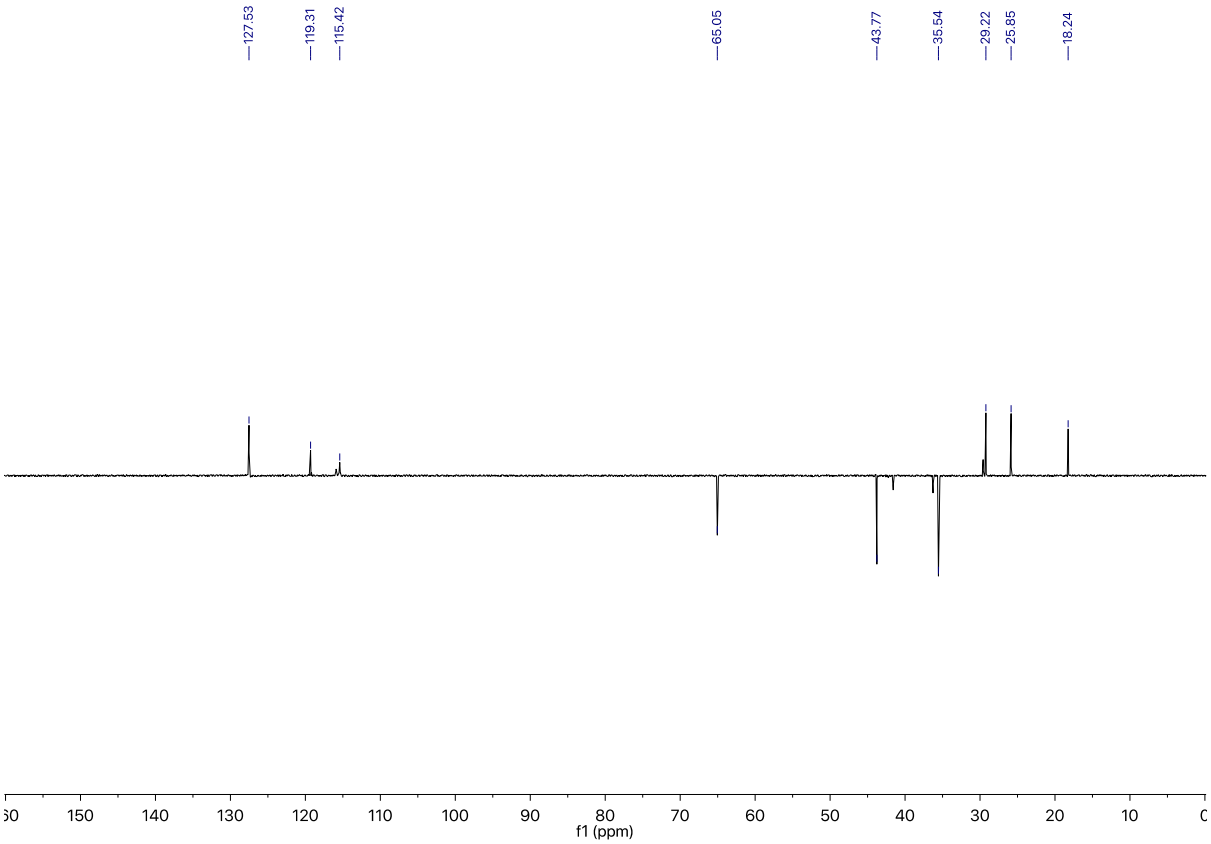
127.53
119.31
115.42
65.05
43.77
35.54
29.22
25.85
18.24
150 140 130 120 110 100 90 80 70 60 50 40 30 20 10
f1 (ppm)

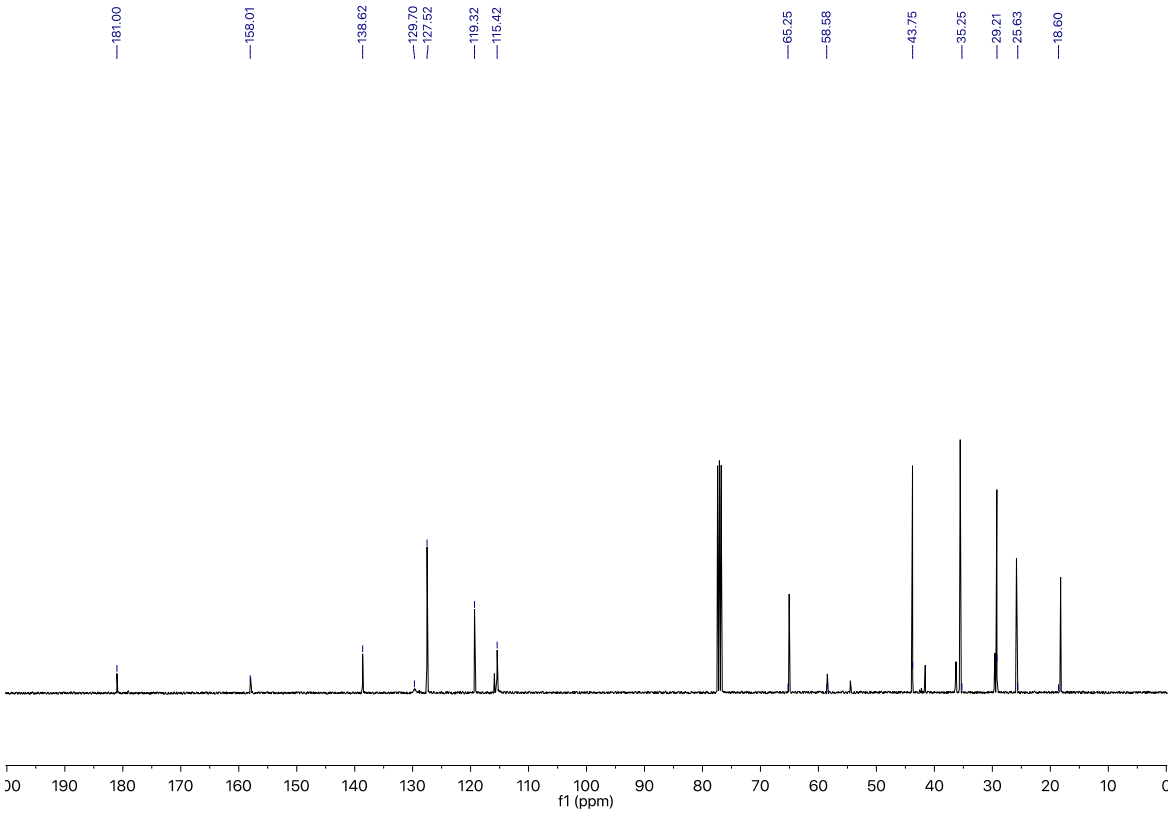
181.00
158.01
138.62
129.70
127.52
119.32
115.42
65.25
58.58
43.75
35.25
29.21
25.63
18.60
190 180 170 160 150 140 130 120 110 100 90 80 70 60 50 40 30 20 10
f1 (ppm)

8.3 ^{13}C NMR SPECTRUM (100 MHZ; CDCL3) of JJH-III-051A

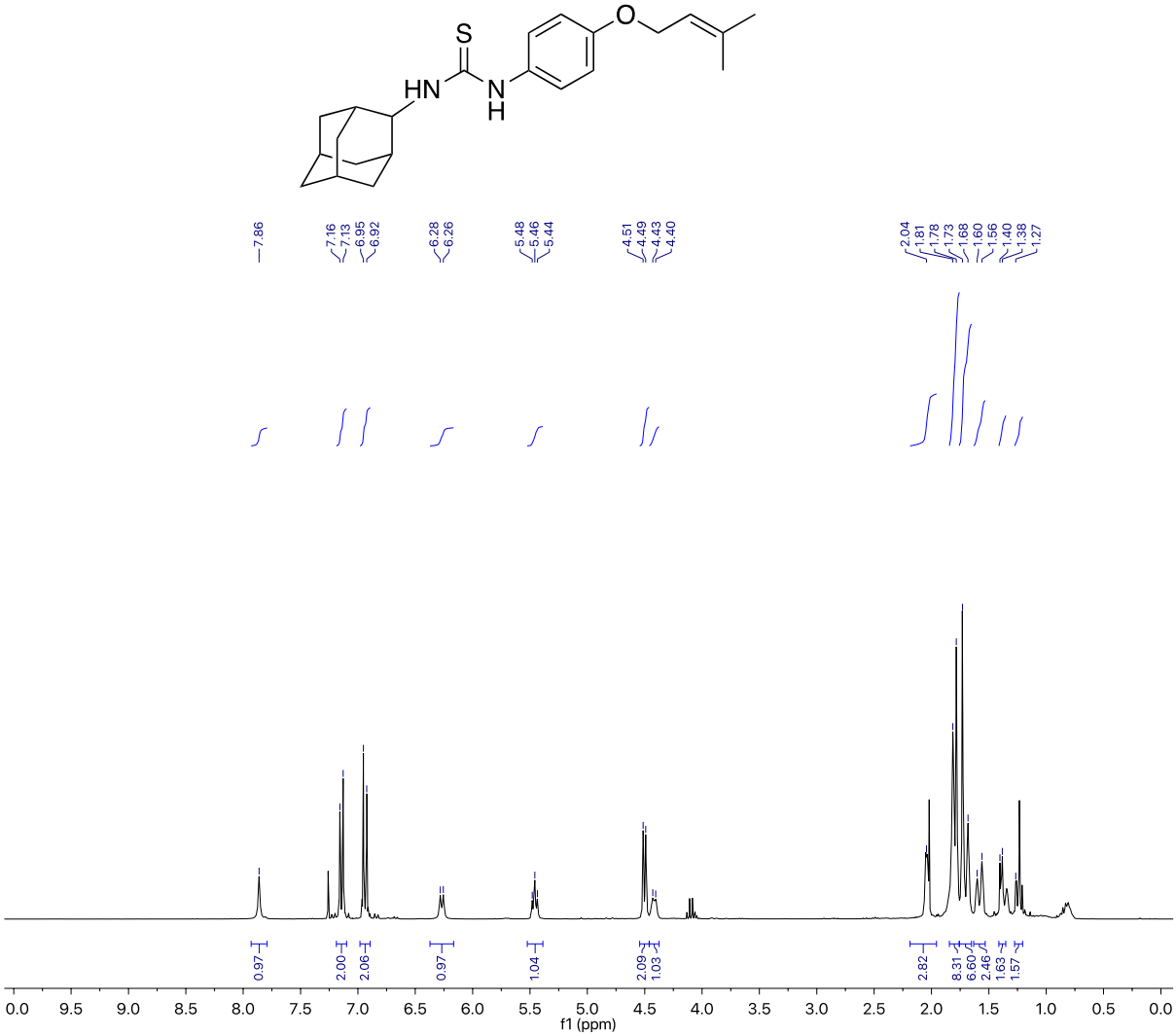

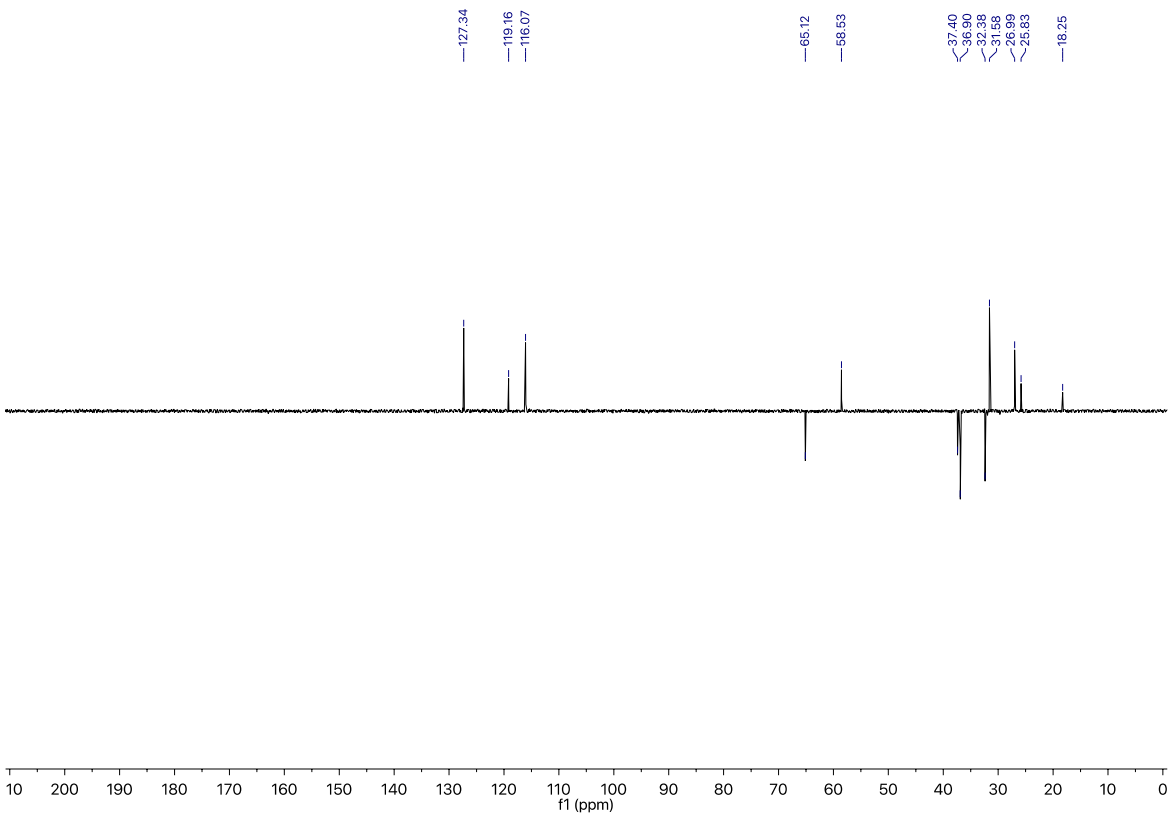
127.34
119.16
116.07
65.12
58.53
37.40
36.90
32.38
31.58
26.99
25.83
18.25
10 200 190 180 170 160 150 140 130 120 110 100 90 80 70 60 50 40 30 20 10 0
f1 (ppm)

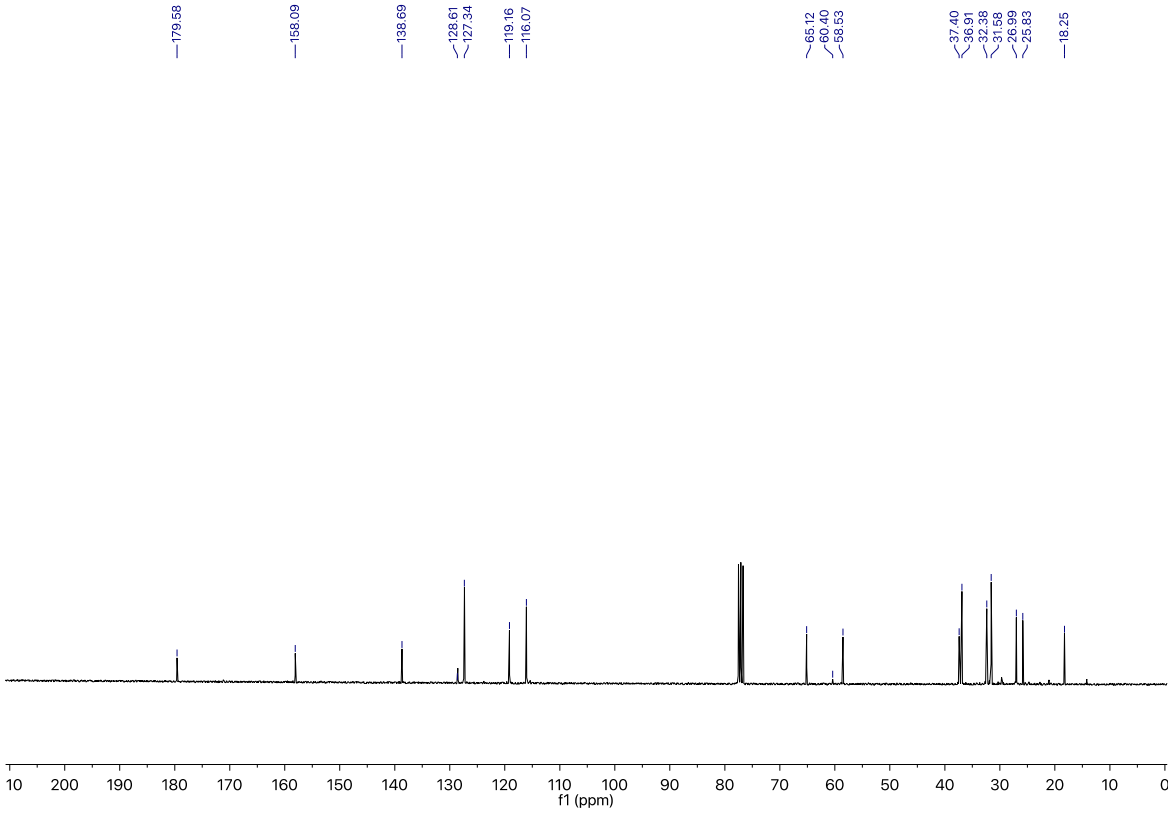
179.58
158.09
138.69
128.61
127.34
119.16
116.07
65.12
60.40
58.53
37.40
36.91
32.38
31.58
26.99
25.83
18.25
10 200 190 180 170 160 150 140 130 120 110 100 90 80 70 60 50 40 30 20 10 0
f1 (ppm)

8.4 ^{13}C NMR SPECTRUM (100 MHZ; CDCL3) of JJH-III-039A

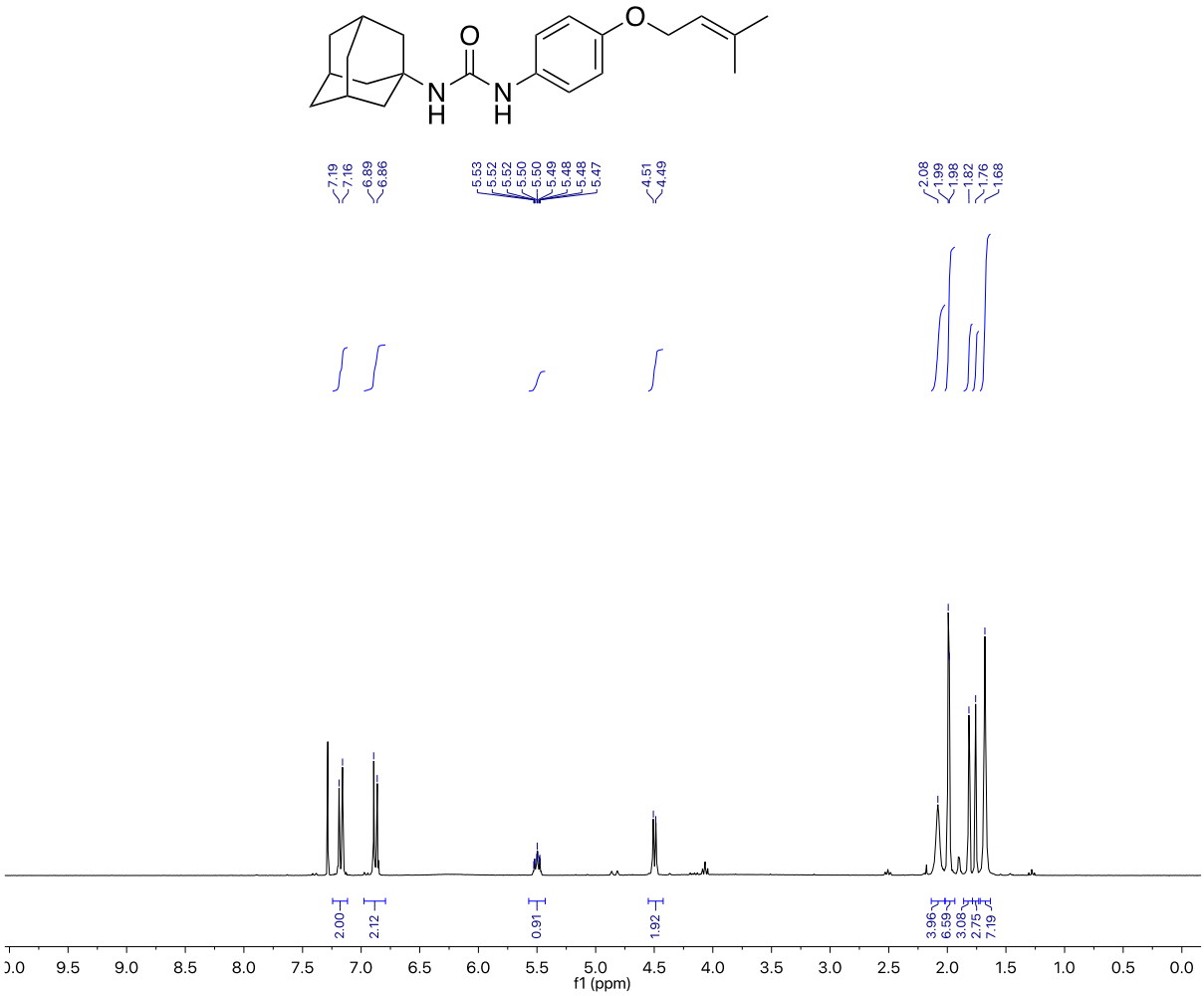

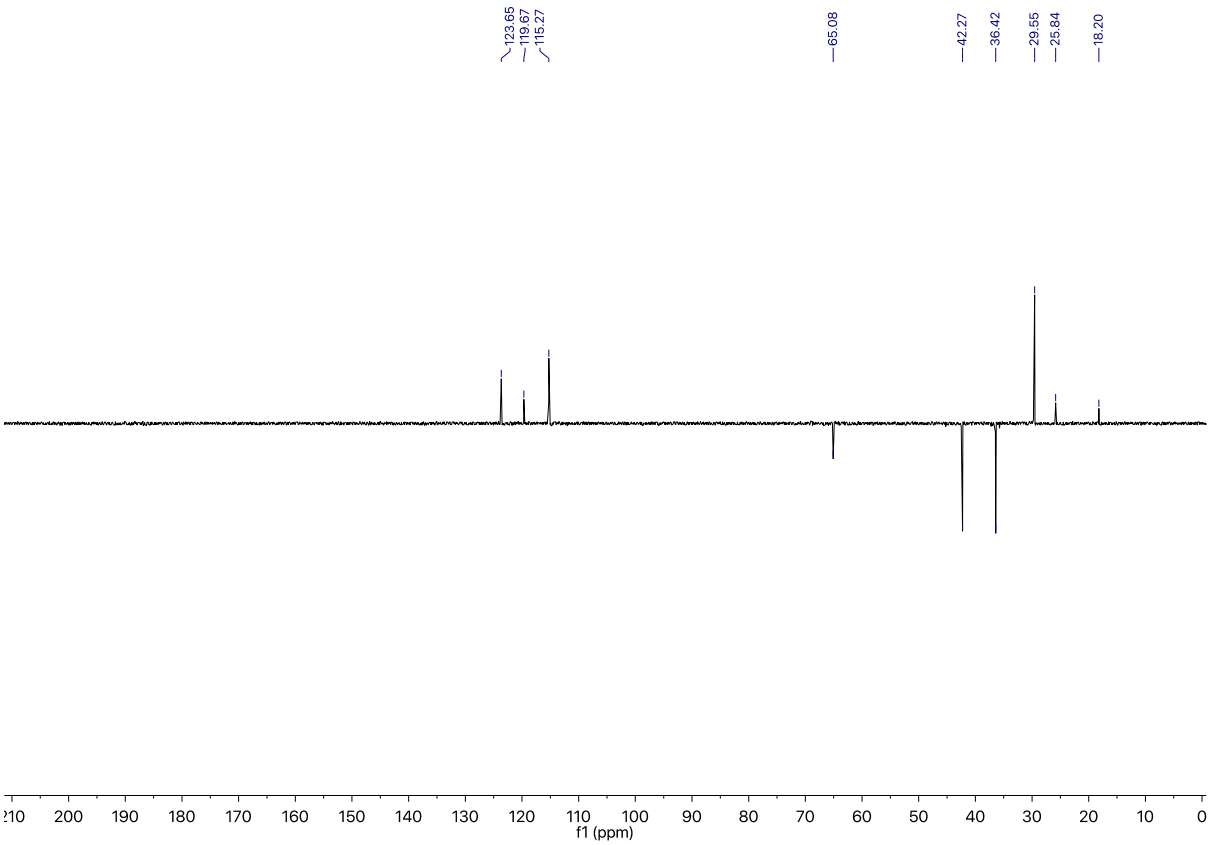
123.65
119.67
115.27
65.08
42.27
36.42
29.55
25.84
18.20
210 200 190 180 170 160 150 140 130 120 110 100 90 80 70 60 50 40 30 20 10 0
f1 (ppm)

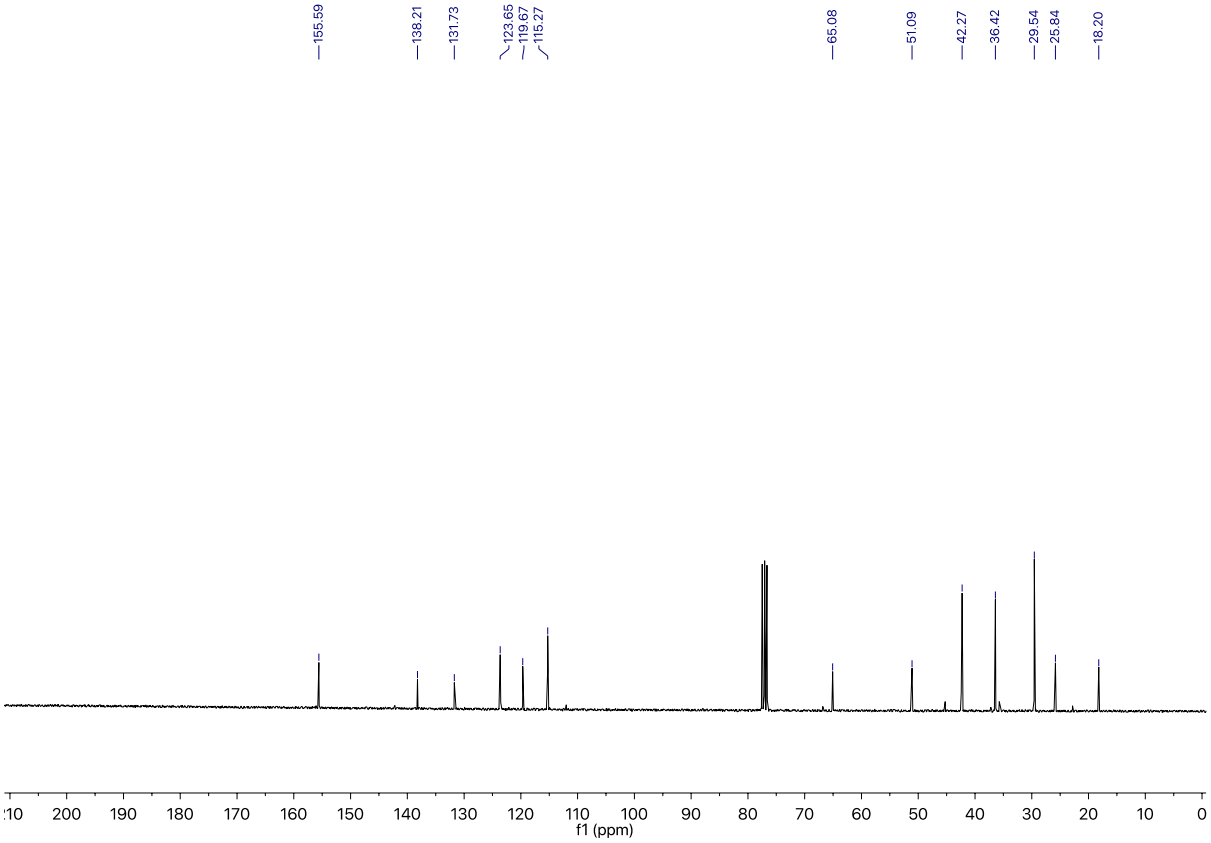
155.59
138.21
131.73
123.65
119.67
115.27
65.08
51.09
42.27
36.42
29.54
25.84
18.20
210 200 190 180 170 160 150 140 130 120 110 100 90 80 70 60 50 40 30 20 10 0
f1 (ppm)

8.5 ^{13}C NMR SPECTRUM (100 MHZ; CDCL3) of JJH-III-052A

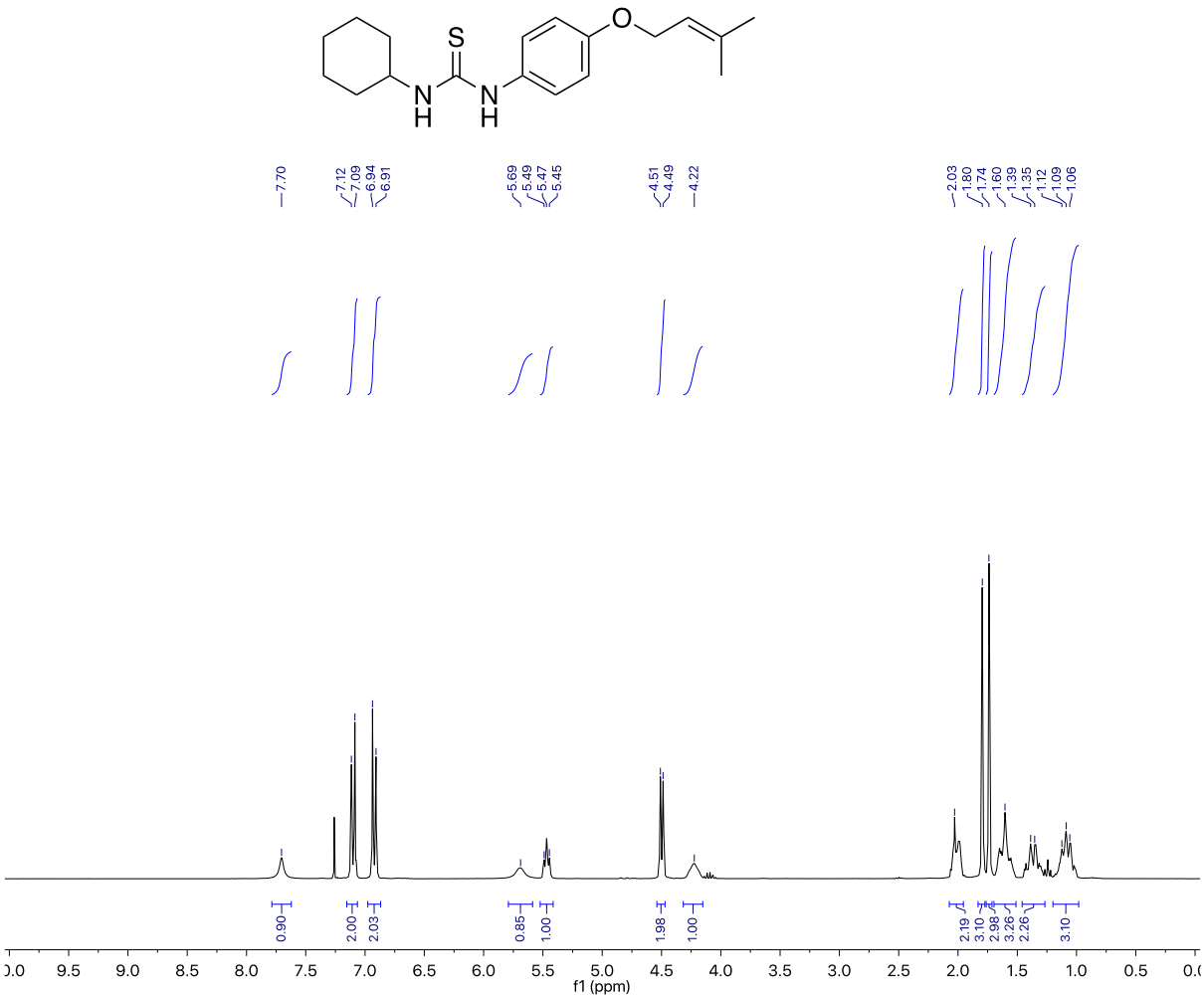

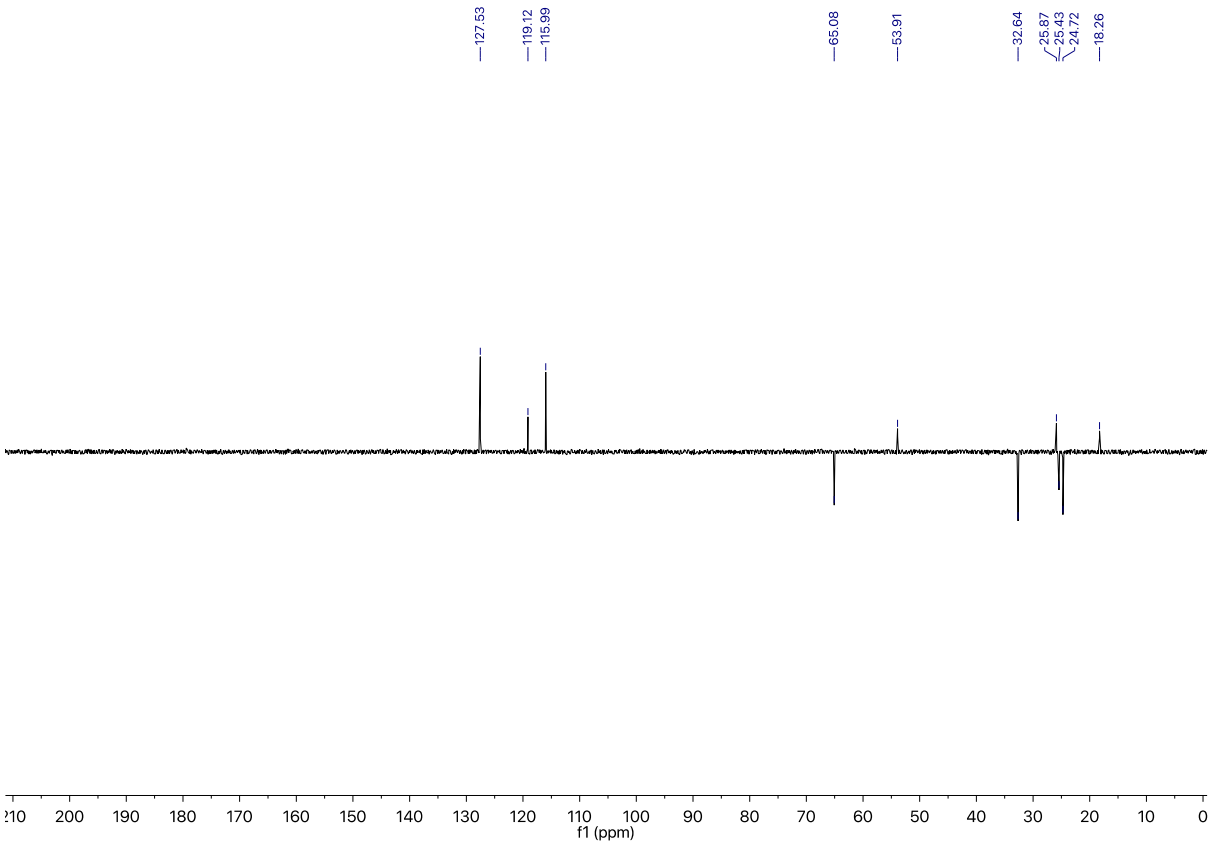
127.53
119.12
115.99
65.08
53.91
32.64
25.87
25.43
24.72
18.26
210 200 190 180 170 160 150 140 130 120 110 100 90 80 70 60 50 40 30 20 10 0
f1 (ppm)

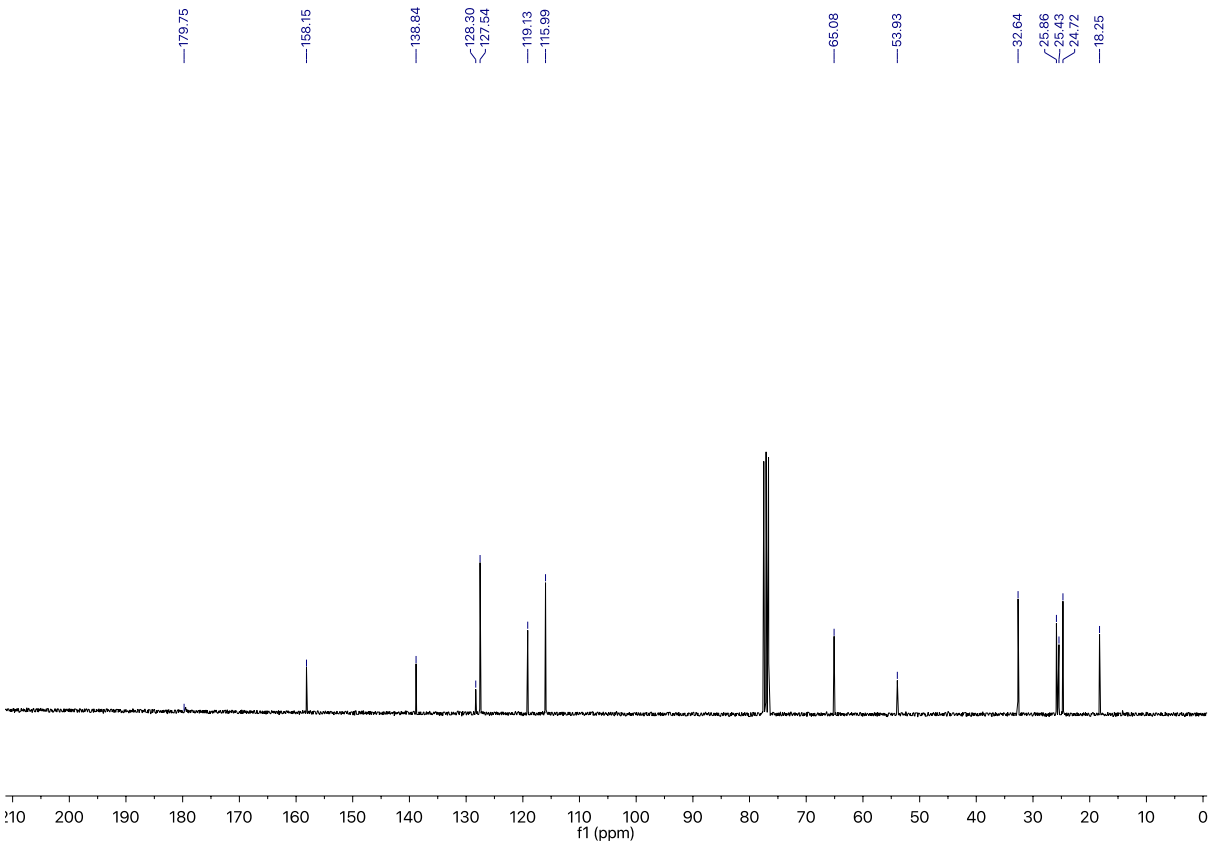
179.75
158.15
138.84
128.30
127.54
119.13
115.99
65.08
53.93
32.64
25.86
25.43
24.72
18.25
210 200 190 180 170 160 150 140 130 120 110 100 90 80 70 60 50 40 30 20 10 0
f1 (ppm)